March 2019

Enhanced Mass Spectrometric Analysis of Peptides and Proteins Using Polymeric Reverse Micelles

Mahalia Adelina Corazon Paningbatan Serrano
University of Massachusetts Amherst

ENHANCED MASS SPECTROMETRIC ANALYSIS OF PEPTIDES AND PROTEINS USING POLYMERIC REVERSE MICELLES

A Dissertation Presented

by

MAHALIA ADELINA CORAZON PANINGBATAN SERRANO

Submitted to the Graduate School of the
University of Massachusetts Amherst in partial fulfillment
of the requirements for the degree of

DOCTOR OF PHILOSOPHY

February 2019

Chemistry Department

ENHANCED MASS SPECTROMETRIC ANALYSIS OF PEPTIDES AND PROTEINS USING POLYMERIC REVERSE MICELLES

A Dissertation Presented

By

MAHALIA ADELINA CORAZON PANINGBATAN SERRANO

Approved as to style and content by:

_____
Richard W. Vachet, Chair

_____
Sankaran Thayumanavan, Member

_____
Stephen J. Eyles, Member

_____
Kathleen F. Arcaro, Member

_____
Richard W. Vachet, Department Head
Chemistry Department

ACKNOWLEDGMENTS

This work would not be possible without the help and contribution of numerous people, and I would like to express my sincerest gratitude to the following:

To Prof. Vachet, for your guidance throughout the highs and lows of my PhD career and for always encouraging me to be a better scientist. Thank you for understanding the struggles of an international student and for always believing in me, especially at times when I am plagued by self-doubt and frustrations. I will always be grateful to you for giving me this opportunity to learn and discover the world of mass spectrometry and for helping me expand my horizon. I look up to you in so many ways (not just because of the height), in the way that you deal with everyday and everyone in the group, with your level-headed mindset even when things are not going our way, with how you teach and how you bring out the best in your students. It has been an honor to have you as my mentor and I do hope to pass on this mentorship to the next generation someday.

To my dissertation committee: Prof. Thayumanavan, Dr. Steve Eyles, Prof. Kathleen Arcaro, and Prof. Matt Holden, for all your critical insights and contributions to this work. Prof. Thai, this work would not be possible without the collaboration with your group and I am truly thankful for all your ideas and for being a second adviser to me. You have always inspired me, from the very first day in Core I, with how you see science and your approach in solving scientific problems. Steve, thank you for agreeing to be in my committee, for training me in the use of the triple quad and the Orbitrap, and for always being there to help me troubleshoot the instruments and have someone to discuss the nitty gritty details of my experiments and methods. Prof. Kathleen, you have always given me feedback on my prospectus, ORP, and dissertation, and all these helped me refine my ideas

and get some perspective on my studies. I also thank Prof. Matt Holden for being in my committee for the first four years, and especially for serving as the chair during my ORP.

To my collaborators: Huan (Joy) He, Bo Zhao, Meizhe Wang, and Jingjing Gao. This work would literally not materialize without your synthetic chemistry expertise. I enjoyed working, conceptualizing and discussing ideas with all of you. I thank Joy for synthesizing and characterizing the PTLAm and PAm polymers used in Chapter II; Bo, for synthesizing polymers P1, P2, P3, P5, P6, P7, and P10, and for being the point person with whom I most often discussed my experimental plans and results; Jingjing, for synthesizing polymer P9.

To Dr. Fateme Tousi, for giving me the industrial internship opportunity in Sanofi, and for being a really inspiring mentor and an amazing scientist.

To the past and present members of the Vachet Lab, for making my time in the lab an enjoyable and unforgettable experience. Thank you for making it fun to work even though graduate school is oftentimes stressful and exhausting.

To the wonderful people from all over the world who I met in UMass, friends I will always cherish: Tiffany, Cola, Hou, Heidi, Carolyn, Laura, Bo, Meizhe, Kong, Alyssa, Gokhan, Derrick, Chengfeng. Thank you for making these past six years worthwhile because of your friendship.

To my Filipino friends who welcomed me in Amherst and gave me a sweet piece of home away from home: Kevin, Tina, Kristine, Myles, Dolly, JB, Bernard, and their families.

To my lifelong friends back home, for a friendship that transcends distance and time. Having you in my life kept me sane and helped me survive grad school.

To my family, whose love gave me constant motivation every day. To my brothers, Tong, Dake and Ninoy, thank you for you support and for always reminding me of what home feels like. To Toshi, for the 12 years and beyond that you filled our lives with love, adventure and joy. To Ate, I could not have made it without you. I am so grateful that we have been through all these adventures together. You have been and always will be my best friend and greatest mentor. Thank you for loving me for me and in spite of me.

And most importantly, to my parents, Nanay and Tatay, for your unwavering love, for believing in me, and for all the sacrifices that you've made in order for me to pursue and achieve my dreams. This would not be possible without you. I dedicate this work to you and I will strive every day to make you proud.

ABSTRACT

ENHANCED MASS SPECTROMETRIC ANALYSIS OF PEPTIDES AND PROTEINS USING POLYMERIC REVERSE MICELLES

FEBRUARY 2019

MAHALIA ADELINA CORAZON PANINGBATAN SERRANO, B.S. UNIVERSITY OF THE PHILIPPINES LOS BAÑOS

Ph.D., UNIVERSITY OF MASSACHUSETTS AMHERST

Directed by: Professor Richard W. Vachet

Mass spectrometry (MS) has become a key and indispensable tool in the identification, characterization, and quantitative analysis of proteins owing to its universality, sensitivity, specificity, and its capability for multiplexed detection. Because biological samples containing these protein analytes are almost always complex systems, various techniques are employed in conjunction with MS to fully harness its analytical potential and enhance its detection capabilities. This dissertation explores the use of amphiphilic polymeric reverse micelles in enriching proteins and peptides from complex biological mixtures and in enhancing their mass spectrometric analysis. Fundamental studies that elucidate the molecular basis for the observed MS signal enhancement that these materials confer are described through structure-property investigations. The molecular features that influence the release of peptides after their encapsulation in these assemblies are examined, and a method for efficient guest release is devised to enable a more quantitative MS analysis. The utility of these materials in simplifying serum and its applicability in significantly enhancing the detection sensitivity in the MS analysis of protein biomarkers is demonstrated.

TABLE OF CONTENTS

Page

ACKNOWLEDGMENTS..... iv

ABSTRACT..... vii

LIST OF TABLES..... xiii

LIST OF FIGURES..... xiv

CHAPTER

I. INTRODUCTION..... 1

Mass Spectrometry for Protein Identification and Detection..... 2

Ionization Methods for Protein MS Analysis..... 4

MALDI..... 4

ESI..... 6

Techniques Coupled to MS to Enhance Protein Analysis..... 7

Disease Biomarkers..... 8

Methods of Biomarker Detection..... 8

Supramolecular Assemblies of Amphiphilic Polymers as Selective Extraction Agents for Protein Enrichment..... 9

References..... 16

II. MALDI-MS SIGNAL ENHANCEMENT OF PEPTIDES THROUGH DONOR-ACCEPTOR INTERACTIONS BETWEEN POLYMER AND MATRIX..... 25

Abstract..... 25

Introduction..... 26

Results and Discussion..... 28

Donor-Acceptor Hypothesis for Signal Enhancement..... 28

Variations in the Structure of the MALDI Matrix..... 30

Variations in the Polymer Structure..... 32

Summary and Conclusions..... 38

Experimental Methods..... 39

Materials and Reagents..... 39

Polymer Synthesis and Characterization..... 40

Preparation of Polymeric Reverse Micelles..... 40

MALDI Matrix Solutions..... 40

Peptide Extraction and Sample Preparation..... 40

Fluorescence Microscopy..... 41

MALDI-MS Analysis..... 41

References..... 42

III. MOLECULAR FEATURES INFLUENCING THE RELEASE OF PEPTIDES FROM AMPHIPHILIC POLYMERIC REVERSE MICELLES..... 45

Abstract..... 45

Introduction..... 46

Results and Discussion..... 48

Cooperative Effects of Disassembly and Charge-Charge Disruption..... 48

Factors Influencing the Release Efficiency..... 53

Summary and Conclusions..... 62

Experimental Methods..... 63

Reagents..... 63

Polymer Synthesis and Characterization..... 64

Preparation of Polymeric Reverse Micelle..... 64

Extraction and Release of Peptides..... 64

MALDI-MS Analysis..... 65

Fluorescence Spectroscopy..... 65

LC-MS Analysis..... 66

References..... 67

IV. SELECTIVE DEPLETION OF ABUNDANT ACIDIC PROTEINS IN SERUM USING POLYMERIC REVERSE MICELLES..... 71

Abstract..... 71

Introduction..... 72

Results and Discussion..... 75

Extraction Selectivity..... 75

Extraction Efficiency and Capacity..... 79

Depletion of Abundant Acidic Proteins in Serum..... 82

Identification of Serum Proteins Depleted..... 83

Effect of Depletion on Detection Sensitivity..... 86

Summary and Conclusions..... 89

Experimental Methods..... 90

Materials and Reagents..... 90

Preparation of Reverse Micelles..... 90

General Extraction Procedure..... 91

Immunoaffinity Albumin and IgG Depletion..... 91

Determination of Extraction Selectivity and Capacity by Intact Protein LC-MS..... 92

SDS-PAGE Analysis..... 93

Total Protein Content..... 93

In-Gel Trypsin Digestion of Protein Bands for Peptide Mass Fingerprinting..... 94

In-Solution Trypsin Digestion for Proteomic Analysis..... 94

LC-MS/MS Analysis..... 95

SRM-MS Analysis of Spiked Bradykinin in Serum..... 96

References..... 97

V. COMBINING pI BRACKETING WITH MRM ANALYSIS FOR MULTIPLEXED AND MORE SENSITIVE DETECTION OF PROTEIN BIOMARKERS..... 101

Abstract..... 101

Introduction..... 102

Results and Discussion..... 105

Target Biomarkers..... 105

Determination of Surrogate Peptide for Cytochrome C..... 107

Selection of Transitions to Monitor and Collision Energy Optimization..... 110

Validation of Transitions and Multiplexed Detection in Serum..... 114

Conclusions and Future Work..... 120

Experimental Methods..... 121

Serum Sample and Target Biomarkers..... 121

Polymer Synthesis, Characterization and Preparation of Reverse Micelles..... 121

Depletion of Abundant Low-pI Serum Proteins..... 122

Digestion with Trypsin and LysC..... 122

Simultaneous Extraction of Biomarkers in Serum by pI Bracketing..... 123

Release of Extracted Peptides by Back-Extraction..... 123

Detection of BK, Hyp^3-BK, and CC Surrogate Peptide in Serum by MRM..... 124

References..... 125

VI. CONCLUSIONS AND FUTURE DIRECTIONS..... 130

References..... 132

APPENDIX: SYNTHETIC SCHEMES AND SUPPLEMENTARY EXPERIMENTS..... 134

BIBLIOGRPHY..... 155

LIST OF TABLES

Table		Page
4.1	Protein identification of bands in SDS-PAGE gel of serum.....	84
4.2	Proteomic analysis of the polymer-bound fraction.....	86
5.1	Target biomarkers, their properties and candidate surrogate peptides for cytochrome c.....	106
5.2	MRM transitions monitored for each target peptide.....	113
A.1	Peptides belonging to α-2-macroglobulin (Uniprot P01023) identified for protein band 1.....	147
A.2	Peptides belonging to transferrin (Uniprot Q53H26) identified for protein band 2.....	148
A.3	Peptides belonging to human serum albumin (Uniprot P02768) identified for protein band 3.....	149
A.4	Peptides belonging to IgG heavy chain identified for protein band 4.....	151
A.5	Peptides belonging to haptoglobin (Uniprot A0A087WU08) identified for protein band 5.....	152
A.6	Peptides belonging to IgG light chain identified for protein band 6.....	152
A.7	Peptides belonging to apolipoprotein A-1 (Uniprot A0A087WU08) identified for protein band 7.....	153

LIST OF FIGURES

Figure		Page
1.1	Several advantages of the use of mass spectrometry for protein analysis.....	2
1.2	Nomenclature for MS/MS peptide fragmentation and chemical structures of product ions produced.....	3
1.3	Illustration of the MALDI-MS process (left) and an example MALDI mass spectrum (right).....	5
1.4	Chemical structures of common MALDI matrices used for peptide and protein analysis.....	5
1.5	Ionization by electrospray (left) and an example ESI mass spectrum for a protein (right).....	6
1.6	Chemical structures of some amphiphilic polymers used in this study.....	11
1.7	Amphiphilic polymers self-assemble into either micelle-type or reverse micelle-type assemblies depending on the solvent.....	11
1.8	General scheme illustrating the pI bracketing method.....	13
1.9	Extraction selectivity using reverse micelles of a negatively charged polymer (left) and a positively charged polymer (right).....	14
2.1	Chemical structures of carboxylate-functionalized homopolymers **P1** and **PAm**.....	27
2.2	General scheme for the pI-dependent selective extraction and MALDI-MS analysis of peptides using reverse micelles of amphiphilic polymers.....	27
2.3	MALDI mass spectra for unextracted 1 μM bradykinin (**A**), and 10 nM bradykinin (RPPGFSPFR, *m/z* 1060.6) extracted using the polymer **P1** (**B**) and using **PAm** (**C**).....	29
2.4	Comparison of MALDI-MS signal for bradykinin peptide (RPPGFSPFR, *m/z* 1060.6) in the absence of the polymer or monomer **(A)**, with the monomer as matrix additive **(B)**, and extracted using polymer **P1 (C)**.....	30

2.5 Chemical structures of different MALDI matrices in the order of increasing electron deficiency on the ring, along with the corresponding MALDI mass spectra and fluorescence images obtained for 100 nM bradykinin extracted by polymer **P1** and analyzed using these MALDI matrices..... 31

2.6 **(A)** Chemical structures of **PTLAm** polymers with varying substituents. **(B-D)** MALDI-MS spectra of a mixture of peptides before and after extraction at pH 8.0 using reverse micelles of the **PTLAm-NO2**, **PTLAm-H**, and **PTLAm-OMe**, respectively. (**E**) MALDI signal intensity of 10 nM bradykinin extracted by each **PTLAm** polymer. **(F)** Fluorescence images show the degree of clustering of peptide (red) and CHCA matrix (green) after extraction using each **PTLAm** polymer..... 33

2.7 Chemical structures and labels of the polyacrylamide-based amphiphilic homopolymers with the carboxylate hydrophilic moiety and variable hydrophobic units containing electron-donating or electron-withdrawing functionalities..... 34

2.8 Fluorescence microscopy images showing the degree of clustering and co-localization of TMR-bradykinin peptide and CHCA matrix..... 36

2.9 Five circular regions selected for each image to quantify the degree of clustering of the peptide in the polymer-matrix-peptide mixture in the organic phase after extraction using each of the **PAm** polymers..... 37

2.10 Correlation of the degree of clustering with the MALDI-MS signal obtained for 50 nM TMR-bradykinin extracted using each **PAm** polymer..... 37

2.11 Co-localization analyis for each fluorescence micrograph..... 38

3.1 Different strategies for guest release from carboxylate-functionalized polymeric reverse micelle assemblies..... 49

3.2 Representative MALDI mass spectra (**A**) 1 μM angiotensin I standard and (**B**) 200 pmol angiotensin I, fully extracted into the organic phase without any release. (**C-J**) Representative MALDI spectra of the resulting aqueous and organic phases after release of 200 pmol angiotensin I from reverse micelles of **P1** using each strategy..... 50

3.3 DLS correlograms (**A**) and hydrodynamic size measurements (**B**) of the polymer assemblies of **P1** in toluene before and after addition of THF. (**C**) UV-Visible absorbance measurements of the organic (ORG) and aqueous (AQ) phases before and after forward and back extraction..... 51

3.4 TAMRA-bradykinin before (**A**) and after (**B**) extraction into reverse micelles of **P1** in toluene. Release of TAMRA-bradykinin under different conditions (**C**), and quantitative determination of the release efficiency by fluorescence measurement of the stripping aqueous phase (**D**)..... 52

3.5 (**A**) Chemical structures of amphiphilic polymers **P1**, **P2**, **P3** and **P4**. Efficiency of peptide release from each polymer by addition of THF then 10% acetic acid (**B**), or by addition of THF then water (**C**). (**D**) Theoretically calculated net charge on the peptide as a function of solution pH..... 54

3.6 Release of malantide peptide (RTKRSGSVYEPLKI, pI 10.3) from reverse micelles of polymer **P3** at different pH of stripping aqueous phase..... 56

3.7 MALDI mass spectra of the stripping aqueous phase (**A**) and the organic phase (**B**) after release at pH 9.5 (using THF + 50 mM Tris, pH 9.5), illustrating that angiotensin I can be selectively released..... 57

3.8 Release efficiency of TAMRA-bradykinin peptide from reverse micelles of homopolymer **P1** (**A**) and a random copolymer **P7** (**B**) as a function of stripping aqueous phase pH..... 59

3.9 **(A**) Structures of polymers **P5**, **P6** and **P7**. (**B**) Release efficiency for bradykinin, quantified by LC-MS, from reverse micelles of polymers with different percentages of carboxylate functional groups..... 60

3.10 Release efficiency of TAMRA-bradykinin from reverse micelles of **P7**, **P6**, **P2** and **P1** using THF and a stripping aqueous phase with increasing electrostatic shielding..... 61

4.1 The abundant proteins in serum..... 72

4.2 Chemical structures of amphiphilic homopolymer **P8** and random copolymer **P9** and a cartoon representation of a positively charged reverse micelle-like nanoassembly encapsulating negatively charged proteins..... 75

4.3 Total ion chromatogram (TIC) of a mixture of 8 μM each of bovine serum albumin (BSA) and cytochrome c (CC) before and after extraction using 1 mg/mL of **P8** in toluene..... 76

4.4 Synthesis of amphiphilic random copolymer **P9**..... 77

4.5 Total ion chromatogram (TIC) of a mixture of 5 μM lysozyme (LZ) and 20 μM bovine serum albumin (BSA) before and after extraction using **P9**..... 77

4.6 SDS-PAGE of a protein mixture before extraction and after each extraction step using nanoassemblies of **P9** (**left**) and using toluene alone (**right**) at pH 7.4..... 78

4.7 Determination of optimum extraction time for protein depletion..... 79

4.8 **(A)** Determination of extraction capacity of **P9**. **(B)** Total protein content of serum (measured by the Bradford assay) before and after depletion using different methods..... 81

4.9 SDS-PAGE analysis of serum spiked with CC **(A)** and LZ **(B** and **C)**, to show the pI-dependent selectivity of extraction in serum..... 82

4.10 SDS-PAGE analysis of serum before and after depletion using the ProtePrep® immunodepletion kit and by multi-step depletion using reverse micelles of **P9** at pH 7.4..... 84

4.11 Comparison of spectral counts (SC) of selected serum proteins before and after depletion..... 87

4.12 SRM chromatograms for bradykinin in serum samples where no depletion was done **(A)**, and with depletion using **P9** prior to analysis **(B)**..... 88

5.1 MRM analysis on a triple quadrupole mass spectrometer..... 103

5.2 Multiplexed detection of target biomarkers by pI bracketing of surrogate peptides and MRM-MS analysis..... 104

5.3 Total ion chromatogram (TIC) for cytochrome c digest and MS spectrum from the product ion scan for TGPNLHGLFGR..... 110

5.4 Extracted ion chromatograms (EIC) for bradykinin (BK, *m/z* 530.8), Hyp^3-bradykinin (Hyp3-BK, *m/z* 538.8) and cytochrome c peptide TGPNLGHLFGR (CC-pep1, *m/z* 584.8) with their corresponding mass spectra..... 111

5.5 Product ion scan MS/MS spectra obtained for bradykinin, Hyp^3-bradykinin, and CC-pep1..... 112

5.6 Collision energy optimization of individual transitions for each peptide..... 113

5.7 Overlaid MRM chromatograms for all the transitions monitored in a serum sample spiked with 10 μM each of BK, Hyp^3-BK and CC protein digest..... 115

5.8 Flowchart of serum sample preparation and enrichment of biomarkers for LC-MRM analysis..... 116

5.9 MRM chromatograms of the quantifying transitions for **(A)** bradykinin, **(B)** Hyp^3-bradykinin, and **(C)** CC-pep1 (TGPNLGHLFGR)..... 118

5.10 Determination of limit of detection (LOD) and limit of quantitation (LOQ) for the MRM assay with and without pI bracketing..... 119

A.1 Synthetic scheme for amphiphilic homopolymer **P1**..... 134

A.2 Determination of extraction capacity of polymer **P1** for bradykinin peptide at pH 8.0..... 135

A.3 Synthetic scheme for polythiolactone-based amphiphilic homopolymers. 136

A.4 DLS data and TEM image for the reverse micelles prepared from polymer **PTLAm-H**..... 137

A.5 MALDI mass spectra of a mixture of peptides before and after extraction at pH 8.0 using reverse micelles of the **PTLAm**-based carboxylate polymers..... 137

A.6 Synthetic scheme for polyacrylamide-based (PAm) amphiphilic homopolymers..... 138

A.7 DLS data, TEM image, and CAC determination for the reverse micelles prepared from polymer **PAm-H**..... 139

A.8 Example of peptide extraction capacity measurement for polymer **PAm-H** at pH 8.0..... 140

A.9 MALDI mass spectra of a mixture of peptides before and after extraction at pH 8.0 using reverse micelles of **PAm-H** polymer..... 141

A.10 Synthesis of random copolymer **P2**..... 141

A.11 Synthesis of random copolymer **P3**..... 142

A.12 Synthesis of random copolymer **P7**..... 143

A.13 Determination of extraction capacities of polymers **P2**, **P3** and **P7** at pH 8.0..... 144

A.14 MALDI mass spectra of a mixture of peptides before and after extraction at pH 8.0 using reverse micelles of **P2** carboxylate polymer.... 145

A.15 Release efficiency of TAMRA-labeled bradykinin peptide from reverse micelles of polymer **P3** at various back-extraction times using THF + acid..... 145

A.16 SDS-PAGE analysis of serum spiked with MG and BCA..... 146

CHAPTER I

INTRODUCTION

Because of the crucial roles that proteins play in biological systems, the development of methods for their analysis has been of prime importance to both chemists and biologists. Over the years, methods with increasing resolution, specificity, accuracy and sensitivity have been developed for protein analysis such as spectrophotometric-based methods, two-dimensional gel electrophoresis, capillary electrophoresis, immunoblotting techniques, microarrays, and chemical or isotope tagging.[1–10] Among the bioanalytical techniques, the advancement of mass spectrometry (MS) for protein analysis is arguably the most impactful,[11,12] so influential that it earned John Fenn and Koichi Tanaka the Nobel Prize in Chemistry in 2002 for developing soft ionization methods that allow for the mass spectrometric detection of these large biopolymers.[13] Indeed, MS has become a key technology in protein analysis and proteomics studies, not only in the qualitative characterization of proteins but in quantitative analysis as well.[14–19] To truly harness the power of mass spectrometers, they are often used in conjunction with other techniques such as chromatography and enrichment methods. With increasing complexity of biological systems under study, so too is the need for approaches that would enable higher sensitivity and more accurate analysis of the proteins under investigation. This becomes particularly relevant in the context of detecting very low levels of proteins in complex biological mixtures such as blood serum and cell lysates. This dissertation describes the use of amphiphilic polymeric reverse micelles as an enrichment method in conjunction with mass spectrometry to enable the enhanced analysis and detection of proteins and peptides.

Mass Spectrometry for Protein Identification and Detection

The use of MS as a tool for protein analysis offers several advantages (Figure 1.1). First, because it is measuring an intrinsic property of the molecule, *i.e.* its mass, MS is capable of detecting proteins free of any tags or labels such as fluorophores that are usually a requirement in other modes of detection. Unambiguous identification of a protein, for instance, can be done based on its unique peptide mass fingerprint.[20,21] The molecular mass is also a direct measure of the protein as opposed to other methods like enzyme-linked immunosorbent assays (ELISA) that rely on binding and secondary signals and reactions

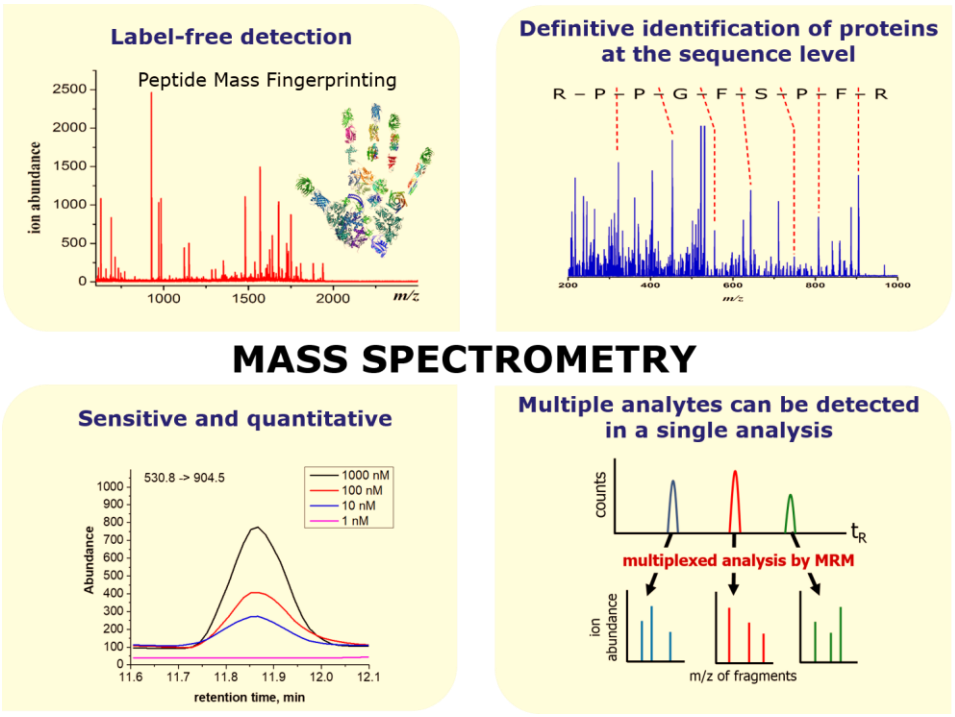

Figure 1.1. Several advantages of the use of mass spectrometry for protein analysis.

for detection. Second, proteins can be definitively identified at the amino acid sequence level through tandem mass spectrometry (MS/MS) and measuring the mass of sequence-specific fragments produced upon MS/MS dissociation (Figure 1.2).[14,16] Because of this

amino acid residue-level resolution, MS can identify site-specific modifications on a protein,[8,22,23] and differentiate various isoforms from one another.[16,24–27] Third, with advancements in instrumentation and sample preparation, highly sensitive and quantitative detection of proteins can be achieved.[28–31] Lastly, the multiplexed capability of MS allows for the simultaneous analysis of multiple proteins in a single run.[32–35]

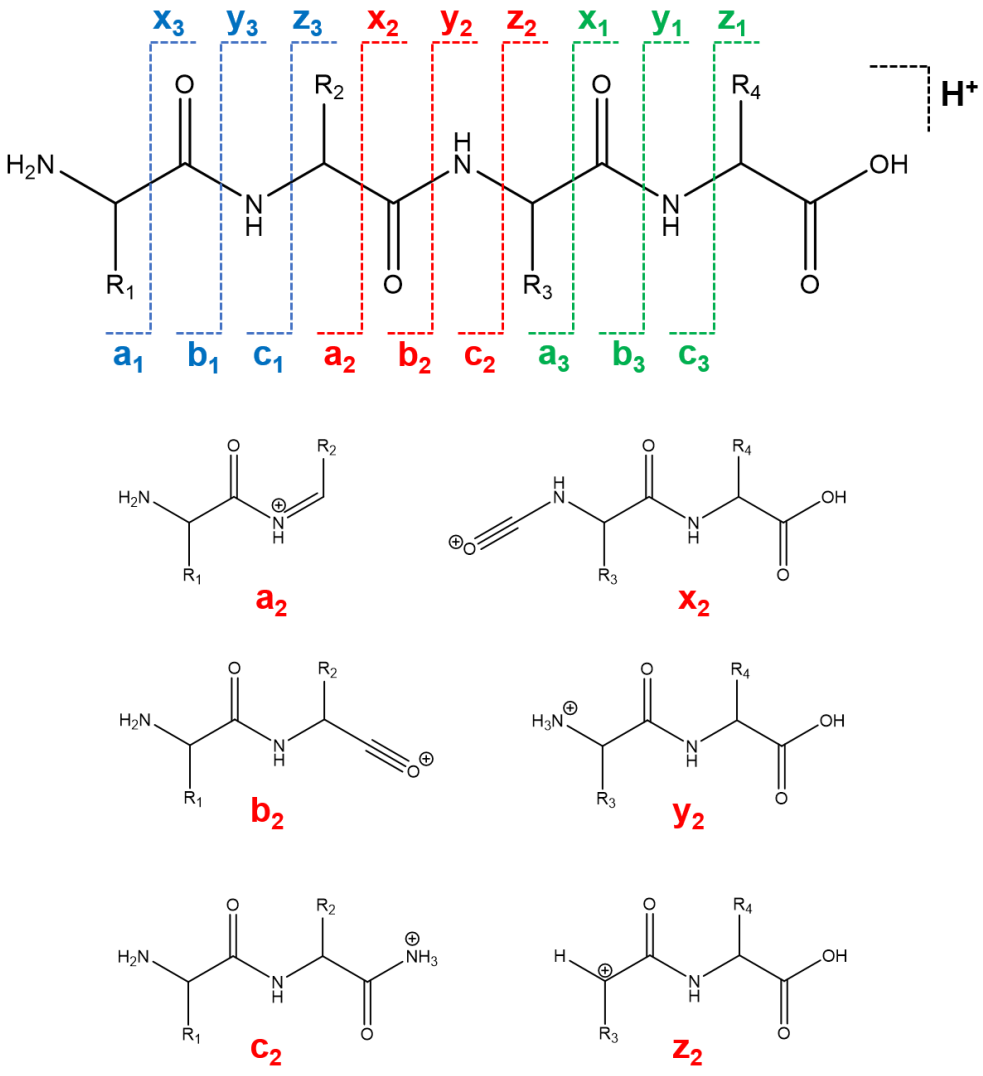

Figure 1.2. Nomenclature for MS/MS peptide fragmentation and chemical structures of product ions produced.

Ionization Methods for Protein MS Analysis

For a molecule to be detected by the mass spectrometer, it has to be ionized and be in the gas phase. However, since proteins are large, polar biomolecules, they are not easily transferred to the gas phase. The advent of mass spectrometric application in the biomolecules realm is attributed to the discovery and development of soft ionization methods, particularly matrix-assisted laser desorption/ionization (MALDI) and electrospray ionization (ESI), that enable the ionization of biomolecules and their transfer to the gas phase with little to no fragmentation.[36]

MALDI. Ionization by MALDI (Figure 1.3) involves the co-crystallization of the peptide and protein analytes with a large molar excess of matrix, which is typically a weak organic acid (Figure 1.4) with absorbance in the wavelength of the laser employed (usually 337 nm or 355 nm).[37,38] Irradiation of this mixture by a pulsed laser causes desorption of the matrix into a gaseous plume, carrying the analyte with it, and causing ionization of the analyte by protonation.[37,39–41] Hence, the MALDI matrix plays crucial roles in the desorption and ionization process by: (1) absorbing the laser energy; (2) dilution of the analyte molecules to prevent analyte-analyte interactions during ionization; and (3) ionization of the peptide/protein analyte by protonation.[37,42–44] Ionization by MALDI typically generates singly protonated species of the peptide or protein analyte with minimal to no fragmentation, hence the term "soft ionization". The protonated analytes are then directed and accelerated with the same amount of kinetic energy (KE) towards the mass analyzer, usually a time-of-flight (TOF) mass analyzer, which separates them according to their mass-to-charge ratio (*m/z*). The ions, having been accelerated with the same KE, will travel the flight tube at different velocities based on their mass since $KE=\frac{1}{2}mv^2$ or

$v=(2KE/m)^{1/2}$, meaning that ions with smaller *m/z* will travel faster and reach the detector first than ions with larger *m/z*.

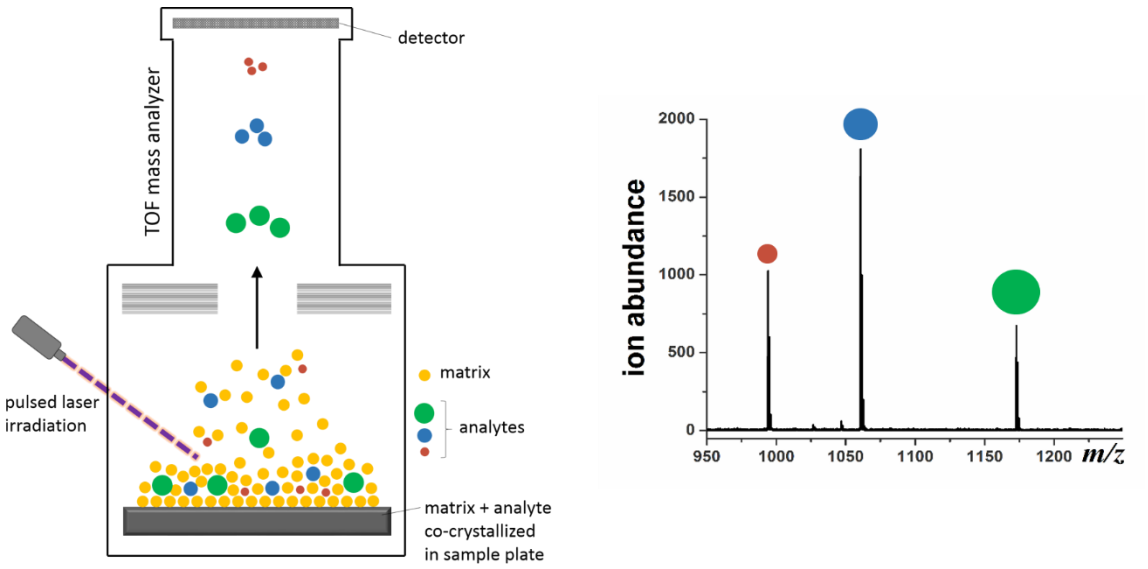

Figure 1.3. Illustration of the MALDI-MS process **(left)** and an example MALDI mass spectrum **(right)**.

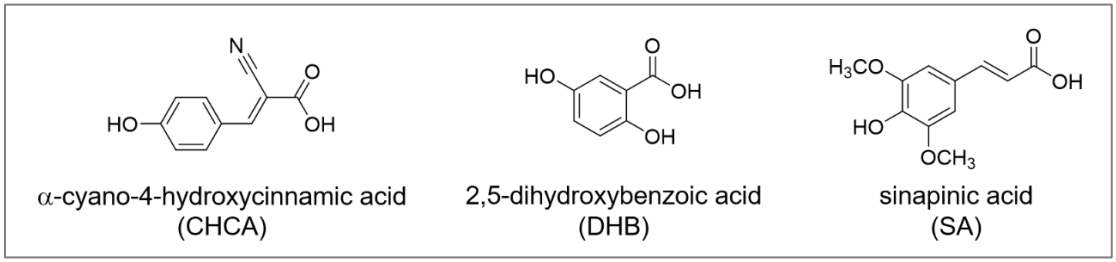

Figure 1.4. Chemical structures of common MALDI matrices used for peptide and protein analysis.

MALDI has several advantages in peptide and protein analysis. Excellent sensitivity (usually femtomole amounts) can be achieved with minimal sample loading. Unlike in ESI, predominantly singly charged species are produced, so the signal is not distributed into a series of charge states, which is one of the reasons why MALDI is able to achieve such high sensitivity. It is also relatively more tolerant to the presence of salts

and buffers.[38] Spectral acquisition is also very fast and samples can be analyzed in a high throughput manner. However, high sensitivity and throughput is offset by poor reproducibility of signal obtained from sample to sample and shot to shot, making quantitation by MALDI a challenge.[45]

ESI. Ionization by electrospray (Figure 1.5) is another soft ionization method that occurs by passing a solution of the analyte through a small capillary. A voltage applied to the capillary produces an aerosol of charged droplets. As the solvent evaporates, the repulsion between like charges within the droplet increases and it undergoes Coulombic explosion to form smaller and smaller charged droplets until finally the analyte molecule finds itself with residual charges attached.[44] For proteins, the main source of charge in the positive mode is through protonation. ESI generates multiply charged ions (Figure 1.5), which allows the *m/z* of high molecular weight molecules like proteins fall within the working range of most mass analyzers. Intact protein mass analysis is mostly done by ESI as the *m/z* represented by each charge state increases the precision of the molecular mass calculation.

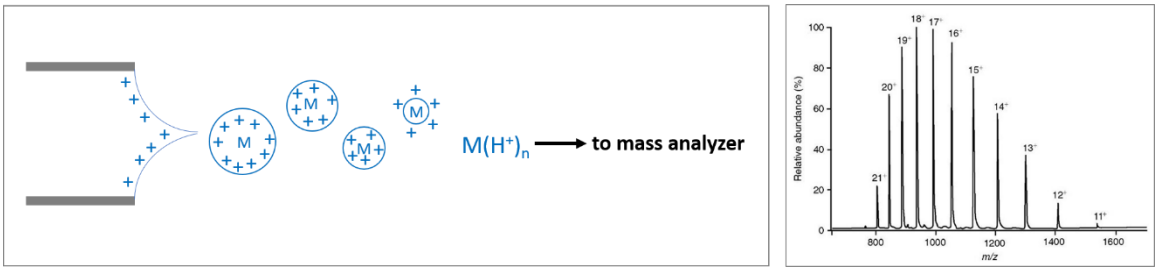

Figure 1.5. Ionization by electrospray **(left)** and an example ESI mass spectrum for a protein **(right)**.

Although less sensitive and less tolerant to salts than MALDI, analysis by ESI is more reproducible and more quantitative since the sample is introduced as a homogeneous

solution rather than a heterogeneous solid mixture as in MALDI. Furthermore, although the continuous flow of sample infusion into ESI results in some sample being wasted, this continuous manner makes ESI amenable to coupling with liquid chromatography (LC) techniques, which provide a dimension of separation prior to MS analysis.

Techniques Coupled to MS to Enhance Protein Analysis

MS analysis of pure protein samples can be relatively straightforward. For complex mixtures, however, prefractionation is often a requirement prior to MS analysis in order to enhance their detection. These include two-dimensional gel electrophoresis, chromatographic techniques such as reversed phase and ion exchange chromatography and combinations of which into multidimensional chromatography, size exclusion chromatography, and capillary electrophoresis.[46–52] These techniques are especially useful in non-targeted shotgun proteomics where a global and comprehensive profiling of the proteins present in a sample is done.[53] In a targeted approach, however, enrichment methods for the protein(s) of interest are usually employed to separate the target protein(s) from the rest of the sample matrix. These enrichment methods include the use of chemically functionalized surfaces, chemical precipitation, porous silicon-based arrays, magnetic beads, functionalized polymers and various immunoaffinity-based methods.[54–63] Prefractionation and enrichment methods are often geared towards increasing the detection sensitivity as ion suppression and matrix interference are common problems in MS analyses.[64,65] This becomes particularly relevant when the protein(s) of interest are present in such low levels amidst a complicated matrix of other highly abundant proteins and biomolecules. One such case is the study of biomarkers from biological samples.

Disease Biomarkers

Biomarkers are molecules, usually proteins and peptides, secreted, shed or released by cells or tissues to biological fluids that indicate the physiological status of the body. In a diseased state, levels of these biomarkers would change and hence are potential indicators of disease onset and/or progression.[66–68] Early detection, especially in diseases like cancer, can allow for increased treatment options and better chances of survival. Besides early detection, monitoring the levels of biomarkers are also used for prognostic and predictive purposes to decide if and which treatment should be administered.[69,70] A method for the sensitive and reliable measurement of the levels of these proteins and peptides is thus of prime importance whether it be for the purpose of early detection or monitoring the disease progression.

Body fluids, particularly blood serum, are rich sources of biomarkers since the protein composition constantly changes as a result of these fluids surveying the diseased tissues or organs. The presence of cancer, for instance, even at its earliest stages, may be revealed through significant changes in protein levels in plasma, either as a result of proteins being overexpressed, abnormally shed from the tumor microenvironment into the blood, or removed from the proteome due to abnormal activation of the proteolytic degradation pathways.[71–73]

Methods of Biomarker Detection

Detection of protein biomarkers is an extremely challenging task, not only due to the complexity of biological systems but also because these proteins are often present in very low abundances. The most widely used clinical method for biomarker detection are immuno-based assays like ELISAs (enzyme-linked immunosorbent assay) that make use

of highly specific and high affinity antibodies directed against specific protein antigens.[74] However, the availability and development of a well-characterized antibody for each target biomarker protein remains to be the main limitation of antibody-based assays. Aside from the high cost and long development times for these antibodies, cross-reactivity with other antigens and inability to discriminate between closely related proteins or isoforms are major issues with immunoassays.[75]

Mass spectrometry, with its ability to definitively identify and detect multiple proteins simultaneously with high accuracy and resolution has become an invaluable tool in biomarker discovery and detection.[76] Unlike immunoassays, no antibodies are required for each analyte and protein identification is based on the sequence obtained by MS/MS, enabling the distinction of even the slightest modification on the protein. However, one of the major challenges for MS in biomarker detection is how to achieve comparable sensitivities as in immunoassays, which is often overcome by employing prefractionation and enrichment techniques.

Supramolecular Assemblies of Amphiphilic Polymers as Selective Extraction Agents for Protein Enrichment

Supramolecular assemblies are structures generated through non-covalent intermolecular interactions such as hydrogen bonding, hydrophobic interactions and electrostatics.[77] These non-covalent interactions, although relatively weaker types of interactions, are extensively used by macromolecules in Nature. They play critical roles in the formation of complex macromolecular structures and in the faithful execution of their function. An excellent example is the formation of the DNA double helix through hydrogen

bonding and π stacking and the hydrogen bond-directed specific pairing of the nucleotide bases that allows for the faithful transfer of genetic information during transcription. Taking inspiration from Nature, artificial supramolecular assemblies have been designed and engineered for a great deal of applications in chemistry, materials science, and biology.[78,79] Polymer-based supramolecular assemblies that form organized structures such as core-shell nanoparticles, micelles, reverse micelles, and vesicles have attracted a lot of interest in recent years for their use in biomimetics,[78,80–82] targeted drug delivery,[83–86] modulating biomolecule activity and reactivity,[87–90] sensing,[91–93] and separations.[94–96]

Amphiphilic polymers are polymers in which the repeating units contain both a hydrophobic and a hydrophilic moiety, examples of those used in this dissertation are shown in Figure 1.6. Based on the hydrophilic-lipophilic balance between these two functionalities, their mutual incompatibility and the immiscibility of one of them in the bulk solvent drives their self-organization into assemblies such as micelles, reverse micelles and vesicles.[97] In an aqueous medium, for instance, amphiphilic polymers would self-assemble into micelle-type assemblies such that the hydrophilic groups orient themselves towards the solvent, shielding the the solvent-immiscible hydrophobic moieties that form a water-excluded core (Figure 1.7). Conversely, in an apolar solvent, reverse micelle-type assemblies are formed whereby the hydrophobic moieties interact with the solvent while the hydrophilic groups form a polar interior away from the solvent.

Reverse micelle assemblies are of particular interest because they are potential nanocontainers for solubilizing polar molecules such as proteins and peptides into the organic phase by hosting them inside their water pool interior. Moreover, these assemblies were found to be kinetically trapped in the solvent where they were initially formed,[94] a

property that is necessary if they were to serve as sequestration agents during liquid-liquid extractions in two immiscible solvents.

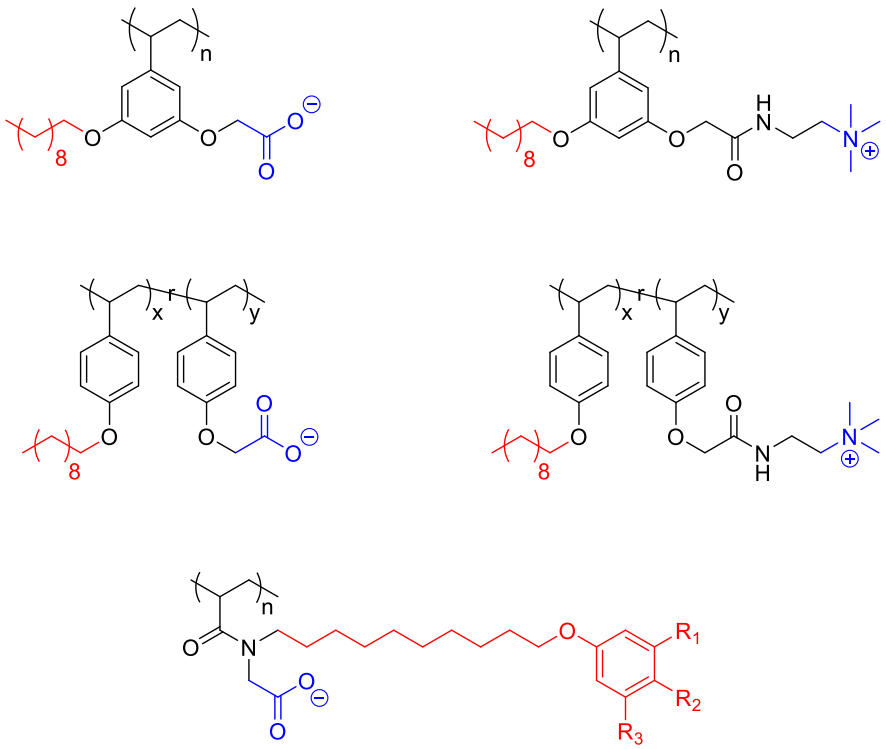

Figure 1.6. Chemical structures of some amphiphilic polymers used in this study. Hydrophobic moieties are shown in red while hydrophilic functionalities are shown in blue.

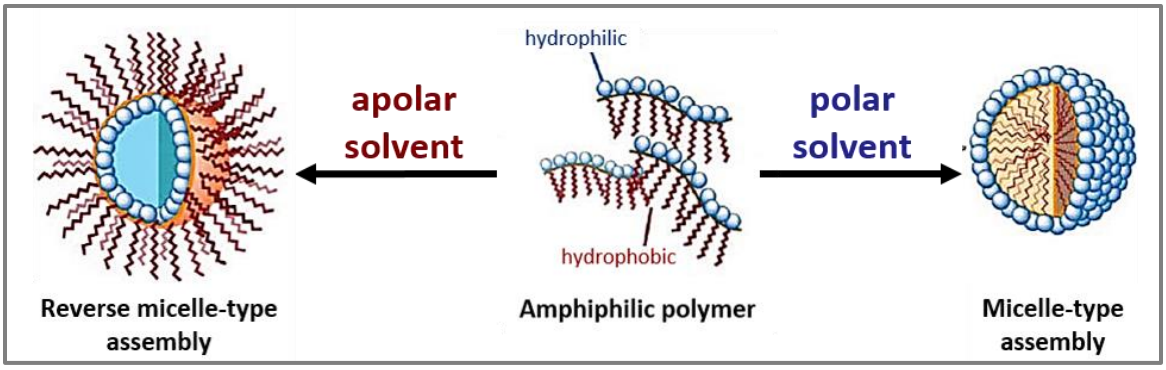

Figure 1.7. Amphiphilic polymers self-assemble into either micelle-type or reverse micelle-type assemblies depending on the solvent. (Figure adopted from reference [97])

Another feature of these materials is that the nature of the hydrophilic group can be tuned to meet various purposes while maintaining the fidelity of the supramolecular assembly. It has been shown that the hydrophilic group imparts the selectivity for which analytes will be sequestered inside the reverse micelles,[95,98,99] and therefore being able to tune these functional groups allows for regulation of their selectivity. Most of the work in this dissertation focuses on the use of charge complementarity between the polymeric reverse micelle hosts and the polypeptide guests as the driving force for this selectivity in a method called isoelectric point (pI) bracketing.

pI bracketing is a method for fractionating a mixture of peptides or proteins based on their isoelectric point through a biphasic extraction using charged reverse micelles (Figure 1.8). A protein's pI is defined as the pH at which its net charge is zero. Proteins are amphoteric molecules due to the diverse functional groups of their amino acid precursors, which contribute either a neutral, positive or negative charge on the protein's overall charge. Positive charges are imparted by protonated basic residues such as arginine, lysine and histidine, as well as the N-terminal amino group. On the other hand, negative charges are contributed by deprotonated acidic residues such as aspartic acid and glutamic acid, as well as the C-terminal carboxylate group. The degrees of protonation and deprotonation of these groups are dependent on the pH of the solution and their respective acid dissociation constant (pK_a), and therefore so too is the pI of the protein.[100] Since pI is an inherent property of all proteins and peptides, this can be used as the basis for their fractionation. At a pH lower than a protein's pI, the protein will have a net positive charge, while at a pH higher than its pI, the protein will have a net negative charge. Therefore, by tuning the pH, selective extraction of peptides and proteins bearing a charge complementary to the

charged interior of polymeric reverse micelles can be achieved (Figure 1.9). Performing sequential extractions also enables bracketing at multiple pI ranges. Furthermore, pI bracketing is also a method of enrichment since a narrower set of extracted peptides are now enriched and concentrated in the organic phase. This approach has been demonstrated to be useful in selectively enriching and detecting very low levels of peptides and proteins in complex mixtures, even in complicated samples such as serum.[96,101]

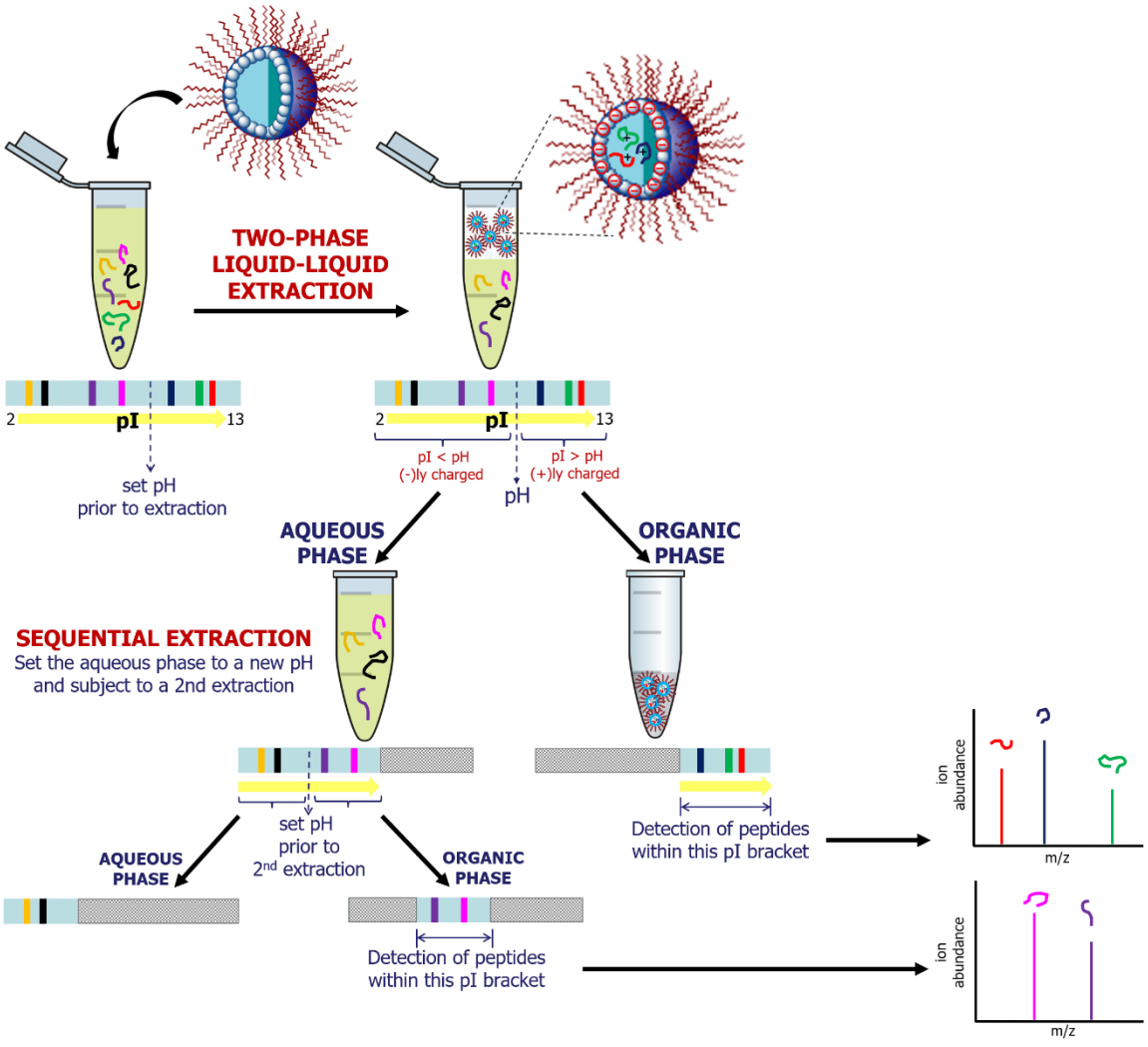

Figure 1.8. General scheme illustrating the pI bracketing method. Based on the extraction pH and their pI, peptides will either be positively or negatively charged. Peptides bearing a charge complementary to the charge of the reverse micelle are extracted and enriched into the organic phase. Sequential extraction enables further pI bracketing of the remaining peptides in the aqueous phase. Each fraction can then be analyzed by MS to for detection and identification.

peptide	m/z	pI	net charge at pH 8
RPPGFSPFR	1060.6	12.4	+
IARRHPYFL	1172.7	11.1	+
DAEFRHDSGYE	1325.5	4.1	–
RTKRSGSVYEPLKI	1633.9	10.7	+
SSEVAGEGDGDSMGHEDLY	1954.8	3.4	–

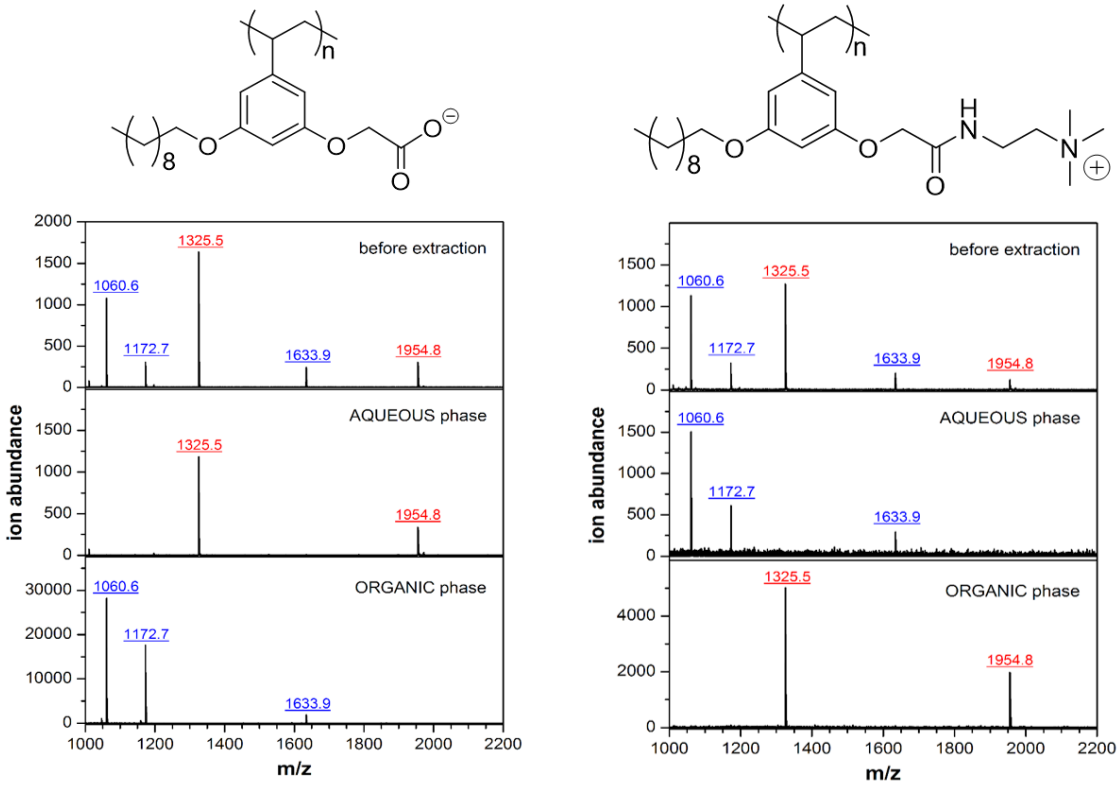

Figure 1.9. Extraction selectivity using reverse micelles of a negatively charged polymer **(left)** and a positively charged polymer **(right)**. Only peptides bearing a charge complementary to the charge of the reverse micelle used for extraction are detected in the organic phase.

Much of the previous success of this method has been with the use of MALDI-MS for detection. The exceptional detection sensitivity achieved by MALDI-MS analysis of the polymer-extracted peptides has been attributed not only to the enrichment capabilities of the method but also to a significant signal enhancement phenomenon that was observed during MALDI-MS analysis. This enhancement of signal, in turn, was attributed to the coalescence of MALDI matrix and peptide analytes into "hotspots" in the presence of the polymer.[102] The molecular basis for this, however, has not been previously addressed. In

Chapter II of this dissertation, investigations into the molecular basis of the signal enhancement phenomenon are discussed. A series of polymers and MALDI matrices were utilized for structure-property studies to elucidate that the polymer mediates the interaction between the peptide analyte and the MALDI matrix, and that only with this favorable interaction does signal enhancement arise.[103]

Despite the success and compatibility of our method with detection by MALDI-MS, its shortcoming when it comes to signal reproducibility becomes an issue when quantitation is desired. Since analysis by ESI-MS is known to be more reproducible and quantitative, I have developed a method for interfacing the extraction protocol with ESI-MS through devising different strategies for efficiently releasing the extracted peptide guests from their supramolecular hosts into ESI-amenable aqueous medium. These strategies are described in Chapter III, along with investigations on the molecular features of the polymer host and the extracted peptides that influence this guest release.[104]

In Chapter IV, the practical utility of these amphiphilic polymer nanoassemblies is demonstrated through its application in selectively depleting abundant acidic proteins in serum. Serum is a particularly challenging sample because of the wide dynamic range of concentration of its constituent proteins, making the analysis of low-level proteins difficult. Depletion of serum albumin, the most abundant serum protein, along with other abundant low-pI proteins was accomplished by extraction using reverse micelles of positively charged polymers, resulting in the enhanced detection of higher pI proteins in the serum proteome. Furthermore, I demonstrate how depletion of serum using these materials enabled a significant increase in the detection sensitivity for a putative cancer biomarker.

Finally, in Chapter V, the method of pI bracketing as a fractionation and enrichment technique was combined with multiple reaction monitoring (MRM) MS to achieve multiplexed detection of peptide and protein biomarkers in serum with significantly enhanced sensitivities. Detection levels in the low ng/mL concentration of these biomarkers in serum demonstrate its potential application in the clinical setting.

References

(1) Duggan, D. E.; Udenfriend, S. The Spectrophotofluorometric Determination of Tryptophan in Plasma and of Tryptophan and Tyrosine in Protein Hydrolysates. *J. Biol. Chem.* **1956**, *223*, 313–319.

(2) O'Farrell, P. H. High Resolution Two-Dimensional Electrophoresis of Proteins. *J. Biol. Chem.* **1975**, *250* (10), 4007–4021.

(3) Eckhardt, A. E.; Hayes, C. E.; Goldstein, I. J. A Sensitive Fluorescent Method for the Detection of Glycoproteins in Polyacrylamide Gels. *Anal. Biochem.* **1976**, *73*, 192–197.

(4) Anderson, L. N.; Esquer-Blasco, R.; Hofmann, J.-P.; Anderson, N. G. A Two-Dimensional Gel Database of Rat Liver Proteins Useful in Gene Regulation and Drug Effects Studies. *Electrophoresis* **1991**, *12*, 907–930.

(5) Horka, M.; Ruzicka, F.; Horky, J.; Hola, V.; Slais, K. Capillary Isoelectric Focusing and Fluorometric Detection of Proteins and Microorganisms Dynamically Modified by Poly(Ethylene Glycol) Pyrenebutanoate. *Anal. Chem.* **2006**, *78*, 8438–8444.

(6) Westermeier, R.; Marouga, R. Protein Detection Methods in Proteomics Research. *Biosci. Rep.* **2005**, *25*, 19–32.

(7) Syahir, A.; Usui, K.; Tomizaki, K.; Kajikawa, K.; Mihara, H. Label and Label-Free Detection Techniques for Protein Microarrays. *Microarrays* **2015**, *4*, 228–244.

(8) Oda, Y.; Huang, K.; Cross, F. R.; Cowburn, D.; Chait, B. T. Accurate Quantitation of Protein Expression and Site-Specific Phosphorylation. *Proc. Natl. Acad. Sci.* **1999**, *96*, 6591–6596.

(9) Smolka, M.; Zhou, H.; Aebersold, R. Quantitative Protein Profiling Using Two-Dimensional Gel Electrophoresis, Isotope-Coded Affinity Tag Labeling, and Mass Spectrometry. *Mol. Cell. Proteomics* **2002**, *1*, 19–29.

(10) Hayashi, T.; Hamachi, I. Traceless Affinity Labeling of Endogenous Proteins for Functional Analysis in Living Cells. *Accounts Chem. Res.* **2012**, *45* (9), 1460–1469.

(11) Aebersold, R.; Mann, M. Mass Spectrometry-Based Proteomics. *Nature* **2003**, *422*, 199–207.

(12) Cravatt, B. F.; Simon, G. M.; Yates, J. R. The Biological Impact of Mass-Spectrometry-Based Proteomics. *Nature* **2007**, *450*, 991–1000.

(13) The Royal Swedish Academy of Sciences. Advanced information on the Nobel Prize in Chemistry 2002. Nobel Prize website. https://assets.nobelprize.org/uploads/2018/06/advanced-chemistryprize2002.pdf.

(14) Schweppe, R. E.; Haydon, C. E.; Lewis, T. S.; Resing, K. A.; Ahn, N. G. The Characterization of Protein Post-Translational Modifications by Mass Spectrometry. *Acc. Chem. Res.* **2003**, *36*, 453–461.

(15) Chen, G.; Warrack, B. M.; Goodenough, A. K.; Wei, H.; Wang-Iverson, D. B.; Tymiak, A. A. Characterization of Protein Therapeutics by Mass Spectrometry: Recent Developments and Future Directions. *Drug Discov. Today* **2011**, *16*, 58–64.

(16) Shaw, J. B.; Li, W.; Holden, D. D.; Zhang, Y.; Griep-Raming, J.; Fellers, R. T.; Early, B. P.; Thomas, P. M.; Kelleher, N. L.; Brodbelt, J. S. Complete Protein Characterization Using Top-down Mass Spectrometry and Ultraviolet Photodissociation. *J. Am. Chem. Soc.* **2013**, *135*, 12646–12651.

(17) Lin, D.; Tabb, D. L.; Yates, J. R. Large-Scale Protein Identification Using Mass Spectrometry. *Biochim. Biophys. Acta - Proteins Proteomics* **2003**, *1646*, 1–10.

(18) Clough, T.; Key, M.; Ott, I.; Ragg, S.; Schadow, G.; Vitek, O. Protein Quantification in Label-Free LC-MS Experiments. *J. Proteome Res.* **2009**, *8*, 5275–5284.

(19) Kennedy, J. J.; Abbatiello, S. E.; Kim, K.; Yan, P.; Whiteaker, J. R.; Lin, C.; Kim, J. S.; Zhang, Y.; Wang, X.; Ivey, R. G.; et al. Demonstrating the Feasibility of Large-Scale Development of Standardized Assays to Quantify Human Proteins. *Nat. Methods* **2014**, *11* (2), 149–155.

(20) Gevaert, K.; Vandekerckhove, J. Protein Identification Methods in Proteomics. *Electrophoresis* **2000**, *21*, 1145–1154.

(21) Park, Z.-Y.; Russell, D. H. Identification of Individual Proteins in Complex Protein Mixtures by High-Resolution, High-Mass-Accuracy MALDI TOF-Mass Spectrometry Analysis of in-Solution Thermal Denaturation/Enzymatic Digestion. *Anal. Chem.* **2001**, *73*, 2558–2564.

(22) Larsen, M. R.; Trelle, M. B.; Thingholm, T. E.; Jensen, O. N. Analysis of Posttranslational Modifications of Proteins by Tandem Mass Spectrometry. *Biotechniques* **2006**, *40*, 790–798.

(23) Olsen, J. V.; Mann, M. Status of Large-Scale Analysis of Post-Translational Modifications by Mass Spectrometry. *Mol. Cell. Proteomics* **2013**, *12*, 3444–3452.

(24) Tipton, J. D.; Tran, J. C.; Catherman, A. D.; Ahlf, D. R.; Durbin, K. R.; Kelleher, N. L. Analysis of Intact Protein Isoforms by Mass Spectrometry. *J. Biol. Chem.* **2011**, *286* (29), 25451–25458.

(25) Stastna, M.; Van Eyk, J. E. Analysis of Protein Isoforms: Can We Do It Better? *Proteomics* **2012**, *12*, 2937–2948.

(26) Ahmad, Y.; Boisvert, F.-M.; Lundberg, E.; Uhlen, M.; Lamond, A. I. Systematic Analysis of Protein Pools, Isoforms, and Modifications Affecting Turnover and Subcellular Localization. *Mol. Cell. Proteomics* **2012**, *11* (3), M111.013680.

(27) Wildsmith, K. R.; Han, B.; Bateman, R. J. Method for the Simultaneous Quantitation of Apolipoprotein E Isoforms Using Tandem Mass Spectrometry. *Anal. Biochem.* **2009**, *395*, 116–118.

(28) Domon, B.; Aebersold, R. Mass Spectrometry and Protein Analysis. *Science* **2006**, *312*, 212–217.

(29) Hanke, S.; Besir, H.; Oesterhelt, D.; Mann, M. Absolute SILAC for Accurate Quantitation of Proteins in Complex Mixtures down to the Attomole Level. *J. Proteome Res.* **2008**, *7*, 1118–1130.

(30) Onisko, B.; Dynin, I.; Requena, J. R.; Silva, C. J.; Erickson, M.; Carter, J. M. Mass Spectrometric Detection of Attomole Amounts of the Prion Protein by NanoLC/MS/MS. *J. Am. Soc. Mass Spectrom.* **2007**, *18*, 1070–1079.

(31) Narumi, R.; Shimizu, Y.; Ukai-Tadenuma, M.; Ode, K. L.; Kanda, G. N.; Shinohara, Y.; Sato, A.; Matsumoto, K.; Ueda, H. R. Mass Spectrometry-Based Absolute Quantification Reveals Rhythmic Variation of Mouse Circadian Clock Proteins. *Proc. Natl. Acad. Sci.* **2016**, *113*, E3461–E3467.

(32) Keshishian, H.; Addona, T.; Burgess, M.; Kuhn, E.; Carr, S. A. Quantitative, Multiplexed Assays for Low Abundance Proteins in Plasma by Targeted Mass Spectrometry and Stable Isotope Dilution. *Mol. Cell. Proteomics* **2007**, *6*, 2212–2229.

(33) Liebler, D. C.; Zimmerman, L. J. Targeted Quantitation of Proteins by Mass Spectrometry. *Biochemistry* **2013**, *52*, 3797–3806.

(34) Grebe, S. K. G.; Singh, R. J. Clinical Peptide and Protein Quantification by Mass Spectrometry (MS). *Trends Anal. Chem.* **2016**, *84*, 131–143.

(35) Gillette, M. A.; Carr, S. A. Quantitative Analysis of Peptides and Proteins in Biomedicine by Targeted Mass Spectrometry. *Nat. Methods* **2013**, *10* (1), 28–34.

(36) Mann, M.; Hendrickson, R. C.; Pandey, A. Analysis of Proteins and Proteomes By Mass Spectrometry. *Annu. Rev. Biochem.* **2001**, *70*, 437–473.

(37) Lewis, J. K.; Wei, J.; Siuzdak, G. Matrix-Assisted Laser Desorption/Ionization Mass Spectrometry in Peptide and Protein Analysis. In *Encyclopedia of Analytical Chemistry*; Meyers, R. A., Ed.; John Wiley & Sons Ltd, 2000; pp 5880–5894.

(38) Glish, G. L.; Vachet, R. W. The Basics of Mass Spectrometry in the Twenty-First Century. *Nat. Rev. Drug Discov.* **2003**, *2* (2), 140–150.

(39) Dreisewerd, K. The Desorption Process in MALDI. *Chem. Rev.* **2003**, *103* (2), 395–425.

(40) Knochenmuss, R.; Zenobi, R. MALDI Ionization: The Role of in-Plume Processes. *Chem. Rev.* **2003**, *103* (2), 441–452.

(41) Karas, M.; Krüger, R. Ion Formation in MALDI: The Cluster Ionization Mechanism. *Chem. Rev.* **2003**, *103* (2), 427–440.

(42) Niehaus, M.; Schnapp, A.; Koch, A.; Soltwisch, J.; Dreisewerd, K. New Insights into the Wavelength Dependence of MALDI Mass Spectrometry. *Anal. Chem.* **2017**, *89*, 7734–7741.

(43) Ahn, S. H.; Park, K. M.; Bae, Y. J.; Kim, M. S. Quantitative Reproducibility of Mass Spectra in Matrix-Assisted Laser Desorption Ionization and Unraveling of the Mechanism for Gas-Phase Peptide Ion Formation. *J. Mass Spectrom.* **2013**, *48* (3), 299–305.

(44) Watson, J. T.; Sparkman, O. D. *Introduction to Mass Spectrometry: Instrumentation, Applications, and Strategies for Data Interpretation, 4th Ed.* John Wiley & Sons Ltd: West Sussex, England, 2007.

(45) Szájli, E.; Fehér, T.; Medzihradszky, K. F. Investigating the Quantitative Nature of MALDI-TOF MS. *Mol. Cell. Proteomics* **2008**, *7* (12), 2410–2418.

(46) Friedman, D. B.; Hill, S.; Keller, J. W.; Merchant, N. B.; Levy, S. E.; Coffey, R. J.; Caprioli, R. M. Proteome Analysis of Human Colon Cancer by Two-Dimensional Difference Gel Electrophoresis and Mass Spectrometry. *Proteomics* **2004**, *4*, 793–811.

(47) Shevchenko, A.; Jensen, O. N.; Podtelejnikov, A. V.; Sagliocco, F.; Wilm, M.; Vorm, O.; Mortensen, P.; Shevchenko, A.; Boucherie, H.; Mann, M. Linking Genome and Proteome by Mass Spectrometry: Large-Scale Identification of Yeast Proteins from Two Dimensional Gels. *Proc. Natl. Acad. Sci.* **1996**, *93*, 14440–14445.

(48) Washburn, M. P.; Wolters, D.; Yates, J. R. Large-Scale Analysis of the Yeast Proteome by Multidimensional Protein Identification Technology. *Nat. Biotechnol.* **2001**, *19*, 242–247.

(49) Peng, J.; Elias, J. E.; Thoreen, C. C.; Licklider, L. J.; Gygi, S. P. Evaluation of Multidimensional Chromatography Coupled with Tandem Mass Spectrometry (LC/LC-MS/MS) for Large-Scale Protein Analysis: The Yeast Proteome. *J. Proteome Res.* **2003**, *2*, 43–50.

(50) Opiteck, G. J.; Jorgenson, J. W.; Anderegg, R. J. Two-Dimensional SEC/RPLC Coupled to Mass Spectrometry for the Analysis of Peptides. *Anal. Chem.* **1997**, *69*, 2283–2291.

(51) Liu, H.; Zhang, L.; Zhu, G.; Zhang, W.; Zhang, Y. An Etched Porous Interface for On-Line Capillary Electrophoresis-Based Two-Dimensional Separation System. *Anal. Chem.* **2004**, *76*, 6506–6512.

(52) Kaiser, T.; Wittke, S.; Just, I.; Krebs, R.; Bartel, S.; Filser, D.; Mischak, H.; Weissinger, E. M. Capillary Electrophoresis Coupled to Mass Spectrometer for Automated and Robust Polypeptide Determination in Body Fluids for Clinical Use. *Electrophoresis* **2004**, *25*, 2044–2055.

(53) Zhang, Y.; Fonslow, B. R.; Shan, B.; Baek, M. C.; Yates, J. R. Protein Analysis by Shotgun/Bottom-up Proteomics. *Chem. Rev.* **2013**, *113* (4), 2343–2394.

(54) Afonso, C.; Budimir, N.; Fournier, F.; Tabet, J.-C. Activated Surfaces for Laser Desorption Mass Spectrometry: Application for Peptide and Protein Analysis. *Curr. Pharm. Des.* **2005**, *11*, 2559–2576.

(55) Chen, F.; Wan, D.; Chang, Z.; Pu, H.; Jin, M. Highly Efficient Separation, Enrichment, and Recovery of Peptides by Silica-Supported Polyethylenimine. *Langmuir* **2014**, *30*, 12250–12257.

(56) Kay, R.; Barton, C.; Ratcliffe, L.; Matharoo-Ball, B.; Brown, P.; Roberts, J.; Teale, P.; Creaser, C. Enrichment of Low Molecular Weight Serum Proteins Using Acetonitrile Precipitation for Mass Spectrometry Based Proteomic Analysis. *Rapid Commun. Mass Spectrom.* **2008**, *22*, 3255–3260.

(57) Tian, R.; Zhang, H.; Ye, M.; Jiang, X.; Hu, L.; Li, X.; Bao, X.; Zou, H. Selective Extraction of Peptides from Human Plasma by Highly Ordered Mesoporous Silica Particles for Peptidome Analysis. *Angew. Chem. Int. Ed. Engl.* **2007**, *46* (6), 962–965.

(58) Whiteaker, J. R.; Zhao, L.; Zhang, H. Y.; Feng, L.-C.; Piening, B. D.; Anderson, L.; Paulovich, A. G. Antibody-Based Enrichment of Peptides on Magnetic Beads for Mass-Spectrometry-Based Quantification of Serum Biomarkers. *Anal. Biochem.* **2007**, *362* (1), 44–54.

(59) Ekstr, S.; Wallman, L.; Helldin, G.; Nilsson, J.; Marko-Varga, G.; Laurell, T. Polymeric Integrated Selective Enrichment Target (ISET) for Solid-Phase-Based Sample Preparation in MALDI–TOF MS. *J. Mass Spectrom.* **2007**, *42*, 1445–1452.

(60) Xiao, H.; Chen, W.; Smeekens, J. M.; Wu, R. An Enrichment Method Based on Synergistic and Reversible Covalent Interactions for Large-Scale Analysis of Glycoproteins. *Nat. Commun.* **2018**, *9*, 1692.

(61) Najam-Ul-Haq, M.; Saeed, A.; Jabeen, F.; Maya, F.; Ashiq, M. N.; Sharif, A. Newly Developed Poly(Allyl Glycidyl Ether/Divinyl Benzene) Polymer for Phosphopeptides Enrichment and Desalting of Biofluids. *ACS Appl. Mater. Interfaces* **2014**, *6*, 3536–3545.

(62) Whiteaker, J. R.; Zhao, L.; Anderson, L.; Paulovich, A. G. An Automated and Multiplexed Method for High Throughput Peptide Immunoaffinity Enrichment and Multiple Reaction Monitoring Mass Spectrometry-Based Quantification of Protein Biomarkers. *Mol. Cell. Proteomics* **2010**, *9*, 184–196.

(63) Guo, A.; Gu, H.; Zhou, J.; Mulhern, D.; Wang, Y.; Lee, K. A.; Yang, V.; Aguiar, M.; Kornhauser, J.; Jia, X.; et al. Immunoaffinity Enrichment and Mass Spectrometry Analysis of Protein Methylation. *Mol. Cell. Proteomics* **2014**, *13* (1), 372–387.

(64) Puangpila, C.; Mayadunne, E.; El Rassi, Z. Liquid Phase Based Separation Systems for Depletion, Prefractionation, and Enrichment of Proteins in Biological Fluids and Matrices for in-Depth Proteomics Analysis-An Update Covering the Period 2011-2014. *Electrophoresis* **2015**, *36*, 238–252.

(65) Panuwet, P.; Hunter, R. E.; D'Souza, P. E.; Chen, X.; Radford, S. A.; Cohen, J. R.; Marder, M. E.; Kartavenka, K.; Ryan, P. B.; Barr, D. B. Biological Matrix Effects in Quantitative Tandem Mass Spectrometry-Based Analytical Methods: Advancing Biomonitoring. *Crit. Rev. Anal. Chem.* **2016**, *46* (2), 93–105.

(66) Wulfkuhle, J. D.; Liotta, L. A.; Petricoin, E. F. Proteomic Applications for the Early Detection of Cancer. *Nat. Rev. Cancer* **2003**, *3*, 267–275.

(67) Misek, D. E.; Kim, E. H. Protein Biomarkers for the Early Detection of Breast Cancer. *Int. J. Proteomics* **2011**, *2011*, 1-9.

(68) Tessitore, A.; Gaggiano, A.; Cicciarelli, G.; Verzella, D.; Capece, D.; Fischietti, M.; Zazzeroni, F.; Alesse, E. Serum Biomarkers Identification by Mass Spectrometry in High Mortality Tumors. *Int. J. Proteomics* **2013**, *2013*, 1–15.

(69) Weigel, M. T.; Dowsett, M. Current and Emerging Biomarkers in Breast Cancer: Prognosis and Prediction. *Endocr. Relat. Cancer* **2010**, *17* (4), R245–R262.

(70) Reyzer, M. L.; Caldwell, R. L.; Dugger, T. C.; Forbes, J. T.; Ritter, C. a; Guix, M.; Arteaga, C. L.; Caprioli, R. M. Early Changes in Protein Expression Detected by Mass Spectrometry Predict Tumor Response to Molecular Therapeutics. *Cancer Res.* **2004**, *64*, 9093–9100.

(71) van Winden, A. W. J.; van den Broek, I.; Gast, M.-C. W.; Engwegen, J. Y. M. N.; Sparidans, R. W.; van Dulken, E. J.; Depla, A. C. T. M.; Cats, A.; Schellens, J. H. M.; Peeters, P. H. M.; et al. Serum Degradome Markers for the Detection of Breast Cancer. *J. Proteome Res.* **2010**, *9*, 3781–3788.

(72) Villanueva, J. et al. Differential Exoprotease Activities Confer Tumor-Specific Serum Peptidome Patterns. *J. Clin. Invest.* **2006**, *116* (1), 271–284.

(73) Sidransky, D. Emerging Molecular Markers of Cancer. *Nat. Rev. Cancer* **2002**, *2*, 210–219.

(74) Nimse, S. B.; Sonawane, M. D.; Song, K.-S.; Kim, T. Biomarker Detection Technologies and Future Directions. *Analyst* **2016**, *141* (3), 740–755.

(75) Hale, J. E. Advantageous Uses of Mass Spectrometry for the Quantification of Proteins. *Int. J. Proteomics* **2013**, *2013*, 1–6.

(76) DeVera, I. E.; Katz, J. E.; Agus, D. B. Clinical Proteomics: The Promises and Challenges of Mass Spectrometry-Based Biomarker Discovery. *Clin. Adv. Hematol. Oncol.* **2006**, *4*, 541–549.

(77) Lehn, J.-M. Toward Complex Matter: Supramolecular Chemistry and Self-Organization. *Proc. Natl. Acad. Sci.* **2002**, *99* (8), 4763–4768.

(78) Tu, Y.; Peng, F.; Adawy, A.; Men, Y.; Abdelmohsen, L. K. E. A.; Wilson, D. A. Mimicking the Cell: Bio-Inspired Functions of Supramolecular Assemblies. *Chem. Rev.* **2016**, *116*, 2023-2078.

(79) Busseron, E.; Ruff, Y.; Moulin, E.; Giuseppone, N. Supramolecular Self-Assemblies as Functional Nanomaterials. *Nanoscale* **2013**, *5* (16), 7098–7140.

(80) Isimjan, T. T.; de Bruyn, J. R.; Gillies, E. R. Self-Assembly of Supramolecular Polymers from β-Strand Peptidomimetic-Poly(Ethylene Oxide) Hybrids. *Macromolecules* **2010**, *43*, 4453–4459.

(81) Jin, H.; Huang, W.; Zhu, X.; Zhou, Y.; Yan, D. Biocompatible or Biodegradable Hyperbranched Polymers: From Self-Assembly to Cytomimetic Applications. *Chem. Soc. Rev.* **2012**, *41* (18), 5986–5997.

(82) Kirkorian, K.; Ellis, A.; Twyman, L. J. Catalytic Hyperbranched Polymers as Enzyme Mimics; Exploiting the Principles of Encapsulation and Supramolecular Chemistry. *Chem. Soc. Rev.* **2012**, *41* (18), 6138–6159.

(83) Bae, Y.; Fukushima, S.; Harada, A.; Kataoka, K. Design of Environment-Sensitive Supramolecular Assemblies for Intracellular Drug Delivery: Polymeric Micelles That Are Responsive to Intracellular pH Change. *Angew. Chemie - Int. Ed.* **2003**, *42* (38), 4640–4643.

(84) Kedar, U.; Phutane, P.; Shidhaye, S.; Kadam, V. Advances in Polymeric Micelles for Drug Delivery and Tumor Targeting. *Nanomedicine: Nanotechnology, Biol. Med.* **2010**, *6*, 714–729.

(85) Zhang, J.; Sun, H.; Ma, P. X. Host-Guest Interaction Mediated Polymeric Assemblies: Multifunctional Nanoparticles for Drug and Gene Delivery. *ACS Nano* **2010**, *4* (2), 1049–1059.

(86) Jia, H.-Z.; Zhang, W.; Zhu, J.-Y.; Yang, B.; Chen, S.; Chen, G.; Zhao, Y.-F.; Feng, J.; Zhang, X.-Z. Hyperbranched–hyperbranched Polymeric Nanoassembly to Mediate Controllable Co-Delivery of SiRNA and Drug for Synergistic Tumor Therapy. *J. Control. Release* **2015**, *216*, 9–17.

(87) Lee, M.; Jang, C.-J.; Ryu, J.-H. Supramolecular Reactor from Self-Assembly of Rod-Coil Molecule in Aqueous Environment. *J. Am. Chem. Soc.* **2004**, *126* (26), 8082–8083.

(88) Sandanaraj, B. S.; Vutukuri, D. R.; Simard, J. M.; Klaikherd, A.; Hong, R.; Rotello, V. M.; Thayumanavan, S. Noncovalent Modification of Chymotrypsin Surface Using an Amphiphilic Polymer Scaffold: Implications in Modulating Protein Function. *J. Am. Chem. Soc.* **2005**, *127* (30), 10693–10698.

(89) Wang, Z.; Van Oers, M. C. M.; Rutjes, F. P. J. T.; Van Hest, J. C. M. Polymersome Colloidosomes for Enzyme Catalysis in a Biphasic System. *Angew. Chemie - Int. Ed.* **2012**, *51* (43), 10746–10750.

(90) Wang, F.; Gomez-Escudero, A.; Ramireddy, R. R.; Murage, G.; Thayumanavan, S.; Vachet, R. W. Electrostatic Control of Peptide Side-Chain Reactivity Using Amphiphilic Homopolymer-Based Supramolecular Assemblies. *J. Am. Chem. Soc.* **2013**, *135* (38), 14179–14188.

(91) Azagarsamy, M. a; Gomez-Escudero, A.; Yesilyurt, V.; Vachet, R. W.; Thayumanavan, S. Amphiphilic Nanoassemblies for the Detection of Peptides and Proteins Using Fluorescence and Mass Spectrometry. *Analyst* **2009**, *134*, 635–649.

(92) González, D. C.; Savariar, E. N.; Thayumanavan, S. Fluorescence Patterns from Supramolecular Polymer Assembly and Disassembly for Sensing Metallo- and Nonmetalloproteins. *J. Am. Chem. Soc.* **2009**, *131*, 7708–7716.

(93) Gillissen, M. a. J.; Voets, I. K.; Meijer, E. W.; Palmans, A. R. a. Single Chain Polymeric Nanoparticles as Compartmentalised Sensors for Metal Ions. *Polym. Chem.* **2012**, *3* (11), 3166.

(94) Basu, S.; Vutukuri, D. R.; Thayumanavan, S. Homopolymer Micelles in Heterogeneous Solvent Mixtures. *J. Am. Chem. Soc.* **2005**, *127* (48), 16794–16795.

(95) Combariza, M. Y.; Savariar, E. N.; Vutukuri, D. R.; Thayumanavan, S.; Vachet, R. W. Polymeric Inverse Micelles as Selective Peptide Extraction Agents for MALDI-MS Analysis. *Anal. Chem.* **2007**, *79* (18), 7124–7130.

(96) Rodthongkum, N.; Chen, Y.; Thayumanavan, S.; Vachet, R. W. Selective Enrichment and Analysis of Acidic Peptides and Proteins Using Polymeric Reverse Micelles and MALDI-MS. *Anal. Chem.* **2010**, *82* (20), 8686–8691.

(97) Kale, T. S.; Klaikherd, A.; Popere, B.; Thayumanavan, S. Supramolecular Assemblies of Amphiphilic Homopolymers. *Langmuir* **2009**, *25* (17), 9660–9670.

(98) Zhao, B.; Serrano, M. A. C.; Wang, M.; Liu, T.; Gordon, M. R.; Thayumanavan, S.; Vachet, R. W. Improved Mass Spectrometric Detection of Acidic Peptides by Variations in the Functional Group pKa Values of Reverse Micelle Extraction Agents. *Analyst* **2018**, *143*, 1434–1443.

(99) Gao, J.; Zhao, B.; Wang, M.; Serrano, M. A. C.; Zhuang, J.; Ray, M.; Rotello, V. M.; Vachet, R. W.; Thayumanavan, S. Supramolecular Assemblies for Transporting Proteins Across an Immiscible Solvent Interface. *J. Am. Chem. Soc.* **2018**, *140*, 2421–2425.

(100) Levene, P. A.; Simms, H. S. Calculation of Isoelectric Points. *J. Biol. Chem.* **1923**, *55*, 801–813.

(101) Rodthongkum, N.; Ramireddy, R.; Thayumanavan, S.; Richard, W. V. Selective Enrichment and Sensitive Detection of Peptide and Protein Biomarkers in Human Serum Using Polymeric Reverse Micelles and MALDI-MS. *Analyst* **2012**, *137* (4), 1024–1030.

(102) Rodthongkum, N.; Chen, Y.; Thayumanavan, S.; Vachet, R. W. Matrix-Assisted Laser Desorption Ionization-Mass Spectrometry Signal Enhancement of Peptides After Selective Extraction with Polymeric Reverse Micelles. *Anal. Chem.* **2010**, *82*, 3686–3691.

(103) Serrano, M. A. C.; He, H.; Zhao, B.; Ramireddy, R. R.; Vachet, R. W.; Thayumanavan, S. Polymer-Mediated Ternary Supramolecular Interactions for Sensitive Detection of Peptides. *Analyst* **2017**, *142*, 118–122.

(104) Serrano, M. A. C.; Zhao, B.; He, H.; Thayumanavan, S.; Vachet, R. W. Molecular Features Influencing the Release of Peptides from Amphiphilic Polymeric Reverse Micelles. *Langmuir* **2018**, *34*, 4595–4602.

CHAPTER II

MALDI-MS SIGNAL ENHANCEMENT OF PEPTIDES THROUGH DONOR-ACCEPTOR INTERACTIONS BETWEEN POLYMER AND MATRIX

Majority of this chapter is published: Serrano, M.A.C.; He, H.; Zhao, B.; Ramireddy, R.R.; Vachet, R.W.; Thayumanavan, S. Polymer-Mediated Ternary Supramolecular Interactions for Sensitive Detection of Peptides. *Analyst* **2017**, *142*, 118-122.

Abstract

A combination of donor-acceptor and electrostatic interactions in a three-component supramolecular system has been shown to form the basis for selective and sensitive detection of peptides by MALDI-MS. Through structure-property studies, different substituents in the polymer and the MALDI matrix were compared to demonstrate that favorable donor-acceptor interactions explain the observed signal enhancement. The ternary supramolecular interactions discovered in this work are enabled by the self-packing behavior of amphiphilic homopolymers and their ability to mediate interactions between the MALDI matrix and peptide, thus enhancing their detection. Elucidating this molecular-level donor-acceptor interaction and how it affects the MALDI-MS ion signal of peptides provides a means of achieving even better MALDI-MS detection limits.

Introduction

Molecular recognition events through ternary supramolecular interactions are quite common in Nature. Prominent examples involve adaptor proteins and enzymes that precisely carry out coupling reactions by first recognizing and binding two different biomolecules and bringing them together.[1–5] Artificial molecular assemblies with such capabilities are relatively limited.[6–9] Herein, we show how amphiphilic homopolymers can act as a 'molecular glue' to effectively and specifically bring together two complementary molecules using disparate non-covalent interactions with each of the molecules. These subtle supramolecular interactions manifest themselves in a macroscopic clustering phenomenon, which in turn has a significant effect on the highly sensitive detection of analyte peptides by MALDI-MS. Strategies to improve MALDI-MS signals have been reported through the use of matrix additives, peptide labelling or derivatization, and/or surface modification of the target plate.[10–18] Our approach is different in that it relies on the inherent properties of the analyte and requires no such type of additives, derivatizations or target surface modification. We report here on how both selectivity and sensitivity can be achieved through favourable ternary supramolecular interactions that can be tuned by variations in the structure of the interacting components.

Recently, our group has developed amphiphilic homopolymers (Figure 2.1) that form kinetically-trapped reverse micelle assemblies in apolar solvents.[19] We have shown previously that these assemblies are capable of selectively sequestering specific peptides based on their isoelectric point (pI) and solution pH.[20–22] This electrostatically-driven interaction causes peptides, which are otherwise insoluble in apolar solvents, to be selectively moved to the apolar phase of a biphasic mixture (Figure 2.2). The versatility of

this method is illustrated by the highly sensitive MALDI-MS detection of peptides in complex mixtures such as protein digests.[20,21] Furthermore, the general applicability of this approach in real samples is demonstrated by the detection of picomolar concentrations of selected peptides in serum.[23] These low detection limits are achieved not only from the selective enrichment that occurs upon extracting the peptides from an aqueous phase to an organic phase, but also from more than an order of magnitude enhancement observed in the MALDI ion signal after extraction.

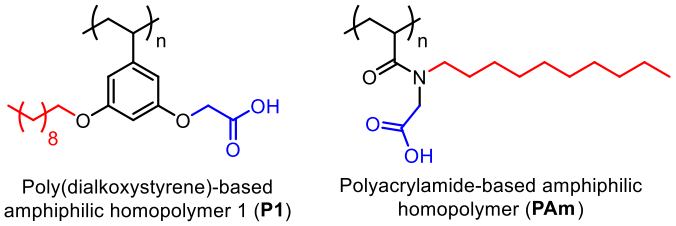

Figure 2.1 Chemical structures of carboxylate-functionalized homopolymers **P1** and **PAm**, based on poly(dialkoxystyrene) and polyacrylamide scaffolds, respectively.

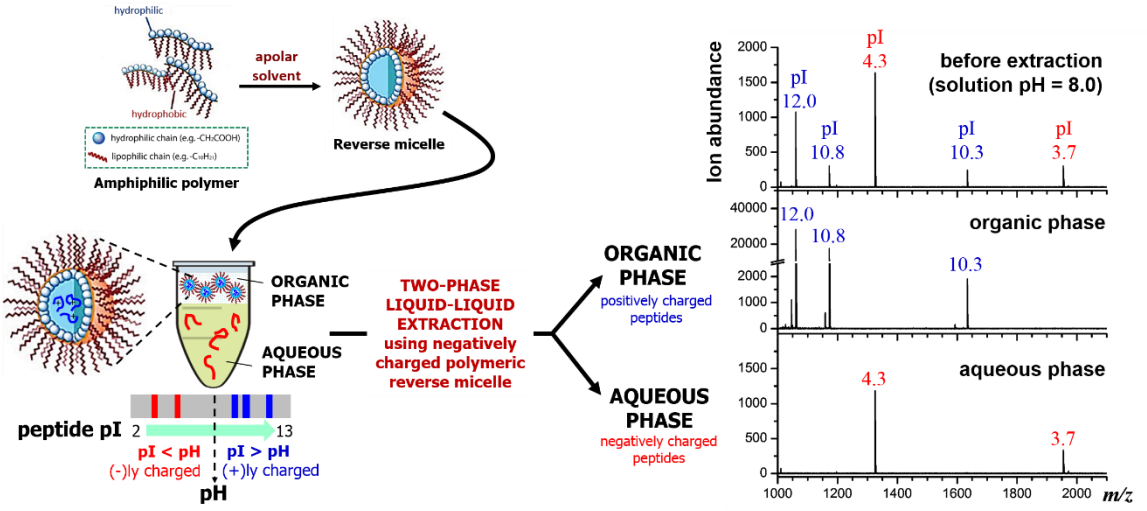

Figure 2.2. General scheme for the pI-dependent selective extraction and MALDI-MS analysis of peptides using reverse micelles of amphiphilic polymers. Using negatively charged polymeric reverse micelles such as **P1** enables the selective extraction of positively charged peptides (pI > pH, with peaks labeled in blue) into the organic phase while leaving the negatively charged peptides (pI < pH, with peaks labeled in red) in the aqueous phase.

While it is understood that the amphiphilic homopolymer, exemplified by the polydialkoxystyrene homopolymer, **P1** shown in Figure 2.1, might play some role in this enhancement,[21] the underlying mechanism for such an enhancement is not understood, and is thus the subject of this study. Elucidating the molecular interactions responsible for this signal enhancement paves the way for improving detection sensitivities and can have tremendous impact on the analysis of complex peptide mixtures and on the detection of low-level peptide and protein biomarkers.

Results and Discussion

Donor-Acceptor Hypothesis for Signal Enhancement

The first clue about the molecular basis for this signal enhancement came from the observation that a polyacrylamide, **PAm** in Figure 2.1, does not provide any signal enhancement (Figure 2.3). This polymer has been shown to form reverse micelle assemblies,[24] similar to those formed by the poly(dialkoxystyrene) **P1**. The key difference is that there is MS signal enhancement only in the case of **P1** (Figure 2.3). Interestingly, there is an associated macroscopic cluster formation in the ternary mixture formed between **P1**, the analyte peptide (bradykinin peptide labeled with TAMRA (TMR-bradykinin) was used for fluorescence visualization), and MALDI matrix, α-cyano-4-hydroxycinnamic acid (CHCA), that does not occur in the presence of **PAm** (Figure 2.3). This led us to hypothesize that the electron-rich aromatic ring of the poly(dialkoxystyrene) polymer **P1** is engaged in a donor-acceptor interaction with the electron-poor aromatic ring of CHCA, while the polymer's carboxylate unit is involved in interacting with the electrostatically complementary peptide. Although these interactions can presumably exist in the presence

of just the monomer bearing the aromatic ring and the carboxylate moiety, results from experiments where the monomer was added to the peptide-matrix mixture in place of its corresponding polymer reveal no significant enhancement in signal (Figure 2.4), suggesting that the multivalent structure of the polymer is needed for signal enhancement. Thus, the polymer structure acts as the effective mediator between the matrix molecule and the peptide.

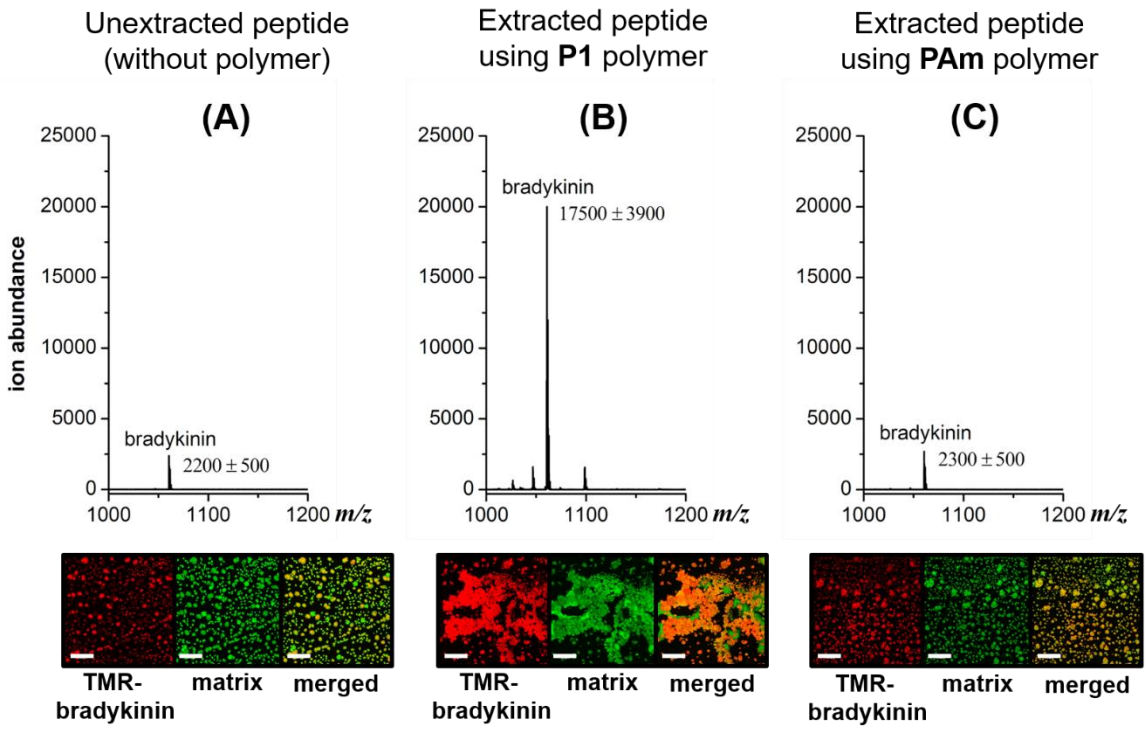

Figure 2.3. MALDI mass spectra for unextracted 1 μM* bradykinin **(A)**, and 10 nM* bradykinin (RPPGFSPFR, *m/z* 1060.6) extracted using the polymer **P1 (B)** and using **PAm (C)**. Corresponding fluorescence microscopy images under each spectrum showing the degree of clustering and co-crystallization of TMR-bradykinin peptide (red) and CHCA matrix (green). Scale bar = 100 μm. *100-fold higher concentration in the unextracted sample (1 μM) relative to extracted sample (10 nM) to account for the 100-fold enrichment during extraction.

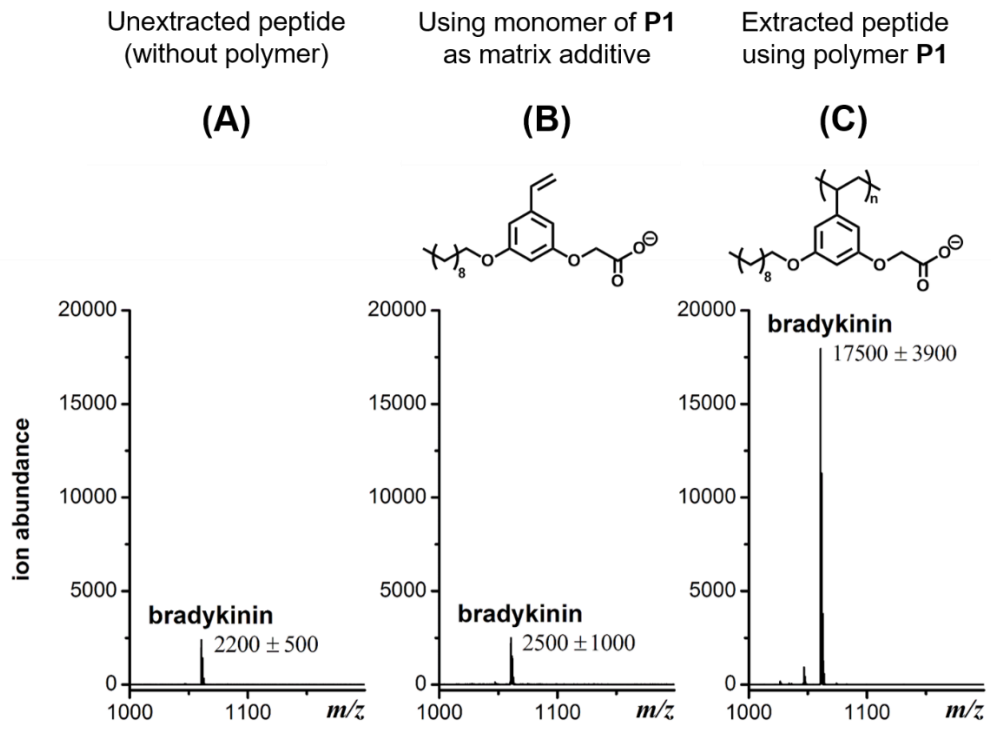

Figure 2.4. Comparison of MALDI-MS signal for bradykinin peptide (RPPGFSPFR, *m/z* 1060.6) in the absence of the polymer or monomer **(A)**, with the monomer as matrix additive **(B)**, and extracted using polymer **P1 (C)**.

Variations in the Structure of the MALDI Matrix

CHCA is the most widely used MALDI matrix for peptides. The aromatic ring in CHCA is considered electron-deficient because of its extended conjugation with the electron-withdrawing cyano group. To test our hypothesis, we first varied the matrix from CHCA to α-cyanocinnamic acid (CCA) and α-cyano-4-chlorocinnamic acid (CClCA). By replacing the –OH group with –H or –Cl, the electron-withdrawing ability of the substituent is varied in the order –OH < -H < -Cl. Upon extraction using polymer **P1** and detection of the positively charged TAMRA-labeled bradykinin peptide (RPPGFSPFR), we find that the MS signal is enhanced by 20% with CCA as the matrix, and more than 100% with CClCA, compared to that of CHCA as the matrix (Figure 2.5). Moreover, corresponding

fluorescence images reveal that clustering of the extracted peptide is the densest with the CClCA matrix (Figure 2.5). This observation is consistent with the hypothesis that the electron-rich polymer **P1** would interact better with more electron-poor matrices, which in turn causes more clustering and affords greater signal enhancement.

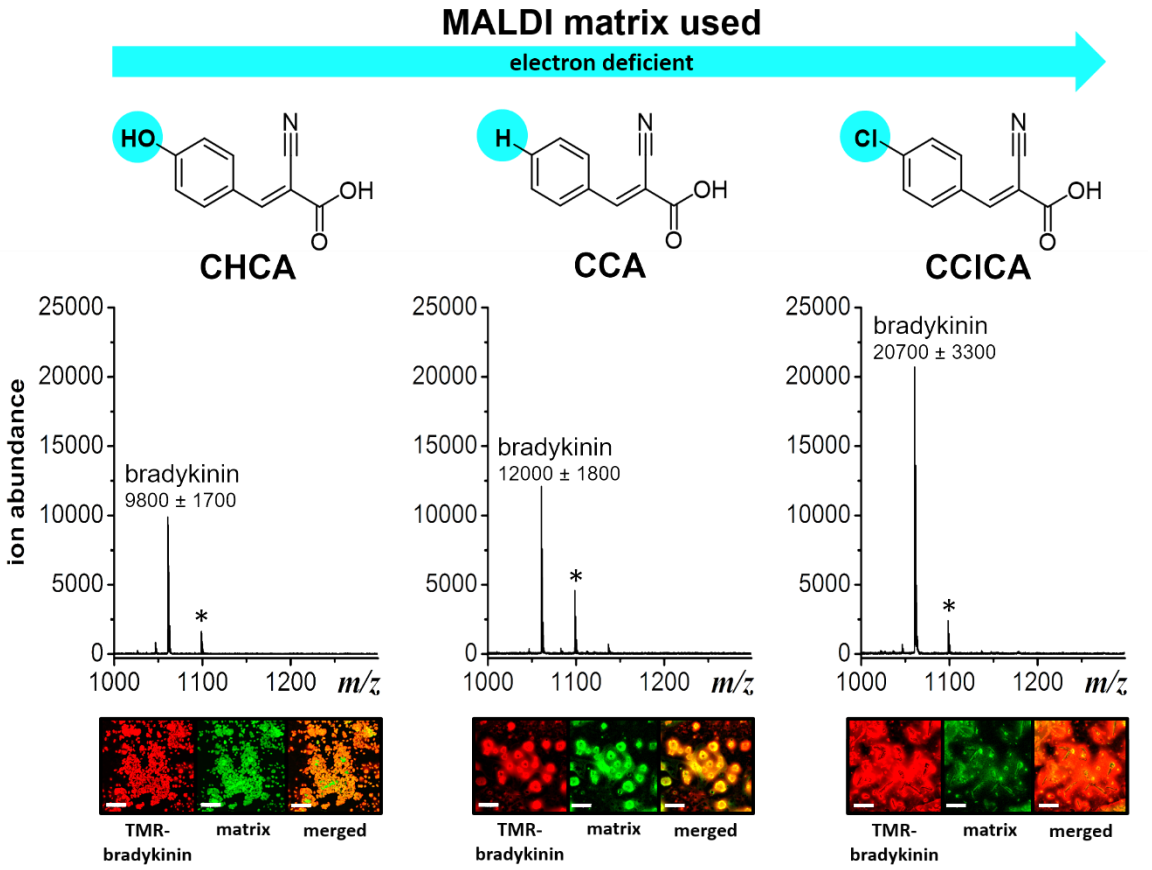

Figure 2.5. Chemical structures of different MALDI matrices in the order of increasing electron deficiency on the ring, along with the corresponding MALDI mass spectra and fluorescence images obtained for 100 nM bradykinin extracted by polymer **P1** and analyzed using these MALDI matrices. Peaks with asterisks are potassium adducts of the peptides. Scale bar on images: 100 µm.

Variations in the Polymer Sructure

To further test our hypothesis, we investigated how varying the electron density on the aromatic ring of the polymer affects MALDI signal enhancement and hotspot formation, while keeping the MALDI matrix constant. In this case, we introduced aromatic rings with electron-donating or electron-withdrawing substituents in a polythiolactone amide (**PTLAm**)-based amphiphilic homopolymer, shown in Figure 2.6 A. These polymers also form reverse micelles and selectively extract positively-charged peptides (Figures 2.6 B to D). Consistent with our hypothesis, using the **PTLAm** polymer with the electron-donating methoxy substituent (**PTLAm-OMe**) resulted in a two-fold enhancement in MALDI signal relative to the unextracted peptide (Figure 2.6 E). Interestingly, the signal was significantly suppressed, when **PTLAM-NO_2**, with its electron-withdrawing nitro group, was used. The unsubstituted **PTLAm** polymer (**PTLAm-H**) did not show a significant difference in MALDI signal relative to the unextracted one. Furthermore, clustering of peptide and matrix into hotspots is apparent in the presence of the **PTLAm-OMe**, but not for either **PTLAm-H** or **PTLAm-NO_2** (Figure 2.6 F), suggesting that a polymer with an electron-rich aromatic ring is needed for hotspot formation and signal enhancement.

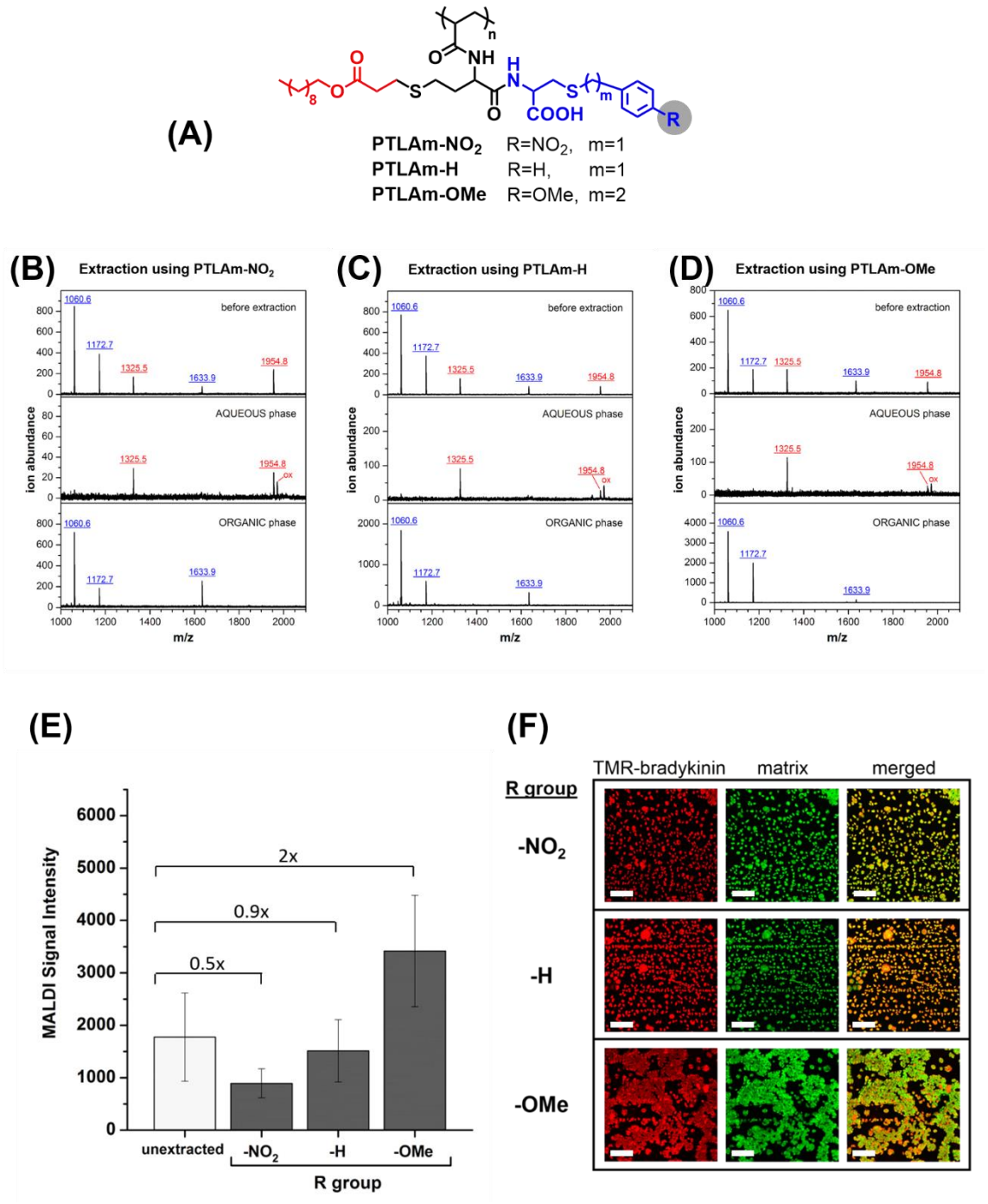

Figure 2.6. (A) Chemical structures of **PTLAm** polymers with varying substituents. **(B-D)** MALDI-MS spectra of a mixture of peptides before and after extraction at pH 8.0 using reverse micelles of the **PTLAm-NO₂**, **PTLAm-H**, and **PTLAm-OMe**, respectively, demonstrating their selectivity. Peptides used: bradykinin (*m/z* 1060.6, pI 12), kinetensin (*m/z* 1172.7, pI 11), β-amyloid(1-11) (*m/z* 1325.5, pI 4.3), malantide (*m/z* 1633.9, pI 10.3), and preproenkephalin (*m/z* 1954.8, pI 3.7). **(E)** MALDI signal intensity of 10 nM bradykinin extracted by each **PTLAm** polymer compared with 1 μM of unextracted bradykinin (100-fold higher concentration to account for 100-fold enrichment during extraction). **(F)** Fluorescence images show the degree of clustering of peptide (red) and CHCA matrix (green) after extraction using each **PTLAm** polymer. Scale bar: 100 μm.

While the **PTLAm** polymers provided access to amphiphilic polymers with aromatic units, we were interested in a scaffold that could provide the opportunity to conveniently introduce subtle changes in the aromatic unit, such as a wide range of electron-donating or -withdrawing substituents on the ring, while keeping the overall structure consistent with the **PAm** structure shown in Figure 2.1. Accordingly, we designed and synthesized a new set of amphiphilic homopolymers with a polyacrylamide (**PAm**) scaffold (Figure 2.7). These polymers provide the opportunity to further test our hypothesis that a ternary supramolecular interaction between the polymer, matrix and the peptide is essential for enhanced detection capabilities. Six polymers with different electron-withdrawing and electron-donating substituents were synthesized.

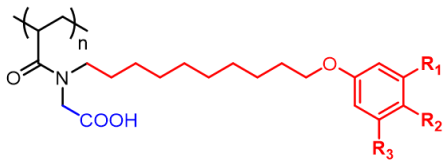

Polyacrylamide (**PAm**)-based carboxylate polymer scaffold

	R_1	R_2	R_3
PAm-NO_2	H	NO_2	H
PAm-CN	H	CN	H
PAm-H	H	H	H
PAm-Me	H	Me	H
PAm-OMe	H	OMe	H
PAm-di-OMe	OMe	H	OMe

Figure 2.7. Chemical structures and labels of the polyacrylamide-based amphiphilic homopolymers with the carboxylate hydrophilic moiety and variable hydrophobic units containing electron-donating or electron-withdrawing functionalities.

Using these polymers for extraction, the degree of matrix-peptide clustering and MALDI signal enhancement after extraction was monitored by fluorescence microscopy and MS, respectively. Through mere visual inspection of the fluorescence micrographs in Figure 2.8, it is evident that a higher degree of clustering is present in samples extracted by polymers with electron-donating groups (**PAm-H**, **PAm-Me**, **PAm-OMe**, **PAm-di-OMe**) compared with those extracted by polymers with electron-withdrawing groups (**PAm-NO_2**

and **PAm-CN**). At first glance, we would expect **PAm-H** to behave similar to the control (unextracted) sample, because of the –H substituent. Note, however, that the base aromatic ring is based on an alkoxyarene, making **PAm-H** a relatively electron-rich aromatic ring. We quantitatively assessed the degree of hotspot formation by measuring the fluorescence intensity per area using the software *ImageJ* [25] (Figure 2.9) and correlated this with the MALDI-MS signal obtained for samples extracted by each polymer. Figure 2.10 reveals that an approximately 3-fold enhancement in signal is obtained when polymers with electron-donating substituents are used for extraction, whereas no appreciable enhancement in signal was observed when extracted by polymers with electron-withdrawing groups. Correspondingly, higher degrees of hotspot formation were calculated for samples extracted using **PAm-H**, **PAm-Me**, **PAm-OMe** and **PAm-di-OMe** compared to **PAm-NO_2** and **PAm-CN**. This correlation shows that the clustering phenomenon indeed translates to enhanced signals in MALDI-MS. A good co-crystallization between the peptide and the MALDI matrix is also crucial to obtaining strong MS signals. Co-localization analyses[26] between the TAMRA-labeled peptide and the MALDI matrix were thus performed for each of the fluorescence micrographs (Figure 2.11) and an index of correlation (I_{corr}) greater than 0.800 was found for all images, suggesting very good co-localization between the peptide and the matrix regardless of the polymer used. However, the enhancement in signal is only observed for those samples which exhibit the cluster formation, that is, when polymers with electron-donating groups are used, indicating that formation of these "hotspots" through the use of polymers with favorable donor-acceptor interaction with the MALDI matrix is key to obtaining the signal enhancement. Formation of densely packed morphologies in the solid state through donor-

acceptor supramolecular interactions has found applications in electronics materials,[27-29] but the work here is the first study, to our knowledge, that tackles its role in mass spectrometric signal enhancement for sensitive molecular detection.

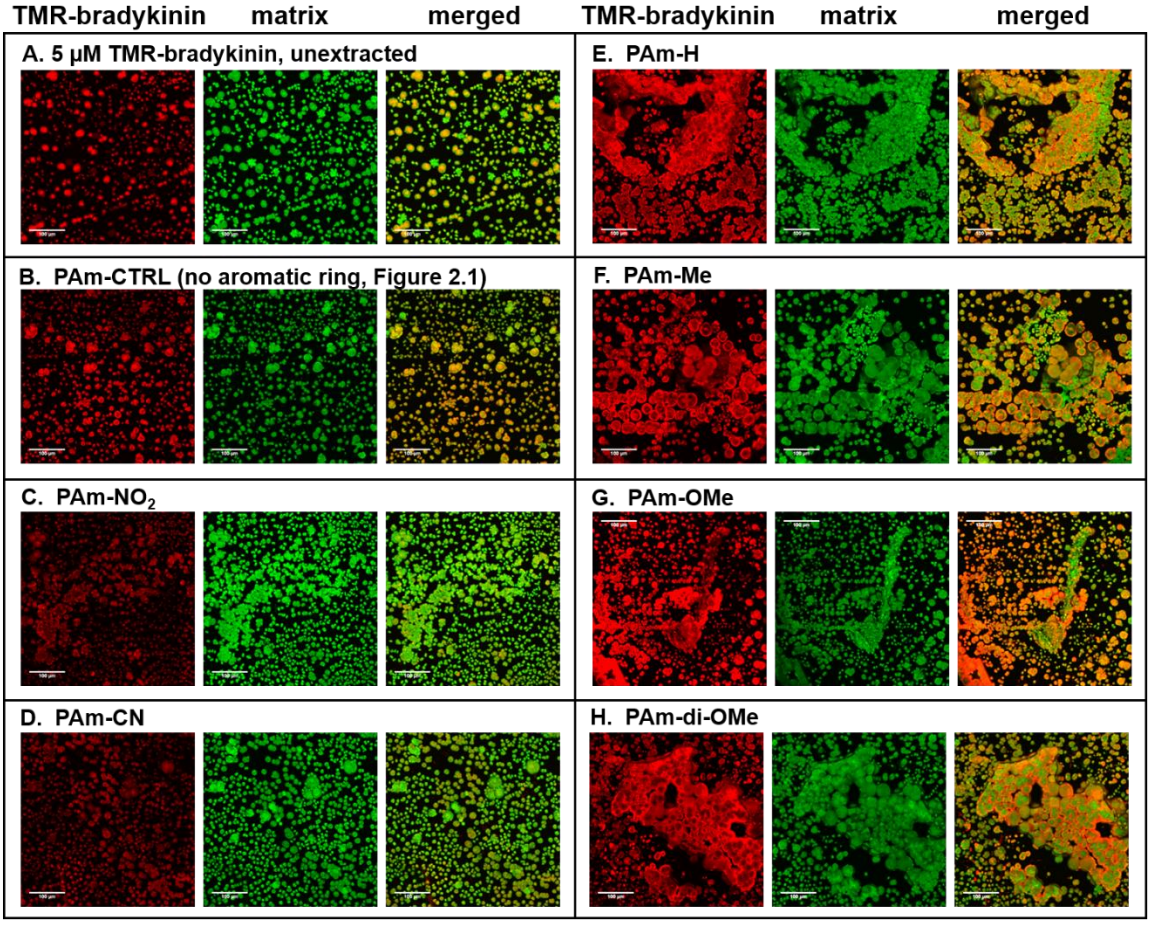

Figure 2.8. Fluorescence microscopy images showing the degree of clustering and co-localization of TMR-bradykinin peptide and CHCA matrix. Images correspond to 5 µM unextracted TMR-bradykinin for panel (**A**) while 50 nM TMR-bradykinin was extracted using the indicated **PAm** polymer for panels (**B**) to (**H**). **PAm-CTRL** refers to the **PAm** polymer without the aromatic ring, shown in Figure 2.1. Scale bar = 100 µm.

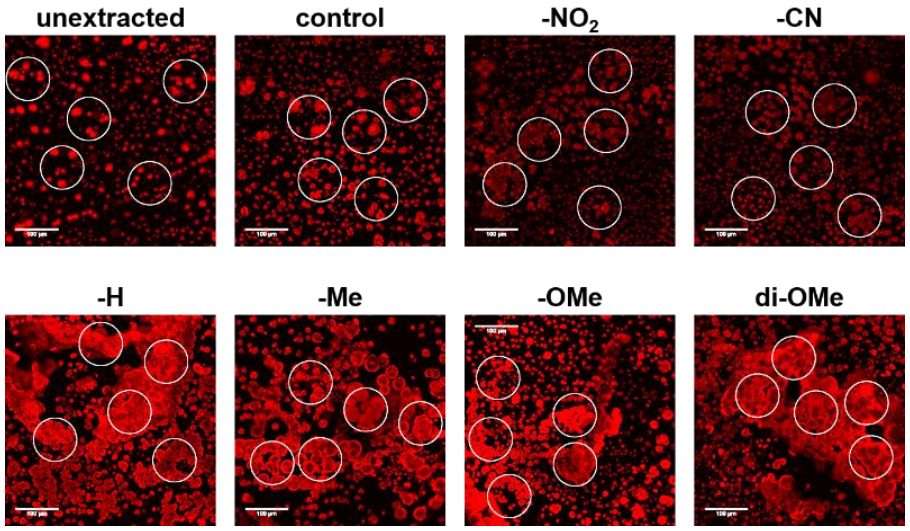

Figure 2.9. Five circular regions (with 100-µm diameter similar to the MALDI laser spot size) selected for each image to quantify the degree of clustering of the peptide in the polymer-matrix-peptide mixture in the organic phase after extraction using each of the **PAm** polymers. The integrated fluorescence for each region was obtained using *ImageJ* software[25] through the 'Measure' command under the 'Analyze' menu. Raw values were corrected by accounting for any background fluorescence in the black region of the image.

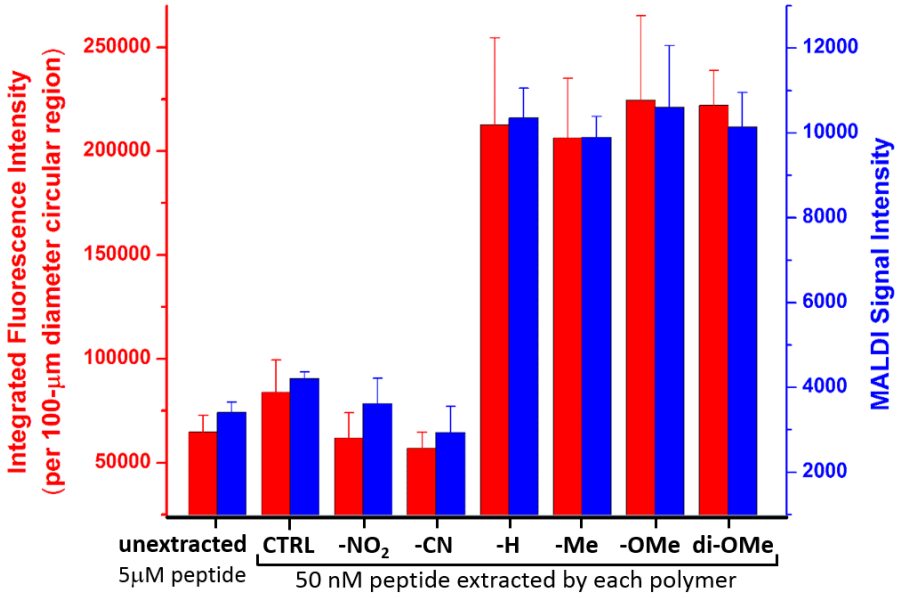

Figure 2.10. Correlation of the degree of clustering (measured from Figure 2.9) with the MALDI-MS signal obtained for 50 nM TMR-bradykinin extracted using each **PAm** polymer. Each red bar represents the average ± standard deviation of the integrated fluorescence density measured for the five circular regions shown in Figure 2.9. Each blue bar represents the average ± SEM of 90 MALDI mass spectra obtained from 3 replicate extractions, each with 3 replicate spots.

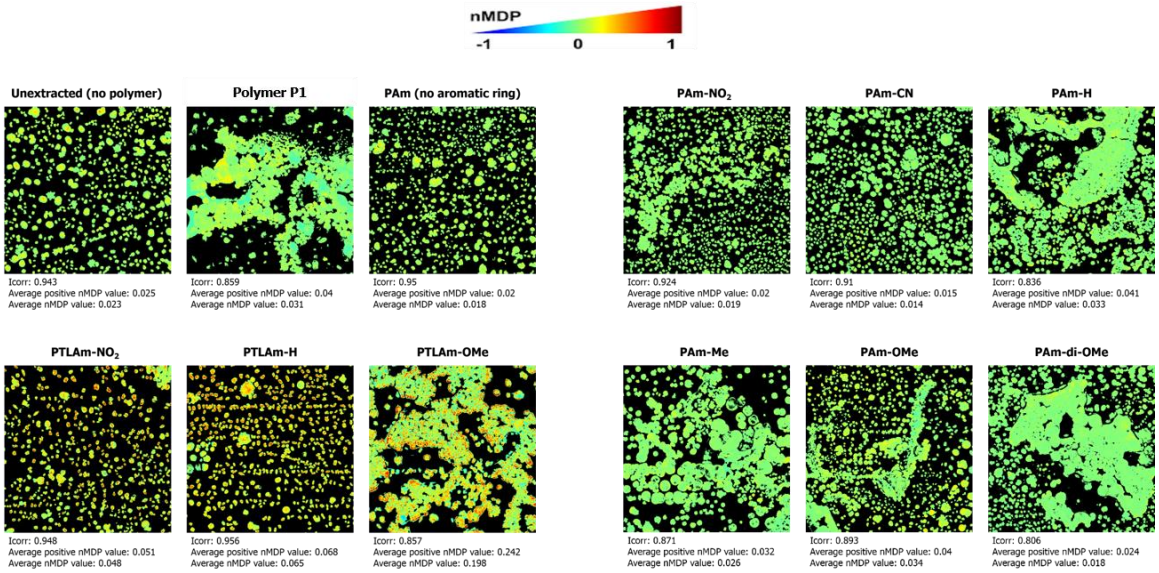

Figure 2.11. Co-localization analysis* with the calculated index of correlation (I_{corr}), average positive nMDP value, and average nMDP value for each fluorescence micrograph. Color scale used to represent the negative nMDP (exclusion) and positive nMDP values (co-localization) on the images is given. *Analyzed using the *Colocalization Colormap* plugin (https://sites.google.com/site/colocalizationcolormap/) for *Fiji*,[26] an image analysis distribution by *ImageJ*. An index of correlation (I_{corr}) is calculated for a pair of images (two different channels representing the peptide and the matrix fluorescence signals). Normalized mean deviation product (nMDP) values ranging from -1 (exclusion) to +1 (co-localization) is calculated between a pair of pixels and the fraction of positively correlated pixels is given by the index of correlation (I_{corr}). A colormap is generated to visualize the co-localization of the two fluorescent species.

Summary and Conclusions

In summary, we have investigated the molecular basis for the observed signal enhancement in peptide detection by MALDI-MS after extraction using reverse micelles of amphiphilic polymers. Through systematic variations in the electronic character of the aromatic ring in the amphiphilic polymer and matrix, we find that favourable donor-acceptor interactions are necessary to form a ternary assembly of the polymer, peptide, and matrix, which is essential for producing peptide-rich zones that maximize ion signal in MALDI-MS. An important point to recognize from all the data presented here is that although the electrostatic interaction between the

polymer and the peptide is required to selectively extract peptides from the aqueous phase into the organic phase, these interactions alone are not sufficient to cause hotspot formation and signal enhancement. All these polymers bear the carboxylate moiety that can conceivably cause the peptides to coalesce into hotspots, but evidently, a favourable aromatic donor-acceptor interaction between the polymer and the matrix is necessary for hotspots to form and signal enhancement to manifest. Thus, the ternary supramolecular interaction formed between the polymer and the peptide through electrostatics, and between the polymer and the matrix through aromatic donor-acceptor interactions, forms the basis for the selective enrichment and sensitive detection of peptides. Overall, these results reveal that amphiphilic polymers can self-pack in such a way that they mediate favourable interactions between peptides and matrix. Such interactions are reminiscent of proteins that upon folding, position other biomolecules in just the right way to perform chemistry that is impossible without the ternary interaction.

Experimental Methods

Materials and Reagents

The peptide bradykinin (RPPGFSPFR) was purchased from the Sigma-Aldrich. TMR-bradykinin (TAMRA dye conjugated at the N-terminal of the peptide) was obtained from Biopeptek Inc. (Malvern, PA). The following peptides were purchased from the American Peptide Company (Sunnyvale, CA): kinetensin (IARRHPYFL), malantide (RTKRSGSVYEPLKI), β-amyloid fragment 1-11 (DAEFRHDSGYE), preproenkephalin (SSEVAGEGDGDSMGHEDLY). Trifluoroacetic acid (TFA), α-cyano-4-hydroxy-

cinnamic acid (CHCA) and α-cyano-4-chlorocinnamic acid (CClCA) were purchased from Sigma-Aldrich, while α-cyanocinnamic acid (CCA) was from Alfa Aesar. Tris(hydroxymethyl)aminomethane (Tris buffer), hydrochloric acid (HCl), ammonium hydroxide (NH_4OH), toluene, tetrahydrofuran (THF) and purified water were obtained from Fisher Scientific. THF was distilled over Na/benzophenone before use.

Polymer Synthesis and Characterization

The synthesis and characterization of the polymers used in this chapter are described in detail in the supporting information of: Serrano, M.A.C.; He, H.; Zhao, B.; Ramireddy, R.R.; Vachet, R.W.; Thayumanavan, S. Polymer-Mediated Ternary Supramolecular Interactions for Sensitive Detection of Peptides. *Analyst* **2017**, *142*, 118-122. These can be found in the Appendix (Figures A.1 to A.8).

Preparation of Polymeric Reverse Micelles

To form reverse micellar assemblies, polymers were dissolved in toluene (0.5 mg/mL) and sonicated until a clear solution was obtained. Two equivalents of water per carboxylate moiety was added to the solution and sonicated again until the solution becomes optically clear.

MALDI Matrix Solutions

CHCA, CCA, and CClCA were all prepared at a concentration of 0.16 M in 350 μL THF:150 μL H_2O:6 μL TFA.

Peptide Extraction and Sample Preparation

Peptide solutions were prepared in 50 mM Tris buffer at the indicated pH. Extractions were done by adding 200 μL of the polymeric reverse micelle solution to 1 mL of the buffered peptide solution, mixing them by vortex for 2 hours, and separating the two phases by centrifugation at 12,500 rpm for 60 minutes. The aqueous phase was carefully drawn out and transferred to a separate tube. The remaining organic phase was dried under a stream of N_2 gas. The dried residue consisting of the polymer and the extracted peptides was reconstituted in 10 μL of THF and then 20 μL of the matrix solution. From this mixture, 1 μL was spotted on the MALDI target plate for MALDI-MS analysis or on indium tin oxide (ITO)-coated glass slides for fluorescence microscopy. Unextracted samples used for comparison were prepared such that they contained the same number of moles of the peptide and the matrix per μL spot, taking into consideration that the extraction process imparts a 100-fold enrichment (1 mL is reconstituted to 10 μL before addition of the matrix).

Fluorescence Microscopy

Fluorescence images were obtained using an Olympus FluoView FV1000 confocal fluorescence microscope. One microliter of sample spotted on ITO-coated glass slides was allowed to dry, and visualized under 10x magnification. The Cy3 channel (λ_{ex}=559 nm, λ_{em}=567 nm) and the ECFP channel (λ_{ex}=405 nm and λ_{em}=476 nm) were used to image TMR-bradykinin and CHCA matrix, respectively. No TMR-bradykinin was visible using the ECFP channel and no CHCA was visible in the Cy3 channel. Images obtained were

1024 x 1024 pixels in size with a scale of 0.478 μm per pixel. Quantitative fluorescence intensity measurements were done using *ImageJ* software.

MALDI-MS Analysis

A Bruker Autoflex III time-of-flight mass spectrometer was used for the MALDI-MS analysis of all samples. Acquisition of all mass spectra was done in reflectron mode with an accelerating voltage of 19 kV. Each spectrum is the average of 300 laser shots at 25% laser power.

References

(1) Flynn, D. C. Adaptor Proteins. *Oncogene* **2001**, *20*, 6270–6272.

(2) Meister, G. Argonaute Proteins: Functional Insights and Emerging Roles. *Nat. Rev. Genet.* **2013**, *14*, 447–459.

(3) Johnson, L. N.; Noble, M. E. M.; Owen, D. J. Active and Inactive Protein Kinases: Structural Basis for Regulation. *Cell* **1996**, *85*, 149–158.

(4) Cusack, S. Aminoacyl-TRNA Synthetases. *Curr. Opin. Struct. Biol.* **1997**, *7*, 881–889.

(5) Pratt, A. J.; MacRae, I. J. The RNA-Induced Silencing Complex: A Versatile Gene-Silencing Machine. *J. Biol. Chem.* **2009**, *284*, 17897–17901.

(6) Barrow, S. J.; Kasera, S.; Rowland, M. J.; Del Barrio, J.; Scherman, O. A. Cucurbituril-Based Molecular Recognition. *Chem. Rev*. **2015**, *115*, 12320–12406.

(7) Kim, H. J.; Heo, J.; Jeon, W. S.; Lee, E.; Kim, J.; Sakamoto, S.; Yamaguchi, K.; Kim, O. Selective Inclusion of a Hetero-Guest Pair in a Molecular Host: Formation of Stable Charge-Transfer Complexes in Cucurbit[8]uril. *Angew. Chemie - Int. Ed.* **2001**, *40*, 1526–1529.

(8) Moon, K.; Grindstaff, J.; Sobransingh, D.; Kaifer, A. E. Cucurbit[8]uril-Mediated Redox-Controlled Self-Assembly of Viologen-Containing Dendrimers. *Angew. Chemie - Int. Ed.* **2004**, *43*, 5496–5499.

(9) Appel, E. a.; Biedermann, F.; Rauwald, U.; Jones, S. T.; Zayed, J. M.; Scherman, O. a. Supramolecular Cross-Linked Networks via Host- Guest Complexation with Cucurbit [8]uril. *J. Am. Chem. Soc.* **2010**, 132, 14251–14260.

(10) Fukuyama, Y.; Tanimura, R.; Maeda, K.; Watanabe, M.; Kawabata, S. I.; Iwamoto, S.; Izumi, S.; Tanaka, K. Alkylated Dihydroxybenzoic Acid as a MALDI Matrix Additive for Hydrophobic Peptide Analysis. *Anal. Chem.* **2012**, *84*, 4237–4243.

(11) Kuyama, H.; Sonomura, K.; Nishimura, O. Sensitive Detection of Phosphopeptides by Matrix-Assisted Laser Desorption/Ionization Mass Spectrometry: Use of Alkylphosphonic Acids as Matrix Additives. *Rapid Commun. Mass Spectrom.* **2008**, *22*, 1109–1116.

(12) Pashkova, A.; Moskovets, E.; Karger, B. L. Coumarin Tags for Improved Analysis of Peptides by MALDI-TOF MS and MS/MS: Enhancement in MALDI MS Signal Intensities. *Anal. Chem.* **2004**, *76*, 4550–4557.

(13) Li, J.; Ma, H.; Wang, X.; Xiong, S.; Dong, S.; Wang, S. Enhanced Detection of Thiol Peptides by Matrix-Assisted Laser Desorption/Ionization Mass Spectrometry after Selective Derivatization with a Tailor-Made Quaternary Ammonium Tag Containing Maleimidyl Group. *Rapid Commun. Mass Spectrom.* **2007**, *21*, 2608–2612.

(14) Kim, J.-S.; Kim, J.-H.; Kim, H.-J. Matrix-Assisted Laser Desorption/Ionization Signal Enhancement of Peptides by Picolinamidination of Amino Groups. *Rapid Commun. Mass Spectrom.* **2008**, *22*, 495–502.

(15) Qiao, X.; Sun, L.; Chen, L.; Zhou, Y.; Yang, K.; Liang, Z.; Zhang, L.; Zhang, Y. Piperazines for Peptide Carboxyl Group Derivatization: Effect of Derivatization Reagents and Properties of Peptides on Signal Enhancement in Matrix-Assisted Laser Desorption/Ionization Mass Spectrometry. *Rapid Commun. Mass Spectrom.* **2011**, *25*, 639–646.

(16) Schuerenberg, M.; Luebbert, C.; Eickhoff, H.; Kalkum, M.; Lehrach, H.; Nordhoff, E. Prestructured MALDI-MS Sample Supports. *Anal. Chem.* **2000**, *72*, 3436–3442.

(17) Xu, Y.; Bruening, M. L.; Watson, J. T. Use of Polymer-Modified MALDI-MS Probes to Improve Analyses of Protein Digests and DNA. *Anal. Chem.* **2004**, *76*, 3106–3111.

(18) Dunn, J.D.; Igrisan, E.A.; Palumbo, A.M.; Reid, G.E.; Bruening, M. L. Phosphopeptide Enrichment Using MALDI Plates Modified with High-Capacity Polymer Brushes. *Anal. Chem.* **2008**, *80*, 5727–5735.

(19) Basu, S.; Vutukuri, D. R.; Thayumanavan, S. Homopolymer Micelles in Heterogeneous Solvent Mixtures. *J. Am. Chem. Soc.* **2005**, *127*, 16794–16795.

(20) Combariza, M.Y.; Savariar, E.N.; Vutukuri, D.R.; Thayumanavan, S.; Vachet, R.W. Polymeric Inverse Micelles as Selective Peptide Extraction Agents for MALDI-MS Analysis. *Anal. Chem.* **2007**, *79*, 7124–7130.

(21) Rodthongkum, N.; Chen, Y.; Thayumanavan, S.; Vachet, R.W. Matrix-Assisted Laser Desorption Ionization-Mass Spectrometry Signal Enhancement of Peptides After Selective Extraction with Polymeric Reverse Micelles. *Anal. Chem.* **2010**, *82*, 3686–3691.

(22) Rodthongkum, N.; Chen, Y.; Thayumanavan, S.; Vachet, R.W. Selective Enrichment and Analysis of Acidic Peptides and Proteins Using Polymeric Reverse Micelles and MALDI-MS. *Anal. Chem*. **2010**, *82*, 8686–8691.

(23) Rodthongkum, N.; Ramireddy, R.; Thayumanavan, S.; Vachet, R.W. Selective Enrichment and Sensitive Detection of Peptide and Protein Biomarkers in Human Serum Using Polymeric Reverse Micelles and MALDI-MS. *Analyst* **2012**, *137*, 1024–1030.

(24) Savariar, E. N.; Aathimanikandan, S. V.; Thayumanavan, S. Supramolecular Assemblies from Amphiphilic Homopolymers: Testing the Scope. *J. Am. Chem. Soc.* **2006**, *128*, 16224–16230.

(25) Rasband, W.S., ImageJ, U. S. National Institutes of Health, Bethesda, Maryland, USA, http://imagej.nih.gov/ij/, 1997-2015.

(26) Schindelin, J.; Arganda-Carreras, I.; Frise, E. *Nature Methods,* **2012**, *9*, 676-682.

(27) Beaujuge, P. M.; Fréchet, J. M. J. Molecular Design and Ordering Effects in π-Functional Materials for Transistor and Solar Cell Applications. *J. Am. Chem. Soc.*, 2011, **133**, 20009-20029.

(28) Li, H.; Sun, S; Mhaisalkar, S.; Zin, M. T.; Lam, Y. M.; Grimdale, A. C. A High Voltage Solar Cell Uing a Donor–Acceptor Conjugated Polymer Based on Pyrrolo[3,4-*f*]-2,1,3-benzothiadiazole-5,7-dione. *J. Mater. Chem. A* **2014**, *2*, 17925-17933.

(29) Peurifoy, S. R.; Guzman, C. X.; Braunschweig, A. B. Topology, Assembly, and Electronics: Three Pillars for Designing Supramolecular Polymers with Emergent Optoelectronic Behavior. *Polym. Chem.* **2015**, *6*, 5529-5539.

CHAPTER III

MOLECULAR FEATURES INFLUENCING THE RELEASE OF PEPTIDES FROM AMPHIPHILIC POLYMERIC REVERSE MICELLES

Majority of this chapter is published: Serrano, M.A.C.; Zhao, B.; He, H.; Thayumanavan, S.; Vachet, R.W. Molecular Features Influencing the Release of Peptides from Amphiphilic Polymeric Reverse Micelles. *Langmuir* **2018**, *34*, 4595-4602.

Abstract

Efficient and controlled release of peptides bound to polymeric reverse micelle assemblies can be achieved through the cooperative effects of disassembly and disruption of charge-charge interactions. Through the examination of various peptides and polymer architectures, the factors that affect the release efficiency of the electrostatically bound peptides have been identified. Peptide guests and polymers with a greater number of complementary charges result in less efficient release than peptides and polymers with lower numbers of charges. Interestingly, the presence of adjacent charged groups on the monomeric unit of the polymer exhibit exceptionally low release efficiency, perhaps due to a chelate-like effect, even when the total polymer charge is lower. Overall, these findings inform the design principles for catch-and-release systems based on polymeric reverse micelles, which offer great versatility and tunability.

Introduction

Polymer-based supramolecular assemblies that form organized structures such as micelles, reverse micelles, and vesicles, have attracted attention in recent years for their use in delivery, separations, catalysis, biomimetics, sensing, and as nanoreactors.[1-11] Such applications often rely on the polymeric assembly acting as a host to accommodate guest molecules through noncovalent interactions. Remarkably, although these host-guest interactions employ relatively weak noncovalent interactions that render the binding reversible and dynamic, the multivalent nature of the polymeric host affords additional strength and versatility to the binding. The existence of cooperativity among the subunits of a supramolecular assembly imparts properties that are different from its individual components, and this manifests not only in the process of host-guest binding/association but also in guest release/dissociation. Understanding the factors that influence guest release is just as important as knowing the mechanism of host-guest binding, as evidenced by the emergence of stimuli-responsive assemblies that take advantage of diverse strategies for regulated guest release.[12-16] Depending on the desired application, either a slow, controlled release may be preferred,[17-19] as in the case of drug delivery, or an immediate, quantitative release may be needed,[20-22] as in the case of separations and purification. In either case, a deeper understanding of the guest release process is necessary to advance such applications, especially in systems involving the capture and release of complex biomolecules.

Encapsulation of biomolecules, particularly peptides and proteins, is typically intended either to isolate them from complex media, protect them from degradation, increase their biostability and sustain their bioactivity, or offer confinement that could

modulate their activity.[23-27] Because these large biopolymers possess diverse chemistries and functionalities in their amino acid precursors, selective capture and release of peptides and proteins into and out of supramolecular hosts require a means of discriminating a selected set of proteins over others. Our group has been particularly interested in the use of amphiphilic polymers, such as the carboxylate-functionalized homopolymer **P1** (Figure 3.1) for the selective extraction of peptides and proteins. The amphiphilic nature of these polymers enables them to self-assemble into reverse micelles in nonpolar solvents, such that the charged functional groups form a hydrophilic core via solvophobic effects while the hydrophobic moieties are oriented outside in contact with the nonpolar solvent. These polymeric reverse micelles serve as ideal supramolecular hosts for extracting peptides and proteins into nonpolar solvents due to the inherent stability of the assemblies,[28,29] tunable selectivity[30,31] and optimizable capacity[32]. In the past, it has been shown how these assemblies can be utilized for the selective enrichment and sensitive detection of peptides and proteins through a simple biphasic extraction.[33] By virtue of a peptide's isoelectric point (pI), which dictates its charge at a given solution pH, the polymeric reverse micelles bearing a charged hydrophilic interior can selectively sequester peptides having a complementary charge into the organic phase. The polymeric reverse micelles can also control the reactivity of peptides that are encapsulated in their interior, enabling residue-selective bioconjugation.[34] However, the factors that control the release of the sequestered biomolecules from the reverse micelles have not been explored. Although there have been numerous studies demonstrating guest release from small molecule surfactant reverse micelles such as AOT (bis(2-ethylhexyl) sulfosuccinate sodium),[20,35-38] systematic studies of the factors that influence guest release from polymeric reverse micelles have been

limited.[4,39] Moreover, because of the high kinetic stability of polymeric reverse micelle assemblies, most guest release mechanisms are of the slow type,[40] simply relying on the inherently dynamic but gradual exchange of guest molecules between the hydrophilic interior of the reverse micelles and the bulk solvent.

In this chapter, I describe investigations into the conditions that affect peptide release efficiency from polymeric reverse micelles and show that efficient guest release requires the disassembly of the reverse micelles and weakening of the non-covalent interactions between polymer and peptide. Furthermore, the features of the supramolecular host (polymeric reverse micelles) and guest (peptide) that influence the release process are examined.

Results and Discussion

Cooperative Effects of Disassembly and Charge-Charge Disruption

In devising strategies for efficient peptide release, simple disruption of electrostatic interactions between the polymer and the peptide that are essential for selective binding was first considered. However, attempts at screening out the electrostatic interaction by increasing the ionic strength was not successful for quantitative recovery. Hence, three strategies (Figure 3.1) were considered: (1) creation of charge-charge repulsion between the peptide and polymer by deprotonating the peptide through the addition of base; (2) neutralization of the polymer's carboxylate groups via the addition of acid to abolish the charge-charge interaction between the polymer and the peptide; and (3) disassembly of the reverse micelles prior to the addition of the stripping aqueous solution.

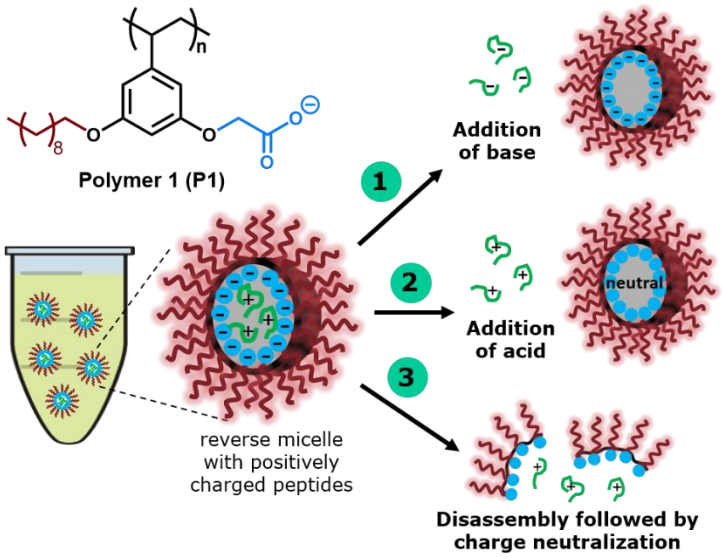

Figure 3.1. Different strategies for guest release from carboxylate-functionalized polymeric reverse micelle assemblies. In the first strategy, addition of aqueous base with pH > pI of the peptide guest makes the peptides net negatively charged and repelled by the negatively charged reverse micelles. In the second strategy, addition of aqueous acid with pH > pKa of the polymer carboxylate groups neutralizes the charge on the reverse micelles. In the third strategy, reverse micelles are first disassembled by the addition of THF, followed by the addition of the stripping aqueous phase.

We tested these strategies with 200 pmol of a model positively charged peptide, angiotensin I (sequence: DRVYIHPFHL, pI 7.9), which can be readily sequestered into the reverse micelles via a biphasic extraction approach described in the experimental section. Peptide release into the stripping aqueous phase was monitored by matrix-assisted laser desorption/ionization mass spectrometry (MALDI-MS) analysis. Using polymer **P1** as an example, we can use the peptide ion signal at *m/z* 1296.7 as an indicator of how much peptide was released using each of the strategies illustrated in Figure 3.1. In parallel, the toluene phase was also analyzed after peptide release to detect any peptides that might remain in the reverse micelles in the organic phase. For reference, Figure 3.2A shows the MALDI-MS signal for an angiotensin I standard that has a concentration of 1 μM (200

pmol in 200 μL), which is the expected concentration if peptide release in the stripping aqueous phase is 100%, while Figure 3.2B shows the MALDI-MS signal for 200 pmol angiotensin I in the reverse micelles in toluene before any peptide is released (*i.e.* 0% release).

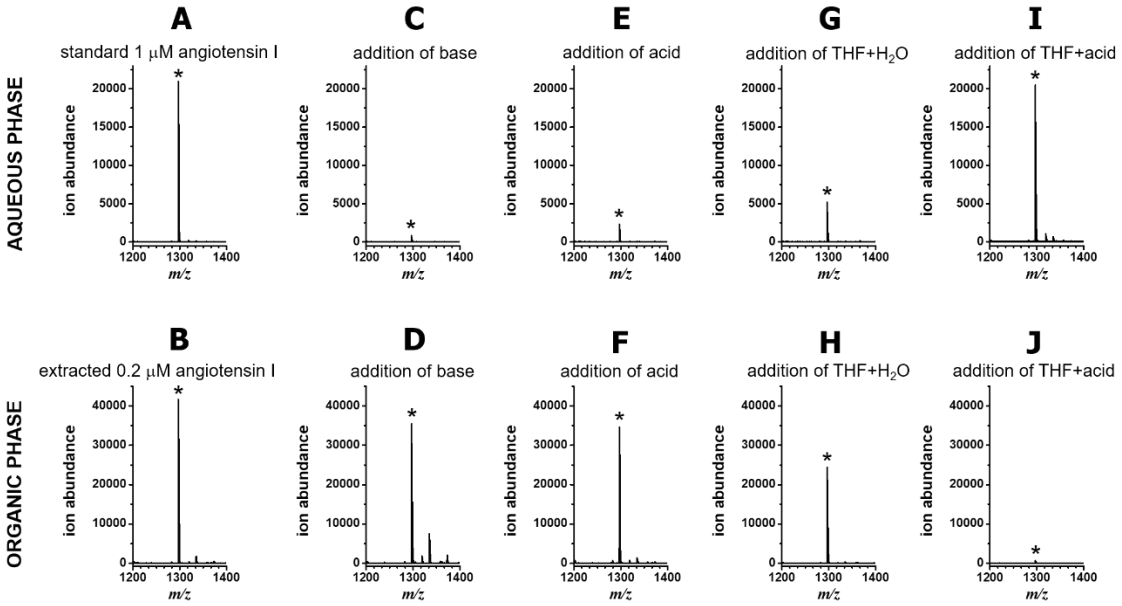

Figure 3.2. Representative MALDI mass spectra for (**A**) 1 μM angiotensin I standard (**m/z* 1296.7) and (**B**) 200 pmol angiotensin I, fully extracted into the organic phase without any release. Representative MALDI spectra of the resulting aqueous and organic phases after release of 200 pmol angiotensin I from reverse micelles of **P1** using 200 mM Tris base at pH 10 (**C** and **D**), using 10% acetic acid at pH 1.7 (**E** and **F**), by the addition of THF then water (**G** and **H**), and by the addition of THF then 10% acetic acid (**I** and **J**). All stripping aqueous phases are 200 μL in volume.

Adding base to deprotonate the peptide (strategy 1) does not yield significant release as indicated by the low MALDI-MS peptide ion signal seen in the stripping aqueous phase (Figure 3.2C) and an abundant amount still remaining in the toluene phase (Figure 3.2D). Adding acid to neutralize the charged groups in the polymeric reverse micelles

(strategy 2) did not release much peptide either (Figure 3.2E), with a significant amount of peptide remaining with the reverse micelles in the toluene phase (Figure 3.2F).

Results from the first two strategies suggest that simply eliminating the charge-charge interaction between the polymer and peptide through a pH change is not sufficient to cause efficient guest release. We posited that their confinement inside the reverse micelle assemblies in the organic phase may be preventing their release into the aqueous phase. We then considered disruption of the assemblies using tetrahydofuran (THF), which is regarded as a good solvent for both the hydrophobic and hydrophilic moieties of the polymer. Adding THF thus eliminates the solvophobic effects that drive self-assembly in the first place. DLS measurements before and after THF addition confirm that the assemblies become unstable (erratic correlograms and unreliable sizes) in a mixture of THF and toluene (Figure 3.3A and 3.3B). Interestingly, UV-Vis measurements indicate that the polymer does not partition to the stripping aqueous phase after THF addition (Figure 3.3C), confirming that the polymer is still in the organic phase but just not as stable assemblies.

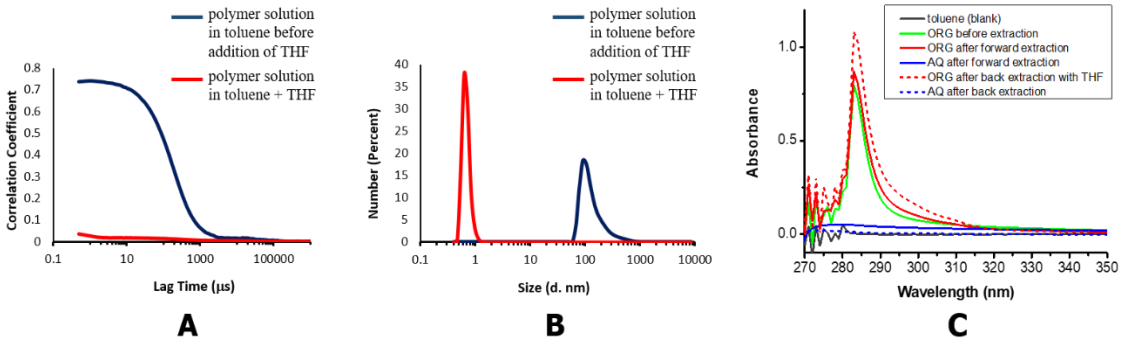

Figure 3.3. DLS correlograms (**A**) and hydrodynamic size measurements (**B**) of the polymer assemblies of **P1** in toluene before and after addition of THF. (**C**) UV-Visible absorbance measurements of the organic (ORG) and aqueous (AQ) phases before and after forward and back extraction.

However, even though THF disassembles the reverse micelles, addition of this solvent is not sufficient to efficiently release the peptides from the organic phase when only water (pH 6) is added as the stripping aqueous phase (Figure 3.2G and Figure 3.2H). However, when acid (pH 1.7) is used as the stripping aqueous phase after THF addition, almost quantitative release of the peptides into the aqueous phase is seen (Figure 3.2I). The peptide signal in this case is close to what is expected if the peptide were initially dissolved in an aqueous solution (Figure 3.2A). Furthermore, almost no peptide remains in the organic phase (Figure 3.2J).

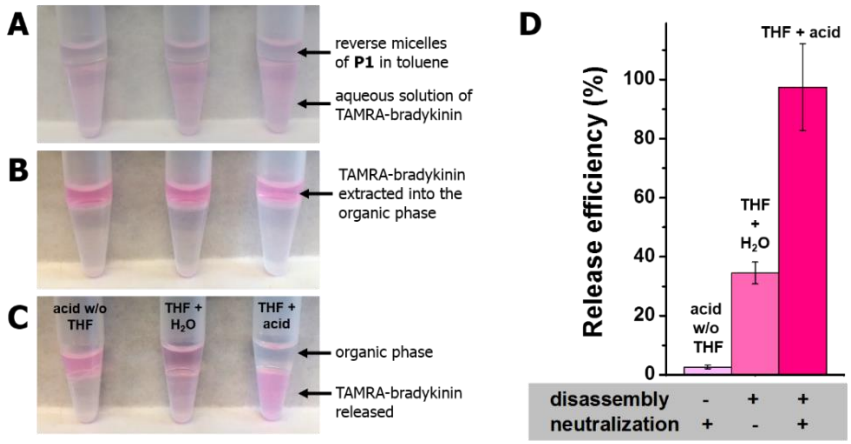

Figure 3.4. TAMRA-bradykinin before (**A**) and after (**B**) extraction into reverse micelles of **P1** in toluene. Release of TAMRA-bradykinin under different conditions (**C**), and quantitative determination of the release efficiency by fluorescence measurement of the stripping aqueous phase (**D**). Initial TAMRA-bradykinin concentration is 0.5 μM in 1mL of buffer, released to a final volume of 200 μL stripping aqueous phase. Each bar is the average ± standard deviation obtained for three replicate samples for each condition.

An illustrative and quantitative indication of guest release can also be observed and measured via the release of the fluorescently labeled guest peptide, TAMRA-bradykinin (sequence: RPPGFSPFR). Figure 3.4 shows the efficiency of guest release using each strategy as measured by fluorescence spectroscopy, which is consistent with results obtained from the MALDI-MS analysis. Taken as a whole, the results in Figures 3.2 and 3.4 indicate that simply neutralizing the electrostatic interaction between polymer and

peptide, nor merely disassembling the reverse micelles in the organic phase is not sufficient to cause efficient guest release from the reverse micelles. Instead, both disassembly and neutralization are necessary for efficient guest release. Thus, it appears that guest release from the polymeric reverse micelles is subject to a significant degree of cooperativity in that both disassembly of the reverse micelles and disruption of the polymer-peptide interactions are necessary.

Factors Influencing the Release Efficiency

Three other amphiphilic polymer scaffolds (see Figure 3.5A) were explored to better understand the structural factors that influence the guest release process. An easily tunable amphiphilic random copolymer (*i.e.* **P2**), which contains a similar styrene-based hydrophobic decyl chain and a hydrophilic carboxylate moiety similar to **P1**, was considered to test the effect of amphiphilic group flexibility as the hydrophobic and hydrophilic groups are not constrained as they are in polymer **P1**. Polymer **P3**, which is also a random copolymer scaffold bearing a hydrophobic decyl chain and a hydrophilic carboxylate group but has an acid-cleavable citraconic acid amide moiety,[41] was chosen to study how charge reversal from negative to positive might drive guest release further due to charge-charge repulsion with the positively charged peptides. A carboxylate-functionalized polyacrylamide-based amphiphilic homopolymer **P4** was also considered to see if a less bulky scaffold would affect guest release. Moreover, several peptides spanning a range of basicity were used as guests in reverse micelles of polymers **P1**-**P4** to investigate what properties of the host (polymer) and guest (peptide) influence release efficiency.

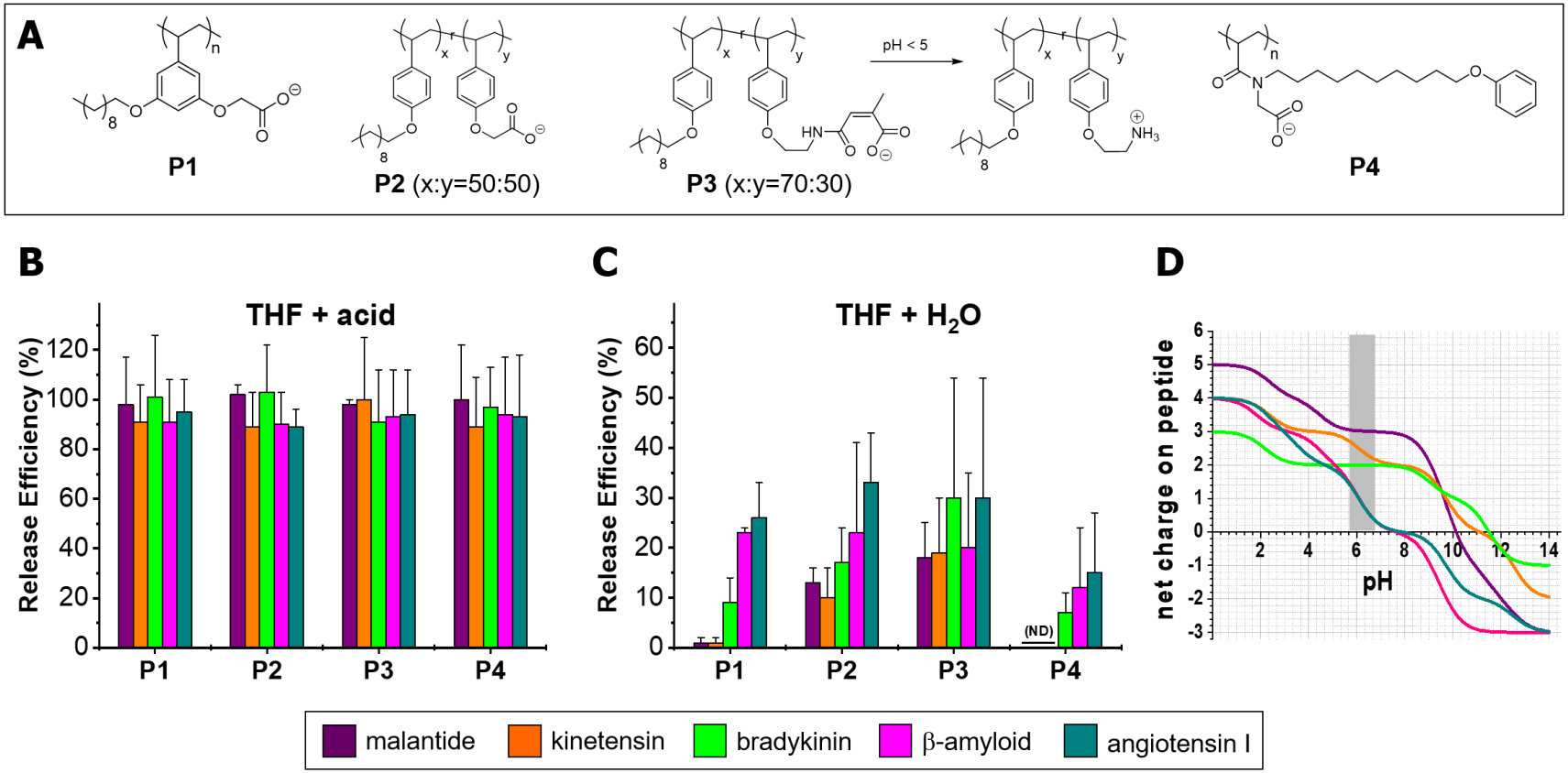

Figure 3.5. (**A**) Chemical structures of amphiphilic polymers **P1**, **P2**, **P3** and **P4**. Efficiency of peptide release from each polymer by addition of THF then 10% acetic acid (**B**), or by addition of THF then water (**C**), as quantified by LC-MS (ND=not detected). Initial concentration of each peptide is 0.2 μM in 1mL of buffer, released to a final volume of 50 μL stripping aqueous phase. Each bar is the average ± standard deviation of three experimental replicates. (**D**) Theoretically calculated net charge‡ on the peptide as a function of solution pH (shaded gray region corresponds to pH range of 5.6-6.5 for water). ‡Values obtained from from *InCharge* software by *EpiQuest* Protein Analysis Software Suite (https://www.epiquest.co.uk/incarge). Peptides studied: malantide (RTKRSGSVYEPLKI, pI=10.3), kinetensin (IARRHPYFL, pI=11), bradykinin (RPPGFSPFR, pI=12), β-amyloid 10-20 fragment (YEVHHQKLVFF, pI=7.6), angiotensin I (DRVYIHPFHL, pI=7.9).

When both THF and acid were added (Figure 3.5B), all guest peptides were released efficiently (90-100%) from the polymers indicating that all the polymers are subject to the same cooperativity noted above. Interestingly, the charge-conversion polymer **P3**, which generates a repulsive interaction upon addition of acid, does not demonstrate a significant advantage over the other three polymers in terms of release efficiency, indicating that disassembly and charge shielding after THF addition is sufficient for effective guest release. However, when only THF and water are used (Figure 3.5C), subtle differences in release efficiency can be observed. At the pH of water (~5.6-6.5), protonation of all the carboxylate groups in the polymer presumably does not occur, resulting in residual electrostatic binding between the polymers and the positively charged peptides. A close look at these data reveals that release efficiency is influenced by the type of polymer and the peptide guest. For instance, less basic peptides like angiotensin I (pI=7.9) are released more easily than highly basic peptides (*vide infra* for comparisons). Also, the random copolymers (**P2** and **P3**) release the peptides into water better than do the homopolymers (**P1** and **P4**), especially for the more basic peptides. These subtle effects evidently arise when the pH of the stripping aqueous solution is closer to neutral, as this condition gives a discriminating effect between weak and strong interactions. Based on these observations, we hypothesize that the strength of electrostatic interaction between the polymer carboxylate groups and the peptides influences the guest release efficiency.

This hypothesis is supported upon considering the peptides' net charges as a function of pH (Figure 3.5D). Using release from polymer **P1** in Figure 3.5C as an example, we find that guest release efficiency increases as the peptide net charge decreases at pH 6. Release of the more basic peptides, malantide, kinetensin, and bradykinin, is much lower

than the release of β-amyloid and angiotensin I, which follows the theoretically calculated net charge on each peptide at pH 6. That is, the higher the net charge, the stronger the peptide's electrostatic interaction with the polymer, and the more difficult it is to be released. Polymers **P2** and **P4** show a similar trend as **P1**, although the trend is less dramatic for the random copolymer **P2**. Overall, under conditions where the carboxylate groups in the polymer are not fully neutralized, the release efficiency depends on the magnitude of the net charge of the peptide at that pH. Polymer **P3**, however, does not clearly show this trend and instead we see better release efficiency for the more basic peptides compared with the other polymers. This is perhaps because some fraction of the acid-cleavable units is being converted to positively charged amine groups at pH 6, thereby giving rise to some repulsive interactions that enable this polymer to more easily release highly positively charged peptides compared to the other polymers that don't have this charge-conversion moiety. To confirm this, we performed the release of malantide, a hard-to-release peptide, at a slightly lower pH where the charge conversion has been shown to occur,[41] and was able to observe a consequent increase in release efficiency as a result of the hydrolysis (Figure 3.6).

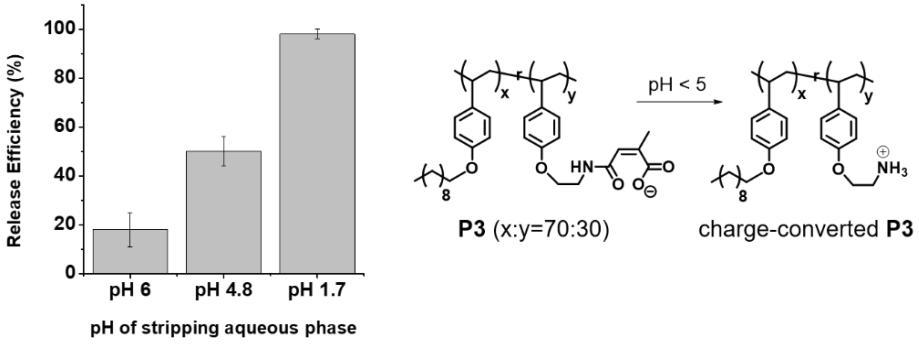

Figure 3.6. Release of malantide peptide (RTKRSGSVYEPLKI, pI 10.3) from reverse micelles of polymer **P3** at different pH of stripping aqueous phase showing an increase in release efficiency as the citraconic acid amide moiety is converted to a positively charged amine group. Each bar represents the average ± standard deviation of three experimental replicates done for each pH.

Interestingly, we can also take advantage of this "release by repulsion" to achieve selective peptide release by using a stripping aqueous phase pH that causes a peptide to have a net negative charge. For example, if kinetensin (pI=11) and angiotensin (pI=7.9) are loaded into reverse micelles of **P1** and then released using THF and a stripping aqueous phase at a pH of 9.5, angiotensin I is selectively released (Figure 3.7A), while kinetensin remains in the organic phase (Figure 3.7B). Presumably, angiotensin I is released because it becomes negatively charged at the pH above its pI, whereas kinetensin remains because it retains its positive charge at the pH below its pI. This observation provides further proof for the importance of electrostatic interactions in the release process, but it also suggests a new mode by which selective release can be achieved, which could have implications for peptide separations/purifications or selective delivery of multiple cargos.

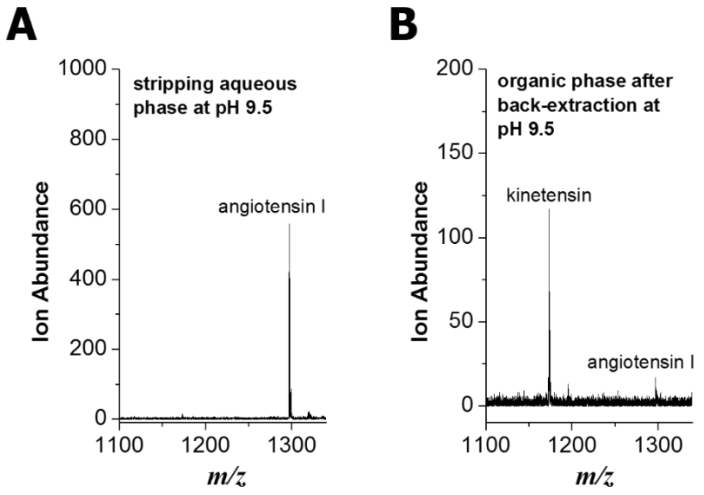

Figure 3.7. MALDI mass spectra of the stripping aqueous phase (**A**) and the organic phase (**B**) after release at pH 9.5 (using THF + 50 mM Tris, pH 9.5), illustrating that angiotensin I can be selectively released.

Further evidence for the importance of electrostatic interactions on guest release is found by varying the number of charges in the polymer via changes in the pH of the stripping aqueous phase used after THF addition. In Figure 3.8A, we find that the release efficiency of TAMRA-bradykinin from reverse micelles of **P1** follows a titration-like dependence as the pH of the stripping aqueous phase (after THF addition) is decreased, presumably as a result of protonation of the polymer carboxylate groups, until quantitative release is achieved at low pH (~2.5). This provides evidence that neutralizing the carboxylate groups (by protonation) weakens the polymer's hold on the peptide upon disassembly by THF. Notably, the pH at which 50% of the peptides are released is around pH 4.7, which may be the effective pK_a of the carboxylic acid groups in the polymer. Interestingly, in previous work we showed that polymer **P1** has the same pH dependency when extracting peptides from an aqueous phase into an organic phase,[42] with an inflection point at around pH 5, highlighting the reversible behavior of this homopolymer. The titration curve-like dependence and effective pK_a observed in Figure 3.8 is similar to what is obtained for a carboxylate-functionalized random copolymer **P7** (Figure 3.8B) suggesting that this behavior is independent of the polymer scaffold. These observations are important as they indicate that the extent of peptide release can be predicted and controlled based on the identity of the charged functional group.

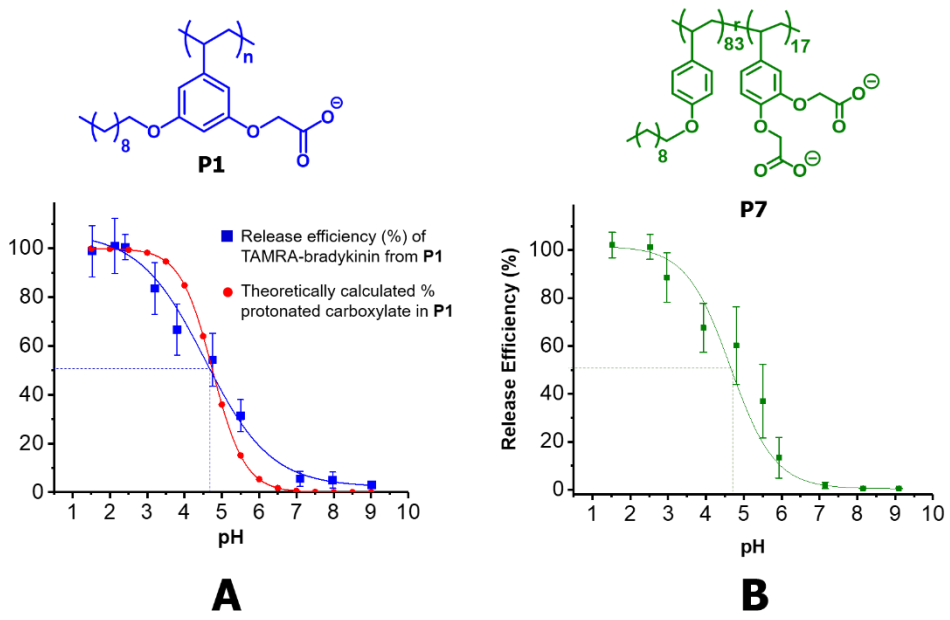

Figure 3.8. Release efficiency of TAMRA-bradykinin peptide from reverse micelles of homopolymer **P1** (**A**) and a random copolymer **P7** (**B**) as a function of stripping aqueous phase pH. Best fit curves are drawn to guide the eye.

Another way to explore the influence of polymer charge density on release efficiency is to vary the percentage of carboxylate groups on the polymer. This can be easily achieved through our random copolymer scaffold by varying the ratio of the hydrophilic and hydrophobic moieties during polymerization.[32] In addition to polymer **P2** which has 50% carboxylate groups, we synthesized random copolymers **P5** and **P6**, containing 20% and 30% carboxylate groups, respectively (Figure 3.9A). As observed before, quantitative peptide release is achieved when THF and acid are used (Figure 3.9B), regardless of the percentage of carboxylate groups in the polymer suggesting that the carboxylate groups are effectively protonated at a low pH. However, when using THF and pure water, peptide release efficiency decreases as the percentage of carboxylate groups in the polymer increases (*i.e.* **P5** < **P6** < **P2** < **P1**), suggesting that a higher carboxylate number in the polymer leads to stronger peptide binding and therefore less efficient peptide release. These results have important implications because while an optimal percentage of

carboxylate groups is required for high binding capacity of the reverse micelles,[32] guest release efficiency is reduced, especially at near neutral conditions.

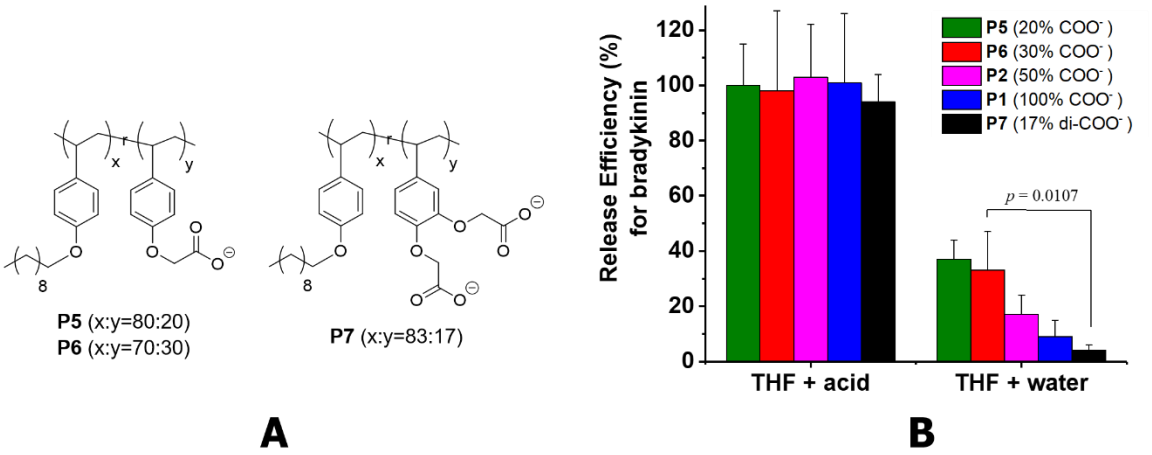

Figure 3.9. (**A**) Structures of polymers **P5**, **P6** and **P7**. (**B**) Release efficiency for bradykinin, quantified by LC-MS, from reverse micelles of polymers with different percentages of carboxylate functional groups. Each bar is the average ± standard deviation of three experimental replicates.

A notable exception to the trend in Figure 3.9B is the result for **P7**, which contains a 17% ratio of a di-carboxylate moiety (or 34% total carboxylate per monomer). With this percentage of carboxylate groups, one would expect peptide release efficiency to be about the same as **P6**, which has 30% carboxylate groups. However, we find that polymer **P7** has an even lower release efficiency than the homopolymer **P1**, which has 100% carboxylate. This observation suggests that the presence of two adjacent carboxylate groups imparts additional avidity through a chelate-like effect that allows the polymer to retain peptides more strongly than what would be expected based on just the global or overall charge density.

The results above demonstrate that peptide release is exquisitely sensitive to pH and polymer charge density, but we also find that peptide release is influenced by ionic strength after disassembly (Figure 3.10). Moreover, the effect of ionic strength is polymer-dependent. For polymers **P6** and **P2**, quantitative release occurs at NaCl concentrations as low as 0.01 M, suggesting that minimal charge shielding is needed to disrupt the electrostatic interaction between polymer and peptide. In contrast, polymers **P1** and **P7** require salt concentrations as high as 1 M to achieve efficient peptide release. The behavior of polymer **P7** is again remarkable, even though it has a lower overall percentage of carboxylate groups than **P1** or **P2**. The bidentate nature of the carboxylate groups in **P7** presumably confers additional strength to its binding with the peptides such that a greater electrostatic shielding is required to release its peptide guests. Perhaps more intriguing is the fact that the forward extraction capacities of polymers **P6** and **P7** were found in our recent work to be very similar.[32] Evidently, the presence of higher local charge density for

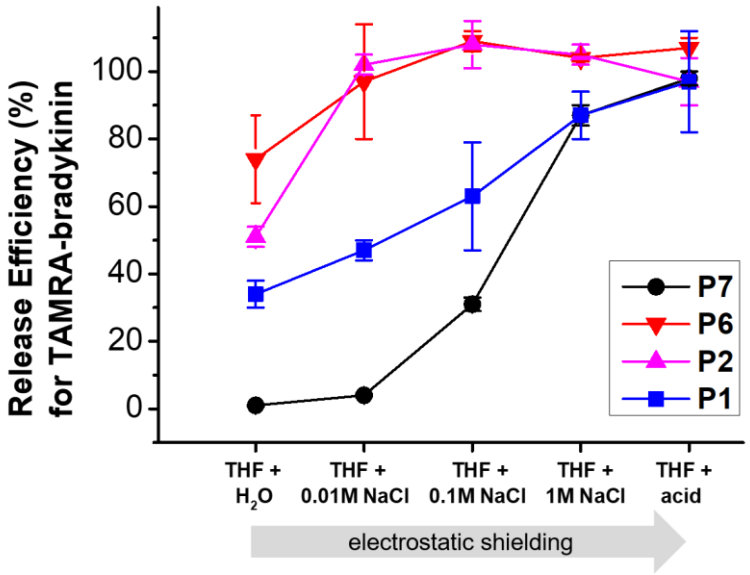

Figure 3.10. Release efficiency of TAMRA-bradykinin from reverse micelles of **P7**, **P6**, **P2** and **P1** using THF and a stripping aqueous phase with increasing electrostatic shielding.

P7 does not influence the forward extraction process like it does guest release. This disparity may be attributed to the fact that peptide extraction from the aqueous phase occurs while the polymer exists as intact reverse micelle assemblies, whereas during peptide release the addition of THF causes them to disassemble, leaving **P7**'s local charge density to dominate polymer-guest interactions.

Summary and Conclusions

In summary, we have evaluated different strategies for releasing guest peptides from polymeric reverse micelles and investigated the features of the guest and the host that affect the release efficiency. We have shown that: (i) both disassembly of the reverse micelles and neutralization of electrostatic interactions between polymer and peptide are required to efficiently release encapsulated guest peptides, indicating a high degree of cooperativity in the release process; (ii) under conditions where full neutralization of the polymer charged groups is not achieved, guest release efficiency is dependent on the strength of interaction between polymer and peptide, which in turn is dictated by the peptide charge and the nature and amount of charge on the polymer; (iii) peptides with a higher magnitude of complementary charge are harder to release but can be rescued with the use of a charge-conversion polymer; (iv) peptides are selectively released if they bear the same charge as the polymer at a given pH of the stripping aqueous phase; (v) release efficiency at different pHs is governed by the effective pK_a of the charged functional groups in the polymer; (vi) higher charge densities in the polymer typically lead to lower release efficiencies; and (vii) polymers bearing two adjacent charged groups in their

monomeric unit lead to lower release efficiencies due to a chelate-like effect brought about by their multidentate binding ability.

Overall, our findings suggest that much like the forward encapsulation process, guest release efficiency is optimizable depending on the aforementioned features of the guest and polymer host. Deeper insights into the underlying features that affect the forward and the reverse processes of encapsulation and guest release thus provides a more complete view for advancing catch-and-release applications involving polymeric reverse micelle assemblies. A method for quantitative release becomes especially critical when these amphiphilic polymeric assemblies are used for separations as in our pI bracketing technique. If quantitative MS measurement of the extracted guests is desired, this would require releasing them into an aqueous medium that is amenable to LC-ESI MS since this would give more reproducible signals and more quantitative analysis than MALDI.

Experimental Methods

Reagents

The peptides bradykinin (RPPGFSPFR) and angiotensin I (DRVYIHPFHL) were purchased from Sigma-Aldrich. TAMRA-bradykinin (TAMRA dye conjugated at the N-terminus of the peptide) was obtained from Biopeptek Inc (Malvern, PA). The following peptides were purchased from the American Peptide Company (Sunnyvale, CA): kinetensin (IARRHPYFL), malantide (RTKRSGSVYEPLKI), β-amyloid fragment 10-20 (DAEFRHDSGYE). Trifluoroacetic acid (TFA), 3-morpholinopropane-1-sulfonic acid (MOPS) buffer and α-cyano-4-hydroxy-cinnamic acid (CHCA) were purchased from Sigma-Aldrich. Tris(hydroxymethyl)-aminomethane (Tris buffer), acetonitrile (ACN),

formic acid (FA), hydrochloric acid (HCl), sodium hydroxide, ammonium hydroxide (NH_4OH), glacial acetic acid, toluene, tetrahydrofuran (THF) and purified water were obtained from Fisher Scientific. THF was distilled over Na/benzophenone before use.

Polymer Synthesis and Characterization

Seven different polymers (**P1**-**P7**) were synthesized to study the effect of the supramolecular host on guest release. The synthetic scheme for each can be found in the Appendix section. Detailed synthesis and characterization are described in published works[29,32,43] and can be found in the accompanying Supplementary Information for each.

Preparation of Polymeric Reverse Micelle

Solutions of the amphiphilic polymers were prepared in toluene to form the reverse micelle assemblies. A concentration of 1×10^{-4} M was prepared by weighing the appropriate amount of polymer and dissolving in toluene by sonication until a clear solution was obtained. To serve as the water pool for the reverse micelles, 2 equivalents of water per carboxylate were added to the solution and sonicated again until optically clear.

Extraction and Release of Peptides

Peptide solutions were prepared in an aqueous buffer of 50 mM MOPS, pH 6.5. Extractions were done by adding 200 μL of the polymeric reverse micelle solution to 1 mL of the buffered peptide solution (0.2 μM of peptides bradykinin, angiotensin I, malantide, kinetensin and β-amyloid (10-20); 0.5 μM of TAMRA-bradykinin), mixing them by vortex for 2 hours, and separating the two phases by centrifugation at 12,500 rpm for 60 minutes. The aqueous phase was carefully drawn out and transferred to a separate tube, leaving the organic phase with the extracted peptides in the original tube. Peptide release was

accomplished by the addition of 100 μL of THF (unless otherwise noted), followed by the addition of the specified stripping aqueous phase (*e.g.* 10% acetic acid, water, buffer, or NaCl solutions). The mixture was vortexed for 2 hours to allow for peptide release from the organic phase into the stripping aqueous phase. The released peptides in the aqueous phase were analyzed either by MALDI-MS, LC-MS, or fluorescence spectroscopy for quantification (protocols and methods described below). The release efficiency was calculated as:

$$Release\ efficiency = \frac{[Concentration\ of\ peptide\ in\ stripping\ aqueous\ phase]}{[initial\ concentration\ of\ peptide] \bullet Concentration\ Factor}\ x\ 100$$

where $Concentration\ Factor = \frac{initial\ volume\ of\ peptide}{final\ vol\ of\ peptide\ in\ stripping\ aqueous\ phase}$

MALDI-MS Analysis

A Bruker UltraFlextreme time-of-flight mass spectrometer was used for the MALDI-MS analysis of the samples. Acquisition of all mass spectra was done in reflectron mode. A matrix solution of CHCA was prepared by dissolving 15 mg in 350 μL THF, 150 μL H_2O and 6 μL TFA. Analysis of the aqueous phase was done by mixing the aqueous sample at 1:1 (v/v) ratio of sample to matrix solution and spotting 1 μL on the MALDI target. Analysis of the organic phase was done by first evaporating the toluene with a stream of N_2 and reconstituting the dried residue with 10 μL of THF and 20 μL of the CHCA matrix solution, then spotting 1 μL of this mixture on the MALDI target.

Fluorescence Spectroscopy

Fluorescence measurements were conducted on a Photon Technology International fluorimeter. Emission scans for TAMRA-bradykinin solutions were acquired from 560 nm

to 620 nm at an excitation wavelength of 550 nm. The fluorescence intensity at 582 nm (λ_{max}) of standard solutions of TAMRA-bradykinin was measured and plotted to generate a calibration curve. The fluorescence intensity of unknown samples were measured at the same wavelength (λ_{max}=582 nm) and their concentrations were determined based on the calibration curve by linear regression analysis.

LC-MS Analysis

Peptides, released into the stripping aqueous phase, were separated by reversed phase capillary liquid chromatography on a Thermo Fisher Scientific Acclaim PepMap 100 C18 column (2 μm particle size, 150 mm length, 0.3 mm I.D.) coupled to a Bruker AmaZon quadrupole ion trap mass spectrometer for detection. LC-grade water with 0.1% FA was used as mobile phase A, while degassed ACN with 0.1% FA was used as mobile phase B. A 5-μL injection volume was used and the flowrate was set to 4 μL/min with the following gradient: 5% B at 0-5 min., ramped to 50% B from 5-30 min., ramped to 95% B from 30-35 min., washed at 95% B from 35-40 min., then down to 5% B from 40-45 min. The LC system was coupled on-line to the mass spectrometer using electrospray ionization with 10 psi nebulizer pressure, 5 L/min dry gas, and 240 °C dry gas temperature. Mass spectra were acquired for the duration of the LC run from *m/z* 200-2000, with a trap drive of 70. Chromatograms and mass spectra were analyzed using Bruker Compass 1.3 DataAnalysis version 4.0 software. The concentration of released peptides (C_x) in the stripping aqueous phase was quantified by the standard addition method where increasing volumes (V_{std}) of known standard peptide concentration (C_{std}) was spiked into fixed volume aliquots (V_x) of the aqueous phase and then diluted to the same final volume. Spiked and unspiked aliquots were run on the LC-MS, and the resulting integrated peak areas for the extracted ion

chromatogram (EIC) of the peptide for each aliquot were plotted against the volume of the spiked standard in the sample (example standard addition plot shown below). From this plot, the concentration of the peptide (C_x) in the unspiked aliquot was calculated as:

$$C_x = \frac{(y\ intercept)(C_{std}\ spiked)}{(slope)(V_x\ of\ aliquot)}$$

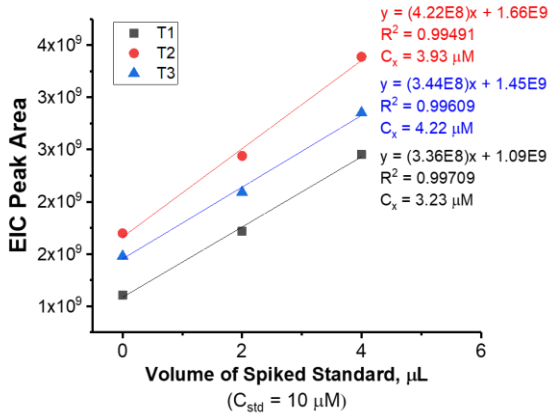

References

(1) Hu, J.; Liu, S. Engineering responsive polymer building blocks with host-guest molecular recognition for functional applications. *Acc. Chem. Res.* **2014**, *47*, 2084–2095.

(2) Gao, G. H.; Park, M. J.; Li, Y.; Im, G. H.; Kim, J.-H.; Kim H. N.; Lee, J. W.; Jeon, P.; Bang, O. Y.; Lee, J. H.; Lee, D. S. The use of pH-sensitive positively charged polymeric micelles for protein delivery. *Biomaterials* **2012**, *33*, 9157–9164.

(3) Du, A. W.; Stenzel, M. H. Drug carriers for the delivery of therapeutic peptides. *Biomacromolecules* **2014**, *15*, 1097–1114.

(4) Jones, M.-C.; Leroux, J.-C. Reverse micelles from amphiphilic branched polymers. *Soft Matter* **2010**, *6*, 5850-5859.

(5) Khmelmitsky, Y. L.; Gladilin, A. K.; Roubailo, V. L.; Martinek, K.; Levashov, A. V. Reversed micelles of polymeric surfactants in nonpolar organic solvents: A new microheterogeneous medium for enzymatic reactions. *Eur. J. Biochem.* **1992**, *206*, 737–745.

(6) Kirkorian, K.; Ellis, A.; Twyman, L. J. Catalytic hyperbranched polymers as enzyme mimics: exploiting the principles of encapsulation and supramolecular chemistry. *Chem. Soc. Rev.* **2012**, *41*, 6138–6159.

(7) Tu, Y.; Peng, F.; Adawy, A.; Men, Y.; Abdelmohsen, L. K. E. A.; Wilson, D. A. Mimicking the cell: Bio-Inspired functions of supramolecular assemblies. *Chem. Rev.* **2016**, *116*, 2023-2078.

(8) Savariar, E. N.; Ghosh, S.; González, D. C.; Thayumanavan, S. Disassembly of noncovalent amphiphilic polymers with proteins and utility in pattern sensing. *J. Am. Chem. Soc.* **2008**, *130*, 5416–5417.

(9) Jin, X.; Zhang, X.; Wu, Z.; Teng, D.; Zhang, X.; Wang, Y; Wang, Z.; Li, C. Amphiphilic random glycopolymer based on phenylboronic acid: synthesis, characterization, and potential as glucose-sensitive matrix. *Biomacromolecules* **2009**, *10*, 1337–1345.

(10) Gillissen, M. A. J.; Voets, I. K.; Meijer, E. W.; Palmans, A. R. A. Single chain polymeric nanoparticles as compartmentalised sensors for metal ions. *Polym. Chem.* **2012**, *3*, 3166-3174.

(11) Cheng, F.; Yang, X.; Peng, H.; Chen, D.; Jiang, M. Well-controlled formation of polymeric micelles with a nanosized aqueous core and their applications as nanoreactors. *Macromolecules* **2007,** *40*, 8007–8014.

(12) Bae, Y.; Fukushima, S.; Harada, A.; Kataoka, K. Design of environment-sensitive supramolecular assemblies for intracellular drug delivery: Polymeric micelles that are responsive to intracellular pH change. *Angew. Chem. Int. Ed.* **2003,** *42*, 4640–4643.

(13) Esser-Kahn, A. P.; Odom, S. A.; Sottos, N. R.; White, S. R.; Moore, J. S. Triggered release from polymer capsules. *Macromolecules* **2011,** *44*, 5539–5553.

(14) Jackson, A. W.; Fulton, D. A. Triggering polymeric nanoparticle disassembly through the simultaneous application of two different stimuli. *Macromolecules* **2012,** *45*, 2699–2708.

(15) Mura, S.; Nicolas, J.; Couvreur, P. Stimuli-responsive nanocarriers for drug delivery. *Nat. Mater.* **2013,** *12*, 991–1003.

(16) Quinn, J. F.; Whittaker, M. R.; Davis, T. P. Glutathione responsive polymers and their application in drug delivery systems. *Polym. Chem.* **2017,** *8*, 97–126.

(17) Chen, Y.; Dong, C. M. pH-Sensitive supramolecular polypeptide-based micelles and reverse micelles mediated by hydrogen-bonding interactions or host-guest chemistry: Characterization and in vitro controlled drug release. *J. Phys. Chem. B* **2010,** *114*, 7461–7468.

(18) Trivedi, R.; Kompella, U. B. Nanomicellar formulations for sustained drug delivery. *Nanomedicine* **2010,** *5*, 485–505.

(19) Lee, J. H.; Yeo, Y. Controlled drug release from pharmaceutical nanocarriers. *Chem. Eng. Sci.* **2015,** *125*, 75–84.

(20) Mathew, D. S.; Juang, R. S. Improved back extraction of papain from AOT reverse micelles using alcohols and a counter-ionic surfactant. *Biochem. Eng. J.* **2005,** *25,* 219–225.

(21) Tonova, K.; Lazarova, Z. Reversed micelle solvents as tools of enzyme purification and enzyme-catalyzed conversion. *Biotechnol. Adv.* **2008,** *26,* 516–532.

(22) Jarudilokkul, S.; Poppenborg, L. H.; Stuckey, D. C. Backward extraction of reverse micellar encapsulated proteins using a counterionic surfactant. *Biotechnol. Bioeng.* **1999,** *62,* 593–601.

(23) Mohan, A.; Rajendran, S. R. C. K.; He, Q. S.; Bazinet, L.; Udenigwe, C. C. Encapsulation of food protein hydrolysates and peptides: a review. *RSC Adv.* **2015,** *5,* 79270–79278.

(24) Mazzola, P. G.; Lopes, A. M.; Hasmann, F. A.; Jozala, A. F.; Penna, T. CV.; Magalhaes, P. O.; Rangel-Yagui, C. O.; Pessoa, A. Jr. Liquid-liquid extraction of biomolecules: an overview and update of the main techniques. *J. Chem. Technol. Biotechnol.* **2008,** *83,* 143–157.

(25) Jones, M. C.; Tewari, P.; Blei, C.; Hales, K.; Pochan, D. J.; Leroux, J.-C. Self-assembled nanocages for hydrophilic guest molecules. *J. Am. Chem. Soc.* **2006,** *128,* 14599–14605.

(26) Audran, R.; Peter, K.; Dannull, J.; Men, Y.; Scandella, E.; Groettrup, M.; Gander, B.; Corradin, G. Encapsulation of peptides in biodegradable microspheres prolongs their MHC class-I presentation by dendritic cells and macrophages *in vitro*. *Vaccine* **2003,** *21,* 1250–1255.

(27) Kumar, M.; Gupta, D.; Singh, G.; Sharma, S.; Bhat, M.; Prashant, C. K.; Dinda, A. K.; Kharbanda, S.; Kufe, D.; Singh, H. Novel polymeric nanoparticles for intracellular delivery of peptide cargos: Antitumor efficacy of the BCL-2 conversion peptide NuBCP-9. *Cancer Res.* **2014,** *74,* 3271–3281.

(28) Kale, T. S.; Klaikherd, A.; Popere, B.; Thayumanavan, S. Supramolecular assemblies of amphiphilic homopolymers. *Langmuir* **2009**, *25* (17), 9660–9670.

(29) Zhao, B.; Serrano, M.A.C.; Gao, J.; Zhuang, J.; Vachet, R.W.; Thayumanavan, S. Self-assembly of random co-polymers for selective binding and detection of peptides. *Polym. Chem.* **2018**, *9*, 1066-1071.

(30) Combariza, M. Y.; Savariar, E. N.; Vutukuri, D. R.; Thayumanavan, S.; Vachet, R. W. Polymeric inverse micelles as selective peptide extraction agents for MALDI-MS analysis. *Anal. Chem.* **2007,** *79,* 7124–7130.

(31) Zhao, B.; Serrano, M. A. C.; Wang, M.; Liu, T.; Gordon, M. R.; Thayumanavan, S.; Vachet, R. W. Improved mass spectrometric detection of acidic peptides by variations in the functional group pKa values of reverse micelle extraction agents. *Analyst* **2018**, *143*, 1434–1443.

(32) Zhao, B.; Zhuang, J.; Serrano, M. A. C.; Vachet, R. W.; Thayumanavan, S. Influence of charge density on host-guest interactions within amphiphilic polymer assemblies in apolar media. *Macromolecules,* 2017, 50, 9734–9741.

(33) Rodthongkum, N.; Ramireddy, R.; Thayumanavan, S.; Richard, W. V. Selective enrichment and sensitive detection of peptide and protein biomarkers in human serum using polymeric reverse micelles and MALDI-MS. *Analyst* **2012,** *137,* 1024–1030.

(34) Wang, F.; Gomez-Escudero, A.; Ramireddy, R. R.; Murage, G.; Thayumanavan, S.; Vachet, R. W. Electrostatic control of peptide side-chain reactivity using amphiphilic homopolymer-based supramolecular assemblies. *J. Am. Chem. Soc.* **2013,** *135,* 14179–14188.

(35) Lee, S.-S.; Hwang, K.-S.; Lee, B.-K.; Hong, D.-P.; Kuboi, R. Interaction between reverse micelles as a key factor governing back-extraction of proteins and its control systems. *Korean J. Chem. Eng.* **2005,** *22,* 611–616.

(36) Chen, J.; Chen, F.; Wang, X.; Zhao, X.; Ao, Q. The forward and backward transport processes in the AOT/hexane reversed micellar extraction of soybean protein. *J. Food Sci. Technol.* **2012,** *51,* 2851–2856.

(37) Yu, Y. C.; Chu, Y.; Ji, J. Y. Study of the factors affecting the forward and back extraction of yeast-lipase and its activity by reverse micelles. *J. Colloid Interface Sci.* **2003,** *267,* 60–64.

(38) Zhao, X.; Chen, F.; Gai, G.; Chen, J.; Xue, W.; Lee, L. Effects of extraction temperature, ionic strength and contact time on efficiency of bis(2-ethylhexyl) sodium sulfosuccinate (AOT) reverse micellar backward extraction of soy protein and isoflavones from soy flour. *J. Sci. Food Agric.* **2008,** *88,* 590–596.

(39) Koyamatsu, Y.; Hirano, T.; Kakizawa, Y.; Okano, F.; Takarada, T.; Maeda, M. pH-responsive release of proteins from biocompatible and biodegradable reverse polymer micelles. *J. Control. Release* **2014,** *173,* 89–95.

(40) Jones, M. C.; Gao, H.; Leroux, J. C. Reverse polymeric micelles for pharmaceutical applications. *J. Control. Release* **2008,** *132*, 208–215.

(41) Kang, S.; Kim, Y.; Song, Y.; Choi, J. U.; Park, E.; Choi, W.; Park, J.; Lee, Y. Comparison of pH-sensitive degradability of maleic acid amide derivatives. *Bioorganic & Medicinal Chemistry Letters* **2014**, *24*, 2364-2367.

(42) Rodthongkum, N.; Washington, J. D.; Savariar, E. N.; Thayumanavan, S.; Vachet, R. W. Generating peptide titration-type curves using polymeric reverse micelles as selective extraction agents along with matrix-assisted laser desorption ionization-mass spectrometry detection. *Anal. Chem.* **2009,** *81,* 5046–53.

(43) Serrano, M. A. C.; Zhao, B.; He, H.; Thayumanavan, S.; Vachet, R. W. Molecular Features Influencing the Release of Peptides from Amphiphilic Polymeric Reverse Micelles. *Langmuir* **2018**, *34* (15), 4595–4602.

CHAPTER IV

SELECTIVE DEPLETION OF ABUNDANT ACIDIC PROTEINS IN SERUM USING POLYMERIC REVERSE MICELLES

Abstract

The analysis of low-level protein biomarkers in serum is precluded by the presence of other highly abundant serum proteins. Hence, the preliminary removal of serum albumin along with other abundant proteins in serum (immunoglobulins, transferrin, haptoglobin, α-2-macroglobulin and apolipoproteins), is often a requirement prior to any biomarker analysis. In this work, we take advantage of the low isoelectric points (pI) of these top abundant proteins to selectively deplete them from serum using functionalized amphiphilic polymeric nanoassemblies. The selectivity of extraction is dependent on the pI of the protein and the extraction pH, which holds true even for extremely complex protein mixtures like serum. High extraction capacity was achieved by optimizing the extraction conditions and was found to be comparable with currently available methods for depletion. Depletion of these abundant acidic proteins allowed for the enhanced detection of higher pI proteins and enabled three orders of magnitude increase in detection sensitivity for a putative cancer biomarker, demonstrating the utility of these polymeric assemblies for enhancing the analysis of the serum proteome.

Introduction

Serum is the most common clinical source of disease biomarkers due to the ease and minimally invasive means of obtaining samples from patients and the fact that it is rich in biomolecules, proteins in particular, that can reflect the overall physiological status of the body. Besides human serum albumin (HSA), which constitutes about 55% of total serum proteins by mass, serum also contains a wide variety of immunoglobulins, signaling peptides and proteins, such as hormones and cytokines, and proteins leaked by tissues into circulation as a result of cell death, damage, abnormal physiology or diseased state.[1] Detection and reliable measurement of low-level proteins is of prime importance for biomarker discovery, early disease diagnosis and disease progression monitoring. However, these efforts are challenged, not only by the sheer complexity of the serum proteome, but also by protein concentrations that vary over ten orders of magnitude. The top six abundant proteins in serum, for instance, comprise about 85% of its total protein content[2] (Figure 4.1), and hence dominate the signal in proteomic analyses[3] and obscure the presence of low-level putative biomarkers.

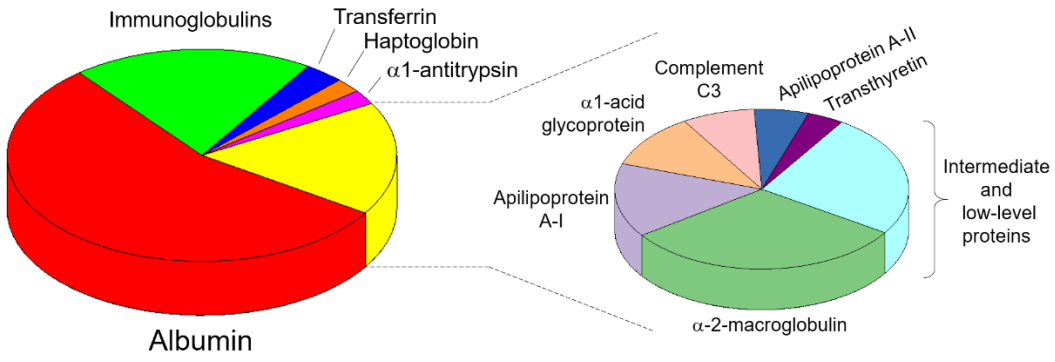

Figure 4.1. The abundant proteins in serum.

In addressing this challenge, various methods have been developed to remove or reduce the concentration of these highly abundant serum proteins to improve the detection of low abundance proteins. Chemical-based strategies that rely on precipitating agents to deplete albumin have been used for a long time,[4–6] but the selectivity of these precipitation techniques is hard to predict and control. Commercially-available immunoaffinity-based depletion methods that use antibodies to selectively remove albumin and other abundant serum proteins have high specificities and remove these proteins efficiently.[2,7–9] However, these commercially available products tend to be costly and suffer from stability and leakage issues when used under harsher conditions or upon storage for long times. Kits and columns using immuno-depletion strategies also have limited sample loading capacity, usually a few tens of microliters of serum. Ligand affinity-based methods, such as immobilized Cibacron Blue dye for depleting albumin,[10–12] and immobilized Protein A/Protein G for binding to the Fc region of immunoglobulins,[13–15] are also commercially available options for selective protein removal. Although less costly and capable of higher sample loading than immuno-depletion methods,[9] these ligand affinity-based methods are more prone to non-specific binding and tend to dilute the sample through several washing and elution steps.

Newer polymer-based depletion methods have been recently explored as they offer advantages in terms of stability and capacity. Their structure and chemistry can be optimized to achieve high sample loading capacity and sufficient selectivity, while working under harsher conditions. Various strategies for imparting selectivity for binding HSA have been reported, such as functionalization of polymers with albumin-binding ligands[16] and via molecular imprinting.[17–19] To our knowledge, however, very few, if any, polymers have

been developed to simultaneously target a wider range of proteins, thereby limiting their applicability if deeper mining of the serum proteome is desired.

Removing a select set of proteins at the same time requires a common property among the proteins. A survey of the properties of the abundant serum proteins reveals that most of them are acidic or low-pI proteins. Taking this into account, we envisioned the use of a polymer that could bind to the top abundant proteins based on their isoelectric point (pI). A protein's pI determines its net charge at a given solution pH; at pH 7, for instance, proteins with pI lower than 7 will be negatively charged. Thus, by virtue of electrostatic interaction, a cationic polymer will have affinity for low-pI proteins. Our group has recently utilized amphiphilic polymers for the selective enrichment of peptides based on their pI values to enhance their detection.[20–23] We have previously demonstrated how these polymeric materials self-assemble into highly stable nanoassemblies in non-polar solvents[24–26] and are capable of selectively enriching complementary peptides when used in the biphasic extraction of complex mixtures.[27–29] In this chapter, I describe investigations on the utility of these materials to extract whole proteins from serum. Using these supramolecular hosts for extracting proteins in this format has several advantages: (*i*) simple preparation of the reverse micelles is achieved by mere self-assembly in a non-polar solvent; (*ii*) the reverse micelle assemblies are highly stable nanocontainers for extraction; (*iii*) the functional group on the polymer can be easily varied; (*iv*) selectivity is tunable by simply controlling the extraction pH; and (*v*) high extraction capacity can be achieved due to multivalent binding. We find that these polymeric assemblies selectively and efficiently deplete abundant acidic proteins from serum and demonstrate how this depletion can improve the detection sensitivity of a cancer biomarker.

Results and Discussion

Extraction Selectivity

Extraction of complex peptide mixtures using nanoassemblies of a positively charged amphiphilic polymer has been previously shown to enable the enrichment of acidic peptides into the organic phase, enhancing their subsequent detection.[27] The polymer used is a styrene-based homopolymer, **P8** (Figure 4.2), functionalized with a quaternary ammonium group that makes it positively charged, and a hydrophobic decyl chain that balances the hydrophilicity of the charged group. This property allows the polymer to self-assemble into reverse micelle-like nanostructures upon dissolution in an apolar solvent. In these assemblies, the charged moieties form a hydrophilic core while the hydrophobic groups are oriented on the outside (Figure 4.2).

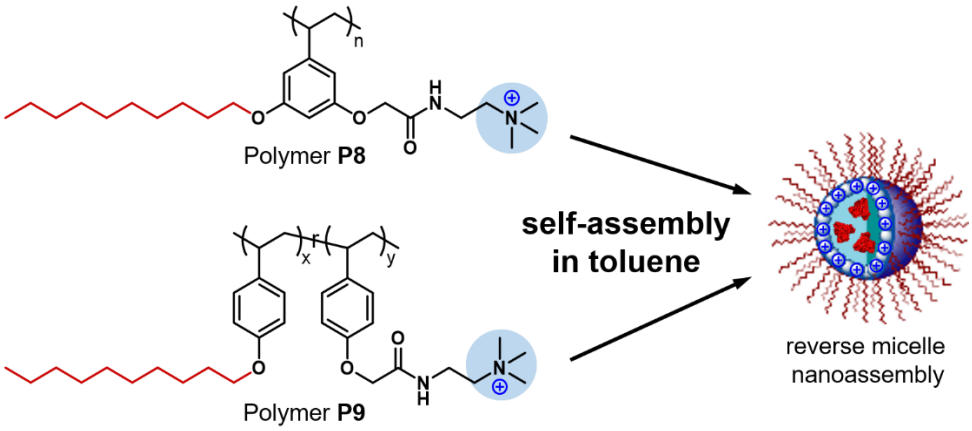

Figure 4.2. Chemical structures of amphiphilic homopolymer **P8** and random copolymer **P9** and a cartoon representation of a positively charged reverse micelle-like nanoassembly encapsulating negatively charged proteins.

Selective binding and extraction of acidic, negatively charged peptides to the nanoassemblies of **P8** are based on electrostatic interactions, which in turn can be tuned by controlling the aqueous phase pH used in the extraction.[27] Because albumin, the most

abundant serum protein, has a low pI value, it was postulated that the same polymer could be used to selectively bind the protein at a pH higher than its pI, while leaving higher pI proteins behind. This idea was tested by extracting an aqueous mixture of bovine serum albumin (BSA, pI=4.7) and cytochrome c (CC, pI=9.6) at pH 7.3 using assemblies of **P8** in toluene. Based on their respective LC peaks before and after extraction (Figure 4.3), it is clear that the high-pI protein, CC, remains in aqueous solution after extraction, while BSA has been removed. This result confirms the ability of the polymeric assembly to remove proteins based on their pI.

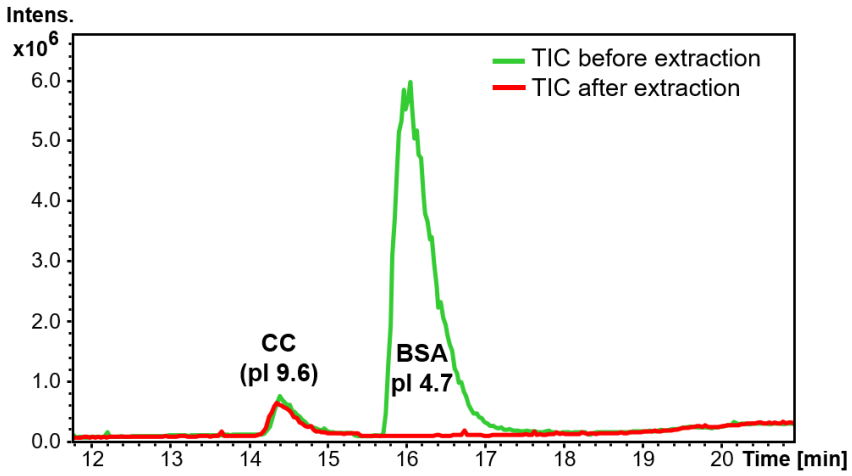

Figure 4.3. Total ion chromatogram (TIC) of a mixture of 8 μM each of bovine serum albumin (BSA) and cytochrome c (CC) before and after extraction using 1 mg/mL of **P8** in toluene.

We also investigated the selective protein extraction capability of a class of random copolymer-based assemblies that we reported recently,[26] as they offer synthetic versatility and simplicity as compared to homopolymers. Polymer **P9** (Figure 4.2) was designed and synthesized with the same alkylammonium and decyl functional groups as homopolymer **P8**. For the synthesis, two monomers were used and were polymerized by nitroxide-mediated radical polymerization (Figure 4.4). In addition to synthetic ease, polymer **P9**

could be solubilized in toluene at higher concentrations than polymer **P8**, making it more useful for protein depletion.

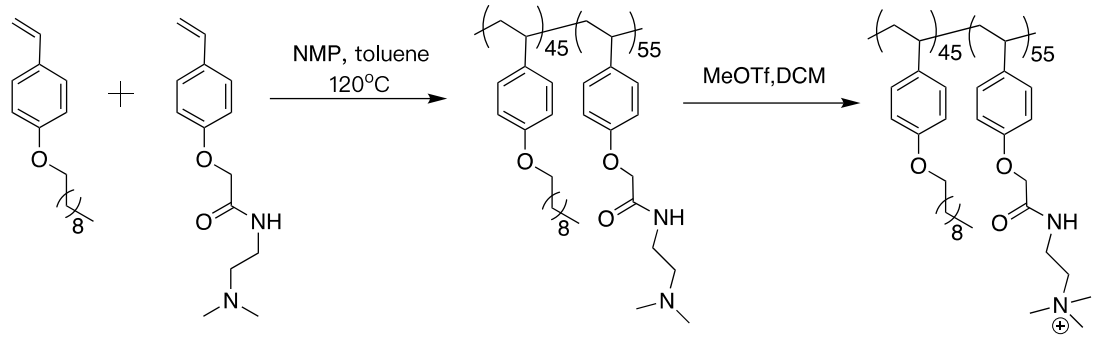

Figure 4.4. Synthesis of amphiphilic random copolymer **P9**.

Similar to **P8**, the extraction selectivity of **P9** was tested on a mixture of BSA and another high-pI protein, lysozyme (LZ, pI=11), and assemblies of this polymer show the same preferential removal of BSA from solution while retaining lysozyme after extraction (Figure 4.5).

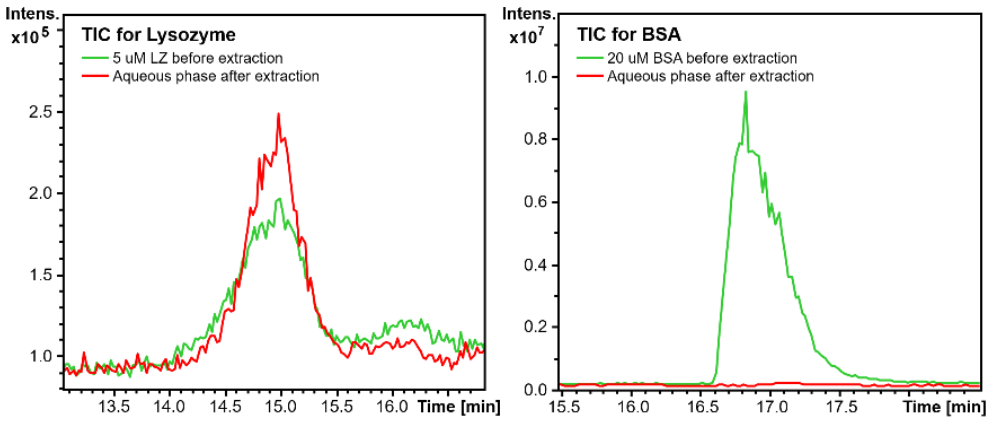

Figure 4.5. Total ion chromatogram (TIC) of a mixture of 5 µM lysozyme (LZ) and 20 µM bovine serum albumin (BSA) before and after extraction using **P9**.

We further tested the extraction selectivity of **P9** using an aqueous mixture of proteins with a range of pI values, including HSA (pI 4.7), BLG (pI 5.1), BCA (pI 6.2), TF (pI 6.8), CC (pI 9.6), and LZ (pI 11). Three sequential extractions using **P9** were performed at pH 7.4 and aliquots from each fraction were run on an SDS-PAGE gel to visualize which proteins are depleted (Figure 4.6A).

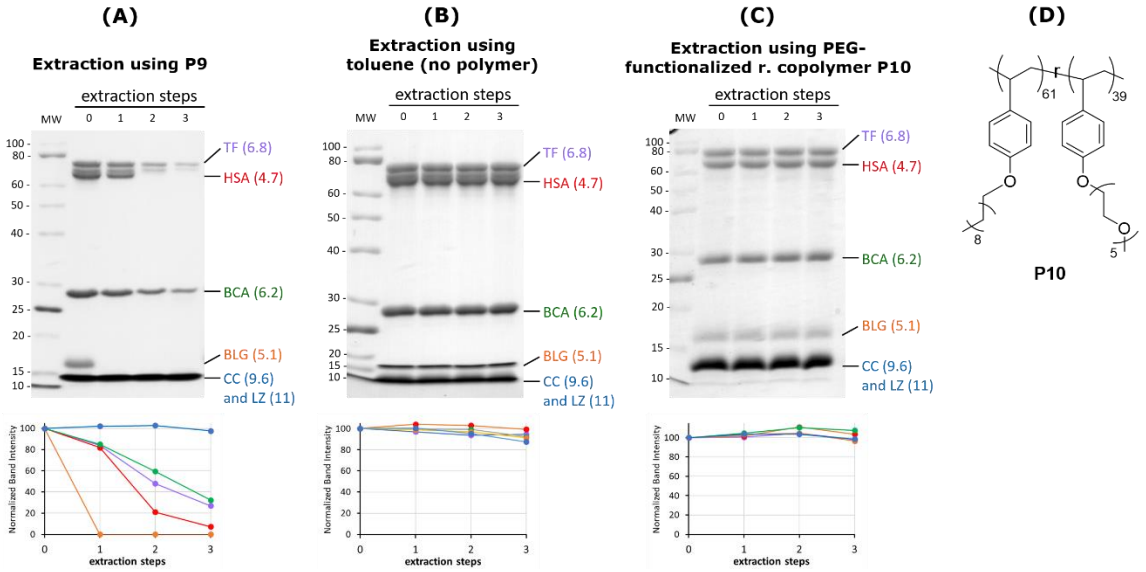

Figure 4.6. SDS-PAGE of a protein mixture before extraction and after each extraction step using nanoassemblies of **P9** (**A**), using toluene alone (**B**), and using nanoassemblies of **P10** (**C**) at pH 7.4. (**D**) Chemical structure of polymer **P10**. One mL containing 0.25 mg/mL of each protein was extracted with 200 µL of 2 mg/mL of either **P9** or **P10** in toluene or toluene alone. Band intensities (normalized to the initial intensity) of each protein in each fraction/lane were measured by *ImageJ* [30] and graphed accordingly as shown at the bottom of each gel image. pI values of each protein are indicated in parentheses. Proteins used: TF=transferrin, HSA=human serum albumin, BCA=bovine carbonic anhydrase, BLG=β-lactoglobulin, CC=cytochrome c, and LZ=lysozyme.

The acidic proteins HSA and BLG were effectively depleted by the polymer after one or two extractions. BCA and TF, which are slightly acidic, were also extracted by the polymer, but to a lesser extent. The inability to fully extract BCA and TF could be for three reasons. First, saturation of the nanoassemblies may have been reached. Second, the assemblies may have a preference for more highly acidic proteins, presumably due to a

greater magnitude of negative charges that can bind to the positively charged polymer sites. Third, a small fraction of the BCA and TF molecules have a net neutral or positive charge at pH 7.4, thereby influencing their extraction. Interestingly, we see no decrease in the amount of the basic proteins, CC and LZ, demonstrating the pI-dependent selectivity of extraction. As negative controls, extractions using only toluene (Figure 4.6B) and using an amphiphilic random co-polymer **P10** (Figure 4.6C), which has charge-neutral polyethylene glycol (PEG) groups as the hydrophilic functionality (Figure 4.6D), were also conducted. The control experiment using only toluene for extraction shows that proteins are not extracted into the organic phase without the polymeric nanoassemblies, while the results for extraction using **P10** prove that (1) the proteins do not get extracted when a charge-neutral amphiphilic polymer is used, and (2) the positively charged quaternary ammonium groups of **P9** are indeed responsible for the extraction selectivity.

Extraction Efficiency and Capacity

To assess the extraction efficiency and capacity of **P9**, the optimum extraction time needed for depletion was first determined. By monitoring the amount of HSA remaining after various extraction times, it was found that 30 minutes is needed to achieve efficient extraction without affecting the selectivity (Figure 4.7).

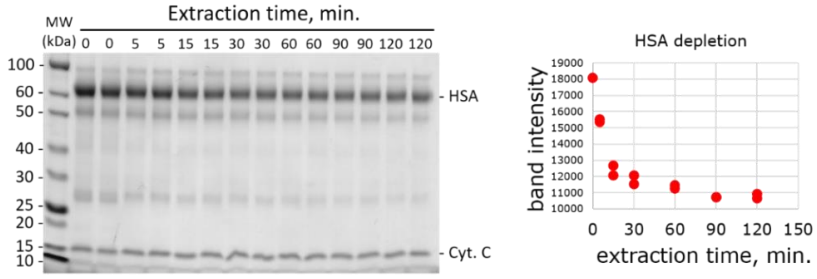

Figure 4.7. Determination of optimum extraction time for protein depletion. Serum spiked with cytochrome c was extracted using **P9** for different lengths of time. HSA depletion was visualized by running each depleted sample on an SDS-PAGE gel and measuring the band intensity by *ImageJ*.[30] Cytochrome c was spiked to check if selectivity is affected by increasing extraction times, which is not the case.

The extraction capacity for **P9** was then determined based on how much albumin can be extracted by a given amount of polymer. BSA solutions (1 mL) buffered at pH 7.4 were prepared at varying concentrations and then were extracted using the polymeric nanoassemblies. The BSA concentration remaining in the aqueous phase after extraction was measured by LC-MS and was used to back-calculate the concentration of BSA that was extracted (Figure 4.8A). Initially, 200 µL of a 1 mg/mL solution of **P9** was used for extraction and the capacity was about 10 µM. At a 2 mg/mL polymer concentration, the extraction capacity increased to about 20 µM of BSA. To increase the capacity even more, the volume of polymer solution used for extraction was doubled to 400 µL. This further improved the capacity to about 40 µM BSA, or the equivalent of 3.3 mg serum albumin extracted per mg of polymer, which is comparable to, if not better than other depletion methods based on polymers.[17] This relatively high extraction capacity can be attributed to the polycationic nature of the reverse micelle hosts, which allows for multiple binding sites with the protein. Our recent findings with peptide extractions reveal that increasing the charge density on the reverse micellar assemblies increases their extraction capacity but only up to a certain point, after which the assemblies become unstable and impairs their binding capacity.[25] It is possible that the optimum charge density has not yet been reached in this case and that the capacity may be increased even more by tuning the polymer structure (ratio of charged moiety and the hydrophilic-lipophilic balance). Structure-property optimization is of great interest, but it is beyond the scope of the current work.

To determine the polymer's capacity to deplete acidic proteins in serum, the amount of proteins extracted from serum was quantified using the Bradford assay. A three-step depletion using 200 µL of 2 mg/mL polymer was able to extract 57% of the total proteins,

while 400 µL of the same polymer concentration extracted 76% of the total proteins, which correlates well with the total proteins measured in the bound protein fraction (Figure 4.8B). A side-by-side comparison with an immuno-based depletion method reveals that a comparable depletion capacity (in terms of total proteins depleted) can be achieved by our polymer after a three-step extraction. It should be noted, however, that the sample loading capacity for the immunodepletion column is limited to 50 µL of serum, whereas our method can allow for higher sample loading capacity.

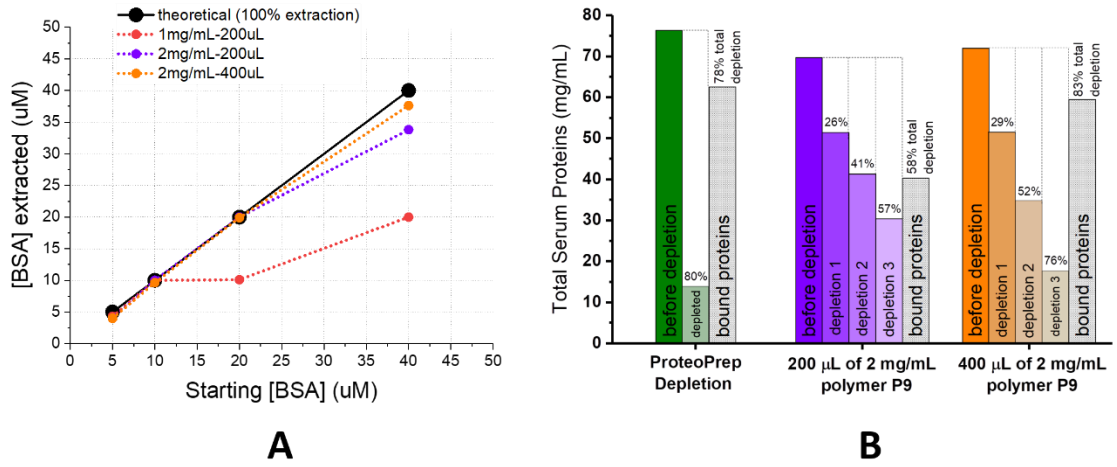

Figure 4.8. (A) Determination of extraction capacity of **P9**. Increasing concentrations of BSA (1 mL volume) were extracted with reverse micelles of **P9** with the indicated polymer concentration and volume. Deviation from the theoretical (100% extraction) line indicates that capacity has been reached as some BSA is left in solution. **(B)** Total protein content of serum (measured by the Bradford assay) before and after depletion using different methods. For all three methods, 50 µL of serum is the loading volume. Polymer depletion was carried out using the indicated polymer volume and concentration at pH 7.4, the same pH as the equilibration buffer for the ProteoPrep® immunoaffinity depletion method. Percentages on top of each bar indicate the percent of total proteins depleted after each step.

Depletion of Abundant Acidic Proteins in Serum

Upon demonstrating its extraction selectivity and capacity in protein mixtures, nanoassemblies of **P9** were employed for depleting the abundant low-pI serum proteins. Because HSA is so high in concentration in serum (up to about 50 mg/mL), it is the main target protein for depletion and the first protein examined. To check if the pI-dependent selectivity still applies to serum extractions, several standard proteins were spiked into serum at high enough concentrations to be visualized on a gel. Serum samples were then subjected to sequential extractions and the proteins remaining after each extraction step were analyzed by SDS-PAGE. Figure 4.9 shows that the extraction selectivity holds true even in a complex protein sample like serum. HSA, being an acidic protein, is clearly being depleted based on its fading gel band intensity, while the basic proteins, CC and LZ, remain

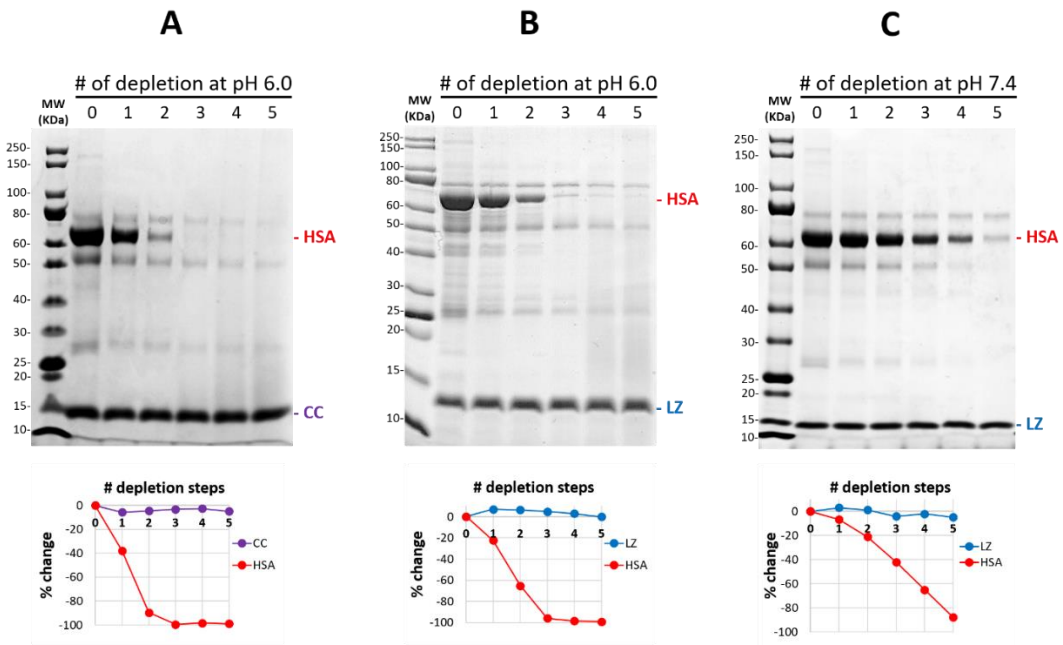

Figure 4.9. SDS-PAGE analysis of serum spiked with CC **(A)** and LZ **(B** and **C)**, to show the pI-dependent selectivity of extraction in serum. Five sequential extractions using 400 µL of 2 mg/mL of **P9** were performed at pH 6.0 for **(A)** and **(B)**, and at pH 7.4 for **(C)**. Changes in protein band intensity after each depletion step (relative to before extraction) were measured using *ImageJ* software and illustrated in a graph below each gel image. HSA is more efficiently depleted when the extraction is done at pH 6.0 than at pH 7.4. Selectivity is still retained at both pH values as shown by the unchanging band intensity for CC and LZ throughout 5 sequential extractions. pI of spiked proteins: CC (pI 9.6), LZ (pI 11).

unchanged throughout 5 sequential extractions. Interestingly, while the selectivity remains effective at both pH 6.0 and pH 7.4, we find that HSA is more efficiently depleted at pH 6.0 than at pH 7.4 (Figures 4.9B and 4.9C), presumably because fewer other proteins get extracted along with HSA at pH 6.0.

Identification of Serum Proteins Depleted

It is apparent that HSA is not the only protein being depleted by the polymer in serum. To determine the identity of the major proteins that are being depleted, an SDS-PAGE gel was run for each fraction: serum before depletion, after each depletion step, and the bound protein fraction (Figure 4.10). Fractions from serum depleted using the anti-HSA/anti-IgG spin column depletion kit was also run side-by-side our polymer-based depletion method for comparison and as a positive control. The prominent bands were excised and subjected to in-gel tryptic digestion for protein identification by LC-MS peptide mass fingerprinting (PMF). The bands were identified based on their apparent MW on the gel and the unique peptides detected from their in-gel tryptic digest as summarized in Table 4.1. Detailed results of the PMF analysis are presented in the Appendix (Tables A.1 to A.7).

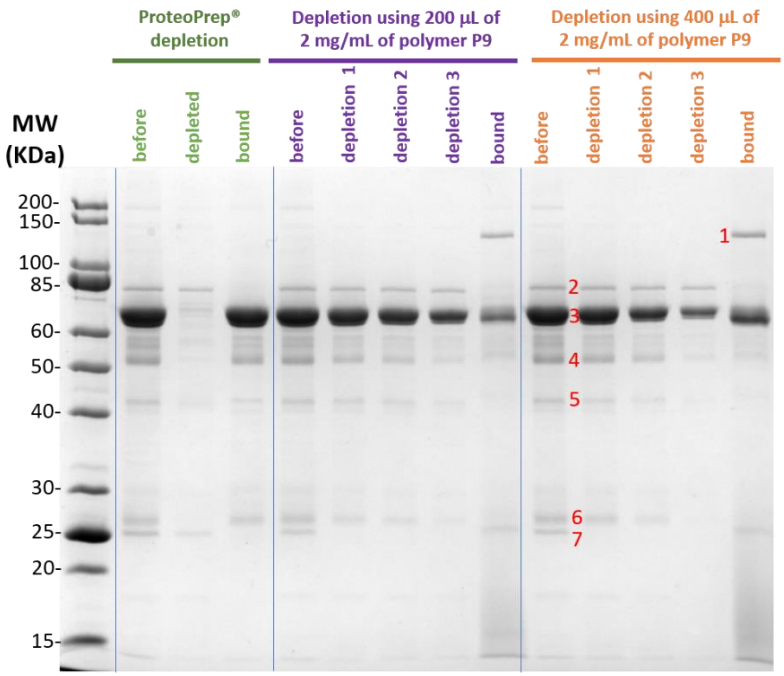

Figure 4.10. SDS-PAGE analysis of serum before and after depletion using the ProtePrep® immunodepletion kit and by multi-step depletion using reverse micelles of **P9** at pH 7.4. Bound proteins from the ProteoPrep column were eluted according to the manufacturer's protocol. Bound proteins from the polymer depletion were back-extracted from the organic phase by the addition of THF and 10% acetic acid.[31] Prominent bands that get depleted are numbered in red and carefully excised for digestion and LC-MS analysis.

Table 4.1. Protein identification of bands in SDS-PAGE gel of serum (from Figure 4.10).

Gel Band	**1**	**2**	**3**	**4**	**5**	**6**	**7**
Protein ID	α-2-macroglobulin	transferrin	serum albumin	IgG heavy chain	haptoglobin	IgG light chain	Apolipoprotein A-1
MW, kDa	163	77	69	52	45	25	28
pI	5.4	6.8	4.7	6-8.5 (variable)	6.1	6-8.5 (variable)	5.6
# Peptides belonging to protein	10	53	66	17	19	8	33
% Coverage	7.5%	57.3%	73.9%	45%	50.9%	46%	72.7%

The depleted proteins were found to be the abundant acidic proteins in serum, with pI values less than the extraction pH of 7.4, except perhaps for IgG whose pI is variable due to the presence of many different isoforms and glycosylation types. Still, some forms of IgG fall within the range of our predicted selectivity. This supports our hypothesis that the abundant low-pI proteins will be preferentially depleted from serum by the polymer. Interestingly, band 1, corresponding to α-2-macroglobulin, was not detected in any of the serum fractions but was prominent in the polymer-bound fraction. It is possible that additional proteins have bound to the polymer but were not detected by SDS-PAGE. Therefore, to get an idea of all the proteins that were depleted, a more in-depth analysis of the bound protein fraction was carried out by tryptic digestion followed by bottom-up proteomic analysis using LC-MS/MS. Listed in Table 4.2 are the proteins identified in the digest, with their calculated pI values. We see the same seven proteins identified in the gel, along with other proteins that have pI values less than or around 7.4 (except again for IgG as explained above), confirming the selectivity of extraction.

Table 4.2. Proteomic analysis of the polymer-bound fraction.

PROTEIN	pI	#Peptides identified	% Coverage	Protein Score (Proteome Discoverer)
Albumin	4.7	31	37.8	679.93
Apolipoprotein B-100	6.6	59	11.1	462.84
Complement C3	5.7	41	16.5	367.80
Apolipoprotein A-I	5.6	24	56.2	322.60
Apolipoprotein A-IV	5.3-5.4	28	44.2	306.21
Serotransferrin	6.8	20	19.5	253.73
Serpin peptidase inhibitor, clade A	5.6	19	29.4	224.24
Complement C4-A	6.7	24	11.9	205.05
Complement C4-B	7.3	24	12.2	204.38
α-2-macroglobulin	5.4	22	13.8	185.35
Inter-α-trypsin inhibitor heavy chain H2	7.0	18	15.7	159.61
Inter-α (Globulin) inhibitor H4	6.9	11	11.6	111.50
Apolipoprotein A-II	4.6	7	51.9	104.15
Clusterin	6.3	11	18.3	101.24
Apolipoprotein E	5.7	11	45.0	100.72
Antithrombin-III	6.7	13	26.1	95.49
Ig gamma-1 chain C region	6-8.5	9	15.2	87.09
Inter-alpha-trypsin inhibitor heavy chain H1	7.6	6	8.1	77.44
Hemopexin	6.4	8	11.7	72.94
Haptoglobin	6.1	7	15.3	62.32
Apolipoprotein C-I	7.5	7	49.4	60.38
Heparin cofactor 2	6.9	9	15.2	55.11
Ig kappa chain C region	6-8.5	2	12.6	54.72
Protein IGKV3-11	6.0	2	12.5	51.43
Ig gamma-3 chain C region	6-8.5	5	11.4	50.66
Apolipoprotein C-III	4.7-5.1	1	16.2	49.54

Effect of Depletion on Detection Sensitivity

Depletion of the highly abundant proteins reduces the extremely wide dynamic range of protein concentration in serum and hopefully improves the detection sensitivity for other proteins and peptides. To demonstrate the effect of our depletion strategy on the detection of other proteins, proteomic analysis of serum was done before and after depletion and the abundance for a select set of proteins were compared. Spectral counting,

a form of label-free LC-MS/MS relative quantitation, was used as a relative measure of protein abundance.[32–34] A comparison of spectral counts of the top abundant serum proteins before and after depletion at pH 6.0 was made for three replicate serum samples, with LZ spiked as a control (Figure 4.11). After depletion, a decrease in abundance of low-pI proteins and an increase in abundance of high-pI proteins were observed. This observation is most evident for the spiked basic protein, LZ, suggesting that this depletion strategy could be particularly advantageous for enhancing the detection of higher-pI proteins.

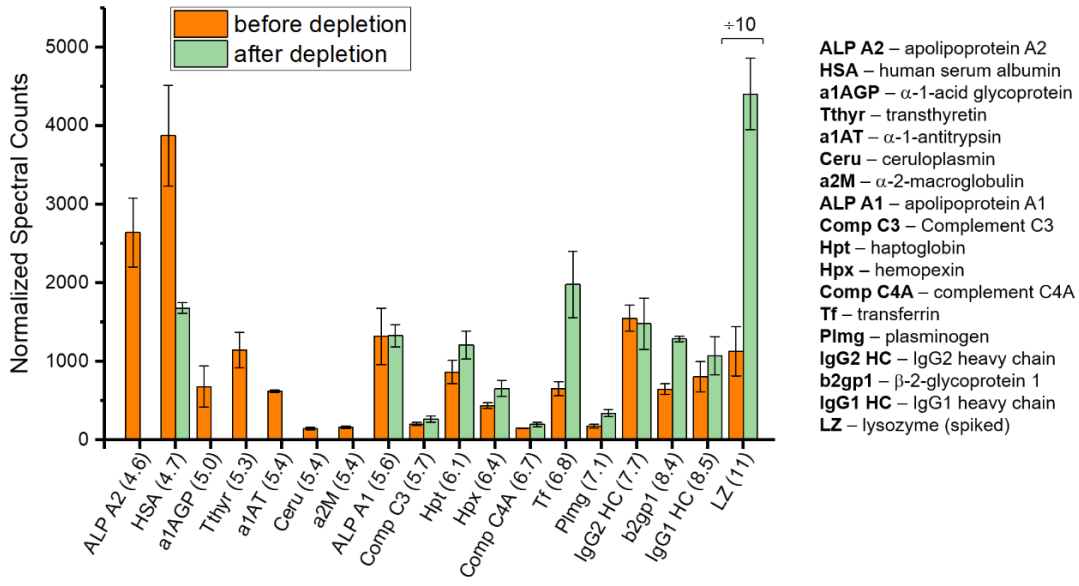

Figure 4.11. Comparison of spectral counts (SC) of selected serum proteins before and after depletion (3 sequential extractions using 400 µL of 2 mg/mL **P9**). Normalized spectral count accounts for the length of the protein by dividing its SC value by the number of amino acid residues. Calculated pI values of each protein are indicated in parentheses.

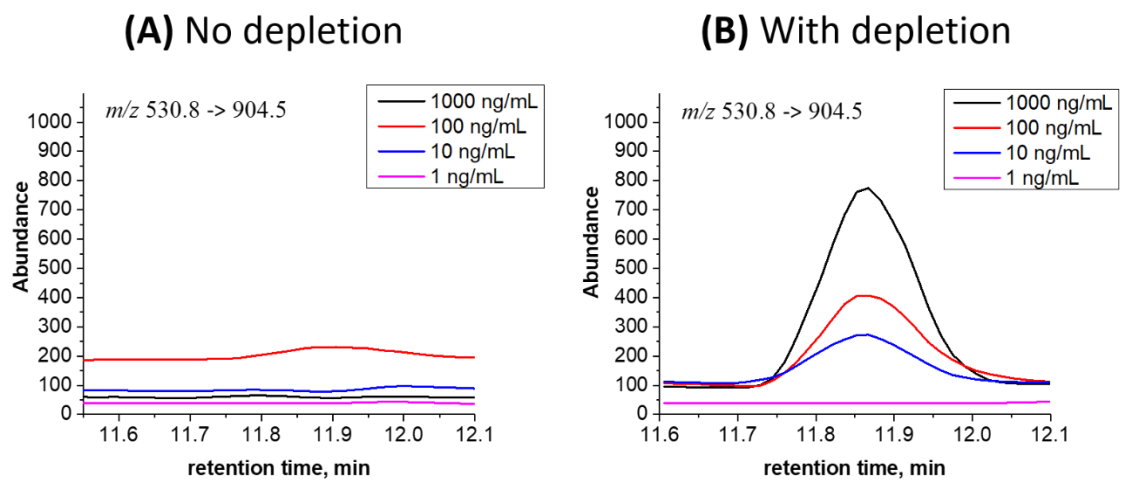

Figure 4.12. SRM chromatograms for bradykinin in serum samples where no depletion was done **(A)**, and with depletion using **P9** prior to analysis **(B)**. *m/z* 530.8 -> 904.5 transition corresponds to the precursor ion (+2 charge state) and product ion (y_8 ion) of bradykinin, respectively, that was monitored in SRM.

The effect of abundant proteins on sensitivity is even more pronounced in the realm of biomarker detection. This is because biomarkers are typically present in ng/mL levels in serum and the abundant proteins typically overwhelm the signal to mask the detection of these low-level proteins. To further demonstrate the effect of our depletion strategy on sensitivity, a putative breast cancer peptide biomarker, bradykinin[35] (RPPGFSPFR, MW 1060 g/mol, pI 12) was spiked at varying known concentrations in serum. The abundant proteins were depleted using our method in one set, while the other set was left undepleted. Detection of the spiked bradykinin peptide in each sample was done by selected reaction monitoring (SRM) measurements on a triple quadrupole mass spectrometer. Bradykinin was undetectable in any of the spiked serum samples where depletion of abundant proteins was not done (Figure 4.12A). On the other hand, bradykinin was detectable down to 10 ng/mL in the spiked serum samples where our depletion strategy was employed prior to analysis (Figure 4.12B), corresponding to at least three orders of magnitude increase in sensitivity compared to the undepleted serum. This underscores the need for abundant

protein depletion in trying to dig deeper into the serum proteome, especially for biomarker detection. Even a method as sensitive as SRM was not able to detect the high spike in the presence of these highly abundant interfering proteins. With the use of these polymeric nanomaterials, however, we were able to demonstrate a significant increase in detection sensitivity to levels that are of clinical utility.

Summary and Conclusions

In this chapter, the utility of reverse micelle nanoassemblies of amphiphilic polymers as functional materials for selectively depleting low-pI proteins from complex mixtures is demonstrated. By functionalizing the polymer with positively charged quaternary ammonium groups, selective binding of negatively charged proteins is achieved. The extraction selectivity is predictable based on the extraction pH and the protein's pI value, and holds true even in extremely complex protein mixtures like serum. The extraction capacity can be maximized by increasing the polymer concentration and volume used for extraction, for which a capacity comparable to currently available methods was achieved. The application of this strategy to effectively deplete the abundant acidic proteins in serum, most especially HSA and other apolipoproteins, was demonstrated, which in turn allowed for the enhanced detection of higher pI proteins. Furthermore, depletion of serum using our approach allowed for three orders of magnitude increase in detection sensitivity for a cancer biomarker. The utility of these materials for improving the analysis of serum and the detection of biomarkers offer a cheaper, tunable, and more stable alternative to costly antibody-based methods.

Experimental Methods

Materials and Reagents

MOPS (3-(N-morpholino)propanesulfonic acid) buffer, glycine, bromophenol blue, and ammonium bicarbonate were purchased from Sigma (St. Louis, MO). Urea was obtained from Acros Orgnics, while dithiothreitol (DTT) and iodoacetamide (IAM) were from Aldrich (Milwaukee, WI). Tris(hydroxymethyl)-aminomethane (Tris), acetonitrile (ACN), formic acid (FA), hydrochloric acid, sodium hydroxide, ammonium hydroxide, glacial acetic acid, toluene, tetrahydrofuran (THF), methanol, 40% acrylamide, sodium dodecyl sulfate (SDS), tetramethylethylenediamine (TEMED), ammomium persulfate, glycerol and purified water were obtained from Fisher Scientific. THF was distilled over Na/benzophenone before use. Pooled normal human serum samples were obtained from Innovative Research (Novi, MI). Protein standards, including bovine serum albumin (BSA), human serum albumin (HSA), chicken egg lysozyme (LZ), bovine cytochrome c (CC), equine myoglobin (MG), β-lactoglobulin (BLG), bovine carbonic anhydrase (BCA), human transferrin (TF), as well as the peptide biomarker bradykinin (RPPGFSPFR), were purchased from Sigma-Aldrich (St. Louis, MO). Molecular weight markers (10-250 kDa) for SDS-PAGE was purchased from New England Biolabs (Ipswich, MA). Sequencing-grade trypsin was acquired from Promega (Madison, WI).

Preparation of Reverse Micelles

Reverse micelles of the polymer were prepared by dissolving the appropriate amount of the solid polymer in a corresponding volume of toluene to make the intended concentration (*e.g.* 1 mg/mL or 2 mg/mL solution). The mixture was sonicated for at least 15 minutes to completely dissolve the solid, and 2 μL of water was added to serve as the

"water pool" interior of the assembly. The mixture was sonicated again for at least 15 minutes to yield a clear solution.

General Extraction Procedure

An aqueous solution of the protein, buffered at the specified pH using either 100 mM Tris or 100 mM MOPS buffer, was mixed with the prepared polymer assemblies in toluene using a vortex mixer for 30 minutes. After extraction, the mixture is centrifuged at 12500 rpm at 15˚C for 60 minutes to separate the aqueous from the toluene layer. The bottom aqueous phase is then carefully drawn out and transferred to another tube for sequential extraction or for subsequent analysis. Sequential extraction is done by adding a fresh solution of the polymeric assemblies to the aqueous phase and repeating the extraction procedure. The extracted or bound proteins in the toluene phase can also be subsequently analyzed by transferring them first to an aqueous medium using a back-extraction strategy described previously.[31] Briefly, 200 µL of THF is added to the organic phase to disrupt the assemblies, followed by the addition of 200 µL of 10% acetic acid (pH~2) to neutralize the electrostatic interaction between the polymer and the proteins. The mixture is placed on a vortex mixer for at least 30 minutes, followed by centrifugation at 3000 rpm for 60 minutes to separate the THF+polymer layer and the aqueous layer containing the back-extracted proteins.

Immunoaffinity Albumin and IgG Depletion

Immunodepletion using the ProteoPrep® albumin and IgG depletion kit (Sigma-Aldrich®, catalog number: PROTIA) was performed on serum samples according to the manufacturer's protocol. Briefly, 50 µL of serum was diluted to 100 µL using the equilibration buffer provided (pH 7.4) and applied to the top of the spin column. After a

10-minute incubation, the spin column was centrifuged for 60 seconds at 10,000 rpm. The flow-through was re-applied to the column bed, incubated for 10 minutes, and then centrifuged again. The remaining unbound proteins were eluted from the column by washing with 125 µL of the equilibration buffer. The combined flow-through contains the depleted serum.

Determination of Extraction Selectivity and Capacity by Intact Protein LC-MS

One-mL solutions containing a constant lysozyme concentration (5 µM) and variable BSA concentrations (5, 10, 20, 40 µM) were prepared in 100 mM MOPS buffered at pH 7.4, and extracted with the nanoassemblies as described in the general extraction procedure. Aliquots of each solution before and after depletion were analyzed by liquid chromatography (LC) on a reversed phase column (Phenomenex Jupiter® C4 column, 5µm, 300 Å, 150 mm x 1.00 mm) coupled to electrospray mass spectrometry (ESI-MS) to separate and measure the proteins in solution. Extraction selectivity and capacity were determined by comparing the LC-MS chromatogram for each protein before and after extraction. A calibration curve for BSA was used to calculate the amount of BSA remaining in solution after extraction and consequently the amount of BSA extracted. The following LC gradient was carried out using 1% acetic acid in water as mobile phase A and 1% acetic acid in ACN as mobile phase B, with 0.3 mL/min as flow rate: 5% B from 0-5 min, 70% B at 20 min, 95% B at 21 min, 95% B at 25 min, 5% B at 30 min, 5% B at 35 min. A Bruker Esquire ion trap mass spectrometer was used as detector with the following settings: nebulizer = 10.0 psi, dry gas = 7.00 L/min, dry temp = 300°C, trap drive = 70, *m/z* scan range = 200-2000.

SDS-PAGE Analysis

Samples for SDS-PAGE were first mixed 1:1 with a 2X loading dye containing 3% DTT, and then heated at 95˚C for 10 minutes. Ten microliters of sample were loaded onto each well of the gel (4% polyacrylamide stacking gel, 10% or 12% polyacrylamide resolving gel). Electrophoretic run was done at 150 V for 40-50 minutes on a 1X Tris/Glycine/SDS running buffer. Staining was done using Coomassie Brilliant Blue R-250 staining solution from Bio-Rad. The gels were imaged on a photo scanner and band intensities were quantified by *ImageJ* analysis[30] using the Analyze -> Gel function.

Total Protein Content

Bradford assays were used to measure the total protein content after each depletion step. The Coomassie protein assay reagent and the albumin standard ampules were obtained from Thermo Scientific (Product Number 23200). Standard solutions (0, 25, 125, 250, 500, 750, 1000, 1500 µg/mL albumin) were prepared by dilution of the stock albumin standard (2000 µg/mL) using the same buffer as the samples. 5 µL of each standard and unknown sample were mixed with 250 µL of the Coomassie reagent for 30 seconds and incubated for 10 minutes at room temperature. Afterwards, the absorbance of each solution at 595 nm was measured on a spectrophotometer. The absorbance readings were corrected by subtracting any absorbance from the blank. A plot of the corrected absorbance against the standard concentration was used to determine the total protein concentration in the samples. Any dilution done for samples with absorbance outside the linear range was accounted for by applying the appropriate dilution factor in the calculations.

In-Gel Trypsin Digestion of Protein Bands for Peptide Mass Fingerprinting

Each protein band of interest were excised from the gel, cut into smaller pieces and placed in a tube. The gel slices were washed and destained twice with 200 µL of 25 mM ammonium bicarbonate (NH_4HCO_3) in 50% ACN for 30 minutes at 37˚C. Protein disulfide bonds were reduced by treating with 50 µL of 50 mM DTT in 50 mM NH_4HCO_3 at 60˚C for 10 minutes. Alkylation of cysteines was carried out using 50 µL of 100 mM iodoacetamide in 50 mM NH_4HCO_3 in the dark at room temperature for 1 hour. The bands were washed twice with 200 µL of 25 mM NH_4HCO_3 in 50% ACN for 30 minutes at 37˚C and then dehydrated with 100% ACN for 10 minutes. To each tube, 48 µL of 50 mM NH_4HCO_3 was added, followed by 2 µL of 0.1 µg/µL sequencing grade trypsin (Promega) solution. Digestion was carried out overnight at 37˚C on a shaking water bath. The supernatant containing the digest was transferred to a sample tube and evaporated to dryness in a speed vac. The dried samples were reconstituted in 20 µL of 5% formic acid in LC-MS water prior to LC-MS/MS analysis.

In-Solution Trypsin Digestion for Proteomic Analysis

For protein samples in aqueous solution (*i.e.* fractions before and after depletion, and back-extracted bound proteins), trypsin digestion was done by first denaturing the proteins in 8 M urea. DTT was added to a final concentration of 500 mM to reduce the disulfides, and then incubated for 30 minutes at 37˚C. Alkylation of the cysteine thiols was accomplished by the addition of iodoacetamide (50 mM final concentration), followed by incubation in the dark at room temperature for 30 minutes. 50 mM ammonium bicarbonate was added to reduce the urea concentration to 1 M prior to addition of trypsin. Sequencing-grade trypsin was added at a 1:20 protein:enzyme ratio. Digestion was carried out by

incubating the samples overnight at 37˚C in a shaking water bath. Two mL of formic acid was added to inactivate trypsin and quench the digestion prior to LC-MS/MS analysis.

LC-MS/MS Analysis

Protein digests were analyzed by LC-MS/MS on an Orbitrap Fusion™ mass spectrometer (Thermo Scientific) coupled to an Easy-nanoLC 1000 UHPLC equipped with a FortisBIO C18 nano-flow column (150 mm x 75μm, 1.7 μm (Fortis Technologies Ltd.)). Nano-LC was run using 0.1% FA in water as mobile phase A, and 0.1% FA in ACN as mobile phase B, with a flow rate of 300 nL/min. For peptide mass fingerprinting of each in-gel tryptic digests, the following gradient was used: 0-1 min (0 to 4% B), 1-41 min (4-55% B), 42-52 min (95% B). For the bottom-up proteomic analysis, the following gradient was used: 0-90 min (0 to 50% B), 90-95 min (50-95% B), 95-115 min (95% B). For mass spectral detection, mass spectra were collected in positive polarity mode using the Orbitrap as the detector with a *m/z* scan range of 350-2000, resolution of 60,000, and automated gain control (AGC) target of 400,000. The most intense ions were selected for MS/MS. Dynamic exclusion was set to exclude precursor ions after being selected 3 times within a 15-second window. Exclusion duration is for 60 s, with a mass tolerance of ±10 ppm. Precursor ions selected for tandem mass spectrometry (MS/MS) were isolated and fragmented by collision induced dissociation (CID), with a collision energy of 35 and CID activation time of 10 ms. Tandem spectra were acquired on the ion trap detector with an AGC target value of 50,000.

Proteome Discoverer v1.4 (Thermo Scientific) was used as the analysis software for peptide identification based on the MS/MS data. Sequest HT was used as the search engine for identifying peptides and proteins by searching against the FASTA sequence for

the Uniprot human proteome database. The search parameters were as follows: trypsin-specific cleavage with a maximum of 4 missed cleavage sites, precursor mass tolerance of 10 ppm and fragment mass tolerance of 0.5 Da, carbamidomethylation of cysteine, oxidation of methionine, and N-terminal glutamine to pyroglutamate as dynamic modifications.

To get the spectral counts for the selected proteins before and after depletion, the raw MS files were first converted to .mfg files. Using several search engines (X!Tandem, MS-GF+, OMSSA, and MyriMatch), peptides and proteins were identified by searching against the FASTA sequence for the Uniprot human proteome database. The search parameters used were as follows: trypsin-specific cleavage, precursor mass tolerance of 10 ppm, carbamidomethylation of cysteine as fixed modification, and oxidation of methionine as variable modifications. PeptideShaker[36] (Compomics) integrates the results from multiple search engines and gives the value for the spectral counts (SC) for each identified protein, which were then compared for the serum samples before and after depletion (3 replicate samples were done).

SRM-MS Analysis of Spiked Bradykinin in Serum

The peptide bradykinin with a sequence of RPPGFSPFR (MW=1060 g/mol) was spiked at different concentrations (0, 1, 10, 100, 1000 nM) in serum. One set of spiked serum was left undepleted, while the other set was depleted by three sequential extractions using 400 µL of 2 mg/mL solution of the positively charged polymeric nanoassemblies. The serum samples were then digested with trypsin. Targeted detection of bradykinin by selected reaction monitoring (SRM) on a Waters TQD triple quadrupole mass spectrometer was employed on the digested serum samples. LC separation of the digest on a Supelco®

Discovery C18 (150mm x 2.1mm, 5µm (Sigma-Aldrich)) reversed phase column was done with with 0.1% FA in water as mobile phase A and 0.1% FA in ACN as mobile phase B under the following gradient: 0-5 min (5% B), 5-15 min (5-50% B), 15-20 min (50-95% B), 20-25 min (95% B), 25-25.1min (95-5% B), 25.1-30 min (5% B). The optimized SRM transition for the bradykinin peptide was determined to be the +2 charge for the precursor ion (*m/z* 530.8) and the y_8 product ion (*m/z* 904.5). SRM for this transition was acquired from 8 to 15 minutes of the LC run with an optimized collision energy of 22 and cone voltage of 44 V. The resulting SRM chromatogram was analyzed and processed using the MassLynx software.

References

(1) Anderson, N. L. The Human Plasma Proteome: History, Character, and Diagnostic Prospects. *Mol. Cell. Proteomics* **2002**, *1* (11), 845–867.

(2) Zolotarjova, N.; Martosella, J.; Nicol, G.; Bailey, J.; Boyes, B. E.; Barrett, W. C. Differences among Techniques for High-Abundant Protein Depletion. *Proteomics* **2005**, *5* (13), 3304–3313.

(3) Hortin, G. L.; Sviridov, D.; Anderson, N. L. High-Abundance Polypeptides of the Human Plasma Proteome Comprising the Top 4 Logs of Polypeptide Abundance. *Clin. Chem.* **2008**, *54*, 1608–1616.

(4) Cohn, E. J.; Strong, L. E.; Hughes, W. L.; Mulford, D. J.; Ashworth, J. N.; Melin, M.; Taylor, H. L. Preparation and Properties of Serum and Plasma Proteins. IV. A System for the Separation into Fractions of the Protein and Lipoprotein Components of Biological Tissues and Fluids. *J. Am. Chem. Soc.* **1946**, *68*, 459–475.

(5) Chen, Y. Y.; Lin, S. Y.; Yeh, Y. Y.; Hsiao, H. H.; Wu, C. Y.; Chen, S. T.; Wang, A. H. J. A Modified Protein Precipitation Procedure for Efficient Removal of Albumin from Serum. *Electrophoresis* **2005**, *26*, 2117–2127.

(6) Liu, G.; Zhao, Y.; Angeles, A.; Hamuro, L. L.; Arnold, M. E.; Shen, J. X. A Novel and Cost Effective Method of Removing Excess Albumin from Plasma/Serum Samples and Its Impacts on LC-MS/MS Bioanalysis of Therapeutic Proteins. *Anal. Chem.* **2014**, *86*, 8336–8343.

(7) Steel, L. F.; Trotter, M. G.; Nakajima, P. B.; Mattu, T. S.; Gonye, G.; Block, T. Efficient and Specific Removal of Albumin from Human Serum Samples. *Mol. Cell. Proteomics* **2003**, *2*, 262–270.

(8) Whiteaker, J. R.; Zhang, H.; Eng, J. K.; Fang, R.; Piening, B. D.; Feng, L.; Lorentzen, T. D.; Schoenherr, R. M.; Keane, J. F.; Holzman, T.; et al. Head-to-Head Comparison of Serum Fractionation Techniques Research Articles. *J. Proteome Res.* **2007**, *6*, 828–836.

(9) Björhall, K.; Miliotis, T.; Davidsson, P. Comparison of Different Depletion Strategies for Improved Resolution in Proteomic Analysis of Human Serum Samples. *Proteomics* **2005**, *5*, 307–317.

(10) Gianazza, E.; Arnaud, P. A General Method for Fractionation of Plasma Proteins. *Biochem. J.* **1982**, *201*, 129–136.

(11) Altintaş, E. B.; Denizli, A. Efficient Removal of Albumin from Human Serum by Monosize Dye-Affinity Beads. *J. Chromatogr. B* **2006**, *832*, 216–223.

(12) Andac, M.; Galaev, I.; Denizli, A. Dye Attached Poly(Hydroxyethyl Methacrylate) Cryogel for Albumin Depletion from Human Serum. *J. Sep. Sci.* **2012**, *35* (9), 1173–1182.

(13) Björck, L.; Kronvall, G. Purification and Some Properties of Streptococcal Protein G, a Novel IgG-Binding Reagent. *J. Immunol.* **1984**, *133*, 969–974.

(14) Moks, T.; Abrahamsen, L.; Nilsson, B.; Hellmann, U. Staphylococcal Protein A Consists of Five IgG Binding Domains. *Eur. J. Biochem.* **1986**, *156*, 637–643.

(15) Choe, W.; Durgannavar, T.; Chung, S. Fc-Binding Ligands of Immunoglobulin G: An Overview of High Affinity Proteins and Peptides. *Materials* **2016**, *9*, 994.

(16) Ding, Z.; Cao, X. Affinity Precipitation of Human Serum Albumin Using a Thermo-Response Polymer with an L-Thyroxin Ligand. *BMC Biotechnol.* **2013**, *13*, 109–118.

(17) Yang, H. H.; Lu, K. H.; Lin, Y. F.; Tsai, S. H.; Chakraborty, S.; Zhai, W. J.; Tai, D. F. Depletion of Albumin and Immunoglobulin G from Human Serum Using Epitope-Imprinted Polymers as Artificial Antibodies. *J. Biomed. Mater. Res. - Part A* **2013**, *101 A*, 1935–1942.

(18) Liu, J.; Deng, Q.; Tao, D.; Yang, K.; Zhang, L.; Liang, Z.; Zhang, Y. Preparation of Protein Imprinted Materials by Hierarchical Imprinting Techniques and Application in Selective Depletion of Albumin from Human Serum. *Sci. Rep.* **2014**, *4*, 1–6.

(19) Li, S.; Yang, K.; Deng, N.; Min, Y.; Liu, L.; Zhang, L.; Zhang, Y. Thermoresponsive Epitope Surface-Imprinted Nanoparticles for Specific Capture and Release of Target Protein from Human Plasma. *ACS Appl. Mater. Interfaces* **2016**, *8*, 5747–5751.

(20) Savariar, E. N.; Aathimanikandan, S. V.; Thayumanavan, S. Supramolecular Assemblies from Amphiphilic Homopolymers: Testing the Scope. *J. Am. Chem. Soc.* **2006**, *128*, 16224–16230.

(21) Combariza, M. Y.; Savariar, E. N.; Vutukuri, D. R.; Thayumanavan, S.; Vachet, R. W. Polymeric Inverse Micelles as Selective Peptide Extraction Agents for MALDI-MS Analysis. *Anal. Chem.* **2007**, *79* (18), 7124–7130.

(22) Rodthongkum, N.; Chen, Y.; Thayumanavan, S.; Vachet, R. W. Matrix-Assisted Laser Desorption Ionization-Mass Spectrometry Signal Enhancement of Peptides after Selective Extraction with Polymeric Reverse Micelles. *Anal. Chem.* **2010**, *82* (9), 3686–3691.

(23) Serrano, M. A. C.; He, H.; Zhao, B.; Ramireddy, R. R.; Vachet, R. W.; Thayumanavan, S. Polymer-Mediated Ternary Supramolecular Interactions for Sensitive Detection of Peptides. *Analyst* **2017**, *142* (1), 118–122.

(24) Basu, S.; Vutukuri, D. R.; Thayumanavan, S. Homopolymer Micelles in Heterogeneous Solvent Mixtures. *J. Am. Chem. Soc.* **2005**, *127* (48), 16794–16795.

(25) Zhao, B.; Zhuang, J.; Serrano, M. A. C.; Vachet, R. W.; Thayumanavan, S. Influence of Charge Density on Host–Guest Interactions within Amphiphilic Polymer Assemblies in Apolar Media. *Macromolecules* **2017**, *50* (24), 9734–9741.

(26) Zhao, B.; Serrano, M. A. C.; Gao, J.; Zhuang, J.; Vachet, R. W.; Thayumanavan, S. Self-Assembly of Random Co-Polymers for Selective Binding and Detection of Peptides. *Polym. Chem.* **2018**, *9* (9), 1066–1071.

(27) Rodthongkum, N.; Chen, Y.; Thayumanavan, S.; Vachet, R. W. Selective Enrichment and Analysis of Acidic Peptides and Proteins Using Polymeric Reverse Micelles and MALDI-MS. *Anal. Chem.* **2010**, *82* (20), 8686–8691.

(28) Rodthongkum, N.; Ramireddy, R.; Thayumanavan, S.; Richard, W. V. Selective Enrichment and Sensitive Detection of Peptide and Proteinbiomarkers in Human Serum Using Polymeric Reverse Micelles and MALDI-MS. *Analyst* **2012**, *137* (4), 1024–1030.

(29) Zhao, B.; Serrano, M. A. C.; Wang, M.; Liu, T.; Gordon, M. R.; Thayumanavan, S.; Vachet, R. W. Improved Mass Spectrometric Detection of Acidic Peptides by Variations in the Functional Group pKa Values of Reverse Micelle Extraction Agents. *Analyst* **2018**, *143* (6), 1434–1443.

(30) Rasband, W. S. ImageJ, U. S. National Institutes of Health, Bethesda, Maryland, USA, 1997-2015. US National Institutes of Health: Bathesda, Maryland, USA.

(31) Serrano, M. A. C.; Zhao, B.; He, H.; Thayumanavan, S.; Vachet, R. W. Molecular Features Influencing the Release of Peptides from Amphiphilic Polymeric Reverse Micelles. *Langmuir* **2018**, *34* (15), 4595–4602.

(32) Rodriguez-Suarez, E.; Whetton, A. D. The Application of Quantification Techniques in Proteomics for Biomedical Research. *Mass Spectrom. Rev.* **2013**, *32*, 1–26.

(33) Zybailov, B.; Coleman, M. K.; Florens, L.; Washburn, M. P. Correlation of Relative Abundance Ratios Derived from Peptide Ion Chromatograms and Spectrum Counting for Quantitative Proteomic Analysis Using Stable Isotope Labeling. *Anal. Chem.* **2005**, *77*, 6218–6224.

(34) Zhu, W.; Smith, J. W.; Huang, C. M. Mass Spectrometry-Based Label-Free Quantitative Proteomics. *J. Biomed. Biotechnol.* **2010**, *2010*, 1–6.

(35) van den Broek, I.; Sparidans, R. W.; Schellens, J. H. M.; Beijnen, J. H. Quantitative Assay for Six Potential Breast Cancer Biomarker Peptides in Human Serum by Liquid Chromatography Coupled to Tandem Mass Spectrometry. *J. Chromatogr. B* **2010**, *878*, 590–602.

(36) Vaudel, M.; Burkhart, J. M.; Zahedi, R. P.; Oveland, E.; Berven, F. S.; Sickmann, A.; Martens, L.; Barsnes, H. PeptideShaker Enables Reanalysis of MS-Derived Proteomics Data Sets: To the Editor. *Nat. Biotechnol.* **2015**, *33*, 22–24.

CHAPTER V

COMBINING pI BRACKETING WITH MRM ANALYSIS FOR MULTIPLEXED AND MORE SENSITIVE DETECTION OF PROTEIN BIOMARKERS

Abstract

The detection of low abundance protein biomarkers poses an immense challenge when present in complex samples such as serum. Pre-fractionation and enrichment methods that would reduce the complexity of the sample are usually necessary prior to analysis such that the biomarker of interest is conveniently separated from as much interference as possible and hence can be more sensitively measured. By utilizing our pI bracketing method, we show that a panel of three cancer biomarkers can be simultaneously enriched based on their pI using reverse micelles of carboxylate-functionalized polymers. Multiplexed detection was achieved using an optimized multiple reaction monitoring (MRM) assay on a triple quadrupole mass spectrometer. Besides its multiplexed detection capability, we further demonstrate the advantage of our method over ELISA through our ability to specifically distinguish an unmodified peptide biomarker from its hydroxylated derivative. By combining pI bracketing as an enrichment technique with MRM analysis, we were able to simultaneously detect all three biomarkers in a single run with significantly enhanced sensitivities. Detection levels in the low ng/mL concentration in serum were achieved, demonstrating its applicability in detecting biomarkers in clinical samples.

Introduction

Detection of biomarkers from serum poses a very challenging task, not only because protein biomarkers are almost always present in very low concentrations (ng/mL and lower), but also because serum is an extremely complex mixture of proteins with concentration ranges spanning at least 9 orders of magnitude.[1,2] Fractionation and enrichment techniques that would simplify the sample being analyzed and isolate the target proteins from the complex matrix are usually needed in order to detect biomarkers at these levels.[3–6]

Among the analytical tools for protein detection, immunoassays such as ELISA (enzyme-linked immunosorbent assay) are considered the gold standard and the most widely used in the clinical setting. Although very sensitive and specific, these assays require an extremely well-characterized, high-affinity antibody for detecting the protein of interest, the development of which is very costly and lengthy.[7,8] Moreover, there are certain cases where these assays are not able to distinguish between different isoforms or sequence variants of a protein, or recognize proteins that have post-translational modifications and truncations.[9,10] ELISAs also typically detect only one specific analyte at a time, which makes the analysis of a panel of biomarkers restricted. Protein microarrays that make use of many individual affinity reagents such as antibodies, lectins, or aptamers immobilized onto a microscopic surface enable multiplexed detection and enhanced sensitivity,[11,12] but are still limited by the availability and quality of the affinity reagents used.

Mass spectrometry or MS-based methods, on the other hand, can resolve proteins at the sequence level, and therefore can distinguish between protein isoforms, truncated forms, and post-translationally modified proteins.[9,13] Moreover, unlike immunoassays

where prior knowledge of the target protein is required to detect it, the universal nature of MS detection opens doors to the discovery of novel disease biomarkers through differential profiling of diseased versus normal states.[14–16] MS is also capable of detecting multiple proteins simultaneously in a single run, making multiplexed analysis of a panel of biomarkers from a single sample possible.[17–19] This is important because diseases like cancer are often heterogeneous in nature and can vary across populations, and thus a single biomarker may not be sufficiently telling of the disease. Analyzing a panel of biomarkers would provide a more effective and accurate means of distinguishing normal from diseased patients.[20,21]

Among the MS-based targeted approaches for protein measurement, multiple reaction monitoring (MRM) has proven to be a powerful method, delivering sensitivity, specificity, and multiplexing all at the same time.[17,19,22–24] MRM is performed specifically on a triple quadrupole instrumentation (Figure 5.1). In this setup, the first quadrupole (Q1) acts as a mass filter that allows only a predefined peptide precursor ion into the second quadrupole (Q2). Q2 then operates as a collision cell that fragments the peptide ions by colliding with a neutral gas. The third quadrupole (Q3) serves as a second mass filter that

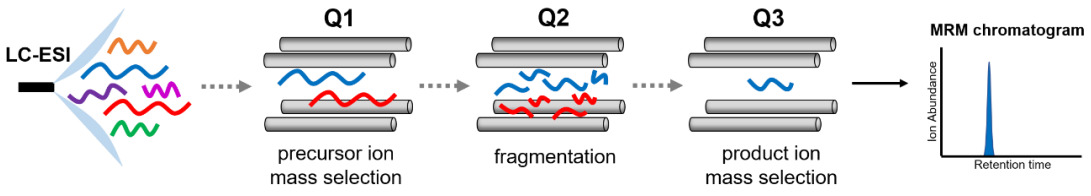

Figure 5.1. MRM analysis on a triple quadrupole mass spectrometer. Peptides eluting from the LC are ionized by electrospray ionization (ESI) and directed towards the mass spectrometer. Precursor ion mass selection in the first quadrupole (Q1) filters out most of the co-eluting peptides that do not fit the predefined precursor mass window. Although an interfering peptide (red) that has the same precursor *m/z* as the target peptide (blue) remains, dissociation in the second quadrupole (Q2) and subsequent product ion mass selection specific for the target peptide's fragment *m/z* in the third quadrupole (Q3) allows for the specific detection of only the target peptide, as represented in the MRM chromatogram.

monitors a specified fragment ion of the peptide. Monitoring a specific precursor and product ion pair (called a "transition") occurs in the millisecond timescale, and hence numerous different transitions can be monitored in a given second along the chromatographic run to yield multiple MRM chromatogram traces that are specific to each transition.[25] Because of the two levels of mass selection for the precursor and product ion, high selectivity and sensitivity is achieved as only the target peptide is collected and any co-eluting interferences are effectively filtered out.[25] This detection specificity makes MRM particularly useful in the analysis of low abundance targets in complex mixtures.

Further increase in sensitivity can be achieved by fractionation and enrichment of the target analytes prior to MRM analysis. It has been previously shown that pI bracketing can be used to simplify serum as a sample and enrich the biomarkers of interest.[26] In this chapter, it is hypothesized that the combination of pI bracketing that can simultaneously extract multiple biomarkers belonging to a certain pI range, and MRM analysis of the enriched fraction, will enable the multiplexed and more sensitive detection of a panel of target biomarkers in serum (Figure 5.2).

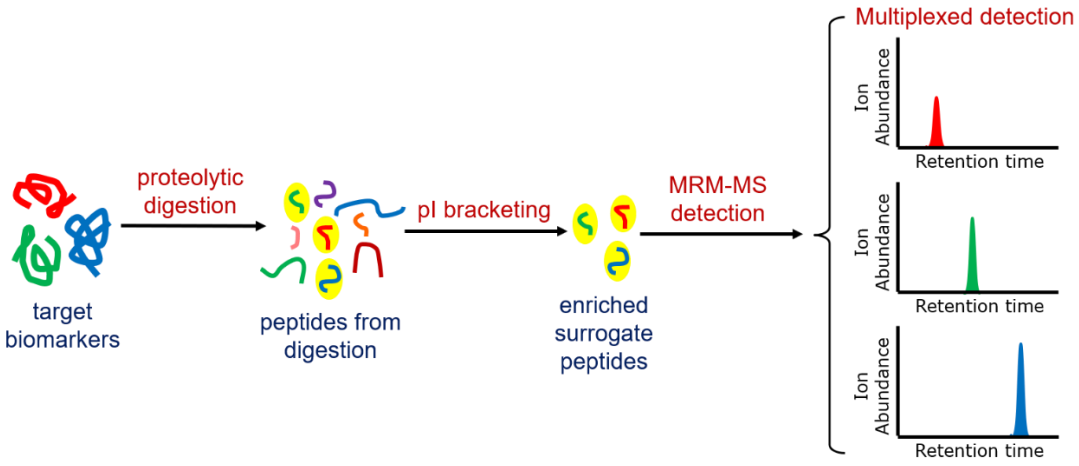

Figure 5.2. Multiplexed detection of target biomarkers by pI bracketing of surrogate peptides and MRM-MS analysis.

Results and Discussion

Target Biomarkers

Three target biomarkers for cancer (Table 5.1) belonging to the same pI bracket were monitored for this study as proof of principle. The peptide bradykinin (BK), with an amino acid sequence of RPPGFSPFR, is a biologically active peptide produced upon proteolysis of kininogen by serine proteases called kallikreins.[27] Along with its derivatives, bradykinin is involved in inflammatory processes and cell proliferation as part of the kallikrein-kinin signaling cascade. Kinin peptides produced upon proteolysis bind to kinin receptors and activate a variety of downstream biological pathways, including the mitogen-activated protein kinase (MAPK), protein kinase C (PKC) and nuclear factor-κB pathways, which are implicated in cancer.[27] Its proline-hydroxylated derivative, hydroxyprolyl^{3}-bradykinin or Hyp^{3}-BK (amino acid sequence RPP^{OH}GFSPFR), is also detectable in circulation and was found present in ascitic fluid from patients with gastric cancer.[28] In a study of the human serum peptidome pattern, bradykinin and its derivatives were found to be differentially expressed in patients with certain types of cancer versus control as a result of altered protease activities in these tumors,[29] and hence can be potentially used as cancer biomarkers.[22,30]

Cytochrome c, on the other hand, is a protein involved in cell energy production and is normally localized in the mitochondria of cells. However, during apoptosis or programmed cell death, as triggered for instance by apoptotic signals such as chemotherapy or radiation, cytochrome c is released from the mitochondria to the cytosol and eventually upon cell death, to the extracellular space.[31] Serum cytochrome c levels, therefore, are considered indicators of the extent of cell death *in vivo* and have been shown to be a

potential prognostic marker for some types of cancer and for monitoring chemotherapeutic efficacy and patient response.[32–34]

Table 5.1. Target biomarkers, their properties and candidate surrogate peptides for cytochrome c.

Target Biomarker	Amino Acid Sequence	Molecular Weight (g/mol)	pI
bradykinin	RPPGFSPFR	1060.2	12.0
Hyp^3-bradykinin	RPP^{OH}FSPFR	1076.2	12.0
cytochrome c protein	MGDVEKGKKIFIMKCSQCHTVEKGGKH KTGPNLHGLFGRKTGQAPGYSYTAANK NKGIIWGEDTLMEYLENPKKYIPGTKMI FVGIKKKEERADLIAYLKKATNE	12234	9.6
cytochrome c peptide 1 (CC-pep1)	TGPNLHGLFGR	1168.3	9.4
cytochrome c peptide 2 (CC-pep2)	TGQAPGYSYTAANK	1428.5	8.2
cytochrome c peptide 3 (CC-pep3)	YIPGTK	677.8	8.6
cytochrome c peptide 4 (CC-pep4)	ADLIAYLK	906.1	5.9

Notes: (1) Lysine (K) and arginine (R) cleavage sites are underlined in the cytochrome c sequence.
(2) Residues with high propensity toward modification (*e.g.* oxidation) are marked in red.
(3) Candidate surrogate peptides for cytochrome c are highlighted in yellow.

These three biomarkers were chosen to show the multiplexed capability of our approach. It is critical to point out that although individual ELISAs are available for bradykinin and cytochrome c, none exists that can detect both. Moreover, there are no available immunoassays that can distinguish between bradykinin and Hyp^3-bradykinin. The hydroxylation in one of the proline residues is presumably too subtle to be sufficiently discriminated by any antibodies. This is where the approach of pI bracketing combined with mass spectrometry could be advantageous. Because the three biomarkers have similar

pI values, all three can be simultaneously extracted from serum, enriched in a single fraction, and specifically identified and detected by MRM based on the mass-to-charge ratios of their precursor and fragment ions.

Determination of Surrogate Peptide for Cytochrome C

In an MRM experiment, proteins are detected based on the presence of their surrogate peptide(s) generated from the prior proteolytic digestion of the protein. The basic assumption in quantification based on the bottom-up approach is that one mole of the surrogate peptide is produced for each mole of the protein during proteolytic digestion. Trypsin is commonly the proteolytic enzyme of choice because of its cleavage specificity (carboxy-side of lysine and arginine residues), efficiency and predictability. Although trypsin digestion of a protein yields a number of peptides that are possible surrogates, careful and strategic selection of the surrogate peptide is crucial to an MRM experiment as they need to correctly and accurately represent the target protein.[35]

One of the criteria for choosing a surrogate peptide is that its amino acid sequence should be unique to the target protein,[25] otherwise the presence of other proteins containing the same sequence would either result in a false positive or contribute a positive error in the measurement. The uniqueness of the peptide sequence to a particular protein can be determined by doing a protein BLAST® search[36] (https://blast.ncbi.nlm.nih.gov/Blast.cgi) of the amino acid sequence of the candidate peptide and searching for matches within the human proteome. If the target protein is the only protein with 100% sequence identity match, then the peptide is unique for that protein. Statistically, the longer the amino acid sequence, the better its chances of being unique. However, too long a peptide often makes

its chromatographic elution towards longer retention times, which is not practical. Therefore, a reasonable peptide length of about 5 to 15 amino acids is desired.

Besides the uniqueness of the peptide sequence, other considerations with regards to the amino acid composition of candidate surrogate peptides are post-translational modifications (PTMs), propensity towards chemically induced modifications, and missed cleavages.[25] PTMs and chemically induced modifications alter the mass of the original peptide and the modification levels are often not consistent or well defined. Therefore, they will not give accurate measure of the protein. Some amino acid residues are prone to modifications during sample preparation and digestion. Methionine (M), cysteine (C) and tryptophan (W), for instance, are prone to oxidation, the levels of which are unpredictable and difficult to control.[37] N-terminal glutamine (Q) tends to convert to pyro-glutamic acid, while N-terminal cysteine that is carbamidomethylated can convert to pyro-carbamidomethylcysteine. Asparagine (N) residues followed by glycine (G) have a high propensity to undergo deamidation to aspartic/isoaspartic acid.[38] These types of residues should thus be avoided as much as possible in selecting candidate surrogates since it is difficult to account for how much modification will occur on the peptide during sample preparation. Peptides with missed cleavages in their sequences are also avoided since the extent of missed cleavage is also hard to control.

Based on the amino acid sequence of the tryptic fragments of cytochrome c, four peptides (listed in Table 5.1) satisfy the aforementioned criteria. These four peptides were also found to be unique to cytochrome c based on a BLAST® search. However, considering that subsequent pI bracketing will be done, the peptide with the closest pI to bradykinin

and Hyp^3-bradykinin is desired. In this regard, peptides 1, 2, and 3 appear to be good surrogate candidates.

The mass spectral properties, *i.e.* ionization efficiency, of the surrogate peptide must also be sufficiently high. Peptides with high ionization efficiency are more easily detectable in the mass spectrometer and hence would result in higher sensitivity for the assay. Some predictors of a peptide's MS detectability include the number of basic residues, peptide length, and hydrophobicity.[39] Besides the MS detectability of the precursor peptide ion, its fragmentation behavior, which is influenced by the peptide sequence, composition and length,[39–41] is also a consideration since the resulting fragment ions are the ones being monitored in MRM. Peptides that give a few highly abundant *b* and *y* product ions are desirable. Cleavage along an X-Pro peptide bond, for instance, usually gives a highly abundant *y* ion.[41] These MS parameters were determined experimentally for cytochrome c by digesting the protein with trypsin, analyzing the digest by LC-MS and determining which peptides exhibit good ionization. Figure 5.3 shows the total ion chromatogram (TIC, top panel) for cytochrome c digest and the peaks identified for each of the four candidate peptides. The most abundant precursor ion peak was observed for the peptide, TGPNLHGLFGR (CC-pep1, highlighted in yellow and confirmed by MS/MS data), and for that reason, CC-pep1 was chosen as the surrogate peptide for cytochrome c. A subsequent MS/MS product ion scan (Figure 5.3, bottom panel) on CC-pep1 gives an idea of the dominant product ions generated upon collision-induced dissociation (CID).

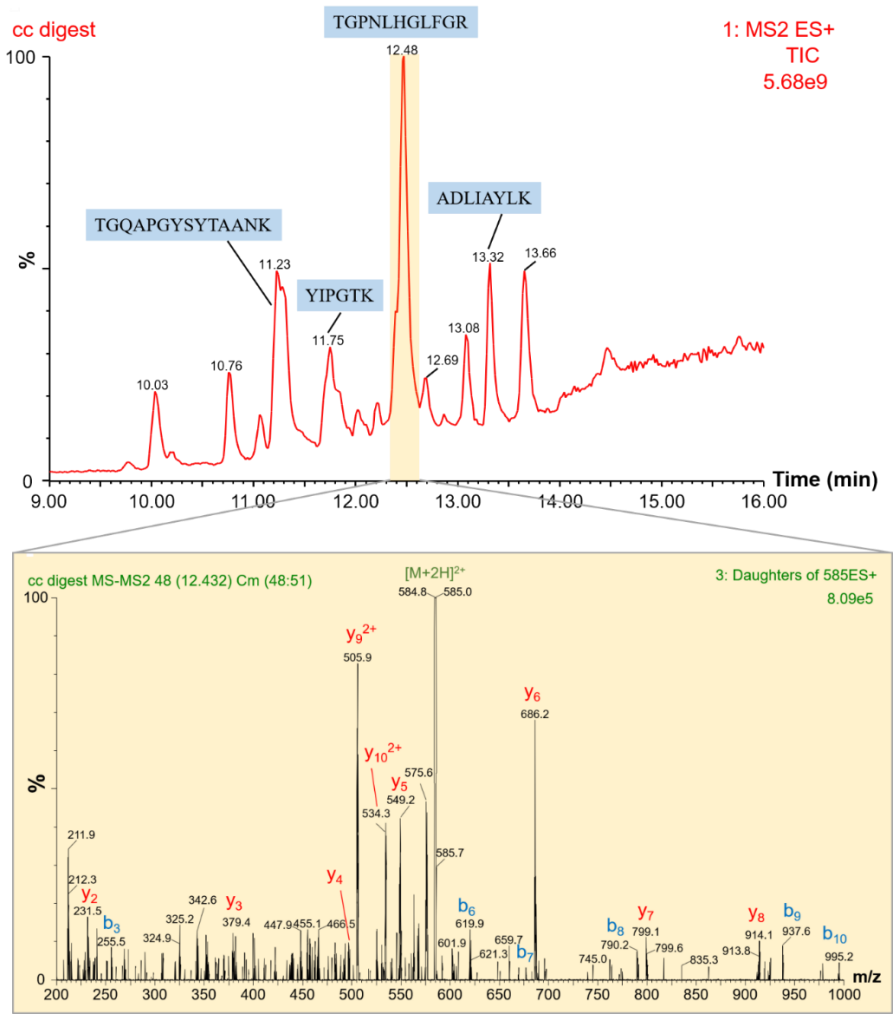

Figure 5.3. Total ion chromatogram (TIC) for cytochrome c digest, with labeled peaks corresponding to the four candidate peptides **(top panel)**. MS spectrum from the product ion scan for TGPNLHGLFGR peptide precursor ion *m/z* 584.8 ($[M+2H]^{2+}$) showing the *b* and *y* product ions produced upon CID **(bottom panel)**.

Selection of Transitions to Monitor and Collision Energy Optimization

Transitions refer to the combination of specific *m/z* of the precursor ion and the product ion defined for the first and the third quadrupole, respectively. Selecting the appropriate transitions for each target peptide is key to a highly specific and sensitive MRM assay. To ensure a highly specific assay, the transitions being monitored must be validated as truly coming from the peptide being targeted and not from some matrix interference. This validation is especially critical when the sample matrix is a complex mixture like

serum. Achieving a highly sensitive assay involves optimizing the parameters such that the most intense response is obtained for the precursor and product ion pair.

The first step in the optimization is determining the most abundant charge state of the precursor ion. Figure 5.4 shows the extracted ion chromatograms for BK, Hyp^3-BK and CC-pep1 and the mass spectra obtained from the highlighted regions in each chromatogram. Based on ion intensity, BK and Hyp^3-BK have precursor ions with +2 as the predominant charge state, while CC-pep1 shows +3 as the most abundant precursor ion charge state.

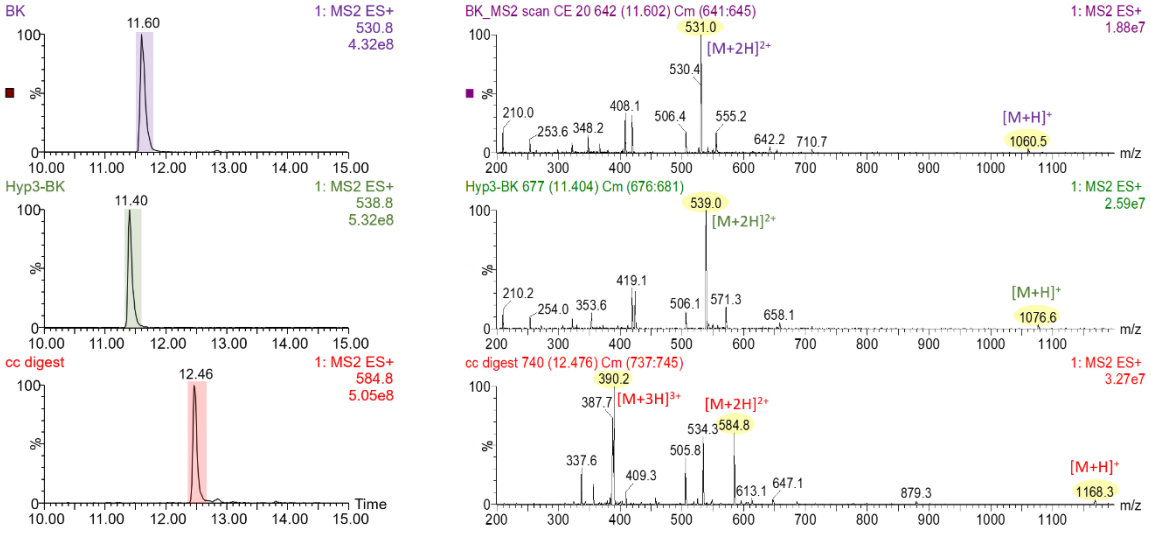

Figure 5.4. (**Left panels**) Extracted ion chromatograms (EIC) for bradykinin (BK, *m/z* 530.8), Hyp^3-bradykinin (Hyp^3-BK, *m/z* 538.8) and cytochrome c peptide TGPNLGHLFGR (CC-pep1, *m/z* 584.8). (**Right panels**) Corresponding mass spectra for BK, Hyp^3-BK, and CC-pep1, extracted from the highlighted regions of their chromatogram. Detected precursor ion peaks of various charge states are highlighted in yellow and labeled accordingly.

Next, a product ion scan is performed to determine the most abundant product ions generated upon fragmentation. The product ion scan mode involves setting the first quadrupole to filter for a specified precursor ion *m/z*, followed by dissociation of the precursor ions in the second quadrupole by CID, and then performing a mass analysis scan

of the product ions generated in the third quadrupole. Figure 5.5 shows the resulting MS/MS spectra from the product ion scans for each peptide. The most abundant product ions are highlighted in yellow and were used to set up the MRM transitions for each peptide. Four transitions were selected for each target peptide as summarized in Table 5.2.

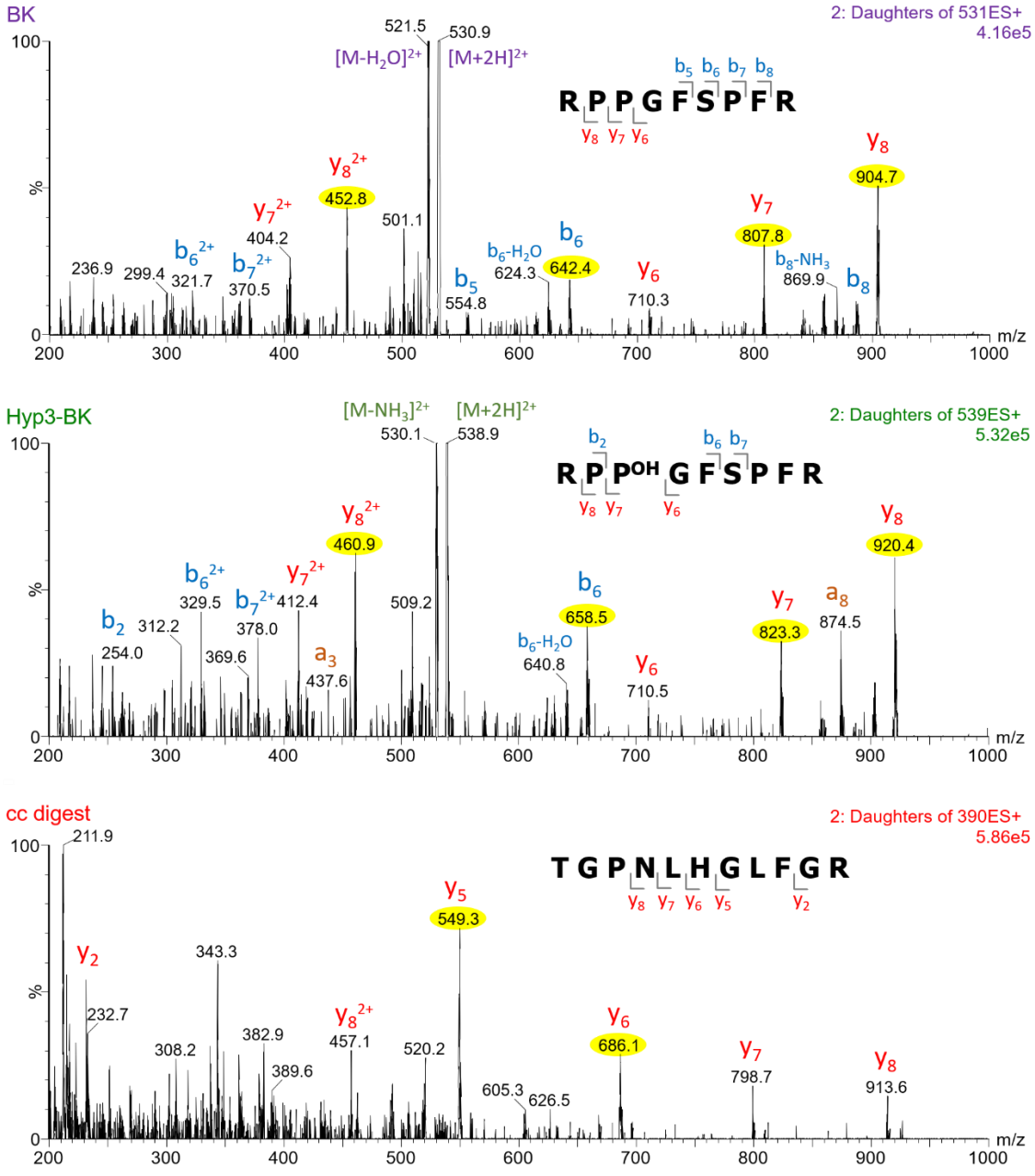

Figure 5.5. Product ion scan MS/MS spectra obtained for bradykinin (**top**), Hyp[3]-bradykinin (**middle**), and CC-pep1 (**bottom**). The most abundant product ions are highlighted in yellow.

Table 5.2. MRM transitions monitored for each target peptide.

Target Peptide	Precursor Ion m/z	Precursor Ion Charge State	Product Ion m/z	Product Ion Type
Bradykinin	530.8	(+2)	452.7	y_8^{2+}
	530.8	(+2)	642.3	b_6
	530.8	(+2)	807.4	y_7
	530.8	(+2)	904.5	y_8
Hyp^3-bradykinin	538.8	(+2)	460.7	y_8^{2+}
	538.8	(+2)	658.3	b_6
	538.8	(+2)	823.4	y_7
	538.8	(+2)	920.5	y_8
CC-pep1	390.2	(+3)	549.3	y_5
	390.2	(+3)	686.4	y_6
	584.8	(+2)	549.3	y_5
	584.8	(+2)	686.4	y_6

For each MRM transition, an optimal collision energy (CE) must be determined to maximize the quantity of product ions generated during CID. Increasing the CE results in greater fragmentation of the precursor ion and hence increases the product ion abundance up to a point where further increases in CE causes secondary fragmentation events that then reduce the product ion intensity.[25] To find the optimum CE for each transition, MRM method events were set up with increasing CE and the resulting intensity was plotted against the CE (Figure 5.6).

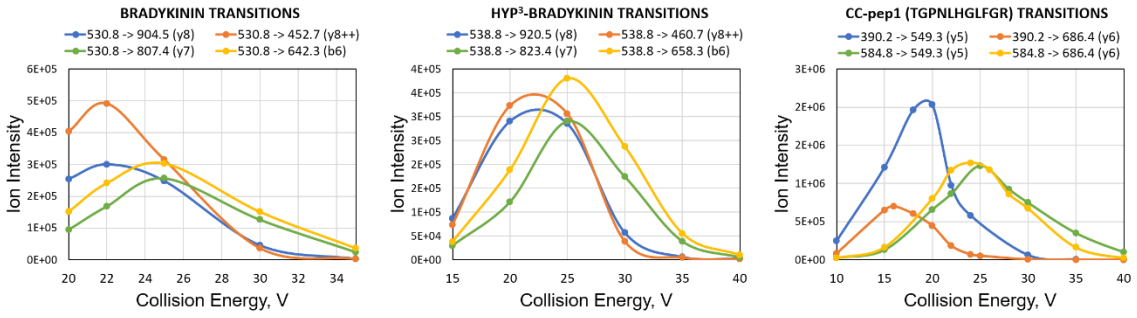

Figure 5.6. Collision energy optimization of individual transitions for each peptide.

Validation of Transitions and Multiplexed Detection in Serum

Using the optimized parameters, we validated if the three biomarkers can be simultaneously detected in a serum matrix. A previously digested serum was spiked with high concentrations of the three target biomarkers (10 µM of BK and Hyp^3-BK peptides and 10 µM of digested CC protein) and was run on a 90-minute LC gradient. Figure 5.7 illustrates the multiplexed capability MRM as all 12 transitions were acquired in a single LC/MRM-MS run. To confirm that the peaks were indeed derived from the target peptide and not from some matrix interference with similar mass, all transitions from that particular peptide should elute at the same retention time. Figure 5.7 shows the co-elution of all the MRM transitions for each peptide, thus confirming the validity of the MRM peaks and demonstrating the specificity of the assay. This type of validation by monitoring multiple transitions for a given peptide is imperative to avoid false positives when the sample matrix is very complex as in the case of serum.[18,25] For instance, although a peak at around 24.2 minutes (labeled with an asterisk) was detected for the transition 584.8->549.3, this can be ruled out as matrix interference since the other transitions did not show a peak at this retention time.

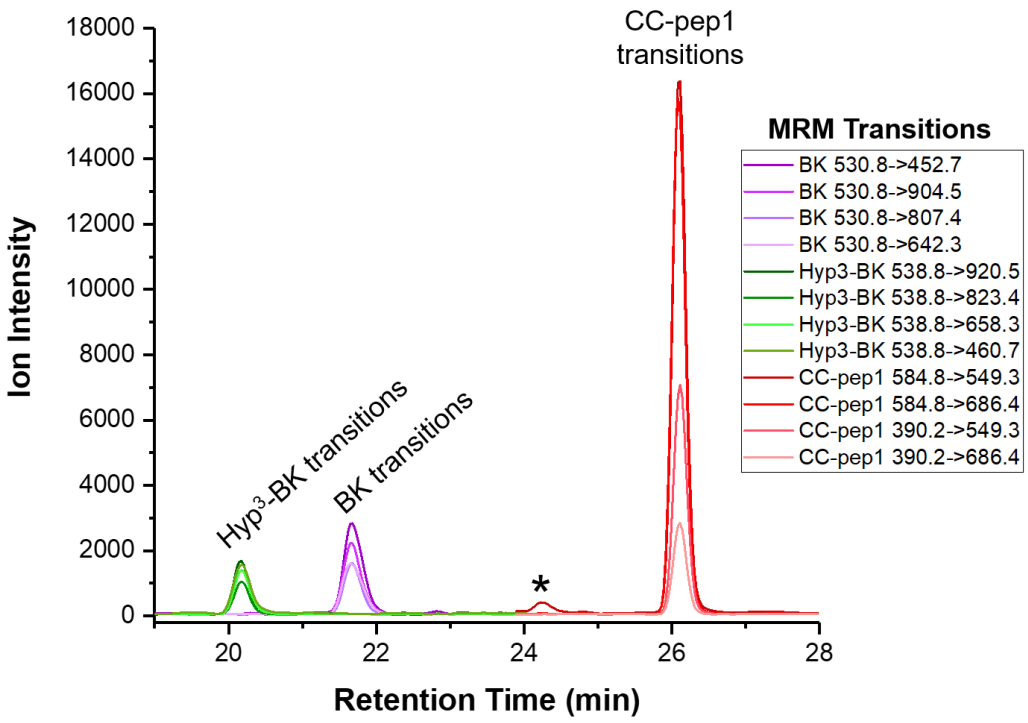

Figure 5.7. Overlaid MRM chromatograms for all the transitions monitored in a serum sample spiked with 10 µM each of BK, Hyp^3-BK and CC protein digest. All 12 transitions were acquired in a single LC/MRM-MS run on a 90-minute LC gradient. Transitions belonging to the same peptide all elute at the same retention time, confirming the validity of these MRM peaks. Peak labeled with an asterisk is ruled out as matrix interference.

Coupling pI Bracketing with MRM to Improve Detection Sensitivity

MRM is inherently more sensitive compared to techniques that employ a "full scan" mode because of its non-scanning nature that filters out potentially interfering ions using a narrow mass window. However, detection sensitivity has been shown to be improved even further by coupling MRM with prior fractionation and enrichment techniques.[6,42–45] Using our pI bracketing approach, we show that the three target biomarkers can be enriched from serum on the basis of their pI and that this enrichment subsequently results in improved detection sensitivity by MRM.

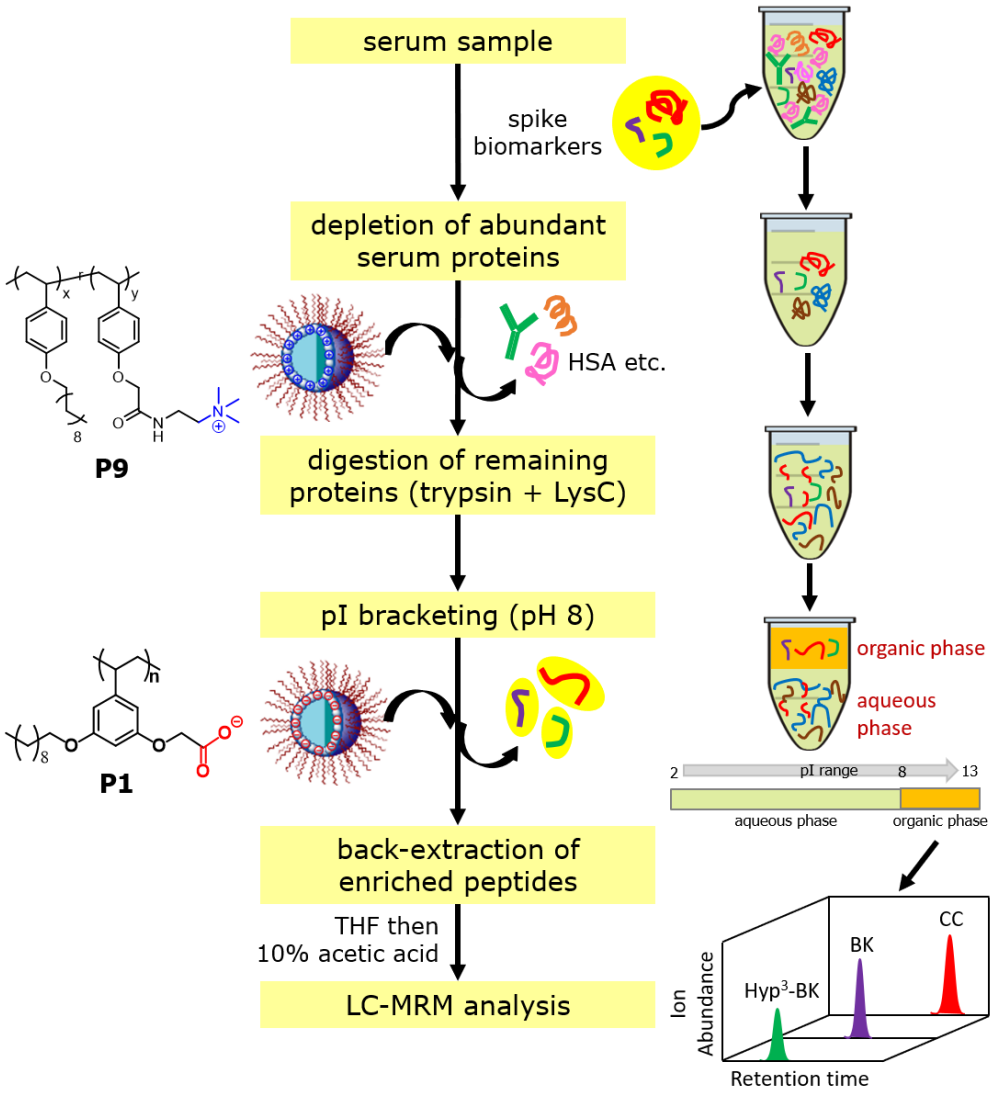

Figure 5.8. Flowchart of serum sample preparation and enrichment of biomarkers for LC-MRM analysis.

Figure 5.8 is a flowchart depicting the pI bracketing of the three biomarkers in serum. Bradykinin, Hyp^3-bradykinin, and cytochrome c protein were spiked at increasing concentrations in serum. HSA and other abundant low-pI serum proteins were then depleted from serum by extraction using a positively charged polymer (**P9** from Chapter IV). The remaining proteins in depleted serum were digested into peptides using a combination of trypsin and LysC enzymes. Extraction using reverse micelles of negatively charged carboxylate homopolymer **P1** at pH 8.0 then selectively extracts positively

charged peptides with pI greater than 8 into the organic phase. Since all three target peptides (BK, Hyp^3-BK and CC-pep1) have pI's above 8, they all get extracted and enriched into the organic phase. Back-extraction of the enriched peptides from the organic phase was accomplished by addition of THF to the toluene phase and subsequent release into an aqueous medium using aqueous acetic acid. Finally, the aqueous phase with the back-extracted peptides was subjected to LC/MRM-MS analysis using the optimized method parameters.

The three biomarkers were detectable in serum at high spiked concentrations; however, at lower spiked concentrations, they became undetectable for serum samples where no pI bracketing was done prior to MRM analysis (Figure 5.9). For samples where pI bracketing was performed, detectable signals were still observed even for the lowest spike (1 ng/mL BK, 1 ng/mL Hyp^3-BK, and 0.1 µg/mL cytochrome c protein or about 10 ng/mL of the CC peptide 1), demonstrating that pI bracketing improves the detection sensitivity of the assay. To quantitatively evaluate its effect on sensitivity, the same protocol was performed on serum samples with even lower spikes to determine the limit of detection (LOD) and limit of quantitation (LOQ) (Figure 5.10). LOD and LOQ were derived from the dose-response line according to the following equations:

$$\boldsymbol{LOD = \frac{3\left(S_{y-int}\right)}{slope} \quad and \quad LOQ = \frac{10\left(S_{y-int}\right)}{slope}}$$

$$where: \quad S_{y-int} = standard\ deviation\ of\ the\ y\ intercept$$

The LOD and LOQ signify the concentration at which the response or signal is differentiable from the blank (unspiked serum) response by 3x (for LOD) or 10x (for LOQ).

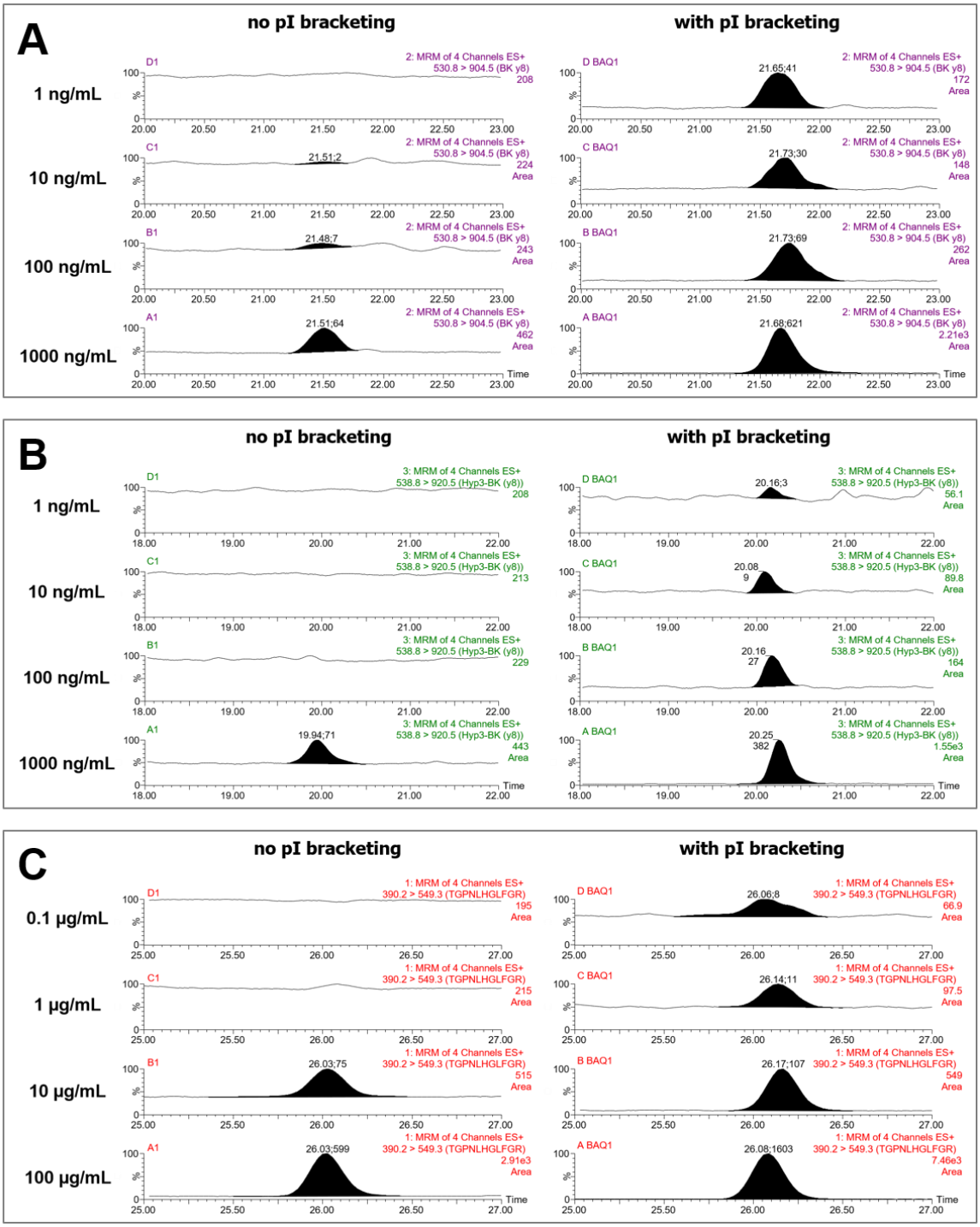

Figure 5.9. MRM chromatograms of the quantifying transitions for **(A)** bradykinin, **(B)** Hyp^3-bradykinin, and **(C)** CC-pep1 (TGPNLGHLFGR) obtained for serum samples spiked with the indicated concentrations of each biomarker. The series of chromatograms on the left represent MRM peaks obtained for samples without pI bracketing while the ones on the right were obtained for samples where pI bracketing was performed prior to MRM analysis. Labels on peaks correspond to the peak top retention time and integrated peak area.

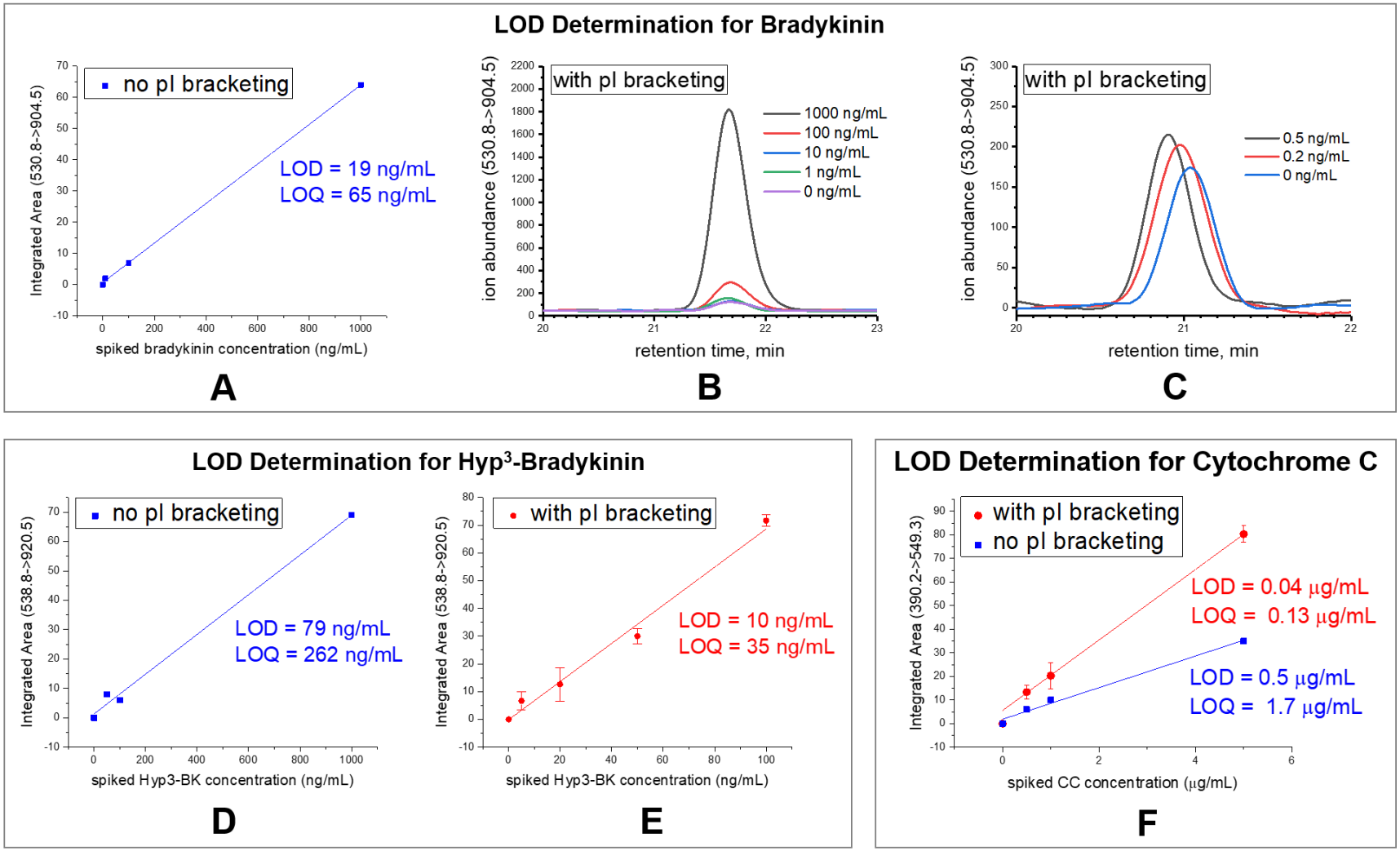

Figure 5.10. Determination of limit of detection (LOD) and limit of quantitation (LOQ) for the MRM assay with and without pI bracketing.

For bradykinin, the LOD and LOQ without pI bracketing were calculated to be 19 ng/mL and 65 ng/mL, respectively (Figure 5.10A). With pI bracketing, however, detectable bradykinin peaks were still obtained down to 0.2 ng/mL and even for the unspiked serum samples (Figures 5.10B and 5.10C), indicating that endogenous bradykinin present in normal serum can be detected. To quantify the absolute concentration of bradykinin, an isotopically labeled internal standard can be used, which would be the subject of future studies. For Hyp^3-bradykinin, about an 8-fold increase in sensitivity was obtained, with an LOD of 10 ng/mL with pI bracketing versus 79 ng/mL for MRM alone (Figures 5.10D and 5.10E). Meanwhile, about a 13-fold increase in cytochrome c detection was observed when pI bracketing was combined with MRM (Figure 5.10F), with an LOD of 0.04 µg/mL with pI bracketing versus 0.5 µg/mL without enrichment. These concentrations correspond to about 4 ng/mL and 48 ng/mL, respectively, of the surrogate peptide, TGPNLHGLFGR, in serum. Overall, these results demonstrate how pI bracketing enrichment increases the sensitivity of the MRM assay for these biomarkers.

Conclusions and Future Work

Using an optimized MRM assay, a panel of three cancer biomarkers were targeted in serum as proof of principle that combining pI bracketing with MRM analysis results in their enhanced detection. pI bracketing using reverse micelles of a negatively charged carboxylate polymer **P1** enabled the simultaneous extraction and enrichment of the three biomarkers from the complex serum matrix and allowed for their multiplexed detection. Bradykinin and its Pro^3-hydroxylated derivative, Hyp^3-bradykinin, were specifically and distinctively detected, a capability that is not currently achievable by any ELISA method.

Comparison of the LOD and LOQ calculated with and without employing pI bracketing prior to MRM analysis proves that detection sensitivity is significantly improved with pI bracketing. LODs in the ng/mL levels in serum were achieved, and we envision the utility of this approach for sensitively detecting multiple low-level biomarkers in serum and in other complex matrices. The same approach can be applied, for instance, to breast milk, cell lysates, urine and other complicated biological fluids. A more in-depth biomarker analysis can also be done by sequentially bracketing the sample further and targeting biomarkers present in other pI fractions. In terms of improving the quantitative aspects of the assay, the use of stable isotopically labeled internal standards will enable a more reliable and absolute quantification. Percent recovery and reproducibility studies will also validate the assay and provide a measure of its accuracy and precision.

Experimental Methods

Serum Sample and Target Biomarkers

Pooled normal human serum samples were obtained from Innovative Research (Novi, MI). Bradykinin peptide ("BK", sequence RPPGFSPFR), 3-hydoxyproline-bradyknin ("Hyp^3-BK", sequence RPP^{OH}GFSPFR), and cytochrome c protein ("CC") were purchased from Sigma (St. Louis, MO).

Polymer Synthesis, Characterization and Preparation of Reverse Micelles

Synthesis and characterization of polymers **P1** and **P9** are described by Basu S., et al. (2005) and Gao, J., et al. (2018), respectively.[46,47] Reverse micelles of the polymer were prepared by dissolving the appropriate amount of the solid polymer in a corresponding

volume of toluene to make the intended concentration. The mixture was sonicated for at least 15 minutes to completely dissolve the solid, and 2 µL of water was added to serve as the "water pool" interior of the reverse micelle. The mixture was sonicated again for at least 15 minutes or until it yieled a clear solution.

Depletion of Abundant Low-pI Serum Proteins

In a manner similar to that described in Chapter IV, reverse micelles of the positively charged polymer, **P9**, were used to deplete the abundant low-pI proteins in serum prior to further analysis. This depletion was accomplished by extracting 1000 µL of 10-fold diluted spiked serum samples with 400 µL of reverse micelles of polymer **P9** (2 mg/mL solution in toluene). Extraction was performed by vortex mixing the samples for 1 hour, after which the samples were centrifuged at 12500 rpm at 15 ˚C for 30 minutes to separate the layer. The depleted aqueous phase was carefully taken out and placed on a separate tube. Sequential extraction of the resulting aqueous phase was repeated two more times for a total of three depletions to effectively remove HSA and other low-pI abundant proteins in the serum samples.

Digestion with Trypsin and LysC

Five hundred microliters of the spiked serum samples buffered at pH 6.0, were placed in a 2-mL tube containing 60 mg of urea. Reduction of any protein disulfide bonds was done by adding 5 µL of 1M dithiothreitol (DTT). Samples were incubated for 30 minutes at room temperature. Afterwards, alkylation of the resulting free cysteine thiols was carried out by the addition of 20 µL of 1 M iodoacetamide (IAM) and incubation in the dark for 30 minutes at room temperature. To reduce the urea concentration to 1M, 420 µL of 200 mM Tris at pH 10 was added. This addition adjusted the pH to about 8 for the

enzymatic digestion. To digest the proteins, 50 µL of 0.2 µg/ µL solution of trypsin (Promega, Madison, WI) and 5 µL of 0.1 µg/ µL solution of LysC (Wako, Japan) were added to each sample and incubated overnight on a 37 ˚C water bath with shaking.

Simultaneous Extraction of Biomarkers in Serum by pI Bracketing

The three target biomarkers – bradykinin (pI 12), Hyp^3-bradykinin (pI 12), and cytochrome c surrogate peptide, TGPNLHGLFGR (pI 9.4) – were extracted simultaneously from digested serum by setting the pH to 8.0 prior to extraction. Using 400 µL of 1 x 10^{-4} M solution of carboxylate homopolymer **P1**, the target peptides were extracted by mixing for 2 hours, followed by centrifugation at 12500 rpm at 25 ˚C for 1 hour to separate the layers. The bottom aqueous phase was carefully drawn out, and the organic phase with the extracted peptides were kept for subsequent back-extraction.

Release of Extracted Peptides by Back-Extraction

In a manner similar to that described in Chapter III, the extracted peptides were released from the reverse micelles in the toluene phase by adding 200 µL of tetrahydrofuran (THF) to disassemble the reverse micelles, followed by 200 µL of 10% acetic acid to neutralize the polymer carboxylate groups. Back-extraction was carried out by mixing the organic phase, THF, and acetic acid mixture for 1 hour by vortex. Centrifugation was done at 10000 rpm for 1 hour (25 ˚C). The back-extraction aqueous phase (B-AQ) containing the released peptides were drawn out and filtered through a 0.1-µm Ultrafree®-MC centrifugal filter (Catalog No. UFC30VV00, Millipore Sigma, St. Louis, MO) to filter out particulates prior to LC-MS analysis. The flow-through B-AQ was evaporated on a speedvac and reconstituted to a 50-µL volume using 10% acetic acid.

Detection of BK, Hyp^3-BK, and CC Surrogate Peptide in Serum by MRM

Multiplexed detection of the target biomarkers was done using the optimized LC-MRM-MS method on a Waters TQD triple quadrupole mass spectrometer coupled to a Waters® ACQUITY UPLC H-class equipped with a Supelco® Discovery C18 reversed phase analytical column (150mm x 2.1mm, 5µm (Sigma-Aldrich, St. Louis, MO)).

LC gradient. The following LC gradient was used at a flow rate of 0.2 mL/min, with 0.1% formic acid in water as mobile phase A and 0.1% formic acid in acetonitrile as mobile phase B: 0-5 min (5% B), 5-65 min (5% to 50% B), 65-70 min (50% to 95% B), 70-80 min (95% B), 80-81 min (95% to 5% B), 81-90 min (5% B).

MS Tune File settings. An electrospray mode with positive polarity (ES+) was used for all mass spectral acquisition. The capillary voltage was set at 3.00 kV, the cone voltage at 44 V, the source temperature at 150 ˚C, the desolvation gas flow at 700 L/hour, and the cone gas flow at 50 L/hour.

Determination of transitions to monitor and optimization of collision energy. Standard solutions containing BK, Hyp^3-BK, and trypsin-digested CC were used to determine the appropriate transitions to monitor for each peptide. LC-MS of the standard mixture was first run to determine their respective retention times and the most intense charge state for the precursor ion of each peptide. A product ion scan (MS/MS scan with dissociation by CID) for the specified precursor ion *m/z* was then implemented to identify high intensity product ions. Based on their retention time, a scheduled MRM was set up for each peptide, specifically monitoring for the precursor ion and product ion pairs ("MRM transitions") for a specified time window. MRM scans for both BK and Hyp^3-BK were implemented from 15 to 23 minutes of the gradient, while that of the CC surrogate

peptide, TGPNLHGLFGR, was implemented from 23 to 28 minutes of the gradient. MRM scans were taken using increasing collision energies (CE) to find the optimum CE for each transition. The "Auto Dwell" function with at least 12 points per peak over a 10-second peak width was selected to apply the appropriate dwell time for acquiring each MRM scan. The most sensitive transition for each peptide based on the peak area of their MRM chromatogram was designated as the "quantifying transition", while the other transitions were kept as "confirmatory transitions" to verify that the correct peptide sequence is being monitored and not a false positive or due to some matrix interference. The optimized MRM transitions corresponding to each target peptide were all combined into one MS method in MassLynx, allowing the simultaneous analysis of the three target peptides in a single run. All unknown samples were then run using this optimized method.

References

(1) Jacobs, J. M.; Adkins, J. N.; Qian, W.-J.; Liu, T.; Shen, Y.; Camp, D. G.; Smith, R. D. Utilizing Human Blood Plasma for Proteomic Biomarker Discovery. *J. Proteome Res.* **2005**, *4*, 1073–1085.

(2) Adkins, J. N. et al. Toward a Human Blood Serum Proteome: Analysis By Multidimensional Separation Coupled With Mass Spectrometry. *Mol. Cell. Proteomics* **2002**, *1*, 947–955.

(3) Whiteaker, J. R.; Zhao, L.; Zhang, H. Y.; Feng, L.-C.; Piening, B. D.; Anderson, L.; Paulovich, A. G. Antibody-Based Enrichment of Peptides on Magnetic Beads for Mass-Spectrometry-Based Quantification of Serum Biomarkers. *Anal. Biochem.* **2007**, *362* (1), 44–54.

(4) Cologna, S. M.; Russell, W. K.; Lim, P. J.; Vigh, G.; Russell, D. H. Combining Isoelectric Point-Based Fractionation, Liquid Chromatography and Mass Spectrometry to Improve Peptide Detection and Protein Identification. *J. Am. Soc. Mass Spectrom.* **2010**, *21* (9), 1612–1619.

(5) Ahn, Y. H.; Kim, K. H.; Shin, P. M.; Ji, E. S.; Kim, H.; Yoo, J. S. Identification of Low-Abundance Cancer Biomarker Candidate TIMP1 from Serum with Lectin Fractionation and Peptide Affinity Enrichment by Ultrahigh-Resolution Mass Spectrometry. *Anal. Chem.* **2012**, *84* (3), 1425–1431.

(6) Razavi, M.; Frick, L. E.; LaMarr, W. A.; Pope, M. E.; Miller, C. A.; Anderson, N. L.; Pearson, T. W. High-Throughput SISCAPA Quantitation of Peptides from Human Plasma Digests by Ultrafast, Liquid Chromatography-Free Mass Spectrometry. *J. Proteome Res.* **2012**, *11* (12), 5642–5649.

(7) Dzieciatkowska, M.; Copeland, M.; You, J.; Wery, J.; Wang, M. Comparison of an Enzyme Immunoassay Versus Mass Spectrometry-Based Assay for the Quantitative Determination of the Procollagen Type I N-Terminal Propeptide in Rat Serum. *Proteomics Insights* **2009**, *2*, 33–38.

(8) Huttenhain, R.; Malmstrom, J.; Picotti, P.; Aebersold, R. Perspectives of Targeted Mass Spectrometry for Protein Biomarker Verification. *Curr. Opin. Chem. Biol.* **2009**, *13*, 1–8.

(9) Hale, J. E. Advantageous Uses of Mass Spectrometry for the Quantification of Proteins. *Int. J. Proteomics* **2013**, *2013*, 1–6.

(10) Krastins, B.; Prakash, A.; Sarracino, D. a; Nedelkov, D.; Niederkofler, E. E.; Kiernan, U. a; Nelson, R.; Vogelsang, M. S.; Vadali, G.; Garces, A.; et al. Rapid Development of Sensitive, High-Throughput, Quantitative and Highly Selective Mass Spectrometric Targeted Immunoassays for Clinically Important Proteins in Human Plasma and Serum. *Clin. Biochem.* **2013**, *46* (6), 399–410.

(11) Hartmann, M.; Roeraade, J.; Stoll, D.; Templin, M. F.; Joos, T. O. Protein Microarrays for Diagnostic Assays. *Anal. Bioanal. Chem.* **2009**, *393*, 1407–1416.

(12) Huang, Y.; Zhu, H. Protein Array-Based Approaches for Biomarker Discovery in Cancer. *Genomics Proteomics Bioinformatics* **2017**, *15* (2), 73–81.

(13) DeVera, I. E.; Katz, J. E.; Agus, D. B. Clinical Proteomics: The Promises and Challenges of Mass Spectrometry-Based Biomarker Discovery. *Clin. Adv. Hematol. Oncol.* **2006**, *4*, 541–549.

(14) Diamandis, E. P. Mass Spectrometry as a Diagnostic and a Cancer Biomarker Discovery Tool. *Mol. Cell. Proteomics* **2004**, *3* (4), 367–378.

(15) Sandanayake, N. S.; Camuzeaux, S.; Sinclair, J.; Blyuss, O.; Andreola, F.; Chapman, M. H.; Webster, G. J.; Smith, R. C.; Timms, J. F.; Pereira, S. P. Identification of Potential Serum Peptide Biomarkers of Biliary Tract Cancer Using MALDI MS Profiling. *BMC Clin. Pathol.* **2014**, *14* (1), 7.

(16) Chung, L.; Moore, K.; Phillips, L.; Boyle, F. M.; Marsh, D. J.; Baxter, R. C. Novel Serum Protein Biomarker Panel Revealed by Mass Spectrometry and Its Prognostic Value in Breast Cancer. *Breast Cancer Res.* **2014**, *16* (3), R63.

(17) Keshishian, H.; Addona, T.; Burgess, M.; Kuhn, E.; Carr, S. A. Quantitative, Multiplexed Assays for Low Abundance Proteins in Plasma by Targeted Mass Spectrometry and Stable Isotope Dilution. *Mol. Cell. Proteomics* **2007**, *6*, 2212–2229.

(18) Gillette, M. A.; Carr, S. A. Quantitative Analysis of Peptides and Proteins in Biomedicine by Targeted Mass Spectrometry. *Nat. Methods* **2013**, *10* (1), 28–34.

(19) Percy, A. J.; Chambers, A. G.; Yang, J.; Hardie, D. B.; Borchers, C. H. Advances in Multiplexed MRM-Based Protein Biomarker Quantitation toward Clinical Utility. *Biochim. Biophys. Acta* **2014**, *1844* (5), 917–926.

(20) Polanski, M.; Anderson, N. L. A List of Candidate Cancer Biomarkers for Targeted Proteomics. *Biomark. Insights* **2007**, *1* (301), 1–48.

(21) Ma, S.; Wang, W.; Xia, B.; Zhang, S.; Yuan, H.; Jiang, H.; Meng, W.; Zheng, X.; Wang, X. Multiplexed Serum Biomarkers for the Detection of Lung Cancer. *EBioMedicine* **2016**, *11*, 210–218.

(22) van den Broek, I.; Sparidans, R. W.; Schellens, J. H. M.; Beijnen, J. H. Quantitative Assay for Six Potential Breast Cancer Biomarker Peptides in Human Serum by Liquid Chromatography Coupled to Tandem Mass Spectrometry. *J. Chromatogr. B* **2010**, *878*, 590–602.

(23) Anderson, L.; Hunter, C. L. Quantitative Mass Spectrometric Multiple Reaction Monitoring Assays for Major Plasma Proteins. *Mol. Cell. Proteomics* **2006**, *5*, 573–588.

(24) Kennedy, J. J.; Abbatiello, S. E.; Kim, K.; Yan, P.; Whiteaker, J. R.; Lin, C.; Kim, J. S.; Zhang, Y.; Wang, X.; Ivey, R. G.; et al. Demonstrating the Feasibility of Large-Scale Development of Standardized Assays to Quantify Human Proteins. *Nat. Methods* **2014**, *11* (2), 149–155.

(25) Lange, V.; Picotti, P.; Domon, B.; Aebersold, R. Selected Reaction Monitoring for Quantitative Proteomics: A Tutorial. *Mol. Syst. Biol.* **2008**, *4* (222), 222.

(26) Rodthongkum, N.; Ramireddy, R.; Thayumanavan, S.; Richard, W. V. Selective Enrichment and Sensitive Detection of Peptide and Proteinbiomarkers in Human Serum Using Polymeric Reverse Micelles and MALDI-MS. *Analyst* **2012**, *137* (4), 1024–1030.

(27) da Costa, P. L. N.; Sirois, P.; Tannock, I. F.; Chammas, R. The Role of Kinin Receptors in Cancer and Therapeutic Opportunities. *Cancer Lett.* **2014**, *345*, 27–38.

(28) Maeda, H.; Matsumura, Y.; Katos, H. Purification and Identification of [Hydroxyprolyl3]Bradykinin in Ascitic Fluid from a Patient with Gastric Cancer. *J. Biol. Chem.* **1988**, *263*, 16051–16054.

(29) Villanueva, J. et al. Differential Exoprotease Activities Confer Tumor-Specific Serum Peptidome Patterns. *J. Clin. Invest.* **2006**, *116* (1), 271–284.

(30) van Winden, A. W. J.; van den Broek, I.; Gast, M.-C. W.; Engwegen, J. Y. M. N.; Sparidans, R. W.; van Dulken, E. J.; Depla, A. C. T. M.; Cats, A.; Schellens, J. H. M.; Peeters, P. H. M.; et al. Serum Degradome Markers for the Detection of Breast Cancer. *J. Proteome Res.* **2010**, *9*, 3781–3788.

(31) Eleftheriadis, T.; Pissas, G.; Liakopoulos, V.; Stefanidis, I. Cytochrome c as a Potentially Clinical Useful Marker of Mitochondrial and Cellular Damage. *Front. Immunol.* **2016**, *7*, 1–5.

(32) Barczyk, K.; Kreuter, M.; Pryjma, J.; Booy, E. P.; Maddika, S.; Ghavami, S.; Berdel, W. E.; Roth, J.; Los, M. Serum Cytochrome c Indicates in Vivo Apoptosis and Can Serve as a Prognostic Marker during Cancer Therapy. *Int. J. Cancer* **2005**, *116*, 167–173.

(33) Osaka, A.; Hasegawa, H.; Yamada, Y.; Yanagihara, K.; Hayashi, T.; Mine, M.; Aoyama, M.; Sawada, T.; Kamihira, S. A Novel Role of Serum Cytochrome c as a Tumor Marker in Patients with Operable Cancer. *J. Cancer Res. Clin. Oncol.* **2009**, *135*, 371–377.

(34) Javid, J.; Mir, R.; Julka, P. K.; Ray, P. C.; Saxena, A. Extracellular Cytochrome c as a Biomarker for Monitoring Therapeutic Efficacy and Prognosis of Non-Small Cell Lung Cancer Patients. *Tumor Biol.* **2015**, *36*, 4253–4260.

(35) Chiva, C.; Sabidó, E. Peptide Selection for Targeted Protein Quantitation. *J. Proteome Res.* **2017**, *16*, 1376–1380.

(36) Altschul, S. F.; Madden, T. L.; Schäffer, A. A.; Zhang, J.; Zhang, Z.; Miller, W.; Lipman, D. J. Gapped BLAST and PSI-BLAST: A New Generation of Protein Database Search Programs. *Nucleic Acids Res.* **1997**, *25*, 3389–3402.

(37) Li, S.; Schöneich, C.; Borchardt, R. T. Chemical Instability of Protein Pharmaceuticals: Mechanisms of Oxidation and Strategies for Stabilization. *Biotechnol. Bioeng.* **1995**, *48*, 490–500.

(38) Tyler-Cross, R.; Schirch, V. Effects of Amino Acid Sequence, Buffers, and Ionic Strength on the Rate and Mechanism of Deamidation of Asparagine Residues in Small Peptides. *J. Biol. Chem.* **1991**, *266*, 22549–22556.

(39) Jarnuczak, A. F.; Lee, D. C. H.; Lawless, C.; Holman, S. W.; Eyers, C. E.; Hubbard, S. J. Analysis of Intrinsic Peptide Detectability via Integrated Label-Free and SRM-Based Absolute Quantitative Proteomics. *J. Proteome Res.* **2016**, *15*, 2945–2959.

(40) Tabb, D. L.; Huang, Y.; Wysocki, V. H.; Yates, J. R. Influence of Basic Residue Content on Fragment Ion Peak Intensities in Low-Energy Collision-Induced Dissociation Spectra of Peptides. *Anal. Chem.* **2004**, *76* (5), 1243–1248.

(41) Kapp, E. A.; Schütz, F.; Reid, G. E.; Eddes, J. S.; Moritz, R. L.; O'Hair, R. A. J.; Speed, T. P.; Simpson, R. J. Mining a Tandem Mass Spectrometry Database to Determine the Trends and Global Factors Influencing Peptide Fragmentation. *Anal. Chem.* **2003**, *75*, 6251–6264.

(42) Kuhn, E.; Wu, J.; Karl, J.; Liao, H.; Zolg, W.; Guild, B. Quantification of C-Reactive Protein in the Serum of Patients with Rheumatoid Arthritis Using Multiple Reaction Monitoring Mass Spectrometry and 13C-Labeled Peptide Standards. *Proteomics* **2004**, *4* (4), 1175–1186.

(43) Whiteaker, J. R.; Zhao, L.; Anderson, L.; Paulovich, A. G. An Automated and Multiplexed Method for High Throughput Peptide Immunoaffinity Enrichment and Multiple Reaction Monitoring Mass Spectrometry-Based Quantification of Protein Biomarkers. *Mol. Cell. Proteomics* **2010**, *9*, 184–196.

(44) Lin, D.; Alborn, W. E.; Slebos, R. J. C.; Liebler, D. C. Comparison of Protein Immunoprecipitation-Multiple Reaction Monitoring with ELISA for Assay of Biomarker Candidates in Plasma. *J. Proteome Res.* **2013**, *12*, 5996–6003.

(45) Mehaffy, C.; Dobos, K. M.; Nahid, P.; Kruh-Garcia, N. A. Second Generation Multiple Reaction Monitoring Assays for Enhanced Detection of Ultra-Low Abundance Mycobacterium Tuberculosis Peptides in Human Serum. *Clin. Proteomics* **2017**, *14*, 21–30.

(46) Basu, S.; Vutukuri, D. R.; Thayumanavan, S. Homopolymer Micelles in Heterogeneous Solvent Mixtures. *J. Am. Chem. Soc.* **2005**, *127* (48), 16794–16795.

(47) Gao, J.; Zhao, B.; Wang, M.; Serrano, M. A. C.; Zhuang, J.; Ray, M.; Rotello, V. M.; Vachet, R. W.; Thayumanavan, S. Supramolecular Assemblies for Transporting Proteins Across an Immiscible Solvent Interface. *J. Am. Chem. Soc.* **2018**, *140* (7), 2421–2425.

CHAPTER VI

CONCLUSIONS AND FUTURE DIRECTIONS

In this dissertation, supramolecular assemblies of amphiphilic polymers were utilized to selectively enrich peptides and proteins from complex mixtures and enhance their mass spectrometric analysis. Through structure-property investigations in Chapter II, it was determined that a favorable aromatic donor-acceptor interaction between the polymer and the MALDI matrix was necessary to bring about enhanced peptide signals in MALDI. Elucidating this mechanism guides the design of materials with signal enhancement capabilities, especially for analyzing peptides that are difficult to detect by MALDI, acidic peptides and phosphopeptides, for instance.

In Chapter III, an efficient mode of release of guest peptides from the reverse micelle assemblies was accomplished through the cooperative effects of disassembly and neutralization of the peptide-polymer charge interaction. Although this strategy was demonstrated to be effective in releasing peptides, its application can also be useful for releasing whole proteins while retaining their biological activity. It has been recently shown that whole proteins can be selectively sequestered inside polymeric reverse micelles in a non-polar solvent without losing their biological activity.[1] Since release by the addition of THF and aqueous acid would likely cause disruption of the native structure of proteins, a different mode of disassembly and neutralization can be employed instead, while still exploiting the cooperative effects. Many different modes of disassembly can be taken advantage of by designing polymers with cleavable linkers,[2] which upon cleavage would conceivably disrupt the hydrophilic-lipophilic balance of the polymers and induce

disassembly of the reverse micelles without affecting the biological activity of the protein cargos. Furthermore, the addition of salt solution was shown to effectively shield the electrostatic interactions between polymer and peptide (Figure 3.10) and would presumably also work for proteins. This could then be an alternative to the addition of aqueous acid after disassembly and enable the release of proteins without denaturation. Another interesting avenue to study is the method of selective guest release, as this can have potential applications in sequential delivery of multiple cargos.

In Chapter IV, abundant low-pI proteins in serum were effectively depleted by extraction using positively charged polymeric reverse micelles, which improved the detection sensitivity for other low-level proteins. Structure-property studies can be done to optimize the polymer structure and improve the extraction capacity further so that depletion can be done efficiently with fewer or even just a single extraction step. To extend the extraction capacity, the solubility of the polymer can also be increased by using a different non-polar solvent such as dichloromethane. It is also of interest to append an HSA-specific ligand to the polymer, such as cibacron blue[3] or thyroxine[4–6] so that the depletion strategy can be applicable to the analysis of low-pI proteins as well. Currently, the depletion strategy is applicable when the protein of interest in serum is a high-pI protein since there are no risks of losses during depletion using the positively charged polymer.

Chapter IV also demonstrated the applicability of the pI bracketing strategy on extracting whole proteins, but other modes of interaction besides one that is based on pI can also be employed. For instance, selective extraction of glycoproteins may be achieved through the use of benzoboroxole moieties that can react specifically with vicinal diols of glycans.[7]

Finally, Chapter V demonstrated that combining the selective enrichment capabilities of pI bracketing with the sensitive and highly specific technique of MRM-MS enables a more sensitive and multiplexed detection of a panel of biomarkers in serum. This approach, however, is not only limited to serum but to other complex biological samples as well that can be sources of biomarkers such as breast milk, cerebrospinal fluid, urine, and cell lysates. It is feasible to use this approach in a wide variety of applications such as in selectively enriching closely related proteins or protein isoforms in cells and then comparing their expression levels, or in determining the extent of modification of a low-level protein. Moreover, this approach can be used in applications other than biomarker analysis. For instance, it can be employed to achieve ultrahigh sensitivity in detecting low-level host cell protein impurities in recombinantly produced biotherapeutic products.[8] Overall, these materials show excellent versatility and utility in enhancing the mass spectrometric analysis of peptides and proteins from complex samples and exhibit great potential for a wide variety of applications.

References

(1) Gao, J.; Zhao, B.; Wang, M.; Serrano, M. A. C.; Zhuang, J.; Ray, M.; Rotello, V. M.; Vachet, R. W.; Thayumanavan, S. Supramolecular Assemblies for Transporting Proteins Across an Immiscible Solvent Interface. *J. Am. Chem. Soc.* **2018**, *140* (7), 2421–2425.

(2) Leriche, G.; Chisholm, L.; Wagner, A. Cleavable Linkers in Chemical Biology. *Bioorg. Med. Chem.* **2012**, *20*, 571–582.

(3) Liu, Y.; Dong, X. Y.; Sun, Y. Protein Separation by Affinity Extraction with Reversed Micelles of Span 85 Modified with Cibacron Blue F3G-A. *Sep. Purif. Technol.* **2007**, *53*, 289–295.

(4) Fasano, M.; Curry, S.; Terreno, E.; Galliano, M.; Fanali, G.; Narciso, P.; Notari, S.; Ascenzi, P. The Extraordinary Ligand Binding Properties of Human Serum Albumin. *IUBMB Life* **2005**, *57* (12), 787–796.

(5) Ding, Z.; Cao, X. Affinity Precipitation of Human Serum Albumin Using a Thermo-Response Polymer with an L-Thyroxin Ligand. *BMC Biotechnol.* **2013**, *13*, 109–118.

(6) Varshney, A.; Sen, P.; Ahmad, E.; Rehan, M.; Subbarao, N.; Khan, R. H. Ligand Binding Strategies of Human Serum Albumin: How Can the Cargo Be Utilized? *Chirality* **2010**, *22*, 77–87.

(7) Xiao, H.; Chen, W.; Smeekens, J. M.; Wu, R. An Enrichment Method Based on Synergistic and Reversible Covalent Interactions for Large-Scale Analysis of Glycoproteins. *Nat. Commun.* **2018**, *9*, 1692.

(8) Madsen, J. A.; Farutin, V.; Carbeau, T.; Wudyka, S.; Yin, Y.; Smith, S.; Anderson, J.; Capila, I. Toward the Complete Characterization of Host Cell Proteins in Biotherapeutics via Affinity Depletions, LC-MS/MS, and Multivariate Analysis. *MAbs* **2015**, *7* (6), 1128–1137.

APPENDIX

SYNTHETIC SCHEMES AND SUPPLEMENTARY EXPERIMENTS

Synthesis of Homopolymer P1

Amphiphilic homopolymer **P1** was synthesized as previously described.[1] The starting material for the monomer is 3,5-dihydroxybenzyl alcohol, which was reacted with one equivalent of 1-iododecane to alkylate one of the phenol groups. The resulting compound was then treated with *tert*-butylbromoacetate. The benzyl alcohol was oxidized by pyridinium chlorochromate (PCC) to give the corresponding aldehyde. Treatment of the aldehyde with methyl triphenylphosponium bromide and potassium *tert*-butoxide in THF yielded the monomer for **P1**. Polymerization was carried out by nitroxide-mediated polymerization (NMP) using a unimolecular initiator. Deprotection of the carboxylate group was then done by treating with base followed by dilute acid to yield **P1**.

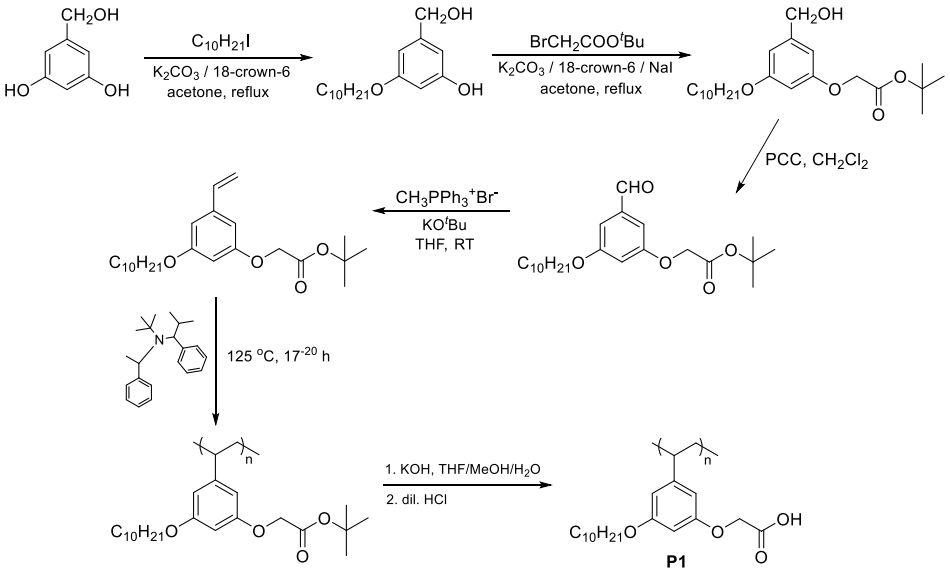

Figure A.1. Synthetic scheme for amphiphilic homopolymer **P1**.

Determination of Extraction Capacity of P1 Reverse Micelle Assemblies

The extraction capacity refers to the concentration of the guest molecule (*e.g.* peptide) that can be accommodated by a given amount of the polymeric reverse micelles. The extraction capacity of **P1** was determined by extracting increasing concentrations of the peptide bradykinin using 200 μL of $1x10^{-4}$ M of polymer and monitoring the peptide peak in the aqueous and organic phases by MALDI-MS. The extraction capacity is taken as the concentration of peptide at which a sudden increase in signal is seen in the aqueous phase or when the signal in the organic phase starts to plateau, indicating that the reverse micelles are saturated and can no longer accommodate more peptides in the organic phase. For **P1**, the capacity was determined to be around 10^{-6} M bradykinin peptide based on Figure A.2.

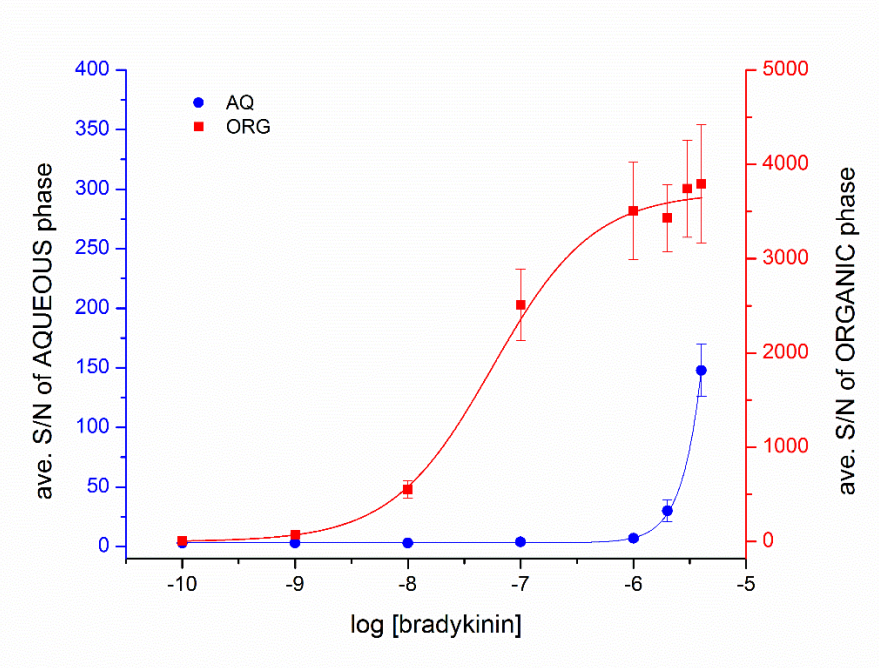

Figure A.2. Determination of extraction capacity of polymer **P1** for bradykinin peptide at pH 8.0.

Synthesis of Polythiolactone-Based (PTLAm) Homopolymers

The PTLAm polymers were synthesized as described in Figure A.3.[2] The PTLAm polymer synthesis was initiated by RAFT polymerization of thiolactone acrylamide,[3] followed by thiolactone ring opening with different amines (blue) and reaction with decyl acrylate (red) in a one pot reaction in DCM/MeOH solvent. GPC of precursor polymer PTLAm: M_n=14.4K, M_w=18.5K, Đ=1.28. ^{1}H-NMR (500 MHz, Chloroform-d) δ 4.92 (br s, 1H), 3.27 (br s, 2H), 2.84 – 1.11 (m, 5H). Due to aggregation issues, NMR for final product is not available. IR spectrum peaks around 1699 cm^{-1} belongs to the C=O of thiolactone, which disappeared after conjugation showing the completion of the modification reaction.

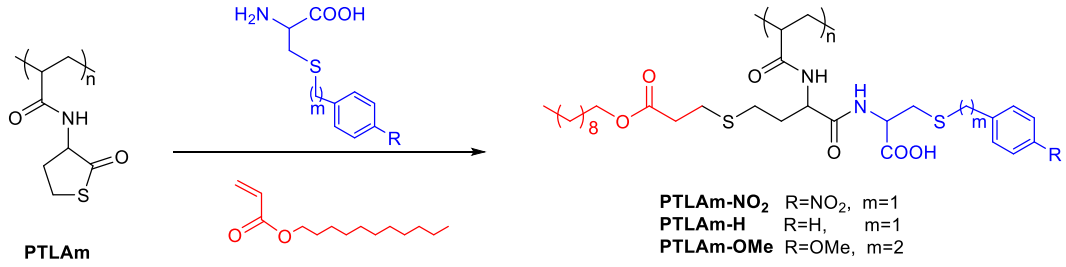

Figure A.3. Synthetic scheme for polythiolactone-based amphiphilic homopolymers.

Characterization of PTLAm Reverse Micelle Assemblies

Dynamic light scattering (DLS) was used to determine the size of the assemblies of polymer **PTLAm-H**. The assemblies were also visualized by transmission electron microscopy.[2]

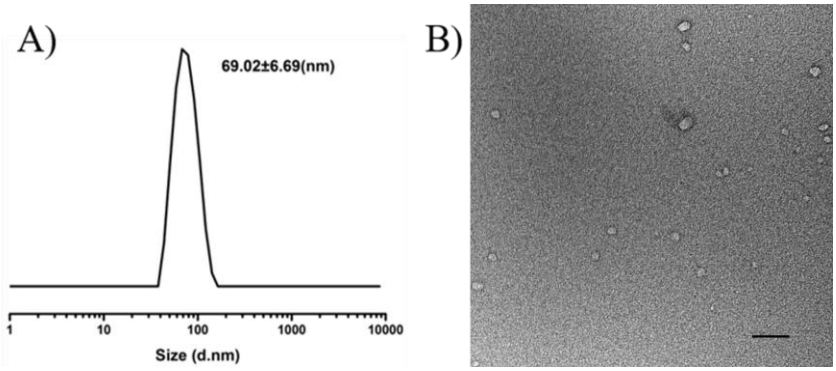

Figure A.4. DLS data (**A**) and TEM image (**B**) for the reverse micelles prepared from polymer **PTLAm-H** at a concentration of 0.5 mg/mL. Scale bar = 50 nm.

Selectivity of Extraction of Peptides Using Reverse Micelles of PTLAm Polymers

The extraction selectivity of PTLAm polymers was tested on a mixture of peptides at pH 8.0. MALDI-MS analysis of the peptide mixture before and after extraction shows that only peptides that are positively charged at pH 8.0 get extracted into the organic phase, as shown in Figure A.5.

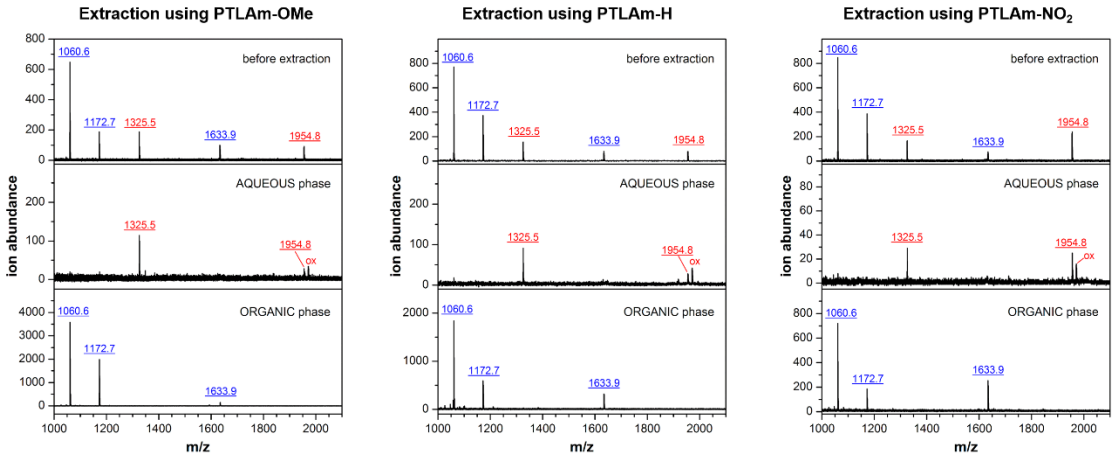

Figure A.5. MALDI mass spectra of a mixture of peptides before and after extraction at pH 8.0 using reverse micelles of the PTLAm-based carboxylate polymers. Only peptides that are positively charged (blue) at pH 8.0 are extracted into the organic phase while peptides that are negatively charged (red) remain in the aqueous phase. Peptides used: bradykinin (RPPGFSPFR, *m/z* 1060.6, pI 12), kinetensin (IARRHPYFL, *m/z* 1172.7, pI 10.8), β-amyloid 1-11 (DAEFRHDSGYE, *m/z* 1325.5, pI 4.3), malantide (RTKRSGSVYEPLKI, *m/z* 1633.9, pI 10.3), preproenkephalin (SSEVAGEGDGDSMGHEDLY, *m/z* 1954.8, pI 3.7).

Synthesis of Polyacrylamide-Based (PAm) Homopolymers

The PAm polymers used in Chapter II were synthesized as described in our published paper.[2] Briefly, the pentafluorophenylacrylate monomer (PFPA) **1a** was synthesized following a published paper[4] using acryloyl chloride and pentafluorophenol in the presence of 1,6-lutidine as the base. The precursor polymer **1b** (PPFPA) was synthesized from **1a** according to published methods.[5] This precursor polymer was then reacted with each of the corresponding secondary amine compounds **3a-g** to obtain the carboxylate functionalized PAm polymers **5a-g** (**PAm-NO$_2$**, **PAm-CN**, **PAm-H**, **PAm-Me**, **PAm-OMe**, **PAm-diOMe**, and **PAm-CTRL**, respectively).

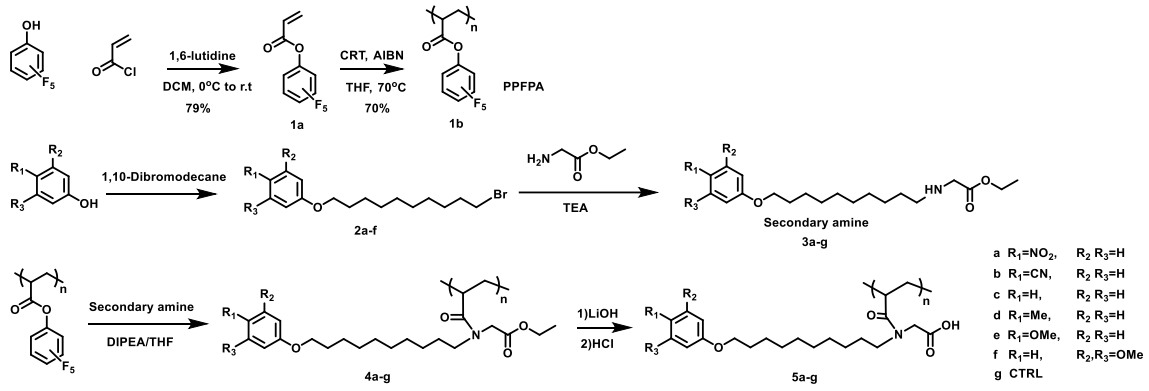

Figure A.6. Synthetic scheme for polyacrylamide-based (PAm) amphiphilic homopolymers.

Characterization of PAm Reverse Micelle Assemblies

The size distributions of PAm-based amphiphilic homopolymer reverse micelles were determined by DLS measurements. The polymers were dissolved in toluene and sonicated until a clear solution was obtained. Two equivalents of water (aqueous NaOH) per carboxylate unit were added to form the water pool inside the reverse micelles. DLS measurements were carried out in a quartz cuvette. The particle sizes obtained for all reverse micelles were between 150 nm and 300 nm based on an average of 3 correlations of 10 minutes each. TEM measurements were performed using a JEOL 2000FX 100K TEM. Samples were prepared by dipping the copper EM grid into the reverse micelle solution and air drying overnight. Critical aggregation concentration (CAC) measurements were done by preparing different concentrations of the polymers in toluene and sonicating for 2 hours to obtain clear solutions. The surface tensions of these solutions were recorded using a tensiometer and plotted against the polymer concentration. As an example, the CAC measurement of polymer **PAm-H** is shown in Figure A.7.

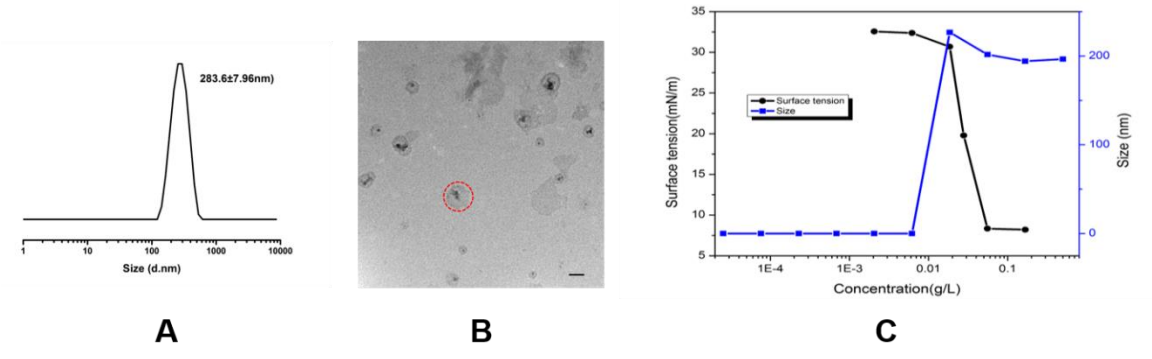

Figure A.7. DLS data (**A**), TEM image (**B**), and CAC determination (**C**) for the reverse micelles prepared from polymer **PAm-H**. Scale bar = 100 nm.

Determination of Extraction Capacity of PAm Reverse Micelle Assemblies

To determine the extraction capacity, increasing concentrations of the peptide bradykinin was extracted using 200 μL of 0.5 mg/mL of each PAm polymer and the peptide peak in the aqueous phase was monitored by MALDI-MS. The extraction capacity is taken as the concentration of peptide at which a sudden increase in signal is seen in the aqueous phase, indicating that the reverse micelles are saturated and can no longer accommodate more peptides in the organic phase.

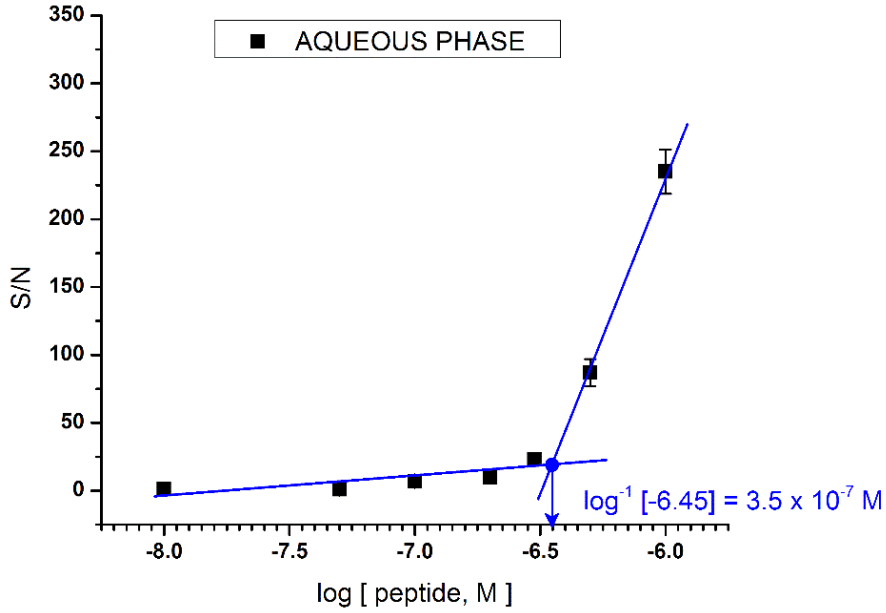

Figure A.8. Example of peptide extraction capacity measurement for polymer **PAm-H** at pH 8.0.

Extraction Selectivity of PAm Polymers

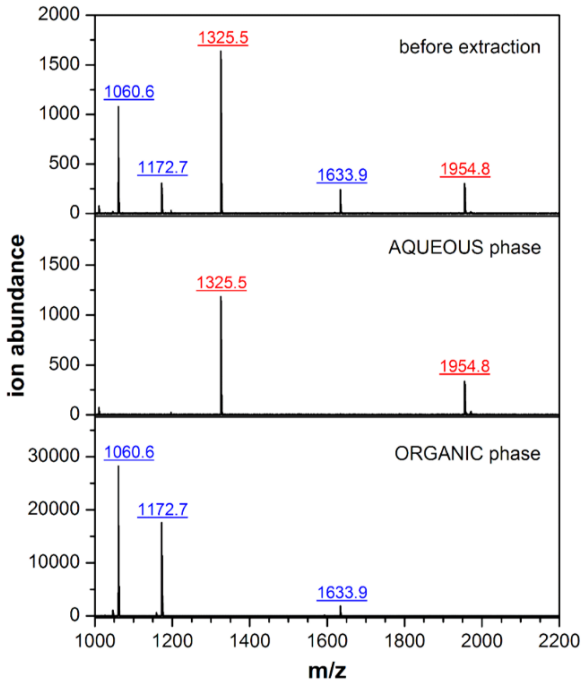

Figure A.9. Example MALDI mass spectra of a mixture of peptides before and after extraction at pH 8.0 using reverse micelles of **PAm-H** carboxylate polymer. Only peptides that are positively charged (blue) at pH 8.0 are extracted into the organic phase while peptides that are negatively charged (red) remain in the aqueous phase. Peptides used: bradykinin (RPPGFSPFR, *m/z* 1060.6, pI 12), kinetensin (IARRHPYFL, *m/z* 1172.7, pI 10.8), β-amyloid 1-11 (DAEFRHDSGYE, *m/z* 1325.5, pI 4.3), malantide (RTKRSGSVYEPLKI, *m/z* 1633.9, pI 10.3), preproenkephalin (SSEVAGEGDGDSMGHEDLY, *m/z* 1954.8, pI 3.7).

Synthesis of Random Copolymer P2

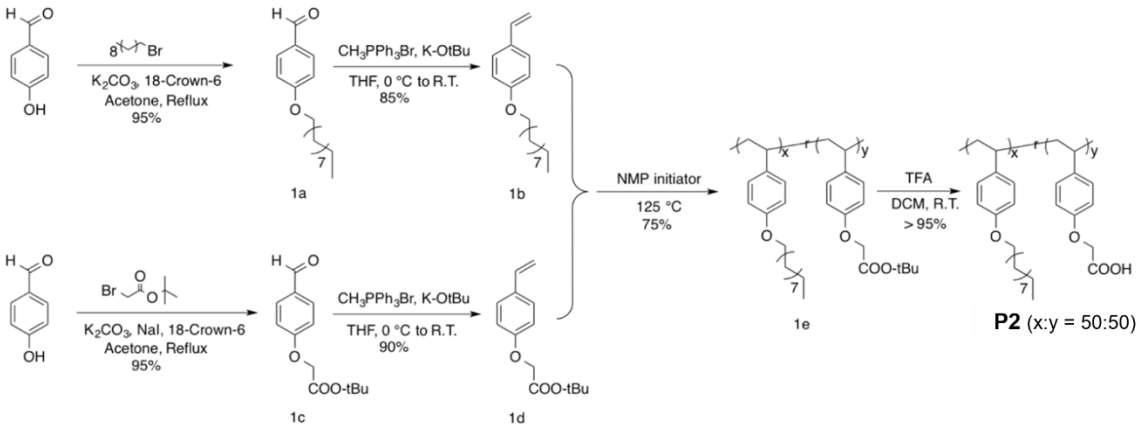

Figure A.10. Synthesis of random copolymer **P2**.

The synthesis and structural characterization (NMR and IR data) of polymer **P2** are described as published.[6] Briefly, the two monomers (compounds **1b** and **1d**) were polymerized at equimolar feed ratios (1.15 mmol of each) by nitroxide-mediated polymerization (NMP) using *N*-*tert*-butyl-*N*-(2-methyl-1-phenylpropyl)-*O*-(1-phenylethyl)hydroxylamine as initiator at 125 ˚C for 12 hours. The resulting product (compound **1e**) was precipitated in MeOH, dried under vacuum, and then deprotected using trifluoroacetic acid (TFA) to yield polymer **P2**.

Synthesis of Random Copolymer P3

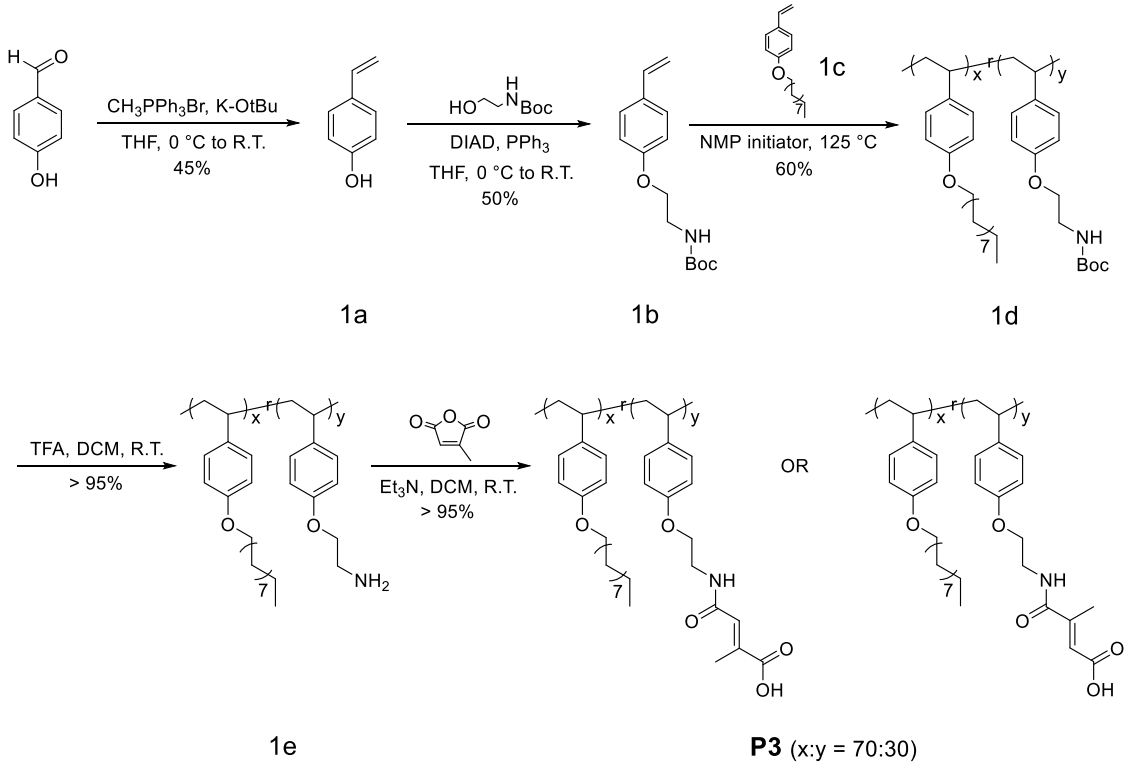

Figure A.11. Synthesis of random copolymer **P3**.

The synthesis and structural characterization (NMR and IR characterization) of polymer **P3** are described as published.[7] The two monomers (compounds **1b** and **1c**) were polymerized by nitroxide-mediated polymerization (NMP) at a feed ratio of 0.38 mmol of **1b** with 0.77 mmol of **1c** using *N*-*tert*-butyl-*N*-(2-methyl-1-phenylpropyl)-*O*-(1-phenylethyl)hydroxylamine as initiator at 125 ˚C for 12 hours. The Boc-protected amine group was deprotected by treatment with TFA. The amine group was then reacted with citraconic anhydride in the presence of a base (triethylamine) to yield polymer **P3** bearing the acid-cleavable citraconic acid amide moiety.

Synthesis of Random Copolymer P7

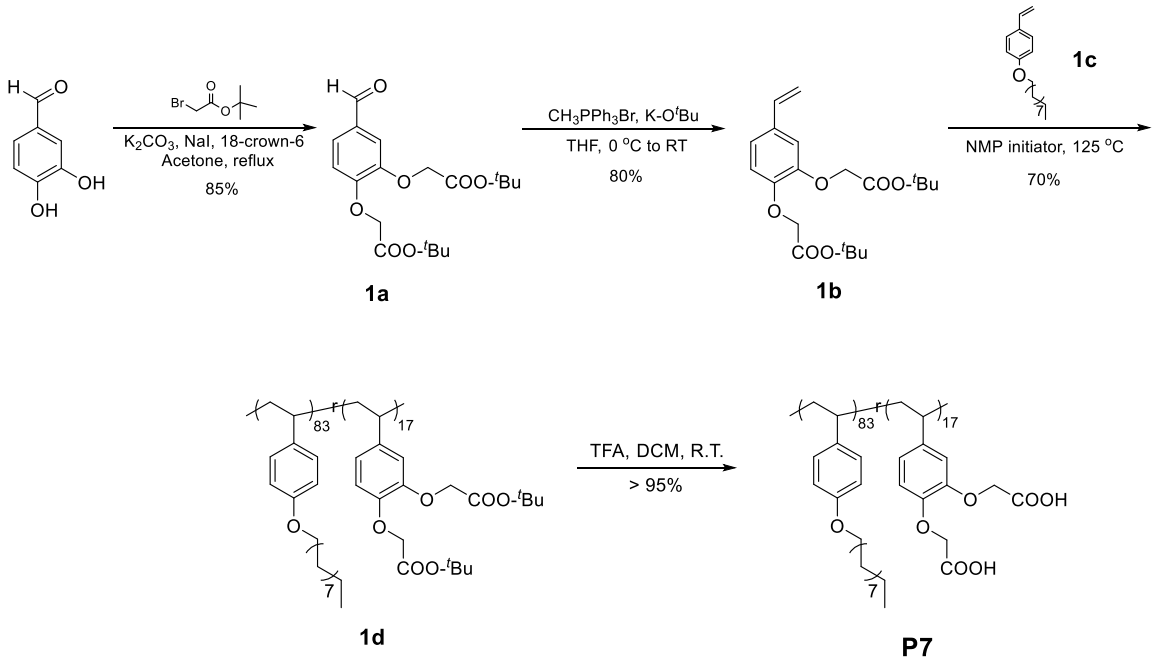

Figure A.12. Synthesis of random copolymer **P7**.

The synthesis and structural characterization (NMR and IR characterization) of polymer **P7** are described as published.[8] Briefly, a feed ratio of 0.14 mmol of **1b** with 0.77 mmol of **1c** was polymerized by nitroxide-mediated polymerization (NMP) using *N*-*tert*-butyl-*N*-(2-methyl-1-phenylpropyl)-*O*-(1-phenylethyl)hydroxylamine as initiator at 125 ˚C for 12 hours to produce random copolymer **1d**. Deprotection of the *tert*-butyl groups was done by treatment with TFA to yield the di-carboxylate functionalized random copolymer **P7**.

Extraction Capacities of Random Copolymers P2, P3, and P7

Increasing concentrations of the peptide bradykinin was extracted using 200 µL of 1 x 10^{-4} M of random copolymer **P2**, **P3**, or **P7** and the peptide peak in the aqueous and organic phases was monitored by MALDI-MS. The extraction capacities for polymers **P2**, **P3**, and **P7** were determined to be 10^{-5} M, 3 x 10^{-6} M, and 10^{-7} M, respectively, based on Figure A.13.

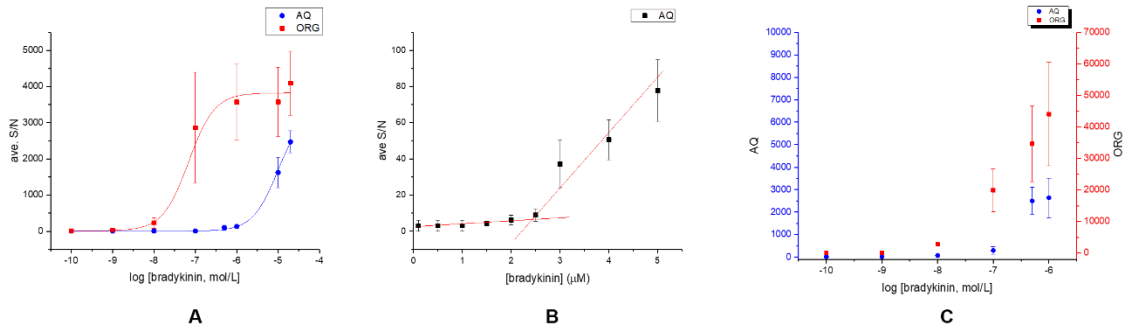

Figure A.13. Determination of extraction capacities of polymers **P2** (**A**), **P3** (**B**) and **P7** (**C**) at pH 8.0.

Extraction Selectivity of P2 Random Copolymer

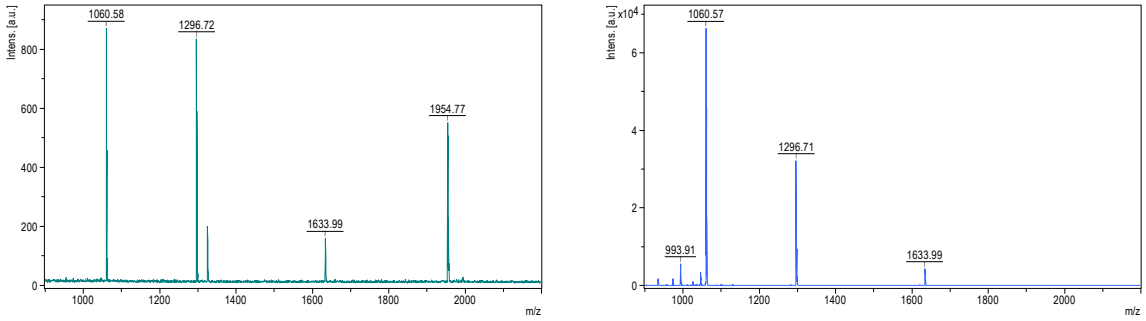

Figure A.14. Example MALDI mass spectra of a mixture of peptides before (**left**) and after (**right**) extraction at pH 8.0 using reverse micelles of **P2** carboxylate polymer. Only peptides that are positively charged at pH 8.0 are extracted into the organic phase (**right**). Peptides used: bradykinin (RPPGFSPFR, *m/z* 1060.6, pI 12), kinetensin (IARRHPYFL, *m/z* 1172.7, pI 10.8), β-amyloid 1-11 (DAEFRHDSGYE, *m/z* 1325.5, pI 4.3), malantide (RTKRSGSVYEPLKI, *m/z* 1633.9, pI 10.3), preproenkephalin (SSEVAGEGDGDSMGHEDLY, *m/z* 1954.8, pI 3.7).

Kinetics of Guest Release

The release efficiency of a TAMRA-labeled bradykinin peptide was monitored at various back-extraction times to determine the kinetics of guest release. The release of peptides by back-extraction using THF followed by the addition of an aqueous acid as stripping aqueous phase was found to be instantaneous, with more than 80% release efficiency achieved within 5 minutes of back-extraction.

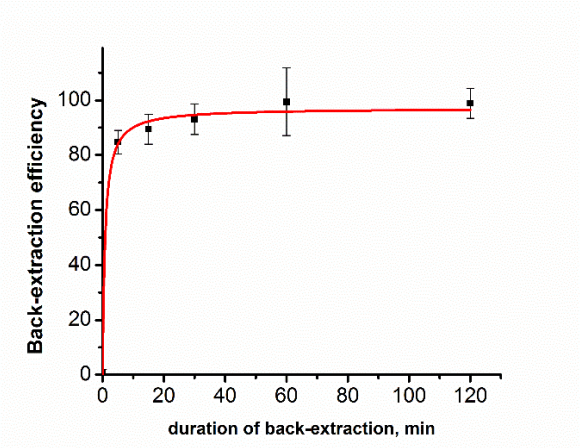

Figure A.15. Release efficiency of TAMRA-labeled bradykinin peptide from reverse micelles of polymer **P3** at various back-extraction times using THF + acid.

Depletion of Serum Spiked with Myoglobin (MG) and Bovine Carbonic Anhydrase (BCA)

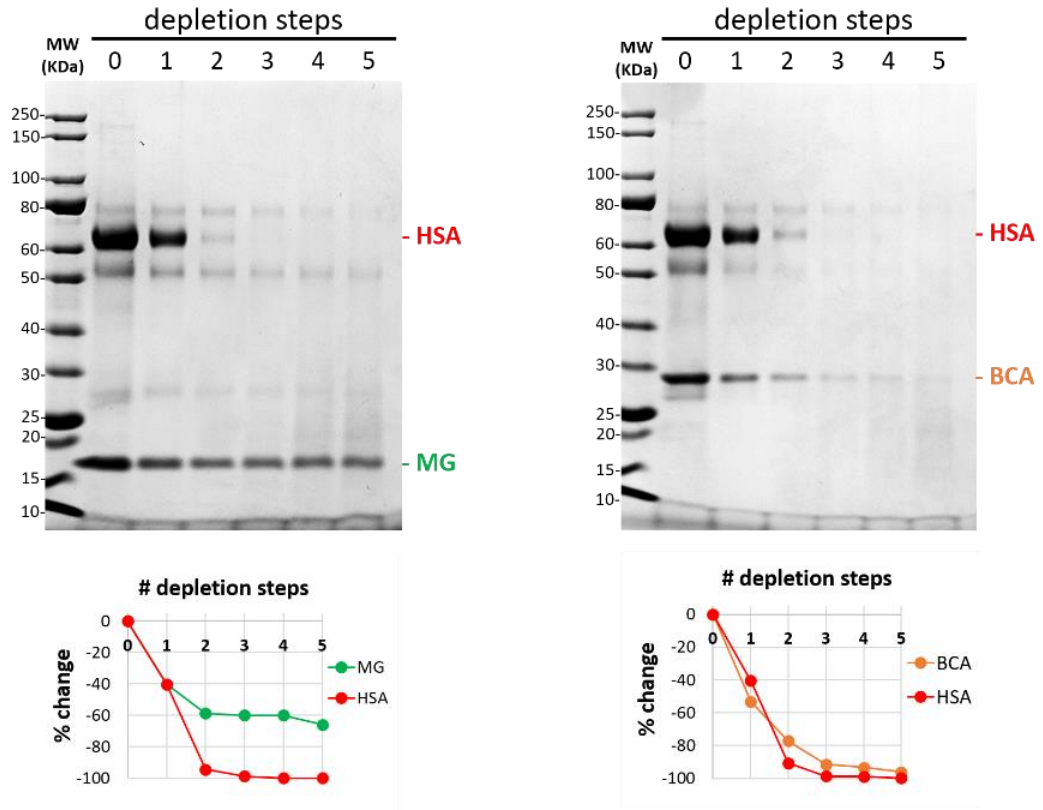

Figure A.16. SDS-PAGE analysis of serum spiked with MG and BCA. Five sequential extractions using 400 µL of 2 mg/mL of **P9** were performed at pH 6.0. Changes in protein band intensity after each depletion step (relative to before extraction) were measured using *ImageJ* software and illustrated in a graph below each gel image. pI of spiked proteins: MG (pI 6.8 and 7.2), BCA (pI 6.2).

Identification of Protein Bands by Peptide Mass Fingerprinting

In Chapter IV, the identities of the major proteins depleted by the polymer were identified by running an SDS-PAGE gel of the depleted fractions and the polymer-bound fractions (Figure 4.10), followed by in-gel tryptic digestion of the prominent bands depleted and then identification by peptide mass fingerprinting (PMF). The summary of the results is given in Table 4.1 of Chapter IV, while the detailed results of the PMF analysis are presented here as Tables A.1 to A.7. Band numbers indicated refer to bands as labeled in Figure 4.10.

Table A.1. Peptides belonging to α-2-macroglobulin (Uniprot P01023) identified for protein band 1.

Confidence	Sequence	# PSMs	# Proteins	# Protein Groups	Protein Group Accessions	Modifications	ΔCn	XCorr	Charge	MH+ [Da]	ΔM [ppm]	RT [min]	# Missed Cleavages
High	NEDSLVFVQTDK	3	2	1	P01023		0.0000	4.27	2	1394.68096	0.78	27.21	0
High	VGFYESDVmGR	3	1	1	P01023	M9(Oxidation)	0.0000	3.68	2	1275.56438	-2.43	24.09	0
High	LPPNVVEESAR	3	1	1	P01023		0.0000	3.47	2	1210.64287	0.15	22.53	0
High	FEVQVTVPK	2	1	1	P01023		0.0000	3.18	2	1046.58745	-0.64	27.89	0
High	ATVLNYLPK	1	4	1	P01023		0.0000	2.61	2	1018.59227	-0.90	30.35	0
High	SDIAPVAR	3	2	1	P01023		0.0000	2.43	2	828.45653	-1.10	17.69	0
Medium	rTTVMVK	3	2	1	P01023	N-Term(Gln->pyro-Glu)	0.0000	1.19	1	817.46729	8.81	29.25	1
Medium	EVLK	1	187	4	P01023;P32456;Q9ULW8;A0A024R8E8		0.1333	1.04	1	488.30756	-0.71	32.91	0
Low	FRVVSMDENFHPLNELIPLVYIQDPKGNR	1	1	1	P01023		0.0000	0.85	2	3440.75762	-6.07	10.85	2

Table A.2. Peptides belonging to transferrin (Uniprot Q53H26) identified for protein band 2.

Confidence	Sequence	# PSMs	# Proteins	# Protein	Protein Group Accessions	Modifications	ΔCn	XCorr	Charge	MH+ [Da]	ΔM [ppm]	RT [min]	# Missed Cleavages
High	SDNcEDTPEAGYFAVAVVK	9	4	2	Q53H26;B4E1B	C4(Carbamidomethyl)	0.0000	7.94	3	2071.92862	0.39	31.58	0
High	KPVDEYKDcHLAQVPSHTVVA	12	6	2	Q53H26;B4E1B	C9(Carbamidomethyl)	0.0000	7.60	3	2549.29007	-1.15	24.69	1
High	KPVEEYANcHLAR	10	5	1	Q53H26	C9(Carbamidomethyl)	0.0000	5.94	3	1586.77256	-1.19	20.70	0
High	SDNcEDTPEAGYFAVAVVKK	3	4	2	Q53H26;B4E1B	C4(Carbamidomethyl)	0.0000	5.49	3	2200.02225	-0.24	29.67	1
High	NLNEKDYELLcLDGTR	6	6	2	Q53H26;B4E1B	C11(Carbamidomethyl	0.0000	5.43	2	1952.93938	0.55	30.74	1
High	cSTSSLLEAcTFR	6	6	2	Q53H26;B4E1B2	C1(Carbamidomethyl); C10(Carbamidomethyl	0.0000	5.39	2	1531.69109	2.02	29.04	0
High	IEcVSAETTEDcIAK	7	6	2	Q53H26;B4E1B2	C3(Carbamidomethyl); C12(Carbamidomethyl	0.0000	5.34	2	1725.76811	0.61	23.04	0
High	HSTIFENLANKADR	3	7	2	Q53H26;B4E1B		0.0000	5.11	3	1615.81528	-2.15	28.58	1
High	DQYELLcLDNTR	6	7	2	Q53H26;B4E1B	C7(Carbamidomethyl)	0.0000	5.03	2	1539.71196	0.73	30.50	0
High	SKEFQLFSSPHGK	13	6	2	Q53H26;B4E1B		0.0000	5.01	3	1491.75940	0.20	26.88	1
High	FDEFFSEGcAPGSK	6	7	2	Q53H26;B4E1B	C9(Carbamidomethyl)	0.0000	4.99	2	1577.65898	0.77	28.74	0
High	EDPQTFYYAVAVVK	12	5	2	Q53H26;B4E1B		0.0000	4.97	2	1629.81621	0.16	33.84	0
High	KcSTSSLLEAcTFR	6	6	2	Q53H26;B4E1B2	C2(Carbamidomethyl); C11(Carbamidomethyl	0.0000	4.84	2	1659.78386	0.54	27.84	1
High	LKcDEWSVNSVGK	6	6	2	Q53H26;B4E1B	C3(Carbamidomethyl)	0.0000	4.83	2	1521.73870	1.33	24.54	1
High	LcmGSGLNLcEPNNK	7	7	2	Q53H26;B4E1B2	C2(Carbamidomethyl); M3(Oxidation); C10(Carbamidomethyl	0.0000	4.81	2	1722.76128	0.23	23.86	0
High	cLKDGAGDVAFVK	6	7	2	Q53H26;B4E1B	C1(Carbamidomethyl)	0.0000	4.73	3	1379.69693	-1.39	24.20	1
High	mYLGYEYVTAIR	12	6	2	Q53H26;B4E1B	M1(Oxidation)	0.0000	4.71	2	1494.73003	0.18	31.39	0
High	ADRDQYELLcLDNTR	10	7	2	Q53H26;B4E1B	C10(Carbamidomethyl	0.0000	4.60	2	1881.87358	-1.30	29.32	1
High	GDVAFVKHQTVPQNTGGK	3	6	2	Q53H26;B4E1B		0.0000	4.53	3	1882.97605	-0.54	20.88	1
High	DcHLAQVPSHTVVAR	9	6	2	Q53H26;B4E1B	C2(Carbamidomethyl)	0.0000	4.40	2	1689.85173	1.61	22.34	0
High	HSTIFENLANK	15	7	2	Q53H26;B4E1B		0.0000	4.29	2	1273.65276	-0.64	26.91	0
High	TAGWNIPmGLLYNK	4	7	2	Q53H26;B4E1B	M8(Oxidation)	0.0000	4.25	2	1593.81084	0.87	34.09	0
High	cDEWSVNSVGK	3	6	2	Q53H26;B4E1B	C1(Carbamidomethyl)	0.0000	4.19	2	1280.56548	6.12	24.15	0
High	DLLFKDSAHGFLK	3	6	2	Q53H26;B4E1B		0.0000	4.00	3	1490.80085	0.39	31.88	1
High	FDEFFSEGcAPGSKK	6	7	2	Q53H26;B4E1B	C9(Carbamidomethyl)	0.0000	3.97	3	1705.75083	-1.12	27.59	1
High	HQTVPQNTGGKNPDPWAK	3	6	2	Q53H26;B4E1B		0.0000	3.93	3	1974.97904	0.46	21.98	1
High	DYELLcLDGTR	2	6	2	Q53H26;B4E1B	C6(Carbamidomethyl)	0.0000	3.89	2	1354.63054	-0.19	31.07	0
High	KDSGFQmNQLR	7	5	2	Q53H26;B4E1B	M7(Oxidation)	0.0000	3.87	2	1339.64226	-0.09	19.10	1
High	DGAGDVAFVK	10	7	2	Q53H26;B4E1B		0.0000	3.80	2	978.48931	0.16	22.85	0
High	EGYYGYTGAFR	15	7	2	Q53H26;B4E1B		0.0000	3.78	2	1283.56853	-0.48	27.35	0
High	DSGFQMNQLR	3	5	2	Q53H26;B4E1B		0.0000	3.73	2	1195.55083	-1.39	25.62	0
High	SASDLTWDNLK	12	7	2	Q53H26;B4E1B		0.0000	3.72	2	1249.60576	-0.16	28.32	0
High	KSASDLTWDNLK	6	7	2	Q53H26;B4E1B		0.0000	3.70	2	1377.70085	-0.06	26.91	1
High	cLVEKGDVAFVK	4	7	2	Q53H26;B4E1B	C1(Carbamidomethyl)	0.0000	3.63	3	1364.72458	0.19	25.99	1
High	DSGFQmNQLR	6	5	2	Q53H26;B4E1B	M6(Oxidation)	0.0000	3.60	2	1211.54778	0.31	20.33	0
High	KASYLDcIR	6	8	2	Q53H26;B4E1B	C7(Carbamidomethyl)	0.0000	3.43	3	1125.57181	-0.30	23.91	1
High	APNHAVVTR	6	6	2	Q53H26;B4E1B		0.0000	3.35	3	964.53211	-0.23	13.96	0
High	EGTcPEAPTDEcKPVK	10	6	2	Q53H26;B4E1B2	C4(Carbamidomethyl); C12(Carbamidomethyl	0.0000	3.32	2	1817.80596	0.79	18.04	0
High	WcALSHHER	9	6	2	Q53H26;B4E1B	C2(Carbamidomethyl)	0.0000	3.31	2	1195.54289	0.27	22.06	0
High	EFQLFSSPHGK	6	6	2	Q53H26;B4E1B		0.0000	3.31	2	1276.63176	-0.27	28.74	0
High	KDSGFQMNQLR	6	5	2	Q53H26;B4E1B		0.0000	3.27	2	1323.64983	1.79	24.28	1
High	ASYLDcIR	7	8	2	Q53H26;B4E1B	C6(Carbamidomethyl)	0.0000	3.16	2	997.47685	-0.32	25.46	0
High	SVIPSDGPSVAcVKK	5	8	2	Q53H26;B4E1B	C12(Carbamidomethyl	0.0000	2.99	2	1543.81853	2.33	23.42	1
High	DLLFRDDTVcLAK	8	6	2	Q53H26;B4E1B	C10(Carbamidomethyl	0.0000	2.95	3	1565.79801	-0.82	31.40	1
High	WcAVSEHEATK	6	8	2	Q53H26;B4E1B	C2(Carbamidomethyl)	0.0000	2.84	3	1317.58921	-0.04	19.40	0
High	SVIPSDGPSVAcVK	6	8	2	Q53H26;B4E1B	C12(Carbamidomethyl	0.0000	2.81	2	1415.72112	0.81	24.91	0
High	DDTVcLAK	6	6	2	Q53H26;B4E1B	C5(Carbamidomethyl)	0.0000	2.80	2	921.43437	-0.31	18.56	0
High	NPDPWAK	6	6	2	Q53H26;B4E1B		0.0000	2.65	2	827.40489	0.27	20.78	0
High	HQTVPQNTGGK	3	6	2	Q53H26;B4E1B		0.0000	2.63	2	1166.59038	-0.79	12.80	0
High	YLGEEYVK	6	6	2	Q53H26;B4E1B		0.0000	2.61	2	1000.49901	0.40	24.57	0
High	GDVAFVK	11	7	2	Q53H26;B4E1B		0.0000	2.30	2	735.40367	0.08	20.87	0
High	DSAHGFLK	13	6	2	Q53H26;B4E1B		0.0000	2.14	2	874.45018	9.61	20.34	0
Medium	sKEFQLFSSPHGK	3	6	2	Q53H26;B4E1B	N-Term(Gln->pyro-	0.0000	2.08	4	1474.73025	-1.57	27.15	1
Medium	WCALSHHER	1	6	2	Q53H26;B4E1B		0.0000	1.86	3	1138.52552	3.87	21.63	0
Medium	DLLFK	6	31	3	P08582;Q53H26;B4E1B2		0.0000	1.47	2	635.37975	5.39	26.93	0
Medium	iECVSAETTEDCIAK	1	6	2	Q53H26;B4E1B	N-Term(Gln->pyro-	0.0392	1.47	3	1594.71018	7.90	32.25	0
Medium	DLLFR	7	13	3	Q15572;Q53H26;B4E1B2		0.0000	1.38	1	663.38251	0.05	27.74	0
Medium	EDPQTFYYAVAVVKK	3	5	2	Q53H26;B4E1B		0.0000	1.37	3	1757.90750	-1.94	31.10	1

Table A.3. Peptides belonging to human serum albumin (Uniprot P02768) identified for protein band 3.

Confidence	Sequence	# PSMs	# Proteins	# Protein Groups	Protein Group Accessi	Modifications	ΔCn	XCorr	Charge	MH+ [Da]	ΔM [ppm]	RT [min]	# Missed Cleavages
High	SHcIAEVENDEmPADLPSLAADFVESK	3	8	1	P02768	C3(Carbamidomethyl); M12(Oxidation)	0.0000	7.34	3	2990.34281	1.09	36.25	0
High	LVRPEVDVmcTAFHDNEETFLK	6	9	1	P02768	M9(Oxidation); C10(Carbamidomethyl)	0.0000	7.34	3	2666.25437	-1.75	30.69	0
High	LVRPEVDVMcTAFHDNEETFLKK	6	9	1	P02768	C10(Carbamidomethyl)	0.0000	6.36	4	2778.36538	2.26	33.90	1
High	ADDKETcFAEEGKK	26	13	1	P02768	C7(Carbamidomethyl)	0.0000	5.82	3	1627.72739	0.29	17.17	2
High	RHPYFYAPELLFFAKR	4	11	1	P02768		0.0000	5.75	4	2055.09804	0.81	44.32	2
High	LVRPEVDVmcTAFHDNEETFLKK	16	9	1	P02768	M9(Oxidation); C10(Carbamidomethyl)	0.0000	5.69	5	2794.35377	-0.08	29.34	1
High	RHPDYSVVLLLR	135	10	1	P02768		0.0000	5.65	3	1467.84601	1.98	48.61	1
High	FPKAEFAEVSK	6	10	1	P02768		0.0000	5.51	3	1252.65735	0.06	24.98	1
High	QEPERNEcFLQHKDDNPNLPR	9	9	1	P02768	C8(Carbamidomethyl)	0.0000	5.45	3	2636.22965	0.95	23.75	2
High	NEcFLQHKDDNPNLPR	10	9	1	P02768	C3(Carbamidomethyl)	0.0000	5.22	2	1996.93535	2.95	23.81	1
High	qEPERNEcFLQHKDDNPNLPR	7	9	1	P02768	N-Term(Gln->pyro-Glu); C8(Carbamidomethyl)	0.0000	5.18	4	2619.20449	1.49	24.79	2
High	VFDEFKPLVEEPQNLIK	19	13	1	P02768		0.0000	5.15	2	2045.09612	0.32	35.43	0
High	LVRPEVDVMCTAFHDNEETFLKK	5	9	1	P02768		0.0000	5.14	4	2721.35512	6.43	29.47	1
High	SLHTLFGDKLcTVATLR	6	9	1	P02768	C11(Carbamidomethyl)	0.0000	5.05	3	1932.04081	1.85	34.18	1
High	AVMDDFAAFVEK	15	13	1	P02768		0.0000	5.02	3	1342.63483	-0.02	34.70	0
High	QNcELFEQLGEYK	15	13	1	P02768	C3(Carbamidomethyl)	0.0000	4.95	2	1657.75566	1.78	31.46	0
High	HPYFYAPELLFFAKR	2	11	1	P02768		0.0000	4.94	3	1898.99503	-0.12	40.77	1
High	ADDKETcFAEEGK	11	13	1	P02768	C7(Carbamidomethyl)	0.0000	4.84	3	1499.64200	6.71	18.22	1
High	qNcELFEQLGEYK	8	13	1	P02768	N-Term(Gln->pyro-Glu); C3(Carbamidomethyl)	0.0000	4.83	2	1640.72673	0.35	33.90	0
High	LKEccEKPLLEK	17	11	1	P02768	C4(Carbamidomethyl); C5(Carbamidomethyl)	0.0000	4.75	3	1546.79294	-2.52	21.34	1
High	VTKccTESLVNR	3	12	1	P02768	C4(Carbamidomethyl); C5(Carbamidomethyl)	0.0000	4.67	3	1466.71250	2.34	18.89	1
High	LVRPEVDVmCTAFHDNEETFLKK	7	9	1	P02768	M9(Oxidation)	0.0000	4.50	3	2737.31522	-6.33	29.45	1
High	qEPERNEcFLQHK	9	9	1	P02768	N-Term(Gln->pyro-Glu); C8(Carbamidomethyl)	0.0000	4.48	3	1697.76798	-1.25	22.22	1
High	YKAAFTEccQAADK	2	10	1	P02768	C8(Carbamidomethyl); C9(Carbamidomethyl)	0.0000	4.46	3	1662.72214	-1.79	20.71	1
High	RPcFSALEVDETYVPK	44	12	1	P02768	C3(Carbamidomethyl)	0.0000	4.35	3	1910.92911	-1.38	33.37	0
High	RHPYFYAPELLFFAK	15	11	1	P02768		0.0000	4.33	2	1898.99346	-0.95	43.16	1
High	DVFLGmFLYEYAR	5	10	1	P02768	M6(Oxidation)	0.0000	4.32	2	1639.78349	0.57	39.75	0
High	LAKTYETTLEK	2	11	1	P02768		0.0000	4.23	3	1296.70429	-0.24	20.44	1
High	AVmDDFAAFVEK	43	13	1	P02768	M3(Oxidation)	0.0000	4.21	2	1358.63176	1.47	31.07	0
High	VPQVSTPTLVEVSR	18	13	1	P02768		0.0000	4.20	3	1511.85486	7.94	28.26	0
High	TcVADESAENcDK	10	9	1	P02768	C2(Carbamidomethyl); C11(Carbamidomethyl)	0.0000	4.07	2	1498.58367	3.43	14.74	0
High	QEPERNEcFLQHK	11	9	1	P02768	C8(Carbamidomethyl)	0.0000	3.99	2	1714.79582	-0.48	20.17	1
High	HPYFYAPELLFFAK	6	11	1	P02768		0.0000	3.99	3	1742.89634	1.26	41.49	0
High	FKDLGEENFK	28	11	1	P02768		0.0000	3.97	3	1226.60520	-0.04	23.78	1
High	YTKKVPQVSTPTLVEVSR	3	13	1	P02768		0.0000	3.95	3	2032.14164	-1.06	26.76	2
High	LVAASQAALGL	79	13	1	P02768		0.0000	3.93	2	1013.59783	-1.19	31.22	0
High	LDELRDEGKASSAK	5	9	1	P02768		0.0000	3.90	3	1518.77350	-1.59	16.94	2
High	YIcENQDSISSK	18	11	1	P02768	C3(Carbamidomethyl)	0.0000	3.87	2	1443.64336	0.89	19.32	0
High	ETYGEmADccAK	15	9	1	P02768	M6(Oxidation); C9(Carbamidomethyl); C10(Carbamidomethyl)	0.0000	3.85	2	1450.52873	0.23	15.45	0
High	KVPQVSTPTLVEVSR	46	13	1	P02768		0.0000	3.82	2	1639.93816	0.21	27.19	1
High	DVcKNYAEAK	6	11	1	P02768	C3(Carbamidomethyl)	0.0000	3.76	3	1197.55460	-1.92	15.54	1
High	AAFTEccQAADK	13	10	1	P02768	C6(Carbamidomethyl); C7(Carbamidomethyl)	0.0000	3.58	2	1371.56890	1.51	18.12	0
High	qTALVELVKHKPK	3	13	1	P02768	N-Term(Gln->pyro-Glu)	0.0000	3.56	3	1473.87989	0.71	29.76	1
High	kVPQVSTPTLVEVSR	1	13	1	P02768	N-Term(Gln->pyro-Glu)	0.0000	3.48	2	1622.91081	-0.28	28.98	1
High	KLVAASQAALGL	5	13	1	P02768		0.0000	3.39	2	1141.69353	-0.41	28.96	1
High	ccTESLVNR	12	12	1	P02768	C1(Carbamidomethyl); C2(Carbamidomethyl)	0.0000	3.33	2	1138.49663	-1.20	18.56	0
High	KQTALVELVK	20	13	1	P02768		0.0000	3.29	2	1128.69829	-0.40	25.64	1
High	ETYGEMADccAK	3	9	1	P02768	C9(Carbamidomethyl); C10(Carbamidomethyl)	0.0000	3.17	2	1434.53264	-0.58	20.06	0
High	HPDYSVVLLLR	32	10	1	P02768		0.0000	3.02	2	1311.74321	0.93	34.38	0
High	DAHKSEVAHR	3	11	1	P02768		0.0000	2.94	3	1149.57676	0.66	12.85	1
High	KYLYEIAR	7	8	1	P02768		0.0000	2.90	2	1055.58769	-0.70	24.74	1
High	EccEKPLLEK	5	11	1	P02768	C2(Carbamidomethyl); C3(Carbamidomethyl)	0.0000	2.87	2	1305.61626	-1.18	18.70	0
High	DLGEENFK	9	11	1	P02768		0.0000	2.86	2	951.44054	-1.38	21.22	0
High	SLHTLFGDK	23	9	1	P02768		0.0000	2.86	3	1017.53821	1.77	25.66	0
High	LVNEVTEFAK	40	9	1	P02768		0.0000	2.83	2	1149.61553	0.40	27.85	0
High	AEFAEVSKLVTDLTK	1	10	1	P02768		0.0000	2.80	3	1650.89280	-1.31	37.61	1
High	dDNPNLPR	4	9	1	P02768	N-Term(Gln->pyro-Glu)	0.0000	2.76	2	923.42076	-1.10	17.74	0
High	LDELRDEGK	20	9	1	P02768		0.0000	2.75	2	1074.55254	9.21	17.26	1

Table A.3 (continuation). Peptides belonging to human serum albumin (Uniprot P02768) identified for protein band 3.

Confidence	Sequence	# PSMs	# Proteins	# Protein Groups	Protein Group Accessions	Modifications	ΔCn	XCorr	Charge	MH+ [Da]	ΔM [ppm]	RT [min]	# Missed Cleavages
High	AEFAEVSK	18	10	1	P02768		0.0000	2.75	2	880.44005	-1.22	18.63	0
High	DDNPNLPR	22	9	1	P02768		0.0000	2.73	2	940.44896	0.67	18.43	0
Medium	TcVADESAENcDKSLHTLFGDK	2	9	1	P02768	C2(Carbamidomethyl); C11(Carbamidomethyl)	0.0000	2.73	4	2497.08462	-5.00	28.64	1
High	AAcLLPK	13	10	1	P02768	C3(Carbamidomethyl)	0.0000	2.71	2	772.43816	-0.59	21.54	0
High	LCTVATLR	3	9	1	P02768		0.0000	2.71	2	876.49864	1.66	24.59	0
High	QTALVELVKHKPK	3	13	1	P02768		0.0000	2.66	3	1490.90174	-2.45	25.42	1
High	NEcFLQHK	6	9	1	P02768	C3(Carbamidomethyl)	0.0000	2.64	2	1075.49932	0.32	19.09	0
High	FQNALLVR	31	13	1	P02768		0.0000	2.59	1	960.56348	0.94	26.32	0
High	kQTALVELVK	1	13	1	P02768	N-Term(Gln->pyro-Glu)	0.0000	2.56	2	1111.67070	-1.34	29.35	1
High	YLYEIAR	25	9	1	P02768		0.0000	2.48	2	927.49278	-0.73	28.34	0
Medium	AVmDDFAAFVEKccK	3	13	1	P02768	M3(Oxidation); C13(Carbamidomethyl); C14(Carbamidomethyl)	0.0000	2.48	3	1806.79007	2.23	30.52	1
High	LcTVATLR	20	9	1	P02768	C2(Carbamidomethyl)	0.0000	2.34	2	933.52062	2.10	22.44	0
High	fQNALLVR	5	13	1	P02768	N-Term(Gln->pyro-Glu)	0.0000	2.26	2	943.53819	2.30	26.36	0
High	QTALVELVK	14	13	1	P02768		0.0000	2.25	1	1000.60382	0.05	27.88	0
High	qTALVELVK	16	13	1	P02768	N-Term(Gln->pyro-Glu)	0.0000	2.24	1	983.57745	0.24	32.67	0
Medium	EQLKAVmDDFAAFVEK	1	13	1	P02768	M7(Oxidation)	0.0261	2.24	3	1856.91520	2.81	33.67	1
High	TYETTLEK	21	11	1	P02768		0.0000	2.13	2	984.48729	-1.17	18.60	0
Medium	ETcFAEEGKK	3	13	1	P02768	C3(Carbamidomethyl)	0.0000	2.05	3	1198.54108	0.13	15.85	1
Medium	lVNEVTEFAK	3	9	1	P02768	N-Term(Gln->pyro-Glu)	0.0000	1.92	2	1132.59477	5.52	28.51	0
Medium	NYAEAK	1	11	1	P02768		0.0000	1.90	2	695.33550	-0.58	11.44	0
High	AWAVAR	9	16	2	P02768;E9		0.0000	1.76	1	673.37775	-0.47	20.03	0
High	LVTDLTK	23	11	1	P02768		0.0000	1.75	1	789.47192	0.31	21.02	0
Medium	CCAAADPHEcYAK	5	13	1	P02768	C10(Carbamidomethyl)	0.0000	1.34	2	1438.54534	-6.63	15.71	0
Low	aDDKETcFAEEGKK	1	13	1	P02768	N-Term(Gln->pyro-Glu); C7(Carbamidomethyl)	0.0000	1.26	4	1610.70998	5.97	16.47	2
Medium	ccAAADPHEcYAK	3	13	1	P02768	N-Term(Gln->pyro-Glu); C2(Carbamidomethyl);	0.0000	1.19	2	1478.56340	9.21	17.04	0
Medium	ETcFAEEGK	1	13	1	P02768	C3(Carbamidomethyl)	0.0000	1.08	2	1070.44780	1.72	25.72	0
Low	ETYGEmADcCAK	1	9	1	P02768	M6(Oxidation); C9(Carbamidomethyl)	0.0556	0.34	2	1393.51921	8.81	15.09	0

Table A.4. Peptides belonging to IgG heavy chain identified for protein band 4.

Confidence	Sequence	# PSMs	# Proteins	# Protein Groups	Protein Group Accessions	Modifications	ΔCn	XCorr	Charge	MH+ [Da]	ΔM [ppm]	RT [min]	# Missed Cleavages
High	TPEVTcVVVDVSHEDPEVK	6	27	4	A0A087X079;Q6GMX6;Q6MZQ6;Q7Z351	C6(Carbamidomethyl)	0.0000	6.35	2	2139.02812	0.28	29.57	0
High	TTPPVLDSDGSFFLYSK	13	21	4	A0A087X079;Q6GMX6;Q6MZQ6;Q7Z351		0.0000	5.30	3	1873.91837	-1.88	34.22	0
High	EPQVYTLPPSRDELTK	17	19	4	A0A087X079;Q6GMX6;Q6MZQ6;Q7Z351		0.0000	4.64	2	1872.97331	1.64	26.82	1
High	fNWYVDGVEVHNAK	3	23	4	A0A087X079;Q6GMX6;Q6MZQ6;Q7Z351	N-Term(Gln->pyro-Glu)	0.0000	4.47	2	1660.77703	0.92	34.28	0
High	STSGGTAALGcLVK	12	47	8	A0A087X079;Q6GMX6;A0A087WXL8;A0A087WVW2;Q6MZQ6;S6C4R2;Q7Z351;S6BGD4	C11(Carbamidomethyl)	0.0000	4.30	2	1321.67839	0.22	26.43	0
High	WQQGNVFScSVmHEALHNHYTQK	7	19	3	A0A087X079;Q6GMX6;P01859	C9(Carbamidomethyl); M12(Oxidation)	0.0000	4.04	3	2817.26017	-0.69	28.44	0
High	FNWYVDGVEVHNAK	19	23	4	A0A087X079;Q6GMX6;Q6MZQ6;Q7Z351		0.0000	3.92	3	1677.80143	-0.37	30.17	0
High	GTTVTVSSASTK	3	2	1	A0A087X079		0.0000	3.87	2	1138.59404	-0.89	16.30	0
High	NSLYLQMNSLR	9	41	7	Q0ZCH9;Q96K68;A2J1N2;Q9UL71;A0A087X2C0;A0A087X079;A2NYQ9		0.0000	3.58	2	1338.68303	-0.34	30.21	0
High	THTcPPcPAPELLGGPSVFLFPPKPK	3	28	4	A0A087X079;Q6GMX6;Q6MZQ6;Q7Z351	C4(Carbamidomethyl); C7(Carbamidomethyl)	0.0000	3.57	4	2844.46499	2.57	37.18	0
High	NSLYLQmNSLR	7	41	7	Q0ZCH9;Q96K68;A2J1N2;Q9UL71;A0A087X2C0;A0A087X079;A2NYQ9	M7(Oxidation)	0.0000	3.53	2	1354.68047	1.52	25.24	0
High	NQVSLTcLVK	8	35	8	A0A087X079;Q6GMX6;P01859;A0A087WXL8;A0A087WVW2;Q6MZQ6;Q6MZX7;Q7Z351	C7(Carbamidomethyl)	0.0000	3.41	2	1161.62883	-0.72	28.04	0
High	TPEVTCVVVDVSHEDPEVK	2	27	4	A0A087X079;Q6GMX6;Q6MZQ6;Q7Z351		0.0000	3.16	3	2082.02542	9.30	28.90	0
High	GPSVFPLAPSSK	16	41	7	A0A087X079;Q6GMX6;Q6MZQ6;S6C4R2;Q7Z351;S6BGD4;Q9Y50		0.0000	3.01	2	1186.64629	-0.36	28.15	0
High	VVSVLTVLHQDWLNGK	3	30	6	A0A087X079;Q6GMX6;A0A087WXL8;A0A087WVW2;Q6MZQ6;Q7Z351		0.0000	2.96	3	1808.00553	-0.58	39.13	0
High	EPQVYTLPPSR	21	33	7	A0A087X079;Q6GMX6;P01859;A0A087WXL8;A0A087WVW2;Q6MZQ6;Q7Z351		0.0000	2.61	2	1286.67290	-0.83	26.70	0
High	DTLMISR	6	41	8	A0A087X079;Q6GMX6;P01859;A0A087WXL8;A0A087WVW2;Q6MZQ6;Q7Z351;Q6MZX7		0.0000	2.59	2	835.43407	-0.23	22.14	0
High	NQVSLTCLVK	3	35	8	A0A087X079;Q6GMX6;P01859;A0A087WXL8;A0A087WVW2;Q6MZQ6;Q6MZX7;Q7Z351		0.0000	2.56	2	1104.60930	1.00	30.61	0
High	DTLmISR	14	41	8	A0A087X079;Q6GMX6;P01859;A0A087WXL8;A0A087WVW2;Q6MZQ6;Q7Z351;Q6MZX7	M4(Oxidation)	0.0000	2.39	2	851.42851	-0.78	19.74	0
High	ALPAPIEK	9	29	6	A0A087X079;Q6GMX6;A0A087WXL8;A0A087WVW2;Q6MZQ6;Q7Z351		0.0000	1.81	1	838.50458	1.49	21.41	0
High	FTISR	10	160	24	A2J1M8;A0A087X079;Q7Z351;P01769;Q96K68;A2J1N2;A2KBC6;G1FM90;A2J1N0;A0A087X2C0;A2NYV1;A2NWW1;A0A087WW89;Q9UL71;A0N7I9;Q9Y509;A2J1N6;A2J1N7;B1N7B6;A0A087WU91;Q6ZW64;Q0ZCH9;Q6MZX9;A2NYQ9		0.0000	1.74	1	623.35077	-0.63	19.84	0
Medium	LTVDK	2	37	8	P01859;Q6MZQ6;Q6MZX7;A0A087X079;Q6GMX6;A0A087WXL8;A0A087WVW2;Q7Z351		0.0000	1.44	2	575.33983	-0.18	14.24	0

Table A.5. Peptides belonging to haptoglobin (Uniprot A0A087WU08) identified for protein band 5.

Confidence	Sequence	# PSMs	# Proteins	# Protein Groups	Protein Group Accessions	Modifications	ΔCn	XCorr	Charge	MH+ [Da]	ΔM [ppm]	RT [min]	# Missed Cleavages
High	SPVGVQPILNEHTFcAGmSK	3	8	1	A0A087WU08	C15(Carbamidomethyl); M18(Oxidation)	0.0000	4.93	3	2188.05082	-0.83	29.07	0
High	YVmLPVADQDQcIR	7	9	1	A0A087WU08	M3(Oxidation); C12(Carbamidomethyl)	0.0000	4.77	2	1723.81426	-0.01	27.36	0
High	ScAVAEYGVYVK	9	10	2	P00739;A0A087WU08	C2(Carbamidomethyl)	0.0000	4.72	2	1345.64519	-0.38	26.05	0
High	VGYVSGWGR	9	9	1	A0A087WU08		0.0000	3.85	2	980.49498	0.10	25.35	0
High	ILGGHLDAK	13	6	2	P00739;A0A087WU08		0.0000	3.68	2	923.53075	-0.21	20.92	0
High	VTSIQDWVQK	6	7	1	A0A087WU08		0.0000	3.54	2	1203.63664	-0.18	27.69	0
High	qKVSVNER	3	9	1	A0A087WU08	N-Term(Gln->pyro-Glu)	0.0000	3.34	2	942.50011	-0.27	16.65	1
High	DIAPTLTLYVGK	3	10	2	P00739;A0A087WU08		0.0000	3.30	2	1290.72978	-0.50	32.14	0
High	HYEGSTVPEKK	9	8	1	A0A087WU08		0.0000	3.25	3	1274.63752	-0.05	15.42	1
High	GSFPWQAK	6	6	2	P00739;A0A087WU08		0.0000	2.99	2	920.46605	3.83	27.61	0
High	KQLVEIEK	6	10	2	P00739;A0A087WU08		0.0000	2.94	2	986.58739	-0.74	20.44	1
High	DIAPTLTLYVGKK	5	10	2	P00739;A0A087WU08		0.0000	2.87	2	1418.82756	1.52	30.43	1
High	DYAEVGR	9	9	1	A0A087WU08		0.0000	2.61	2	809.37798	-1.07	16.50	0
High	HYEGSTVPEK	12	9	1	A0A087WU08		0.0000	2.40	2	1146.53801	-4.01	15.11	0
High	qLVEIEK	10	10	2	P00739;A0A087WU08	N-Term(Gln->pyro-Glu)	0.0000	2.38	1	841.46661	0.01	27.06	0
High	QLVEIEK	7	10	2	P00739;A0A087WU08		0.0000	2.20	1	858.49310	-0.06	21.94	0
High	VmPIcLPSK	3	10	2	P00739;A0A087WU08	M2(Oxidation); C5(Carbamidomethyl)	0.0000	2.08	2	1060.55327	0.25	24.42	0
High	FTDHLK	12	9	1	A0A087WU08		0.0000	2.02	2	760.39934	0.66	17.37	0
Medium	VmPIcLPSKDYAEVGR	3	9	1	A0A087WU08	M2(Oxidation); C5(Carbamidomethyl)	0.0000	1.76	3	1850.91025	-2.03	27.63	1
Medium	QKVSVNER	2	9	1	A0A087WU08		0.0000	1.76	3	959.52729	0.39	13.98	1
Medium	VMPIcLPSK	3	10	2	P00739;A0A087WU08	C5(Carbamidomethyl)	0.0000	1.65	2	1044.55937	1.22	27.63	0
Medium	VSVNER	3	9	1	A0A087WU08		0.0000	1.49	2	703.37297	-0.55	13.57	0

Table A.6. Peptides belonging to IgG light chain identified for protein band 6.

Confidence	Sequence	# PSMs	# Proteins	# Protein Groups	Protein Group Accessions	Modifications	ΔCn	XCorr	Charge	MH+ [Da]	ΔM [ppm]	RT [min]	# Missed Cleavages
High	HKVYAcEVTHQGLSSPVTK	5	16	5	A0A087X130;A0A087WYL9;Q6PIL8;Q6P5S8;V9HW34	C6(Carbamidomethyl)	0.0000	7.47	3	2141.07969	-0.55	24.46	1
High	VDNALQSGNSQESVTEQDSK	7	16	5	A0A087X130;A0A087WYL9;Q6PIL8;Q6P5S8;V9HW34		0.0000	6.38	2	2135.96904	0.11	18.86	0
High	ASQSVSSNLAWYQQKPGQAPR	2	3	1	A0A087X130		0.0000	4.65	3	2303.15018	-1.14	26.73	0
High	DSTYSLSSTLTLSK	3	16	5	A0A087X130;A0A087WYL9;Q6PIL8;Q6P5S8;V9HW34		0.0000	4.34	2	1502.75823	-0.17	28.67	0
High	VYAcEVTHQGLSSPVTK	8	16	5	A0A087X130;A0A087WYL9;Q6PIL8;Q6P5S8;V9HW34	C4(Carbamidomethyl)	0.0000	4.09	3	1875.92429	-1.44	23.55	0
High	LLIYGASTR	6	8	3	P01605;Q9UL85;A0A087X130		0.0000	2.73	2	993.57366	0.87	26.40	0
High	TVAAPSVFIFPPSDEQLK	2	25	8	A0A087X130;A0A087WYL9;Q6PIL8;Q6P5S8;V9HW34;S6AWD3;S6B2A1;S6BGE9		0.0000	2.56	2	1946.03447	3.81	35.61	0
High	SFNRGEc	3	16	5	A0A087X130;A0A087WYL9;Q6PIL8;Q6P5S8;V9HW34	C7(Carbamidomethyl)	0.0000	2.42	2	869.35735	0.32	13.75	1

Table A.7. Peptides belonging to apolipoprotein A-1 (Uniprot A0A087WU08) identified for protein band 7.

Confidence	Sequence	# PSMs	# Proteins	# Protein Groups	Protein Group Accessions	Modifications	ΔCn	XCorr	Charge	MH+ [Da]	ΔM [ppm]	RT [min]	# Missed Cleavages
High	LLDNWDSVTSTFSK	3	2	1	P02647		0.0000	5.08	2	1612.78020	-3.22	33.33	0
High	DSGRDYVSQFEGSALGK	7	1	1	P02647		0.0000	4.78	2	1815.85149	0.35	28.81	1
High	AKVQPYLDDFQK	2	2	1	P02647		0.0000	4.71	3	1451.75159	-0.94	26.26	1
High	DYVSQFEGSALGK	6	1	1	P02647		0.0000	4.63	2	1400.67278	2.49	29.65	0
High	qEmSKDLEEVKAK	3	2	1	P02647	N-Term(Gln->pyro-Glu); M3(Oxidation)	0.0000	4.45	3	1533.74659	0.00	19.16	2
High	AKVQPYLDDFQKK	4	2	1	P02647		0.0000	4.40	3	1579.84787	-0.04	25.11	2
High	VKDLATVYVDVLK	6	1	1	P02647		0.0000	4.30	2	1462.85503	2.33	32.71	1
High	ETEGLRQEmSKDLEEVK	6	2	1	P02647	M9(Oxidation)	0.0000	4.14	3	2036.97965	-0.46	21.99	2
High	ATEHLSTLSEK	8	3	1	P02647		0.0000	3.96	3	1215.62235	0.61	18.66	0
High	qEmSKDLEEVK	3	2	1	P02647	N-Term(Gln->pyro-Glu); M3(Oxidation)	0.0000	3.89	2	1334.61540	0.68	19.68	1
High	VEPLRAELQEGAR	6	2	1	P02647		0.0000	3.78	2	1467.79473	2.20	24.44	1
High	qKVEPLRAELQEGAR	7	2	1	P02647	N-Term(Gln->pyro-Glu)	0.0000	3.69	3	1706.91684	-0.97	26.01	2
High	qKLHELQEK	9	2	1	P02647	N-Term(Gln->pyro-Glu)	0.0000	3.57	2	1135.60942	-1.07	18.97	1
High	LEALKENGGAR	6	4	1	P02647		0.0000	3.42	2	1157.62615	-1.07	17.22	1
High	DLATVYVDVLK	3	1	1	P02647		0.0000	3.35	2	1235.68804	-0.16	34.47	0
High	THLAPYSDELR	7	4	1	P02647		0.0000	3.27	2	1301.64641	-1.59	23.94	0
High	WQEEmELYR	8	2	1	P02647	M5(Oxidation)	0.0000	3.26	2	1299.56719	-0.22	24.49	0
High	QKVEPLRAELQEGAR	7	2	1	P02647		0.0000	3.22	2	1723.94426	-0.46	24.56	2
High	QEmSKDLEEVK	5	2	1	P02647	M3(Oxidation)	0.0000	3.20	2	1351.64202	0.72	17.24	1
High	ARAHVDALR	2	3	1	P02647		0.0000	3.10	3	1008.57016	0.37	18.32	1
High	VQPYLDDFQKK	11	2	1	P02647		0.0000	3.09	2	1380.71648	0.46	25.23	1
High	QGLLPVLESFK	3	2	1	P02647		0.0000	3.07	2	1230.70879	-0.43	37.27	0
High	LSPLGEEmR	5	3	1	P02647	M8(Oxidation)	0.0000	3.06	2	1047.51506	1.03	20.89	0
High	KWQEEmELYR	6	2	1	P02647	M6(Oxidation)	0.0000	3.03	2	1427.66338	0.66	24.11	1
High	THLAPYSDELRQR	3	3	1	P02647		0.0000	2.94	3	1585.80667	-0.95	23.31	1
High	LSPLGEEMR	3	3	1	P02647		0.0000	2.83	2	1031.51885	-0.22	24.61	0
High	qKVEPLR	6	2	1	P02647	N-Term(Gln->pyro-Glu)	0.0000	2.54	2	852.49382	0.00	19.18	1
High	AKPALEDLR	6	2	1	P02647		0.0000	2.50	2	1012.57891	0.27	21.89	0
High	VQPYLDDFQK	9	2	1	P02647		0.0000	2.40	2	1252.62554	3.72	26.88	0
Medium	QEmSKDLEEVKAK	3	2	1	P02647	M3(Oxidation)	0.0000	2.33	4	1550.77285	-0.19	16.98	2
High	AELQEGAR	3	2	1	P02647		0.0000	2.26	2	873.44237	-0.17	14.00	0
High	LHELQEK	3	2	1	P02647		0.0000	2.21	2	896.48259	-1.17	15.26	0
High	ETEGLRQEmSK	9	2	1	P02647	M9(Oxidation)	0.0000	2.12	2	1323.62016	-0.61	14.06	1
High	DLEEVK	4	6	1	P02647		0.0000	1.99	1	732.37793	0.65	16.33	0
Medium	LAEYHAK	3	4	1	P02647		0.0000	1.97	2	831.43675	0.97	14.29	0
Medium	QKLHELQEK	6	2	1	P02647		0.0000	1.96	2	1152.63701	-0.16	16.69	1
Medium	LSPLGEEmRDR	5	3	1	P02647	M8(Oxidation)	0.0000	1.58	2	1318.64263	0.43	20.06	1
Medium	qLNLK	3	10	3	P02647;B7ZLD4;Q7RTS7	N-Term(Gln->pyro-Glu)	0.0000	1.45	1	598.35565	-0.44	22.98	0
Medium	QKVEPLR	6	2	1	P02647		0.0000	1.30	2	869.51976	-0.70	15.92	1

References

(1) Basu, S.; Vutukuri, D. R.; Thayumanavan, S. Homopolymer Micelles in Heterogeneous Solvent Mixtures. *J. Am. Chem. Soc.* **2005**, *127* (48), 16794–16795.

(2) Serrano, M. A. C.; He, H.; Zhao, B.; Ramireddy, R. R.; Vachet, R. W.; Thayumanavan, S. Polymer-Mediated Ternary Supramolecular Interactions for Sensitive Detection of Peptides. *Analyst* **2017**, *142* (1), 118–122.

(3) Reinicke, S.; Espeel, P.; Stamenović, M. M.; Du Prez, F. E. One-Pot Double Modification of p(NIPAAm): A Tool for Designing Tailor-Made Multiresponsive Polymers. *ACS Macro Lett.* **2013**, *2* (6), 539–543.

(4) Zhuang, J.; Jiwpanich, S.; Deepak, V. D.; Thayumanavan, S. Facile Preparation of Nanogels Using Activated Ester Containing Polymers. *ACS Macro Lett.* **2012**, *1* (1), 175–179.

(5) Eberhardt, M.; Mruk, R.; Zentel, R.; Théato, P. Synthesis of Pentafluorophenyl(Meth)Acrylate Polymers: New Precursor Polymers for the Synthesis of Multifunctional Materials. *Eur. Polym. J.* **2005**, *41* (7), 1569–1575.

(6) Zhao, B.; Serrano, M. A. C.; Gao, J.; Zhuang, J.; Vachet, R. W.; Thayumanavan, S. Self-Assembly of Random Co-Polymers for Selective Binding and Detection of Peptides. *Polym. Chem.* **2018**, *9* (9), 1066–1071.

(7) Serrano, M. A. C.; Zhao, B.; He, H.; Thayumanavan, S.; Vachet, R. W. Molecular Features Influencing the Release of Peptides from Amphiphilic Polymeric Reverse Micelles. *Langmuir* **2018**, *34* (15), 4595–4602.

(8) Zhao, B.; Zhuang, J.; Serrano, M. A. C.; Vachet, R. W.; Thayumanavan, S. Influence of Charge Density on Host–Guest Interactions within Amphiphilic Polymer Assemblies in Apolar Media. *Macromolecules* **2017**, *50* (24), 9734–9741.

BIBLIOGRAPHY

Adkins, J. N.; Varnum, S. M.; Auberry, K. J.; Moore, R. J.; Angell, N. H.; Smith, R. D.; Springer, D. L.; Pounds, J. G. Toward a Human Blood Serum Proteome: Analysis by Multidimensional Separation Coupled with Mass Spectrometry. *Mol. Cell. Proteomics* **2002**, *1*, 947–955.

Aebersold, R.; Mann, M. Mass Spectrometry-Based Proteomics. *Nature* **2003**, *422*, 199–207.

Afonso, C.; Budimir, N.; Fournier, F.; Tabet, J.-C. Activated Surfaces for Laser Desorption Mass Spectrometry: Application for Peptide and Protein Analysis. *Curr. Pharm. Des.* **2005**, *11*, 2559–2576.

Ahmad, Y.; Boisvert, F.-M.; Lundberg, E.; Uhlen, M.; Lamond, A. I. Systematic Analysis of Protein Pools, Isoforms, and Modifications Affecting Turnover and Subcellular Localization. *Mol. Cell. Proteomics* **2012**, *11* (3), M111.013680.

Ahn, S. H.; Park, K. M.; Bae, Y. J.; Kim, M. S. Quantitative Reproducibility of Mass Spectra in Matrix-Assisted Laser Desorption Ionization and Unraveling of the Mechanism for Gas-Phase Peptide Ion Formation. *J. Mass Spectrom.* **2013**, *48* (3), 299–305.

Ahn, Y. H.; Kim, K. H.; Shin, P. M.; Ji, E. S.; Kim, H.; Yoo, J. S. Identification of Low-Abundance Cancer Biomarker Candidate TIMP1 from Serum with Lectin Fractionation and Peptide Affinity Enrichment by Ultrahigh-Resolution Mass Spectrometry. *Anal. Chem.* **2012**, *84* (3), 1425–1431.

Altintaş, E. B.; Denizli, A. Efficient Removal of Albumin from Human Serum by Monosize Dye-Affinity Beads. *J. Chromatogr. B* **2006**, *832*, 216–223.

Altschul, S. F.; Madden, T. L.; Schäffer, A. A.; Zhang, J.; Zhang, Z.; Miller, W.; Lipman, D. J. Gapped BLAST and PSI-BLAST: A New Generation of Protein Database Search Programs. *Nucleic Acids Res.* **1997**, *25*, 3389–3402.

Andac, M.; Galaev, I.; Denizli, A. Dye Attached Poly(Hydroxyethyl Methacrylate) Cryogel for Albumin Depletion from Human Serum. *J. Sep. Sci.* **2012**, *35* (9), 1173–1182.

Anderson, L. N.; Esquer-Blasco, R.; Hofmann, J.-P.; Anderson, N. G. A Two-Dimensional Gel Database of Rat Liver Proteins Useful in Gene Regulation and Drug Effects Studies. *Electrophoresis* **1991**, *12*, 907–930.

Anderson, L.; Hunter, C. L. Quantitative Mass Spectrometric Multiple Reaction Monitoring Assays for Major Plasma Proteins. *Mol. Cell. Proteomics* **2006**, *5*, 573–588.

Anderson, N. L. The Human Plasma Proteome: History, Character, and Diagnostic Prospects. *Mol. Cell. Proteomics* **2002**, *1* (11), 845–867.

Appel, E.; Biedermann, F.; Rauwald, U.; Jones, S. T.; Zayed, J. M.; Scherman, O. Supramolecular Cross-Linked Networks via Host- Guest Complexation with Cucurbit [8]uril. *J. Am. Chem. Soc.* **2010**, *132*, 14251–14260.

Audran, R.; Peter, K.; Dannull, J.; Men, Y.; Scandella, E.; Groettrup, M.; Gander, B.; Corradin, G. Encapsulation of Peptides in Biodegradable Microspheres Prolongs Their MHC Class-I Presentation by Dendritic Cells and Macrophages *In Vitro*. *Vaccine* **2003,** *21*, 1250–1255.

Azagarsamy, M. a; Gomez-Escudero, A.; Yesilyurt, V.; Vachet, R. W.; Thayumanavan, S. Amphiphilic Nanoassemblies for the Detection of Peptides and Proteins Using Fluorescence and Mass Spectrometry. *Analyst* **2009**, *134*, 635–649.

Bae, Y.; Fukushima, S.; Harada, A.; Kataoka, K. Design of Environment-Sensitive Supramolecular Assemblies for Intracellular Drug Delivery: Polymeric Micelles That are Responsive to Intracellular pH Change. *Angew. Chem. Int. Ed.* **2003,** *42*, 4640–4643.

Barczyk, K.; Kreuter, M.; Pryjma, J.; Booy, E. P.; Maddika, S.; Ghavami, S.; Berdel, W. E.; Roth, J.; Los, M. Serum Cytochrome c Indicates in Vivo Apoptosis and Can Serve as a Prognostic Marker during Cancer Therapy. *Int. J. Cancer* **2005**, *116*, 167–173.

Barrow, S. J.; Kasera, S.; Rowland, M. J.; Del Barrio, J.; Scherman, O. A. Cucurbituril-Based Molecular Recognition. *Chem. Rev.* **2015**, *115*, 12320–12406.

Basu, S.; Vutukuri, D. R.; Thayumanavan, S. Homopolymer Micelles in Heterogeneous Solvent Mixtures. *J. Am. Chem. Soc.* **2005**, *127* (48), 16794–16795.

Beaujuge, P. M.; Fréchet, J. M. J. Molecular Design and Ordering Effects in π-Functional Materials for Transistor and Solar Cell Applications. *J. Am. Chem. Soc.*, **2011**, *133*, 20009-20029.

Björck, L.; Kronvall, G. Purification and Some Properties of Streptococcal Protein G, a Novel IgG-Binding Reagent. *J. Immunol.* **1984**, *133*, 969–974.

Björhall, K.; Miliotis, T.; Davidsson, P. Comparison of Different Depletion Strategies for Improved Resolution in Proteomic Analysis of Human Serum Samples. *Proteomics* **2005**, *5*, 307–317.

Busseron, E.; Ruff, Y.; Moulin, E.; Giuseppone, N. Supramolecular Self-Assemblies as Functional Nanomaterials. *Nanoscale* **2013**, *5* (16), 7098–7140.

Chen, F.; Wan, D.; Chang, Z.; Pu, H.; Jin, M. Highly Efficient Separation, Enrichment, and Recovery of Peptides by Silica-Supported Polyethylenimine. *Langmuir* **2014**, *30*, 12250–12257.

Chen, G.; Warrack, B. M.; Goodenough, A. K.; Wei, H.; Wang-Iverson, D. B.; Tymiak, A. A. Characterization of Protein Therapeutics by Mass Spectrometry: Recent Developments and Future Directions. *Drug Discov. Today* **2011**, *16*, 58–64.

Chen, J.; Chen, F.; Wang, X.; Zhao, X.; Ao, Q. The Forward and Backward Transport Processes in the AOT/Hexane Reversed Micellar Extraction of Soybean Protein. *J. Food Sci. Technol.* **2012,** *51*, 2851–2856.

Chen, Y. Y.; Lin, S. Y.; Yeh, Y. Y.; Hsiao, H. H.; Wu, C. Y.; Chen, S. T.; Wang, A. H. J. A Modified Protein Precipitation Procedure for Efficient Removal of Albumin from Serum. *Electrophoresis* **2005**, *26*, 2117–2127.

Chen, Y.; Dong, C. M. pH-Sensitive Supramolecular Polypeptide-Based Micelles and Reverse Micelles Mediated by Hydrogen-Bonding Interactions or Host-Guest Chemistry: Characterization and *In Vitro* Controlled Drug Release. *J. Phys. Chem. B* **2010,** *114*, 7461–7468.

Cheng, F.; Yang, X.; Peng, H.; Chen, D.; Jiang, M. Well-Controlled Formation of Polymeric Micelles with a Nanosized Aqueous Core and Their Applications as Nanoreactors. *Macromolecules* **2007,** *40*, 8007–8014.

Chiva, C.; Sabidó, E. Peptide Selection for Targeted Protein Quantitation. *J. Proteome Res.* **2017**, *16*, 1376–1380.

Choe, W.; Durgannavar, T.; Chung, S. Fc-Binding Ligands of Immunoglobulin G: An Overview of High Affinity Proteins and Peptides. *Materials* **2016**, *9*, 994.

Chung, L.; Moore, K.; Phillips, L.; Boyle, F. M.; Marsh, D. J.; Baxter, R. C. Novel Serum Protein Biomarker Panel Revealed by Mass Spectrometry and Its Prognostic Value in Breast Cancer. *Breast Cancer Res.* **2014**, *16* (3), R63.

Clough, T.; Key, M.; Ott, I.; Ragg, S.; Schadow, G.; Vitek, O. Protein Quantification in Label-Free LC-MS Experiments. *J. Proteome Res.* **2009**, *8*, 5275–5284.

Cohn, E. J.; Strong, L. E.; Hughes, W. L.; Mulford, D. J.; Ashworth, J. N.; Melin, M.; Taylor, H. L. Preparation and Properties of Serum and Plasma Proteins. IV. A System for the Separation into Fractions of the Protein and Lipoprotein Components of Biological Tissues and Fluids. *J. Am. Chem. Soc.* **1946**, *68*, 459–475.

Cologna, S. M.; Russell, W. K.; Lim, P. J.; Vigh, G.; Russell, D. H. Combining Isoelectric Point-Based Fractionation, Liquid Chromatography and Mass Spectrometry to Improve Peptide Detection and Protein Identification. *J. Am. Soc. Mass Spectrom.* **2010**, *21* (9), 1612–1619.

Combariza, M. Y.; Savariar, E. N.; Vutukuri, D. R.; Thayumanavan, S.; Vachet, R. W. Polymeric Inverse Micelles as Selective Peptide Extraction Agents for MALDI-MS Analysis. *Anal. Chem.* **2007**, *79* (18), 7124–7130.

Cravatt, B. F.; Simon, G. M.; Yates, J. R. The Biological Impact of Mass-Spectrometry-Based Proteomics. *Nature* **2007**, *450*, 991–1000.

Cusack, S. Aminoacyl-TRNA Synthetases. *Curr. Opin. Struct. Biol.* **1997**, *7*, 881–889.

da Costa, P. L. N.; Sirois, P.; Tannock, I. F.; Chammas, R. The Role of Kinin Receptors in Cancer and Therapeutic Opportunities. *Cancer Lett.* **2014**, *345*, 27–38.

DeVera, I. E.; Katz, J. E.; Agus, D. B. Clinical Proteomics: The Promises and Challenges of Mass Spectrometry-Based Biomarker Discovery. *Clin. Adv. Hematol. Oncol.* **2006**, *4*, 541–549.

Diamandis, E. P. Mass Spectrometry as a Diagnostic and a Cancer Biomarker Discovery Tool. *Mol. Cell. Proteomics* **2004**, *3* (4), 367–378.

Ding, Z.; Cao, X. Affinity Precipitation of Human Serum Albumin Using a Thermo-Response Polymer with an L-Thyroxin Ligand. *BMC Biotechnol.* **2013**, *13*, 109–118.

Domon, B.; Aebersold, R. Mass Spectrometry and Protein Analysis. *Science* **2006**, *312*, 212–217.

Dreisewerd, K. The Desorption Process in MALDI. *Chem. Rev.* **2003**, *103* (2), 395–425.

Du, A. W.; Stenzel, M. H. Drug Carriers for the Delivery of Therapeutic Peptides. *Biomacromolecules* **2014**, *15*, 1097–1114.

Duggan, D. E.; Udenfriend, S. The Spectrophotofluorometric Determination of Tryptophan in Plasma and of Tryptophan and Tyrosine in Protein Hydrolysates. *J. Biol. Chem.* **1956**, *223*, 313–319.

Dunn, J.D.; Igrisan, E.A.; Palumbo, A.M.; Reid, G.E.; Bruening, M. L. Phosphopeptide Enrichment Using MALDI Plates Modified with High-Capacity Polymer Brushes. *Anal. Chem.* **2008**, *80*, 5727–5735.

Dzieciatkowska, M.; Copeland, M.; You, J.; Wery, J.; Wang, M. Comparison of an Enzyme Immunoassay Versus Mass Spectrometry-Based Assay for the Quantitative Determination of the Procollagen Type I N-Terminal Propeptide in Rat Serum. *Proteomics Insights* **2009**, *2*, 33–38.

Eberhardt, M.; Mruk, R.; Zentel, R.; Théato, P. Synthesis of Pentafluorophenyl(Meth)Acrylate Polymers: New Precursor Polymers for the Synthesis of Multifunctional Materials. *Eur. Polym. J.* **2005**, *41* (7), 1569–1575.

Eckhardt, A. E.; Hayes, C. E.; Goldstein, I. J. A Sensitive Fluorescent Method for the Detection of Glycoproteins in Polyacrylamide Gels. *Anal. Biochem.* **1976**, *73*, 192–197.

Ekstr, S.; Wallman, L.; Helldin, G.; Nilsson, J.; Marko-Varga, G.; Laurell, T. Polymeric Integrated Selective Enrichment Target (ISET) for Solid-Phase-Based Sample Preparation in MALDI–TOF MS. *J. Mass Spectrom.* **2007**, *42*, 1445–1452.

Eleftheriadis, T.; Pissas, G.; Liakopoulos, V.; Stefanidis, I. Cytochrome c as a Potentially Clinical Useful Marker of Mitochondrial and Cellular Damage. *Front. Immunol.* **2016**, *7*, 1–5.

Esser-Kahn, A. P.; Odom, S. A.; Sottos, N. R.; White, S. R.; Moore, J. S. Triggered release from polymer capsules. *Macromolecules* **2011,** *44*, 5539–5553.

Fasano, M.; Curry, S.; Terreno, E.; Galliano, M.; Fanali, G.; Narciso, P.; Notari, S.; Ascenzi, P. The Extraordinary Ligand Binding Properties of Human Serum Albumin. *IUBMB Life* **2005**, *57* (12), 787–796.

Flynn, D. C. Adaptor Proteins. *Oncogene* **2001**, *20*, 6270–6272.

Friedman, D. B.; Hill, S.; Keller, J. W.; Merchant, N. B.; Levy, S. E.; Coffey, R. J.; Caprioli, R. M. Proteome Analysis of Human Colon Cancer by Two-Dimensional Difference Gel Electrophoresis and Mass Spectrometry. *Proteomics* **2004**, *4*, 793–811.

Fukuyama, Y.; Tanimura, R.; Maeda, K.; Watanabe, M.; Kawabata, S. I.; Iwamoto, S.; Izumi, S.; Tanaka, K. Alkylated Dihydroxybenzoic Acid as a MALDI Matrix Additive for Hydrophobic Peptide Analysis. *Anal. Chem.* **2012**, *84*, 4237–4243.

Gao, G. H.; Park, M. J.; Li, Y.; Im, G. H.; Kim, J.-H.; Kim H. N.; Lee, J. W.; Jeon, P.; Bang, O. Y.; Lee, J. H.; Lee, D. S. The Use of pH-Sensitive Positively Charged Polymeric Micelles for Protein Delivery. *Biomaterials* **2012**, *33***,** 9157–9164.

Gao, J.; Zhao, B.; Wang, M.; Serrano, M. A. C.; Zhuang, J.; Ray, M.; Rotello, V. M.; Vachet, R. W.; Thayumanavan, S. Supramolecular Assemblies for Transporting Proteins Across an Immiscible Solvent Interface. *J. Am. Chem. Soc.* **2018**, *140* (7), 2421–2425.

Gevaert, K.; Vandekerckhove, J. Protein Identification Methods in Proteomics. *Electrophoresis* **2000**, *21*, 1145–1154.

Gianazza, E.; Arnaud, P. A General Method for Fractionation of Plasma Proteins. *Biochem. J.* **1982**, *201*, 129–136.

Gillette, M. A.; Carr, S. A. Quantitative Analysis of Peptides and Proteins in Biomedicine by Targeted Mass Spectrometry. *Nat. Methods* **2013**, *10* (1), 28–34.

Gillissen, M. A. J.; Voets, I. K.; Meijer, E. W.; Palmans, A. R. A. Single Chain Polymeric Nanoparticles as Compartmentalised Sensors for Metal Ions. *Polym. Chem.* **2012**, *3*, 3166-3174.

Glish, G. L.; Vachet, R. W. The Basics of Mass Spectrometry in the Twenty-First Century. *Nat. Rev. Drug Discov.* **2003**, *2* (2), 140–150.

González, D. C.; Savariar, E. N.; Thayumanavan, S. Fluorescence Patterns from Supramolecular Polymer Assembly and Disassembly for Sensing Metallo- and Nonmetalloproteins. *J. Am. Chem. Soc.* **2009**, *131*, 7708–7716.

Grebe, S. K. G.; Singh, R. J. Clinical Peptide and Protein Quantification by Mass Spectrometry (MS). *Trends Anal. Chem.* **2016**, *84*, 131–143.

Guo, A.; Gu, H.; Zhou, J.; Mulhern, D.; Wang, Y.; Lee, K. A.; Yang, V.; Aguiar, M.; Kornhauser, J.; Jia, X.; et al. Immunoaffinity Enrichment and Mass Spectrometry Analysis of Protein Methylation. *Mol. Cell. Proteomics* **2014**, *13* (1), 372–387.

Hale, J. E. Advantageous Uses of Mass Spectrometry for the Quantification of Proteins. *Int. J. Proteomics* **2013**, *2013*, 1–6.

Hanke, S.; Besir, H.; Oesterhelt, D.; Mann, M. Absolute SILAC for Accurate Quantitation of Proteins in Complex Mixtures down to the Attomole Level. *J. Proteome Res.* **2008**, *7*, 1118–1130.

Hartmann, M.; Roeraade, J.; Stoll, D.; Templin, M. F.; Joos, T. O. Protein Microarrays for Diagnostic Assays. *Anal. Bioanal. Chem.* **2009**, *393*, 1407–1416.

Hayashi, T.; Hamachi, I. Traceless Affinity Labeling of Endogenous Proteins for Functional Analysis in Living Cells. *Accounts Chem. Res.* **2012**, *45* (9), 1460–1469.

Horka, M.; Ruzicka, F.; Horky, J.; Hola, V.; Slais, K. Capillary Isoelectric Focusing and Fluorometric Detection of Proteins and Microorganisms Dynamically Modified by Poly(Ethylene Glycol) Pyrenebutanoate. *Anal. Chem.* **2006**, *78*, 8438–8444.

Hortin, G. L.; Sviridov, D.; Anderson, N. L. High-Abundance Polypeptides of the Human Plasma Proteome Comprising the Top 4 Logs of Polypeptide Abundance. *Clin. Chem.* **2008**, *54*, 1608–1616.

Hu, J.; Liu, S. Engineering Responsive Polymer Building Blocks with Host-Guest Molecular Recognition for Functional Applications. *Acc. Chem. Res.* **2014**, *47***,** 2084–2095.

Huang, Y.; Zhu, H. Protein Array-Based Approaches for Biomarker Discovery in Cancer. *Genomics Proteomics Bioinformatics* **2017**, *15* (2), 73–81.

Huttenhain, R.; Malmstrom, J.; Picotti, P.; Aebersold, R. Perspectives of Targeted Mass Spectrometry for Protein Biomarker Verification. *Curr. Opin. Chem. Biol.* **2009**, *13*, 1–8.

Isimjan, T. T.; de Bruyn, J. R.; Gillies, E. R. Self-Assembly of Supramolecular Polymers from β-Strand Peptidomimetic-Poly(Ethylene Oxide) Hybrids. *Macromolecules* **2010**, *43*, 4453–4459.

Jackson, A. W.; Fulton, D. A. Triggering Polymeric Nanoparticle Disassembly Through the Simultaneous Application of Two Different Stimuli. *Macromolecules* **2012,** *45*, 2699–2708.

Jacobs, J. M.; Adkins, J. N.; Qian, W.-J.; Liu, T.; Shen, Y.; Camp, D. G.; Smith, R. D. Utilizing Human Blood Plasma for Proteomic Biomarker Discovery. *J. Proteome Res.* **2005**, *4*, 1073–1085.

Jarnuczak, A. F.; Lee, D. C. H.; Lawless, C.; Holman, S. W.; Eyers, C. E.; Hubbard, S. J. Analysis of Intrinsic Peptide Detectability via Integrated Label-Free and SRM-Based Absolute Quantitative Proteomics. *J. Proteome Res.* **2016**, *15*, 2945–2959.

Jarudilokkul, S.; Poppenborg, L. H.; Stuckey, D. C. Backward Extraction of Reverse Micellar Encapsulated Proteins Using a Counterionic Surfactant. *Biotechnol. Bioeng.* **1999,** *62*, 593–601.

Javid, J.; Mir, R.; Julka, P. K.; Ray, P. C.; Saxena, A. Extracellular Cytochrome c as a Biomarker for Monitoring Therapeutic Efficacy and Prognosis of Non-Small Cell Lung Cancer Patients. *Tumor Biol.* **2015**, *36*, 4253–4260.

Jia, H.-Z.; Zhang, W.; Zhu, J.-Y.; Yang, B.; Chen, S.; Chen, G.; Zhao, Y.-F.; Feng, J.; Zhang, X.-Z. Hyperbranched–hyperbranched Polymeric Nanoassembly to Mediate Controllable Co-Delivery of siRNA and Drug for Synergistic Tumor Therapy. *J. Control. Release* **2015**, *216*, 9–17.

Jin, H.; Huang, W.; Zhu, X.; Zhou, Y.; Yan, D. Biocompatible or Biodegradable Hyperbranched Polymers: From Self-Assembly to Cytomimetic Applications. *Chem. Soc. Rev.* **2012**, *41* (18), 5986–5997.

Jin, X.; Zhang, X.; Wu, Z.; Teng, D.; Zhang, X.; Wang, Y; Wang, Z.; Li, C. Amphiphilic Random Glycopolymer Based on Phenylboronic Acid: Synthesis, Characterization, and Potential as Glucose-Sensitive Matrix. *Biomacromolecules* **2009**, *10*, 1337–1345.

Johnson, L. N.; Noble, M. E. M.; Owen, D. J. Active and Inactive Protein Kinases: Structural Basis for Regulation. *Cell* **1996**, *85*, 149–158.

Jones, M. C.; Gao, H.; Leroux, J. C. Reverse Polymeric Micelles for Pharmaceutical Applications. *J. Control. Release* **2008,** *132*, 208–215.

Jones, M. C.; Tewari, P.; Blei, C.; Hales, K.; Pochan, D. J.; Leroux, J.-C. Self-Assembled Nanocages for Hydrophilic Guest Molecules. *J. Am. Chem. Soc.* **2006,** *128,* 14599–14605.

Jones, M.-C.; Leroux, J.-C. Reverse Micelles from Amphiphilic Branched Polymers. *Soft Matter* **2010**, *6*, 5850-5859.

Kaiser, T.; Wittke, S.; Just, I.; Krebs, R.; Bartel, S.; Filser, D.; Mischak, H.; Weissinger, E. M. Capillary Electrophoresis Coupled to Mass Spectrometer for Automated and Robust Polypeptide Determination in Body Fluids for Clinical Use. *Electrophoresis* **2004**, *25*, 2044–2055.

Kale, T. S.; Klaikherd, A.; Popere, B.; Thayumanavan, S. Supramolecular Assemblies of Amphiphilic Homopolymers. *Langmuir* **2009**, *25* (17), 9660–9670.

Kang, S.; Kim, Y.; Song, Y.; Choi, J. U.; Park, E.; Choi, W.; Park, J.; Lee, Y. Comparison of pH-Sensitive Degradability of Maleic Acid Amide Derivatives. *Bioorganic & Medicinal Chemistry Letters* **2014**, *24*, 2364-2367.

Kapp, E. A.; Schütz, F.; Reid, G. E.; Eddes, J. S.; Moritz, R. L.; O'Hair, R. A. J.; Speed, T. P.; Simpson, R. J. Mining a Tandem Mass Spectrometry Database to Determine the Trends and Global Factors Influencing Peptide Fragmentation. *Anal. Chem.* **2003**, *75*, 6251–6264.

Karas, M.; Krüger, R. Ion Formation in MALDI: The Cluster Ionization Mechanism. *Chem. Rev.* **2003**, *103* (2), 427–440.

Kay, R.; Barton, C.; Ratcliffe, L.; Matharoo-Ball, B.; Brown, P.; Roberts, J.; Teale, P.; Creaser, C. Enrichment of Low Molecular Weight Serum Proteins Using Acetonitrile Precipitation for Mass Spectrometry Based Proteomic Analysis. *Rapid Commun. Mass Spectrom.* **2008**, *22*, 3255–3260.

Kedar, U.; Phutane, P.; Shidhaye, S.; Kadam, V. Advances in Polymeric Micelles for Drug Delivery and Tumor Targeting. *Nanomedicine: Nanotechnology, Biol. Med.* **2010**, *6*, 714–729.

Kennedy, J. J.; Abbatiello, S. E.; Kim, K.; Yan, P.; Whiteaker, J. R.; Lin, C.; Kim, J. S.; Zhang, Y.; Wang, X.; Ivey, R. G.; et al. Demonstrating the Feasibility of Large-Scale Development of Standardized Assays to Quantify Human Proteins. *Nat. Methods* **2014**, *11* (2), 149–155.

Keshishian, H.; Addona, T.; Burgess, M.; Kuhn, E.; Carr, S. A. Quantitative, Multiplexed Assays for Low Abundance Proteins in Plasma by Targeted Mass Spectrometry and Stable Isotope Dilution. *Mol. Cell. Proteomics* **2007**, *6*, 2212–2229.

Khmelmitsky, Y. L.; Gladilin, A. K.; Roubailo, V. L.; Martinek, K.; Levashov, A. V. Reversed Micelles of Polymeric Surfactants in Nonpolar Organic Solvents: A New Microheterogeneous Medium for Enzymatic Reactions. *Eur. J. Biochem.* **1992**, *206***,** 737–745.

Kim, H. J.; Heo, J.; Jeon, W. S.; Lee, E.; Kim, J.; Sakamoto, S.; Yamaguchi, K.; Kim, O. Selective Inclusion of a Hetero-Guest Pair in a Molecular Host: Formation of Stable Charge-Transfer Complexes in Cucurbit[8]uril. *Angew. Chemie - Int. Ed.* **2001**, *40*, 1526–1529.

Kim, J.-S.; Kim, J.-H.; Kim, H.-J. Matrix-Assisted Laser Desorption/Ionization Signal Enhancement of Peptides by Picolinamidination of Amino Groups. *Rapid Commun. Mass Spectrom.* **2008**, *22*, 495–502.

Kirkorian, K.; Ellis, A.; Twyman, L. J. Catalytic Hyperbranched Polymers as Enzyme Mimics; Exploiting the Principles of Encapsulation and Supramolecular Chemistry. *Chem. Soc. Rev.* **2012**, *41* (18), 6138–6159.

Knochenmuss, R.; Zenobi, R. MALDI Ionization: The Role of in-Plume Processes. *Chem. Rev.* **2003**, *103* (2), 441–452.

Koyamatsu, Y.; Hirano, T.; Kakizawa, Y.; Okano, F.; Takarada, T.; Maeda, M. pH-Responsive Release of Proteins from Biocompatible and Biodegradable Reverse Polymer Micelles. *J. Control. Release* **2014,** *173*, 89–95.

Krastins, B.; Prakash, A.; Sarracino, D. a; Nedelkov, D.; Niederkofler, E. E.; Kiernan, U. a; Nelson, R.; Vogelsang, M. S.; Vadali, G.; Garces, A.; et al. Rapid Development of Sensitive, High-Throughput, Quantitative and Highly Selective Mass Spectrometric Targeted Immunoassays for Clinically Important Proteins in Human Plasma and Serum. *Clin. Biochem.* **2013**, *46* (6), 399–410.

Kuhn, E.; Wu, J.; Karl, J.; Liao, H.; Zolg, W.; Guild, B. Quantification of C-Reactive Protein in the Serum of Patients with Rheumatoid Arthritis Using Multiple Reaction Monitoring Mass Spectrometry and 13C-Labeled Peptide Standards. *Proteomics* **2004**, *4* (4), 1175–1186.

Kumar, M.; Gupta, D.; Singh, G.; Sharma, S.; Bhat, M.; Prashant, C. K.; Dinda, A. K.; Kharbanda, S.; Kufe, D.; Singh, H. Novel Polymeric Nanoparticles for Intracellular Delivery of Peptide Cargos: Antitumor Efficacy of the BCL-2 Conversion Peptide NuBCP-9. *Cancer Res.* **2014,** *74*, 3271–3281.

Kuyama, H.; Sonomura, K.; Nishimura, O. Sensitive Detection of Phosphopeptides by Matrix-Assisted Laser Desorption/Ionization Mass Spectrometry: Use of Alkylphosphonic Acids as Matrix Additives. *Rapid Commun. Mass Spectrom.* **2008**, *22*, 1109–1116.

Lange, V.; Picotti, P.; Domon, B.; Aebersold, R. Selected Reaction Monitoring for Quantitative Proteomics: A Tutorial. *Mol. Syst. Biol.* **2008**, *4* (222), 222.

Larsen, M. R.; Trelle, M. B.; Thingholm, T. E.; Jensen, O. N. Analysis of Posttranslational Modifications of Proteins by Tandem Mass Spectrometry. *Biotechniques* **2006**, *40*, 790–798.

Lee, J. H.; Yeo, Y. Controlled Drug Release from Pharmaceutical Nanocarriers. *Chem. Eng. Sci.* **2015,** *125*, 75–84.

Lee, M.; Jang, C.-J.; Ryu, J.-H. Supramolecular Reactor from Self-Assembly of Rod-Coil Molecule in Aqueous Environment. *J. Am. Chem. Soc.* **2004**, *126* (26), 8082–8083.

Lee, S.-S.; Hwang, K.-S.; Lee, B.-K.; Hong, D.-P.; Kuboi, R. Interaction Between Reverse Micelles as a Key Factor Governing Back-Extraction of Proteins and Its Control Systems. *Korean J. Chem. Eng.* **2005,** *22*, 611–616.

Lehn, J.-M. Toward Complex Matter: Supramolecular Chemistry and Self-Organization. *Proc. Natl. Acad. Sci.* **2002**, *99* (8), 4763–4768.

Leriche, G.; Chisholm, L.; Wagner, A. Cleavable Linkers in Chemical Biology. *Bioorg. Med. Chem.* **2012**, *20*, 571–582.

Levene, P. A.; Simms, H. S. Calculation of Isoelectric Points. *J. Biol. Chem.* **1923**, *55*, 801–813.

Lewis, J. K.; Wei, J.; Siuzdak, G. Matrix-Assisted Laser Desorption/Ionization Mass Spectrometry in Peptide and Protein Analysis. In *Encyclopedia of Analytical Chemistry*; Meyers, R. A., ed.; John Wiley & Sons Ltd, 2000; pp 5880–5894.

Li, H.; Sun, S; Mhaisalkar, S.; Zin, M. T.; Lam, Y. M.; Grimdale, A. C. A High Voltage Solar Cell Uing a Donor–Acceptor Conjugated Polymer Based on Pyrrolo[3,4-*f*]-2,1,3-benzothiadiazole-5,7-dione. *J. Mater. Chem. A* **2014**, *2*, 17925-17933.

Li, J.; Ma, H.; Wang, X.; Xiong, S.; Dong, S.; Wang, S. Enhanced Detection of Thiol Peptides by Matrix-Assisted Laser Desorption/Ionization Mass Spectrometry after Selective Derivatization with a Tailor-Made Quaternary Ammonium Tag Containing Maleimidyl Group. *Rapid Commun. Mass Spectrom.* **2007**, *21*, 2608–2612.

Li, S.; Schöneich, C.; Borchardt, R. T. Chemical Instability of Protein Pharmaceuticals: Mechanisms of Oxidation and Strategies for Stabilization. *Biotechnol. Bioeng.* **1995**, *48*, 490–500.

Li, S.; Yang, K.; Deng, N.; Min, Y.; Liu, L.; Zhang, L.; Zhang, Y. Thermoresponsive Epitope Surface-Imprinted Nanoparticles for Specific Capture and Release of Target Protein from Human Plasma. *ACS Appl. Mater. Interfaces* **2016**, *8*, 5747–5751.

Liebler, D. C.; Zimmerman, L. J. Targeted Quantitation of Proteins by Mass Spectrometry. *Biochemistry* **2013**, *52*, 3797–3806.

Lin, D.; Alborn, W. E.; Slebos, R. J. C.; Liebler, D. C. Comparison of Protein Immunoprecipitation-Multiple Reaction Monitoring with ELISA for Assay of Biomarker Candidates in Plasma. *J. Proteome Res.* **2013**, *12*, 5996–6003.

Lin, D.; Tabb, D. L.; Yates, J. R. Large-Scale Protein Identification Using Mass Spectrometry. *Biochim. Biophys. Acta - Proteins Proteomics* **2003**, *1646*, 1–10.

Liu, G.; Zhao, Y.; Angeles, A.; Hamuro, L. L.; Arnold, M. E.; Shen, J. X. A Novel and Cost Effective Method of Removing Excess Albumin from Plasma/Serum Samples and Its Impacts on LC-MS/MS Bioanalysis of Therapeutic Proteins. *Anal. Chem.* **2014**, *86*, 8336–8343.

Liu, H.; Zhang, L.; Zhu, G.; Zhang, W.; Zhang, Y. An Etched Porous Interface for On-Line Capillary Electrophoresis-Based Two-Dimensional Separation System. *Anal. Chem.* **2004**, *76*, 6506–6512.

Liu, J.; Deng, Q.; Tao, D.; Yang, K.; Zhang, L.; Liang, Z.; Zhang, Y. Preparation of Protein Imprinted Materials by Hierarchical Imprinting Techniques and Application in Selective Depletion of Albumin from Human Serum. *Sci. Rep.* **2014**, *4*, 1–6.

Liu, Y.; Dong, X. Y.; Sun, Y. Protein Separation by Affinity Extraction with Reversed Micelles of Span 85 Modified with Cibacron Blue F3G-A. *Sep. Purif. Technol.* **2007**, *53*, 289–295.

Ma, S.; Wang, W.; Xia, B.; Zhang, S.; Yuan, H.; Jiang, H.; Meng, W.; Zheng, X.; Wang, X. Multiplexed Serum Biomarkers for the Detection of Lung Cancer. *EBioMedicine* **2016**, *11*, 210–218.

Madsen, J. A.; Farutin, V.; Carbeau, T.; Wudyka, S.; Yin, Y.; Smith, S.; Anderson, J.; Capila, I. Toward the Complete Characterization of Host Cell Proteins in Biotherapeutics via Affinity Depletions, LC-MS/MS, and Multivariate Analysis. *MAbs* **2015**, *7* (6), 1128–1137.

Maeda, H.; Matsumura, Y.; Katos, H. Purification and Identification of [Hydroxyprolyl3]Bradykinin in Ascitic Fluid from a Patient with Gastric Cancer. *J. Biol. Chem.* **1988**, *263*, 16051–16054.

Mann, M.; Hendrickson, R. C.; Pandey, A. Analysis of Proteins and Proteomes By Mass Spectrometry. *Annu. Rev. Biochem.* **2001**, *70*, 437–473.

Mathew, D. S.; Juang, R. S. Improved Back Extraction of Papain from AOT Reverse Micelles Using Alcohols and a Counter-Ionic Surfactant. *Biochem. Eng. J.* **2005,** *25*, 219–225.

Mazzola, P. G.; Lopes, A. M.; Hasmann, F. A.; Jozala, A. F.; Penna, T. CV.; Magalhaes, P. O.; Rangel-Yagui, C. O.; Pessoa, A. Jr. Liquid-liquid extraction of biomolecules: an overview and update of the main techniques. *J. Chem. Technol. Biotechnol.* **2008,** *83*, 143–157.

Mehaffy, C.; Dobos, K. M.; Nahid, P.; Kruh-Garcia, N. A. Second Generation Multiple Reaction Monitoring Assays for Enhanced Detection of Ultra-Low Abundance Mycobacterium Tuberculosis Peptides in Human Serum. *Clin. Proteomics* **2017**, *14*, 21–30.

Meister, G. Argonaute Proteins: Functional Insights and Emerging Roles. *Nat. Rev. Genet.* **2013**, *14*, 447–459.

Misek, D. E.; Kim, E. H. Protein Biomarkers for the Early Detection of Breast Cancer. *Int. J. Proteomics* **2011**, *2011*, 1-9.

Mohan, A.; Rajendran, S. R. C. K.; He, Q. S.; Bazinet, L.; Udenigwe, C. C. Encapsulation of Food Protein Hydrolysates and Peptides: A Review. *RSC Adv.* **2015,** *5*, 79270–79278.

Moks, T.; Abrahamsen, L.; Nilsson, B.; Hellmann, U. Staphylococcal Protein A Consists of Five IgG Binding Domains. *Eur. J. Biochem.* **1986**, *156*, 637–643.

Moon, K.; Grindstaff, J.; Sobransingh, D.; Kaifer, A. E. Cucurbit[8]uril-Mediated Redox-Controlled Self-Assembly of Viologen-Containing Dendrimers. *Angew. Chemie - Int. Ed.* **2004**, *43*, 5496–5499.

Mura, S.; Nicolas, J.; Couvreur, P. Stimuli-Responsive Nanocarriers for Drug Delivery. *Nat. Mater.* **2013,** *12*, 991–1003.

Najam-Ul-Haq, M.; Saeed, A.; Jabeen, F.; Maya, F.; Ashiq, M. N.; Sharif, A. Newly Developed Poly(Allyl Glycidyl Ether/Divinyl Benzene) Polymer for Phosphopeptides Enrichment and Desalting of Biofluids. *ACS Appl. Mater. Interfaces* **2014**, *6*, 3536–3545.

Narumi, R.; Shimizu, Y.; Ukai-Tadenuma, M.; Ode, K. L.; Kanda, G. N.; Shinohara, Y.; Sato, A.; Matsumoto, K.; Ueda, H. R. Mass Spectrometry-Based Absolute Quantification Reveals Rhythmic Variation of Mouse Circadian Clock Proteins. *Proc. Natl. Acad. Sci.* **2016**, *113*, E3461–E3467.

Niehaus, M.; Schnapp, A.; Koch, A.; Soltwisch, J.; Dreisewerd, K. New Insights into the Wavelength Dependence of MALDI Mass Spectrometry. *Anal. Chem.* **2017**, *89*, 7734–7741.

Nimse, S. B.; Sonawane, M. D.; Song, K.-S.; Kim, T. Biomarker Detection Technologies and Future Directions. *Analyst* **2016**, *141* (3), 740–755.

O'Farrell, P. H. High Resolution Two-Dimensional Electrophoresis of Proteins. *J. Biol. Chem.* **1975**, *250* (10), 4007–4021.

Oda, Y.; Huang, K.; Cross, F. R.; Cowburn, D.; Chait, B. T. Accurate Quantitation of Protein Expression and Site-Specific Phosphorylation. *Proc. Natl. Acad. Sci.* **1999**, *96*, 6591–6596.

Olsen, J. V.; Mann, M. Status of Large-Scale Analysis of Post-Translational Modifications by Mass Spectrometry. *Mol. Cell. Proteomics* **2013**, *12*, 3444–3452.

Onisko, B.; Dynin, I.; Requena, J. R.; Silva, C. J.; Erickson, M.; Carter, J. M. Mass Spectrometric Detection of Attomole Amounts of the Prion Protein by NanoLC/MS/MS. *J. Am. Soc. Mass Spectrom.* **2007**, *18*, 1070–1079.

Opiteck, G. J.; Jorgenson, J. W.; Anderegg, R. J. Two-Dimensional SEC/RPLC Coupled to Mass Spectrometry for the Analysis of Peptides. *Anal. Chem.* **1997**, *69*, 2283–2291.

Osaka, A.; Hasegawa, H.; Yamada, Y.; Yanagihara, K.; Hayashi, T.; Mine, M.; Aoyama, M.; Sawada, T.; Kamihira, S. A Novel Role of Serum Cytochrome c as a Tumor Marker in Patients with Operable Cancer. *J. Cancer Res. Clin. Oncol.* **2009**, *135*, 371–377.

Panuwet, P.; Hunter, R. E.; D'Souza, P. E.; Chen, X.; Radford, S. A.; Cohen, J. R.; Marder, M. E.; Kartavenka, K.; Ryan, P. B.; Barr, D. B. Biological Matrix Effects in Quantitative Tandem Mass Spectrometry-Based Analytical Methods: Advancing Biomonitoring. *Crit. Rev. Anal. Chem.* **2016**, *46* (2), 93–105.

Park, Z.-Y.; Russell, D. H. Identification of Individual Proteins in Complex Protein Mixtures by High-Resolution, High-Mass-Accuracy MALDI TOF-Mass Spectrometry Analysis of in-Solution Thermal Denaturation/Enzymatic Digestion. *Anal. Chem.* **2001**, *73*, 2558–2564.

Pashkova, A.; Moskovets, E.; Karger, B. L. Coumarin Tags for Improved Analysis of Peptides by MALDI-TOF MS and MS/MS: Enhancement in MALDI MS Signal Intensities. *Anal. Chem.* **2004**, *76*, 4550–4557.

Peng, J.; Elias, J. E.; Thoreen, C. C.; Licklider, L. J.; Gygi, S. P. Evaluation of Multidimensional Chromatography Coupled with Tandem Mass Spectrometry (LC/LC-MS/MS) for Large-Scale Protein Analysis: The Yeast Proteome. *J. Proteome Res.* **2003**, *2*, 43–50.

Percy, A. J.; Chambers, A. G.; Yang, J.; Hardie, D. B.; Borchers, C. H. Advances in Multiplexed MRM-Based Protein Biomarker Quantitation toward Clinical Utility. *Biochim. Biophys. Acta* **2014**, *1844* (5), 917–926.

Peurifoy, S. R.; Guzman, C. X.; Braunschweig, A. B. Topology, Assembly, and Electronics: Three Pillars for Designing Supramolecular Polymers with Emergent Optoelectronic Behavior. *Polym. Chem.* **2015**, *6*, 5529-5539.

Polanski, M.; Anderson, N. L. A List of Candidate Cancer Biomarkers for Targeted Proteomics. *Biomark. Insights* **2007**, *1* (301), 1–48.

Pratt, A. J.; MacRae, I. J. The RNA-Induced Silencing Complex: A Versatile Gene-Silencing Machine. *J. Biol. Chem.* **2009**, *284*, 17897–17901.

Puangpila, C.; Mayadunne, E.; El Rassi, Z. Liquid Phase Based Separation Systems for Depletion, Prefractionation, and Enrichment of Proteins in Biological Fluids and Matrices for in-Depth Proteomics Analysis-An Update Covering the Period 2011-2014. *Electrophoresis* **2015**, *36*, 238–252.

Qiao, X.; Sun, L.; Chen, L.; Zhou, Y.; Yang, K.; Liang, Z.; Zhang, L.; Zhang, Y. Piperazines for Peptide Carboxyl Group Derivatization: Effect of Derivatization Reagents and Properties of Peptides on Signal Enhancement in Matrix-Assisted Laser Desorption/Ionization Mass Spectrometry. *Rapid Commun. Mass Spectrom.* **2011**, *25*, 639–646.

Quinn, J. F.; Whittaker, M. R.; Davis, T. P. Glutathione Responsive Polymers and Their Application in Drug Delivery Systems. *Polym. Chem.* **2017,** *8*, 97–126.

Rasband, W.S., ImageJ, U. S. National Institutes of Health, Bethesda, Maryland, USA, http://imagej.nih.gov/ij/, 1997-2015.

Razavi, M.; Frick, L. E.; LaMarr, W. A.; Pope, M. E.; Miller, C. A.; Anderson, N. L.; Pearson, T. W. High-Throughput SISCAPA Quantitation of Peptides from Human Plasma Digests by Ultrafast, Liquid Chromatography-Free Mass Spectrometry. *J. Proteome Res.* **2012**, *11* (12), 5642–5649.

Reinicke, S.; Espeel, P.; Stamenović, M. M.; Du Prez, F. E. One-Pot Double Modification of p(NIPAAm): A Tool for Designing Tailor-Made Multiresponsive Polymers. *ACS Macro Lett.* **2013**, *2* (6), 539–543.

Reyzer, M. L.; Caldwell, R. L.; Dugger, T. C.; Forbes, J. T.; Ritter, C. a; Guix, M.; Arteaga, C. L.; Caprioli, R. M. Early Changes in Protein Expression Detected by Mass Spectrometry Predict Tumor Response to Molecular Therapeutics. *Cancer Res.* **2004**, *64*, 9093–9100.

Rodriguez-Suarez, E.; Whetton, A. D. The Application of Quantification Techniques in Proteomics for Biomedical Research. *Mass Spectrom. Rev.* **2013**, *32*, 1–26.

Rodthongkum, N.; Chen, Y.; Thayumanavan, S.; Vachet, R. W. Matrix-Assisted Laser Desorption Ionization-Mass Spectrometry Signal Enhancement of Peptides After Selective Extraction with Polymeric Reverse Micelles. *Anal. Chem.* **2010**, *82*, 3686–3691.

Rodthongkum, N.; Chen, Y.; Thayumanavan, S.; Vachet, R. W. Selective Enrichment and Analysis of Acidic Peptides and Proteins Using Polymeric Reverse Micelles and MALDI-MS. *Anal. Chem.* **2010**, *82* (20), 8686–8691.

Rodthongkum, N.; Ramireddy, R.; Thayumanavan, S.; Richard, W. V. Selective enrichment and sensitive detection of peptide and protein biomarkers in human serum using polymeric reverse micelles and MALDI-MS. *Analyst* **2012,** *137*, 1024–1030.

Rodthongkum, N.; Washington, J. D.; Savariar, E. N.; Thayumanavan, S.; Vachet, R. W. Generating peptide titration-type curves using polymeric reverse micelles as selective extraction agents along with matrix-assisted laser desorption ionization-mass spectrometry detection. *Anal. Chem.* **2009,** *81*, 5046–53.

Sandanaraj, B. S.; Vutukuri, D. R.; Simard, J. M.; Klaikherd, A.; Hong, R.; Rotello, V. M.; Thayumanavan, S. Noncovalent Modification of Chymotrypsin Surface Using an Amphiphilic Polymer Scaffold: Implications in Modulating Protein Function. *J. Am. Chem. Soc.* **2005**, *127* (30), 10693–10698.

Sandanayake, N. S.; Camuzeaux, S.; Sinclair, J.; Blyuss, O.; Andreola, F.; Chapman, M. H.; Webster, G. J.; Smith, R. C.; Timms, J. F.; Pereira, S. P. Identification of Potential Serum Peptide Biomarkers of Biliary Tract Cancer Using MALDI MS Profiling. *BMC Clin. Pathol.* **2014**, *14* (1), 7-17.

Savariar, E. N.; Aathimanikandan, S. V.; Thayumanavan, S. Supramolecular Assemblies from Amphiphilic Homopolymers: Testing the Scope. *J. Am. Chem. Soc.* **2006**, *128*, 16224–16230.

Savariar, E. N.; Ghosh, S.; González, D. C.; Thayumanavan, S. Disassembly of Noncovalent Amphiphilic Polymers with Proteins and Utility in Pattern Sensing. *J. Am. Chem. Soc.* **2008**, *130*, 5416–5417.

Schindelin, J.; Arganda-Carreras, I.; Frise, E.; Kaynig, V.; Longair, M.; Pietzsch, T.; Preibisch, S.; Rueden, C.; Saalfeld, S.; Schmid, B.; et al. Fiji: An Open-Source Platform for Biological-Image Analysis. *Nat. Methods* **2012**, *9* (7), 676–682.

Schuerenberg, M.; Luebbert, C.; Eickhoff, H.; Kalkum, M.; Lehrach, H.; Nordhoff, E. Prestructured MALDI-MS Sample Supports. *Anal. Chem.* **2000**, *72*, 3436–3442.

Schweppe, R. E.; Haydon, C. E.; Lewis, T. S.; Resing, K. A.; Ahn, N. G. The Characterization of Protein Post-Translational Modifications by Mass Spectrometry. *Acc. Chem. Res.* **2003**, *36*, 453–461.

Serrano, M. A. C.; He, H.; Zhao, B.; Ramireddy, R. R.; Vachet, R. W.; Thayumanavan, S. Polymer-Mediated Ternary Supramolecular Interactions for Sensitive Detection of Peptides. *Analyst* **2017**, *142* (1), 118–122.

Serrano, M. A. C.; Zhao, B.; He, H.; Thayumanavan, S.; Vachet, R. W. Molecular Features Influencing the Release of Peptides from Amphiphilic Polymeric Reverse Micelles. *Langmuir* **2018**, *34* (15), 4595–4602.

Shaw, J. B.; Li, W.; Holden, D. D.; Zhang, Y.; Griep-Raming, J.; Fellers, R. T.; Early, B. P.; Thomas, P. M.; Kelleher, N. L.; Brodbelt, J. S. Complete Protein Characterization Using Top-down Mass Spectrometry and Ultraviolet Photodissociation. *J. Am. Chem. Soc.* **2013**, *135*, 12646–12651.

Shevchenko, A.; Jensen, O. N.; Podtelejnikov, A. V.; Sagliocco, F.; Wilm, M.; Vorm, O.; Mortensen, P.; Shevchenko, A.; Boucherie, H.; Mann, M. Linking Genome and Proteome by Mass Spectrometry: Large-Scale Identification of Yeast Proteins from Two Dimensional Gels. *Proc. Natl. Acad. Sci.* **1996**, *93*, 14440–14445.

Sidransky, D. Emerging Molecular Markers of Cancer. *Nat. Rev. Cancer* **2002**, *2*, 210–219.

Smolka, M.; Zhou, H.; Aebersold, R. Quantitative Protein Profiling Using Two-Dimensional Gel Electrophoresis, Isotope-Coded Affinity Tag Labeling, and Mass Spectrometry. *Mol. Cell. Proteomics* **2002**, *1*, 19–29.

Stastna, M.; Van Eyk, J. E. Analysis of Protein Isoforms: Can We Do It Better? *Proteomics* **2012**, *12*, 2937–2948.

Steel, L. F.; Trotter, M. G.; Nakajima, P. B.; Mattu, T. S.; Gonye, G.; Block, T. Efficient and Specific Removal of Albumin from Human Serum Samples. *Mol. Cell. Proteomics* **2003**, *2*, 262–270.

Syahir, A.; Usui, K.; Tomizaki, K.; Kajikawa, K.; Mihara, H. Label and Label-Free Detection Techniques for Protein Microarrays. *Microarrays* **2015**, *4*, 228–244.

Szájli, E.; Fehér, T.; Medzihradszky, K. F. Investigating the Quantitative Nature of MALDI-TOF MS. *Mol. Cell. Proteomics* **2008**, *7* (12), 2410–2418.

Tabb, D. L.; Huang, Y.; Wysocki, V. H.; Yates, J. R. Influence of Basic Residue Content on Fragment Ion Peak Intensities in Low-Energy Collision-Induced Dissociation Spectra of Peptides. *Anal. Chem.* **2004**, *76* (5), 1243–1248.

Tessitore, A.; Gaggiano, A.; Cicciarelli, G.; Verzella, D.; Capece, D.; Fischietti, M.; Zazzeroni, F.; Alesse, E. Serum Biomarkers Identification by Mass Spectrometry in High Mortality Tumors. *Int. J. Proteomics* **2013**, *2013*, 1–15.

The Royal Swedish Academy of Sciences. Advanced information on the Nobel Prize in Chemistry 2002. Nobel Prize website. https://assets.nobelprize.org/uploads/2018/06/advanced-chemistryprize2002.pdf.

Tian, R.; Zhang, H.; Ye, M.; Jiang, X.; Hu, L.; Li, X.; Bao, X.; Zou, H. Selective Extraction of Peptides from Human Plasma by Highly Ordered Mesoporous Silica Particles for Peptidome Analysis. *Angew. Chem. Int. Ed. Engl.* **2007**, *46* (6), 962–965.

Tipton, J. D.; Tran, J. C.; Catherman, A. D.; Ahlf, D. R.; Durbin, K. R.; Kelleher, N. L. Analysis of Intact Protein Isoforms by Mass Spectrometry. *J. Biol. Chem.* **2011**, *286* (29), 25451–25458.

Tonova, K.; Lazarova, Z. Reversed Micelle Solvents as Tools of Enzyme Purification and Enzyme-Catalyzed Conversion. *Biotechnol. Adv.* **2008,** *26,* 516–532.

Trivedi, R.; Kompella, U. B. Nanomicellar Formulations for Sustained Drug Delivery. *Nanomedicine* **2010,** *5,* 485–505.

Tu, Y.; Peng, F.; Adawy, A.; Men, Y.; Abdelmohsen, L. K. E. A.; Wilson, D. A. Mimicking the Cell: Bio-Inspired Functions of Supramolecular Assemblies. *Chem. Rev.* **2016**, *116*, 2023-2078.

Tu, Y.; Peng, F.; Adawy, A.; Men, Y.; Abdelmohsen, L. K. E. A.; Wilson, D. A. Mimicking the Cell: Bio-Inspired Functions of Supramolecular Assemblies. *Chem. Rev.* **2016**, *116*, 2023-2078.

Tyler-Cross, R.; Schirch, V. Effects of Amino Acid Sequence, Buffers, and Ionic Strength on the Rate and Mechanism of Deamidation of Asparagine Residues in Small Peptides. *J. Biol. Chem.* **1991**, *266*, 22549–22556.

van den Broek, I.; Sparidans, R. W.; Schellens, J. H. M.; Beijnen, J. H. Quantitative Assay for Six Potential Breast Cancer Biomarker Peptides in Human Serum by Liquid Chromatography Coupled to Tandem Mass Spectrometry. *J. Chromatogr. B* **2010**, *878*, 590–602.

van Winden, A. W. J.; van den Broek, I.; Gast, M.-C. W.; Engwegen, J. Y. M. N.; Sparidans, R. W.; van Dulken, E. J.; Depla, A. C. T. M.; Cats, A.; Schellens, J. H. M.; Peeters, P. H. M.; Beijnen, J. H.; van Gils, C. H. Serum Degradome Markers for the Detection of Breast Cancer. *J. Proteome Res.* **2010**, *9*, 3781–3788.

Varshney, A.; Sen, P.; Ahmad, E.; Rehan, M.; Subbarao, N.; Khan, R. H. Ligand Binding Strategies of Human Serum Albumin: How Can the Cargo Be Utilized? *Chirality* **2010**, *22*, 77–87.

Vaudel, M.; Burkhart, J. M.; Zahedi, R. P.; Oveland, E.; Berven, F. S.; Sickmann, A.; Martens, L.; Barsnes, H. PeptideShaker Enables Reanalysis of MS-Derived Proteomics Data Sets: To the Editor. *Nat. Biotechnol.* **2015**, *33*, 22–24.

Villanueva, J. et al. Differential Exoprotease Activities Confer Tumor-Specific Serum Peptidome Patterns. *J. Clin. Invest.* **2006**, *116* (1), 271–284.

Wang, F.; Gomez-Escudero, A.; Ramireddy, R. R.; Murage, G.; Thayumanavan, S.; Vachet, R. W. Electrostatic Control of Peptide Side-Chain Reactivity Using Amphiphilic Homopolymer-Based Supramolecular Assemblies. *J. Am. Chem. Soc.* **2013,** *135*, 14179–14188.

Wang, Z.; Van Oers, M. C. M.; Rutjes, F. P. J. T.; Van Hest, J. C. M. Polymersome Colloidosomes for Enzyme Catalysis in a Biphasic System. *Angew. Chemie - Int. Ed.* **2012**, *51* (43), 10746–10750.

Washburn, M. P.; Wolters, D.; Yates, J. R. Large-Scale Analysis of the Yeast Proteome by Multidimensional Protein Identification Technology. *Nat. Biotechnol.* **2001**, *19*, 242–247.

Watson, J. T.; Sparkman, O. D. *Introduction to Mass Spectrometry: Instrumentation, Applications, and Strategies for Data Interpretation, 4th Ed.* John Wiley & Sons Ltd: West Sussex, England, 2007.

Weigel, M. T.; Dowsett, M. Current and Emerging Biomarkers in Breast Cancer: Prognosis and Prediction. *Endocr. Relat. Cancer* **2010**, *17* (4), R245–R262.

Westermeier, R.; Marouga, R. Protein Detection Methods in Proteomics Research. *Biosci. Rep.* **2005**, *25*, 19–32.

Whiteaker, J. R.; Zhang, H.; Eng, J. K.; Fang, R.; Piening, B. D.; Feng, L.; Lorentzen, T. D.; Schoenherr, R. M.; Keane, J. F.; Holzman, T.; et al. Head-to-Head Comparison of Serum Fractionation Techniques Research Articles. *J. Proteome Res.* **2007**, *6*, 828–836.

Whiteaker, J. R.; Zhao, L.; Anderson, L.; Paulovich, A. G. An Automated and Multiplexed Method for High Throughput Peptide Immunoaffinity Enrichment and Multiple Reaction Monitoring Mass Spectrometry-Based Quantification of Protein Biomarkers. *Mol. Cell. Proteomics* **2010**, *9*, 184–196.

Whiteaker, J. R.; Zhao, L.; Zhang, H. Y.; Feng, L.-C.; Piening, B. D.; Anderson, L.; Paulovich, A. G. Antibody-Based Enrichment of Peptides on Magnetic Beads for Mass-Spectrometry-Based Quantification of Serum Biomarkers. *Anal. Biochem.* **2007**, *362* (1), 44–54.

Wildsmith, K. R.; Han, B.; Bateman, R. J. Method for the Simultaneous Quantitation of Apolipoprotein E Isoforms Using Tandem Mass Spectrometry. *Anal. Biochem.* **2009**, *395*, 116–118.

Wulfkuhle, J. D.; Liotta, L. A.; Petricoin, E. F. Proteomic Applications for the Early Detection of Cancer. *Nat. Rev. Cancer* **2003**, *3*, 267–275.

Xiao, H.; Chen, W.; Smeekens, J. M.; Wu, R. An Enrichment Method Based on Synergistic and Reversible Covalent Interactions for Large-Scale Analysis of Glycoproteins. *Nat. Commun.* **2018**, *9*, 1692.

Xu, Y.; Bruening, M. L.; Watson, J. T. Use of Polymer-Modified MALDI-MS Probes to Improve Analyses of Protein Digests and DNA. *Anal. Chem.* **2004**, *76*, 3106–3111.

Yang, H. H.; Lu, K. H.; Lin, Y. F.; Tsai, S. H.; Chakraborty, S.; Zhai, W. J.; Tai, D. F. Depletion of Albumin and Immunoglobulin G from Human Serum Using Epitope-Imprinted Polymers as Artificial Antibodies. *J. Biomed. Mater. Res. - Part A* **2013**, *101 A*, 1935–1942.

Yu, Y. C.; Chu, Y.; Ji, J. Y. Study of the Factors Affecting the Forward and Back Extraction of Yeast-Lipase and Its Activity by Reverse Micelles. *J. Colloid Interface Sci.* **2003,** *267*, 60–64.

Zhang, J.; Sun, H.; Ma, P. X. Host-Guest Interaction Mediated Polymeric Assemblies: Multifunctional Nanoparticles for Drug and Gene Delivery. *ACS Nano* **2010**, *4* (2), 1049–1059.

Zhang, Y.; Fonslow, B. R.; Shan, B.; Baek, M. C.; Yates, J. R. Protein Analysis by Shotgun/Bottom-up Proteomics. *Chem. Rev.* **2013**, *113* (4), 2343–2394.

Zhao, B.; Serrano, M. A. C.; Gao, J.; Zhuang, J.; Vachet, R. W.; Thayumanavan, S. Self-Assembly of Random Co-Polymers for Selective Binding and Detection of Peptides. *Polym. Chem.* **2018**, *9* (9), 1066–1071.

Zhao, B.; Serrano, M. A. C.; Wang, M.; Liu, T.; Gordon, M. R.; Thayumanavan, S.; Vachet, R. W. Improved Mass Spectrometric Detection of Acidic Peptides by Variations in the Functional Group pKa Values of Reverse Micelle Extraction Agents. *Analyst* **2018**, *143*, 1434–1443.

Zhao, B.; Zhuang, J.; Serrano, M. A. C.; Vachet, R. W.; Thayumanavan, S. Influence of Charge Density on Host–Guest Interactions within Amphiphilic Polymer Assemblies in Apolar Media. *Macromolecules* **2017**, *50* (24), 9734–9741.

Zhao, X.; Chen, F.; Gai, G.; Chen, J.; Xue, W.; Lee, L. Effects of Extraction Temperature, Ionic Strength and Contact Time on Efficiency of Bis(2-ethylhexyl) Sodium Sulfosuccinate (AOT) Reverse Micellar Backward Extraction of Soy Protein and Isoflavones from Soy Flour. *J. Sci. Food Agric.* **2008,** *88*, 590–596.

Zhu, W.; Smith, J. W.; Huang, C. M. Mass Spectrometry-Based Label-Free Quantitative Proteomics. *J. Biomed. Biotechnol.* **2010**, *2010*, 1–6.

Zhuang, J.; Jiwpanich, S.; Deepak, V. D.; Thayumanavan, S. Facile Preparation of Nanogels Using Activated Ester Containing Polymers. *ACS Macro Lett.* **2012**, *1* (1), 175–179.

Zolotarjova, N.; Martosella, J.; Nicol, G.; Bailey, J.; Boyes, B. E.; Barrett, W. C. Differences among Techniques for High-Abundant Protein Depletion. *Proteomics* **2005**, *5* (13), 3304–3313.

Zybailov, B.; Coleman, M. K.; Florens, L.; Washburn, M. P. Correlation of Relative Abundance Ratios Derived from Peptide Ion Chromatograms and Spectrum Counting for Quantitative Proteomic Analysis Using Stable Isotope Labeling. *Anal. Chem.* **2005**, *77*, 6218–6224.